Vitor João Salgueiro Rosa

SYNTHESIS, CHARACTERIZATION AND REACTIVITY OF NEW COBALT, PALLADIUM AND NICKEL COMPLEXES BEARING α-DIIMINES AND P,O LIGANDS

Lisboa

2008

Vitor João Salgueiro Rosa

SYNTHESIS, CHARACTERIZATION AND REACTIVITY OF NEW COBALT, PALLADIUM AND NICKEL COMPLEXES BEARING α-DIIMINES AND P,O LIGANDS

Dissertação apresentada para a obtenção do
Grau de Doutor em Química,
Especialidade Química Inorgânica
Pela Universidade Nova de Lisboa,
Faculdade de Ciências e Tecnologia

Lisboa
2008

"Posso ser tão mau como os piores mas, graças
a Deus, também posso ser tão bom como os melhores"
Walt Whitman American poet (1819-1892)

"…our knowledge can be only finite, while
our ignorance must necessarily be infinite."
Karl Popper British philosopher of science (1902-1994)

Ao Tomás

ACKNOWLEDGEMENTS

To Prof. Teresa Avilés, the supervisor of this thesis, for all her help and guidance through this work, and her truly friendship. For providing motivation and help to allow me to overcome the frustration that usually strikes synthetic chemists. I would like to thank her also for the help and criticism during the making of this thesis.

To Dr. Carlos Lodeiro, for his always useful advices and support, and for his input in absorption studies.

To Prof. Richard Welter, for all the help in the determination of single crystals X-ray structures, his patience and friendship.

To Prof. Teixeira Gomes to helping me at the beginning of this journey that was this thesis, for the polymerization of ethylene tests and for the pleasant collaboration we had and hoping that it continues.

To Berta Covelo for X-ray studies, Prof. Carlos Brondino for the EPR studies, Prof. Gabriel Aullón for the theoretical studies and Pierre Braunstein for his useful chemical insights and collaboration.

To "Fundação para a Ciência e a Tecnologia", for financial support through the PRAXIS XXI program, with the grant SFRH/BD/13777/2003.

To the New University of Lisbon and in particular the Chemistry Department of the Faculty of Science and Technology, for giving me the possibility to access and use the technical, material and human resources, in particular the assistance of Dr. Maria do Rosário Caras Altas in recording the NMR data.

To Christophe, Jean-Thomas and Samuel and Magno for their friendship and all the help they provided me at Strasbourg.

To all my laboratory colleagues, in particular Bruno, Betty and Tiago for their kindness, and to all my friends, in particular Jorge for his help in the revision of this thesis and his constant support.

And finally, thanks to my family, in particular my mother without whom I would never be who I am.

ABSTRACT

This work describes the synthesis and characterization of a series of new α-diimine and P,O, β-keto and acetamide phosphines ligands, and their complexation to Ni(II), Co(II), Co(III) and Pd(II) to obtain a series of new compounds aiming to study their structural characteristics and to test their catalytic activity. All the compounds synthesized were characterized by the usual spectroscopic and spectrometric techniques: Elemental Analysis, MALDI-TOF-MS spectrometry, IR, UV-vis, ^{1}H, ^{13}C and ^{31}P NMR spectroscopies. Some of the paramagnetic compounds were also characterized by EPR. For the majority of the compounds it was possible to solve their solid state structure by single crystal X-ray diffraction. Tests for olefin polymerization were performed in order to determine the catalytic activity of the Co(II) complexes.

Chapter I presents a brief introduction to homogenous catalysis, highlighting the reactions catalyzed by the type of compounds described in this thesis, namely olefin polymerization and oligomerization and reactions catalyzed by the complexes bearing α-diimines and P,O type ligands.

Chapter II is dedicated to the description of the synthesis of new α-diimines cobalt (II) complexes, of general formula [CoX_2(α-diimine)], where X = Cl or I and the α-diimines are bis(aryl)acenaphthenequinonediimine) (Ar-BIAN) and 1,4-diaryl-2,3-dimethyl-1,4-diaza-1,3-butadiene (Ar-DAB). Structures solved by single crystal X-ray diffraction were obtained for all the described complexes. For some of the compounds, X-band EPR measurements were performed on polycrystalline samples, showing a high-spin Co(II) (S = 3/2) ion, in a distorted axial environment. EPR single crystal experiments on two of the compounds allowed us to determine the ***g*** tensor orientation in the molecular structure.

In **Chapter III** we continue with the synthesis and characterization of more cobalt (II) complexes bearing α-diimines of general formula [CoX_2(α-diimine)], with X = Cl or I and α-diimines are bis(aryl)acenaphthenequinonediimine) (Ar-BIAN) and 1,4-diaryl-2,3-dimethyl-1,4-diaza-1,3-butadiene (Ar-DAB). The structures of three of the new compounds synthesized were determined by single crystal X-ray diffraction. A NMR paramagnetic characterization of

all the compounds described is presented. Ethylene polymerization tests were done to determine the catalytic activity of several of the Co(II) complexes described in **Chapter II** and **III** and their results are shown.

In **Chapter IV** a new rigid bidentate ligand, bis(1-naphthylimino)acenaphthene, and its complexes with Zn(II) and Pd(II), were synthesized. Both the ligand and its complexes show *syn* and *anti* isomers. Structures of the ligand and the *anti* isomer of the Pd(II) complex were solved by single crystal X-ray diffraction. All the compounds were characterized by elemental analysis, MALDI-TOF-MS spectrometry, and by IR, UV-vis, ^{1}H, ^{13}C, ^{1}H-^{1}H COSY, ^{1}H-^{13}C HSQC, ^{1}H-^{13}C HSQC-TOCSY and ^{1}H-^{1}H NOESY NMR when necessary.

DFT studies showed that both conformers of $[PdCl_2(BIAN)]$ are isoenergetics and can be obtain experimentally. However, we can predict that the isomerization process is not available in square-planar complex, but is possible for the free ligand. The molecular geometry is very similar in both isomers, and only different orientations for naphthyl groups can be expected.

Chapter V describes the synthesis of new P, O type ligands, β-keto phosphine, $R_2PCH_2C(O)Ph$, and acetamide phosphine $R_2PNHC(O)Me$, as well as a series of new cobalt (III) complexes namely $[(\eta^5\text{-}C_5H_5)CoI_2\{Ph_2PCH_2C(O)Ph\}]$, and $[(\eta^5\text{-}C_5H_5)CoI_2\{Ph_2PNHC(O)Me\}]$. Treating these Co(III) compounds with an excess of Et_3N, resulted in complexes η^2-phosphinoenolate $[(\eta^5\text{-}C_5H_5)CoI\{Ph_2PCH{\cdots}C(\cdots O)Ph\}]$ and η^2-acetamide phosphine $[(\eta^5\text{-}C_5H_5)CoI\{Ph_2PN{\cdots}C(\cdots O)Me\}]$. Nickel (II) complexes were also obtained: *cis*-$[Ni(Ph_2PN{\cdots}C(\cdots O)Me)_2]$ and *cis*-$[Ni((i\text{-}Pr)_2PN{\cdots}C(\cdots O)Me)_2]$. Their geometry and isomerism were discussed. Seven structures of the compounds described in this chapter were determined by single crystal X-ray diffraction.

The general conclusions of this work can be found in **Chapter VI**.

RESUMO

Neste trabalho descreve-se a síntese e caracterização de uma série de novos ligandos, do tipo α-diimina e do tipo P,O, β-keto e acetamido fosfina, e a sua complexação a Ni(II), Co(II), Co (III) e Pd(II) obtendo-se séries de novos compostos com o objectivo de estudar as suas características estruturais e testar a sua actividade catalítica. Todos os compostos sintetizados foram caracterizados pelos métodos espectroscópicos e espectrométricos usuais: análise elementar, espectrometria MALDI-TOF-MS, e espectroscopias de IV, UV-vis, ^{1}H, ^{13}C e ^{31}P RMN. No caso de alguns dos compostos paramagnéticos foi também utilizada RPE. Na maioria dos compostos foi possível determinar as estruturas no estado sólido por difracção de raios-X. Foram efectuados testes de catálise de polimerização de etileno para determinar a actividade de vários dos complexos de Co(II).

No **Capítulo I** é feita uma breve introdução á catálise homogénea, salientando as reacções catalizadas pelo tipo de compostos descritos nesta tese, nomeadamente a polimerização e oligomerização de olefinas e reacções catalizadas pelos complexos contendo ligandos α-diiminicos e do tipo P,O.

O **Capítulo II** está dedicado à descrição da síntese de novos complexos de cobalto (II) com ligandos α-diiminas, de formula geral [CoX_2(α-diimina)], nos quais X = Cl ou I e as α-diiminas são a bis(arilo)acenaftenoquinonadiimina) (Ar-BIAN) e a 1,4-diaril-2,3-dimetil-1,4-diaza-1,3-butadieno (Ar-DAB). Foi possível obter estruturas através da difracção de raios-X de todos os complexos descritos. Medidas de RPE banda X com amostras policristalinas foram feitas nalguns dos compostos descritos mostrando um spin-alto do ião Co(II) (S = 3/2) num ambiente axialmente distorcido. Experiências de RPE de mono cristal, de dois dos compostos, permitiram-nos determinar a orientação do tensor $\boldsymbol{g}$ dentro da estrutura molecular.

No **Capítulo III** continua-se a descrição da síntese de complexos de cobalto (II) com α-diiminas de formula geral [CoX_2(α-diimina)], nos quais X = Cl ou I e as α-diiminas são a bis(arilo)acenaftenoquinonadiimina) (Ar-BIAN) e a 1,4-diaril-2,3-dimetil-1,4-diaza-1,3-butadieno (Ar-DAB). Além da determinação das estruturas por difracção de raios-X de mono cristal de três dos compostos sintetizados também foi feito um estudo de RMN paramagnética

dos compostos descritos. Foram efectuados testes de catálise de polimerização de etileno para determinar a actividade de vários dos complexos de Co(II) descritos no **Capitulo II** e **III**, e os resultados apresentados.

No **Capítulo IV** um novo ligando rígido bidentado, o bis(1-naftilolimino)acenafteno, e os respectivos complexos de Zn(II) e Pd(II), foram sintetizados. Tanto o ligando como os seus complexos apresentam isómeros *syn* e *anti*. As estruturas de estado sólido do ligando e do isómero *anti* do composto de Pd(II) foram determinadas por difracção raios-X de cristal único. Todos os compostos foram caracterizados por analise elementar, espectrometria MALDI-TOF-MS, e por espectroscopias de IV, UV-vis, ^{1}H, ^{13}C, ^{1}H-^{1}H COSY, ^{1}H-^{13}C HSQC, ^{1}H-^{13}C HSQC-TOCSY e ^{1}H-^{1}H NOESY RMN quando necessário.

Estudos de DFT mostraram que os confórmeros do $[PdCl_2(BIAN)]$ são isoenergéticos e podem ser ambos obtidos experimentalmente. No entanto, pode-se deduzir que o processo de isomerização não é possível num complexo quadrangular planar, mas é possível para o ligando livre. A geometria molecular é muito semelhante para ambos os isómeros, sendo unicamente esperado observar diferentes orientações dos grupos naftilo.

No **Capítulo V** descreve-se a síntese de novos ligandos do tipo P,O, β-keto fosfina, $R_2PCH_2C(O)Ph$, e acetamido fosfina $R_2PNHC(O)Me$, assim como a de uma série de novos complexos de cobalto (III) $[(\eta^5\text{-}C_5H_5)CoI_2\{Ph_2PCH_2C(O)Ph\}]$, $[(\eta^5\text{-}C_5H_5)CoI_2\{Ph_2PNHC(O)Me\}]$. Por tratamento destes compostos com um excesso de Et_3N, sintetizou-se o complexo η^2-fosfinoenolato $[(\eta^5\text{-}C_5H_5)CoI\{Ph_2PCH{\cdots}C({\cdots}O)Ph\}]$ e o complexo η^2-acetamidofosfina $[(\eta^5\text{-}C_5H_5)CoI\{Ph_2PN{\cdots}C({\cdots}O)Me\}]$. Complexos de níquel (II) também foram obtidos: o *cis*-$[Ni(Ph_2PN{\cdots}C({\cdots}O)Me)_2]$ e o *cis*-$[Ni((i\text{-}Pr)_2PN{\cdots}C({\cdots}O)Me)_2]$. As suas geometrias e isomeria foram discutidas. Foram determinadas as estruturas moleculares de sete dos compostos descritos neste capítulo, através de difracção de raios-X.

Podem-se encontrar no **Capítulo VI**, as conclusões gerais deste trabalho.

ABBREVIATIONS

Ac	Acetyl
Ar	Aryl
Atm	Atmosphere
BIAN	bis(aryl)acenaftenoquinonediimine
Bn	Benzyl
Bu	Butyl
t-Bu	*tert*-Butyl
CDV	Calorimetria diferencial de varrimento
^{13}C NMR	Carbon Nuclear Magnetic Resonance
Conc.	Concentration
d	Duplet
DAB	1,4-diaryl-2,3-dimethyl-1,4-diaza-1,3-butadiene
dba	dibenzylideneacetone
DFT	Density functional theory
dmba	ortometalateddemethylbenzylamine
DSC	differential scanning calorimetry
EI	Electronic Impact Ionization
EPR	Electronic Paramagnetic Resonance
eq.	Equivalent
Et	Ethyl
h	Hour
^{1}H NMR	Proton Nuclear Magnetic Resonance
HPLC	High performance liquid chromatography
HSQC	Heteronuclear single quantum. Correlation
Hz	Hertz
^{i}Pr	Isopropyl
IR	Infra Red spectrometry
IV	Espectrometria infravermelha
J	Coupling constant
m	Multiplet
MALDI	Matrix assisted laser desorption/ionization

MAO	Methylaluminoxane
Me	Methyl
min.	Minute
MS	Mass Spectrometry
NOESY	Nuclear Overhauser effect spectroscopy
NMR	Nuclear Magnetic Resonance
PE	Polyethylene
Ph	Phenyl
s	Singlet
t	Triplet
T (ºC)	Temperature Celsius
t.a.	Temperature ambient
THF	Tetrehydrofuran
TOCSY	Total Correlation Spectroscopy
TOF-MS-EI	Time-of-Fly Mass Spectrometry Electron Impact
TOF-MS-FD	Time-of-Fly Mass Spectrometry Field Desorption
δ	Chemical Shifting
λ	Wave length
ν	Wave number

TABLE OF CONTENTS

INDEX OF FIGURES

INDEX OF SCHEMES

INDEX OF TABLES

INDEX OF COMPOUNDS

Chapter II

Structure	Nº	Name or molecular formula	C.
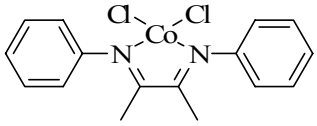	**1a**	[Co(Ph-DAB)Cl_2]	II
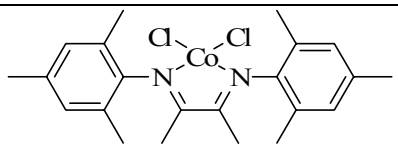	**1b**	[Co(*o,o',p*-$Me_3C_6H_2$DAB)Cl_2]	II
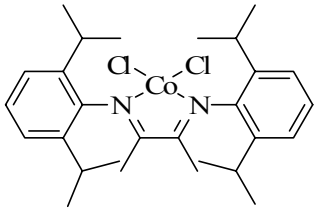	**1c**	[Co(*o,o'*-$^{i}Pr_2C_6H_3$-DAB)Cl_2]	II
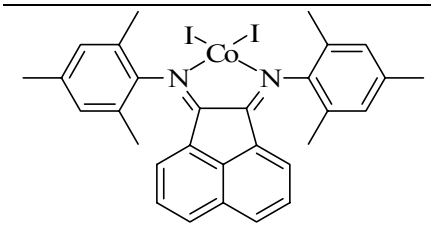	**2'b**	[Co(*o,o',p*-$Me_3C_6H_2$-BIAN)I_2]	II

Chapter III

Structure	Nº	Name	C.
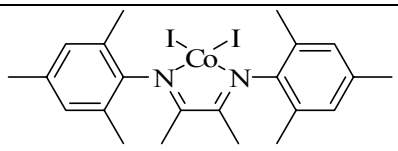	**1**	[CoI_2(*o,o',p*-$Me_3C_6H_2$-DAB)]	III

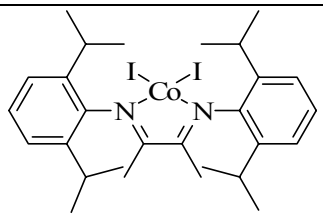	**2**	[CoI_2(*o,o'*-$^{i}Pr_2C_6H_3$-DAB)]	III
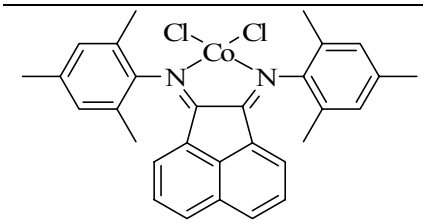	**3**	[$CoCl_2$(*o,o',p*-$Me_3C_6H_2$-BIAN)]	III
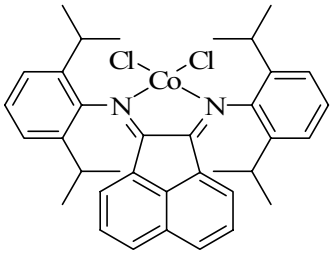	**4**	[$CoCl_2$(*o,o'*-$^{i}Pr_2C_6H_3$-BIAN)]	III
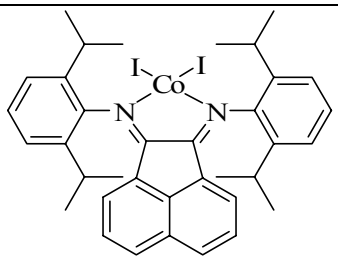	**5**	[CoI_2(*o,o'*-$^{i}Pr_2C_6H_3$-BIAN)]	III

Chapter IV

Structure	Nº	Name	C.
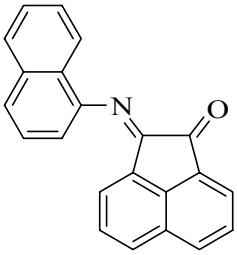	**L**	Mono (1-naphthylimino)acenaphthene	IV
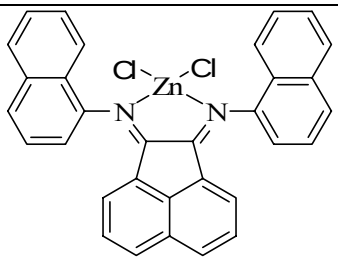	**1**	Bis(1-naphthylimino)acenaphthene zinc dichloride	IV

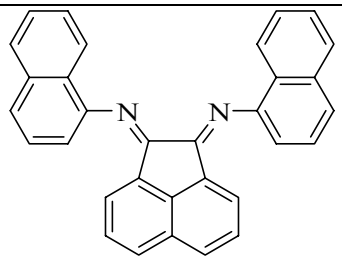	**L1**	Bis(1-naphthylimino)acenaphthene	IV
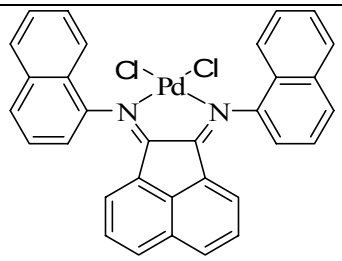	**2**	Bis (1-naphthylimino)acenaphthene palladium dichloride	IV

Chapter V

Structure	Nº	Name	C.
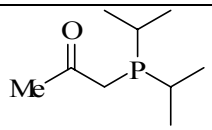	**HL1**	$[(^{i}Pr)_2PCH_2C(O)Ph]$	V
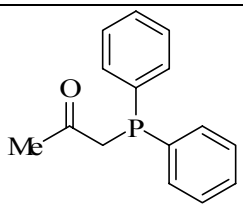	**HL2**	$[Ph_2PCH_2C(O)Ph]$	V
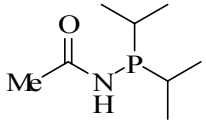	**HL3**	$[(^{i}Pr)_2PNHC(O)Me]$	V
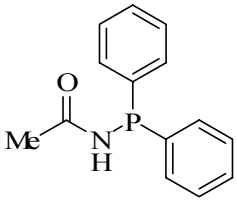	**HL4**	$[Ph_2PNHC(O)Me]$	V
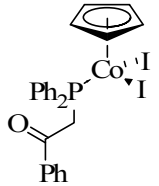	**3**	$[(\eta^5\text{-}C_5H_5)CoI_2\{Ph_2PCH_2C(O)Ph\}]$	V

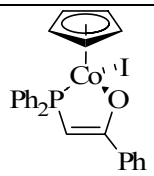	**4**	$[(\eta^5\text{-}C_5H_5)CoI\{Ph_2PCH{\cdots}C(\cdots O)Ph\}]$	V
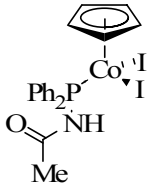	**5**	$[(\eta^5\text{-}C_5H_5)CoI_2\{Ph_2PNHC(O)Me\}]$	V
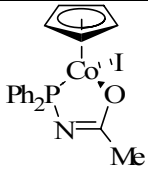	**6**	$[(\eta^5\text{-}C_5H_5)CoI\{Ph_2PN{\cdots}C(\cdots O)Me\}]$	V
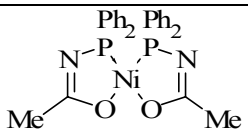	**10**	*cis*-$[Ni(Ph_2PN{\cdots}C(\cdots O)Me)_2]$	V
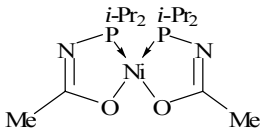	**11**	*cis*-$[Ni((^{i}Pr)_2PN{\cdots}C(\cdots O)Me)_2]$	V

Chapter I

GENERAL INTRODUCTION

Index

I.1 Catalysis: General definition

Catalysis is the process by which the rate of a chemical reaction (or biological process) is increased by means of the addition of a species known as a catalyst to the reaction. What makes a catalyst different from a chemical reagent is that whilst it participates in the reaction, is not consumed in it. That is, the catalysts may undergo several chemical transformations during the reaction, but at the conclusion of the process, the catalyst is regenerated to its initial form. As a catalyst is regenerated in a reaction, often only a very small amount is needed to increase the rate of the reaction. A catalyst works by providing an alternative reaction pathway to the reaction product. The rate of the reaction is increased as this alternative route has lower activation energy than the reaction route not mediated by the catalyst. The lower the activation energy, the faster is the rate of the reaction.

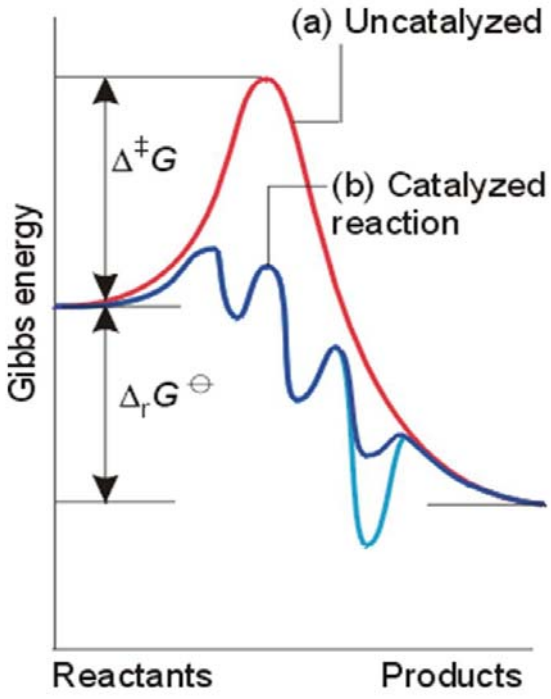

Figure I.1 Schematic representation of the energetics in a catalytic cycle. The uncatalyzed reaction (a) has a higher Gibbs energy of activation $\Delta^{\ddagger}G$ than any step in the catalyzed reaction (b). The Gibbs energy of reaction, $\Delta_r G^{\ominus}$, for the overall reaction is unchanged from (a) to (b).

Catalysis allows the production in mild conditions, in terms of pressure and temperature, of new and interesting materials.

Catalysts are classified as homogeneous if they are present in the same phase as the reagents. This normally means that they are present as solutes in a liquid reaction mixture. Catalysts are heterogeneous if they are present in a different phase from that of the reactants. Both types of catalysis are fundamentally similar. Of the two, heterogeneous catalysis has a much greater economic impact.

The importance of catalysis in industry is growing exponentially over the last decades of the 20th century.

I.2 Ethylene oligomerisation and polymerization.

The first transition metals catalysts for the polymerization of ethylene were developed by Ziegler and Natta. They were based on early transition metals such as titanium, zirconium, vanadium or chromium. These catalysts came 20 years after the discovery of ethylene polymerization. The waxy solid had been formed, by accident, by the heating of a mixture of ethylene and benzaldehyde at 170°C, during high-pressure experiments conducted in 1933 by ICI scientists Reginald Gibson and Eric Fawcett.

The commercial production of polyolefins from ethylene and propylene suffered an enormous development from the use of the Ziegler-Natta type catalysts ($TiCl_4/AlEt_3$).[1-3] Their ability to polymerize ethylene at relatively low temperatures and pressure is one of their most interesting qualities.

Efforts were made just after their discovery to obtain homogeneous models of the heterogeneous catalysts to perform mechanistic studies easily. These efforts were rewarded in 1957 when Natta and Breslow, in different research groups, showed that Et_3Al and Et_2AlCl could activate $TiCl_2(Cp)_2$ for olefin polymerization. On the other hand these homogeneous catalysts presented lower activities to ethylene polymerization than the heterogeneous ones.[4,5]

In the early 1980s, this field was remarkably renewed thanks to the work of Sinn and Kaminsky. They reported that catalysts based on group 4 metallocenes (biscyclopentadienyl derivatives), activated by partly hydrolyzed $AlMe_3$, were suited for the polymerization of both ethylene and alpha-olefins.[6,7] The discovery of the methylaluminoxane (MAO) was a great breakthrough. Its use allowed a much better control of the properties of polyethylene and

polypropylene and in some cases the improvement of the catalytic system properties. The "metallocene revolution" was part of a rapid advance in the catalysis of olefin polymerization. These new metallocene based catalysts were very different in various aspects, compared to early ones, mainly their homogenous characteristics. The increasing importance in MAO and group 4 metallocenes, followed by the development of constrained geometry catalysts such as half sandwich amide complexes, resulted in their common use in industrial processes (scheme I.1).[8, 9]

Scheme I.1 Group 4 metallocenes (A) and constrained geometry catalysts (half-sandwich) (B) (X = Halide. M = Zr, Cr).

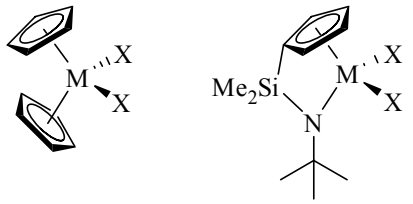

A B

Since that finding, several advances have been made in which variation of the zirconocene symmetry was found to strongly influence the resulting polyolefin microstructure.[10-14]

The extraordinary potential of these zirconocenes is not without certain limitations, they have limited temperature stability and the tendency to produce lower molecular weight materials under convenient commercial operating conditions. To solve these problems commercial and academic laboratories are developing efforts to produce more suitable coordination compounds, in which replacement of the cyclopentadienyl ligand fragment and/or the metal center is anticipated to yield increased selectivity and/or productivity.

The high oxophilicity of early transition metal catalysts (titanium, zirconium, or chromium) causes them to be poisoned by most functionalized olefins, particularly the commercially available polar comonomers, representing one of their main drawbacks. The use of late metal transition is one way to overcome this problem. Many attempts were made in this direction.

Reports on late transition metal complexes able to successfully catalyze polymerization of ethylene and alpha-olefins were scarce until twenty years ago. Even though some earlier work on nickel catalyst systems of the type employed in the Shell Higher Olefin Process (SHOP) had revealed the potential for late transition metals to polymerize ethylene, compared to early metal catalysts, late metal complexes systems had a higher rate of chain transfer. The SHOP type catalysts will be discussed later on this introduction.[15-18]

In the mid-1990s, a new type of catalysts was discovered, based on late transition metals and quite simple ligands, leading to novel polymer microstructures.[19-22] The interest in developing a new generation of "non-metallocene" catalysts was to exploit the potential of other metals in ethylene polymerization. Brookhart's Ni(II) and Pd(II) complexes, stabilized by bulky α-diimines ligands, produced grades of branched polyethylene, varying in concentration and individual branch length, starting exclusively from ethylene and accommodating even polar monomers (Scheme I.2).[20, 23-36]

In the case of the methyl precursors there is no need to use an activator, such as MAO, and the complexes can be used directly in ethylene homopolymerization. However the bis-halide derivates need a co-catalyst in order to activate them.

Scheme I.2 Alpha-diimine Ni(II) and Pd(II) catalyst precursors.

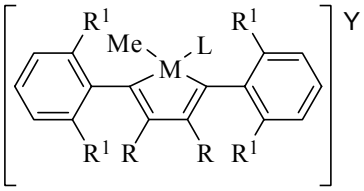

M = Ni, PD
R = Me, H, 0.5 naphthalene-1,8 diyl
R^1 = Me, ^{i}Pr
L = OEt_2
Y^- = BAr_4^-, SbF_6^-

The discovery of new ligand systems and activators has contributed to overcome this gap and make late transition metal catalysts as efficient as metallocenes and even more versatile.

Due to their enhanced functional group tolerance, such later transition metal systems also offered the commercially attractive possibility of being able to incorporate polar comonomers into polyolefin materials, to produce modified surface properties at low levels of comonomer incorporation, to change the bulk properties of the polyolefin at the higher levels

of incorporation, or to provide a low temperature/pressure route to existing materials such as ethylene-vinyl acetate (EVA) copolymer.

In 1998 a new class of neutral Ni(II) complexes stabilized by salicylaldiminato ligands was independently reported by Johnson[37] and Grubbs(Scheme I.3).[38-41]

The properties of these precursors can be tuned by varying the nature and size of their substituents, allowing for a wide range of polyethylene types, from moderately branched to linear. These systems are usually activated by Lewis-acid co-catalysts such as $B(C_6F_5)_3$ or $B(PPh)_3$.

Scheme I.3 Salicylaldiminato nickel(II) catalysts for ethylene homo- and copolymerization.

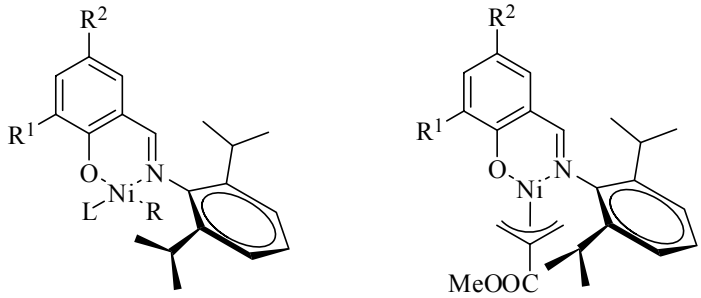

Iminocarboxamides allow for the production of high molecular weights polymers with a narrow molecular weight distribution (scheme I.4).[42, 43]

Scheme I.4 α-iminocarboxamide

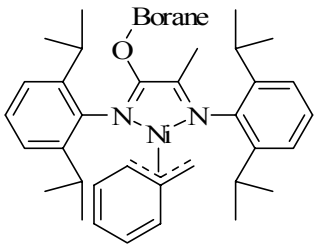

In the same year, Brookhart, Bennett and Gibson independently discovered that five-coordinate 2,6-bis(arylimino)pyridyl Fe(II) and Co(II) dihalides, activated by MAO, are effective catalysts for the conversion of ethylene either to high-density polyethylene or to alpha-olefins with Schulz–Flory[44-46] distribution (scheme I.5). These new types of catalysts showed an activity as high as the most efficient metallocenes.[47-52]

Scheme I.5 General structure of the 2,6-bis(imino)pyridyl Fe(II) or Co(II) dihalides used by Brookhart and Gibson for ethylene polymerization/oligomerization on activation with MAO.

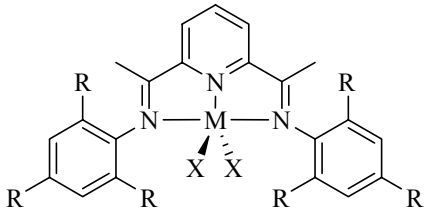

M = Co, Fe
X = Cl, Br
R = alkyl, aryl groups

There is considerable current academic and industrial interest in catalytic ethylene oligomerization, in particular for the production of linear a-olefins in the C4–C10 range whose demand is growing fast. The need for identifying and fine-tuning the parameters which influence the activity and selectivity of metal catalysts is generating much effort at the interface between ligand design, coordination/organometallic chemistry and homogeneous catalysis.

Developments similar to that of ethylene polymerisation catalysts have been experienced for the alpha-olefins catalysts. Originally linear alpha-olefins were produced by the Ziegler (Alfen) process which consists of a controlled oligomerisation of ethylene in the presence of $AlEt_3$ at 90–120 ◦C at a monomer pressure of 100 bar.[53-55]

However well-defined late transition metals such as Ni(II) and Pd(II) in conjunction with chelating ligands, such as diimine or salicyl imino, Fe(II) di-halides complexed with 2,6-bis(organylimino)pyridines and Co(II) di-halides, complexed with iminopyridines constitute a valid and, in some cases, better alternative.[22, 56-62]

I.3 Catalysts bearing α-diimine ligands

Metal complexes active in polymerization, must have suitable ligands in order to accomplish four important roles:

1) Control over the metal coordination number.

2) Control over the metal coordination geometry.

3) Control over the formal oxidation state of the metal.

4) Steric protection of the active site and influence over (stereo) selectivity.

A large variety of ligands has been used in catalytic reactions. Changing the nature and characteristics of the ligands allows tuning of the catalysts proprieties. One of the most employed ligands are the sterically demanding α-diimines[63].

α-diimines can be divided on two main groups: firstly the R-DAB (DAB = 1,4-diaza-1,3-butadienes) and secondly R-BIAN (R-BIAN = bis(aryl)acenaphthenequinonediimine) having an acenaphthene backbone (Scheme I.6). R can be a wide variety of organic substituents, mostly substituted aryl.

Scheme I.6 DAB = 1,4-diaza-1,3-butadienes and R-BIAN = bis(aryl)acenaphthenequinonediimine

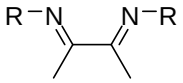

R-DAB

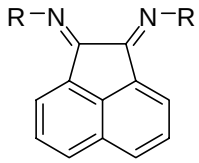

R-BIAN

The first reports of R-DAB metal complexes were done by Krumholz back in 1953. He described the synthesis of some ferrous complexes of general formula $[Fe(Me\text{-}DAB)_3]I_2$.

Molecules containing the 1,4-diaza-1,3-butadiene skeleton have attracted much interest because of both their versatile coordination behavior and the interesting properties of

their metal complexes. In particular, extensive chemistry has been carried out with 2,2'-bipyridine and phenanthroline, which are both known to coordinate to metal centers in the chelate bonding mode.

The coordination chemistry of the most simple representative of this class of compounds: the 1,4-diaza-1,3-butadienes, RN=CR'-CR''=NR, has been extensively studied. These compounds are particularly fascinating since they have a flexible N=C-C=N skeleton, they appear to have unusual electron donor and acceptor properties as compared to the above mentioned bidentate nitrogen donors, and they can potentially act in a variety of coordination modes.

R-DAB species are very versatile ligands, due to the fact that these ligands are strong sigma-donor and pi-acceptor and the possibility to change the R substituents allows the modification of both the electronic and the steric properties in a sensible way.

In comparison to most diimine ligands, BIAN derivates are more rigid. This rigidity imposes both the correct geometry for coordination and most of all imparts a high chemical stability with respect to hydrolysis and rupture of the C-C central bond. The latter is a common problem with most diimine ligands and prevents their use for many catalytic systems when long catalyst life times are a requisite, as is always the case for industrial applications.

It is possible to easily change the backbone and *N*-substituents of both R-DAB and R-BIAN ligands, allowing for the control of the steric and electronic effects at the metal centre.

α-diimines are well known to form stable complexes with transition metal and a large number of late transition metal complexes bearing α-diimine[63] ligands have been extensively studied in the commercial production of polyolefin from ethene and propene.[20-22, 64-72] Recently some results in the insertion polymerization of ethylene have been reported using tetrahedral Co(II) complexes with related ligands.[58, 73, 74]

Most complexes bearing α-diimine ligands are prepared by simply mixing a metal salt with the respective ligand in an equimolar stoichiometry. (Scheme I.7)

Scheme I.7 Reaction of α-diimines ligands with late transition metals.

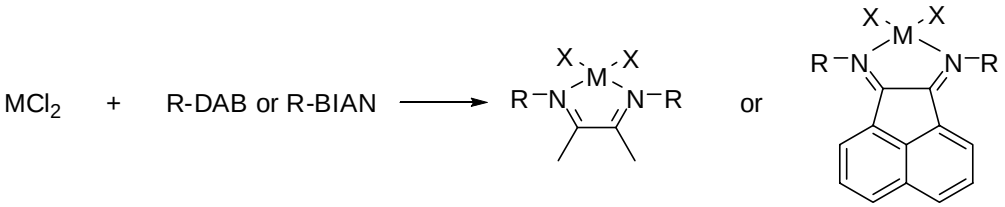

M = Cu, Co, Zn, Pd, Ni etc...
R = Ar, naphthyl
X = Cl, I, Br

Some R-DAB and R-BIAN ligands are either not know as free molecules or have only a very limited stability. For the R-BIAN ligands the synthesis of complexes by an *in situ* preparation is a well known approach also known as the "template method" (scheme I.8).

Scheme I.8 Template method

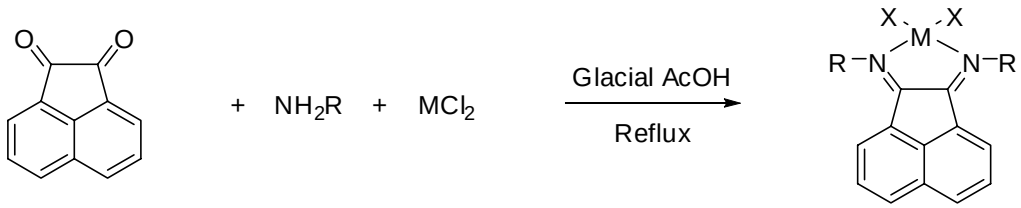

This method is now used to prepare asymmetric alpha-diimines ligands since the demetallation of the complex is simple to perform.

Given the high importance that bidentate chelating nitrogen ligands have shown in homogeneous catalysis,[75-78] they have been the subject of different studies regarding the relative binding strengths,[79-81] as well as their reactivity with main group metals.[82, 83] The effect of steric hindrance on the most stable complex has been examined for some R-DAB complexes,[63, 84-86] but electronic effects were not investigated.

Compounds of the Ar,Ar-BIAN family (Ar,Ar-BIAN = bis(aryl)-acenaphthenequinonediimine) have been known for some time,[87, 88] but have been brought to

the general attention only in recent years by Elsevier and his group.[89] Since then, they have found widespread use as ligands especially for palladium, ruthenium and nickel and the corresponding complexes have been employed as catalysts for a wide variety of reactions, such as alkene hydrogenation,[90] polymerization,[20, 33, 91] aziridination, and cyclopropanation (Scheme I.9),[92] alkene–CO copolymerization (Scheme I.10),[93] alkyne coupling in the presence of halogens or organic halides and tin compounds[94, 95] (Scheme I.11) or just tin compounds (Scheme I.13),[96] selective hydrogenation of alkynes to alkenes (Scheme I.12),[97] allylic aminations of olefins by nitroarenes in the presence of CO (Scheme I.14),[98-100] the synthesis of pyrroles and oxazines from dienes, nitroarenes and CO (Scheme I.14),[100] the reduction of nitroarenes to anilines by CO/ H2O (Scheme I.15),[101, 102] the cross-coupling reaction between organic halides and organomagnesium, -zinc, and -tin reagents,[103-105] the Suzuki–Miyaura cross coupling (Scheme I.16),[106] the synthesis of 4-quinolones and 2,3-dihydroquinolones from 2′-nitrochalcones and CO (Scheme I.17),[107-109] the synthesis of indoles from o-nitrostyrenes and CO (Scheme I.19),[110] and the Heck arylation of olefins (Scheme I.18).[111] For some of these syntheses, the use of the Ar,Ar-BIAN ligands was instrumental in achieving high performance of the catalytic system.

Scheme I.9 Aziridination and Cyclopropanation of Styrene with Cu^{+}.

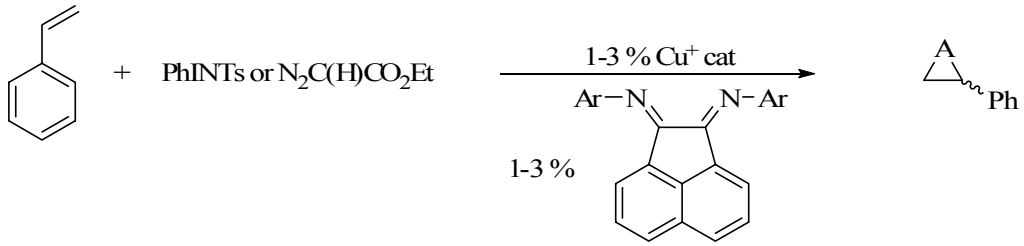

Scheme I.10 Alkene–CO copolymerization.

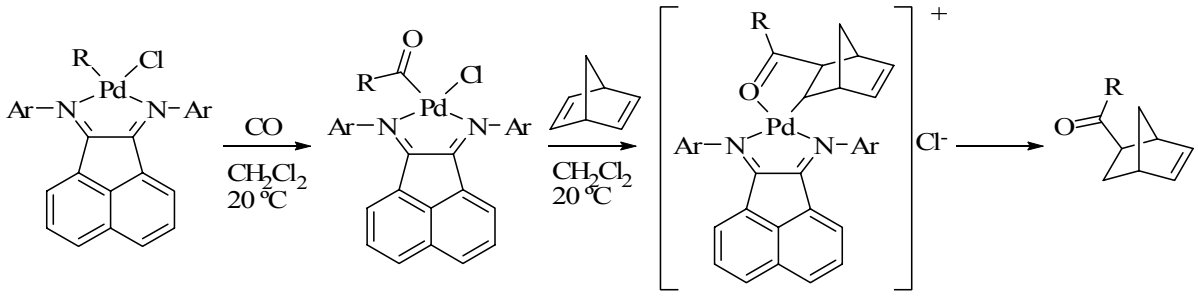

R = Me, Et, *i*-Pr, Ph

Scheme I.11 Alkyne coupling in the presence of halogens or organic halides and tin compounds.

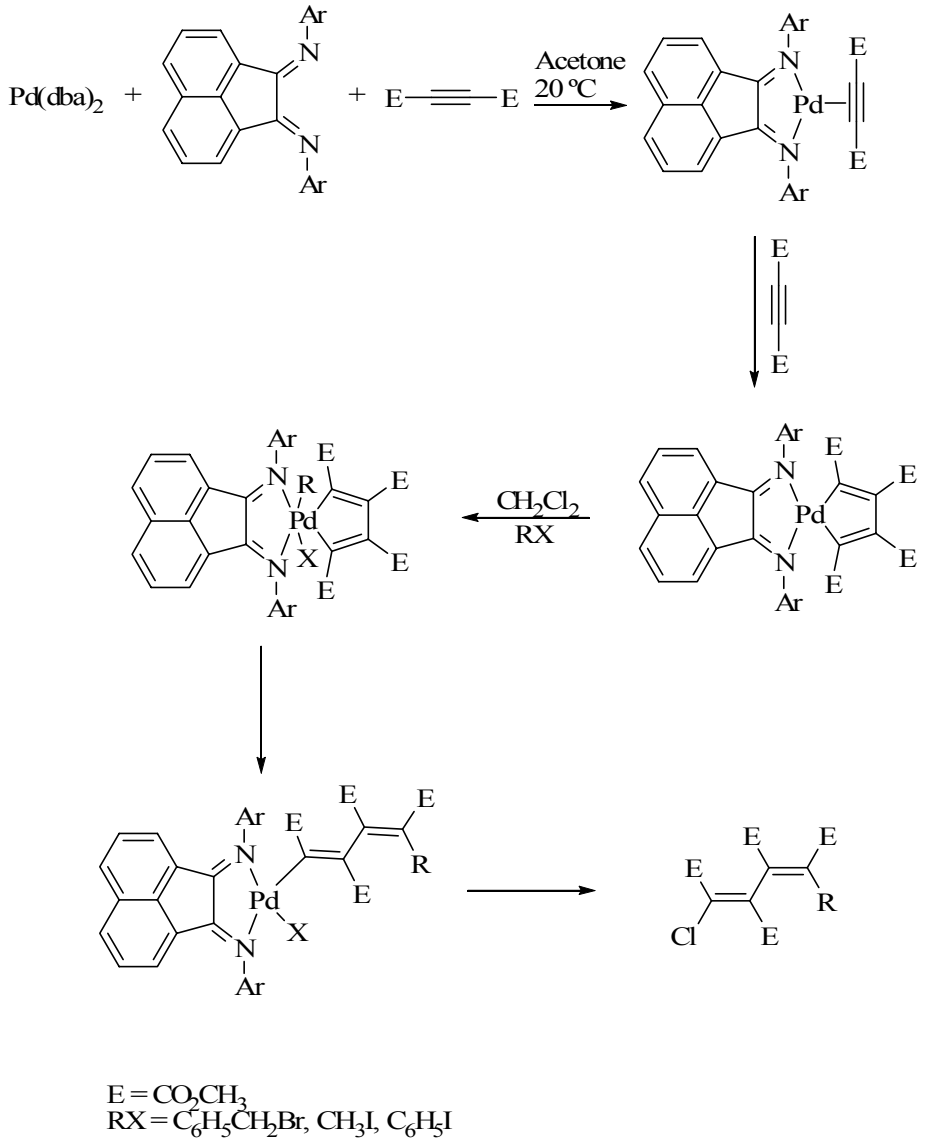

Scheme I.12 Selective hydrogenation of alkynes to alkenes.

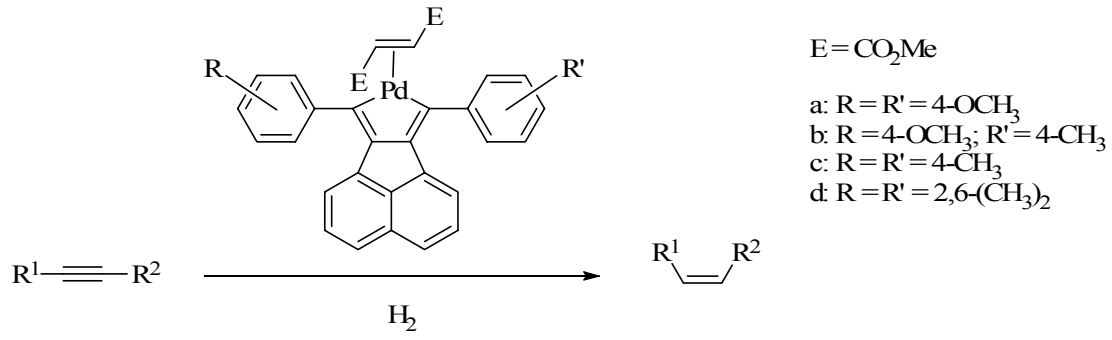

Scheme I.13 Alkyne coupling in the presence of tin compounds.

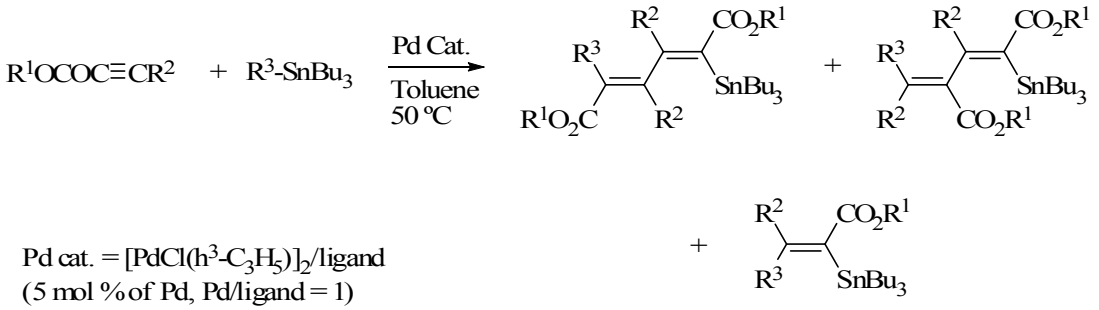

Ligands

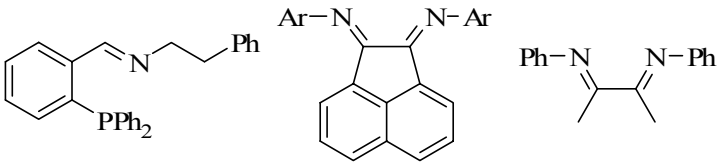

Scheme I.14 **1**) Allylic aminations of olefins by nitroarenes in the presence of CO. **2)** The synthesis of pyrroles and oxazines from dienes, nitroarenes and CO.

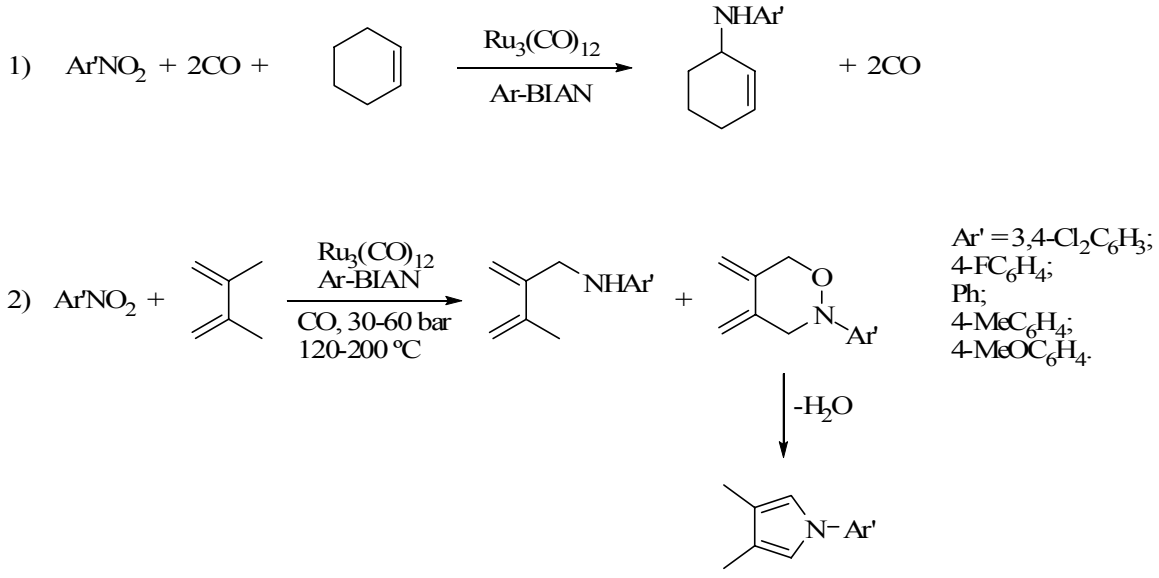

Scheme I.15 The reduction of nitroarenes to anilines by CO/ H_2O.

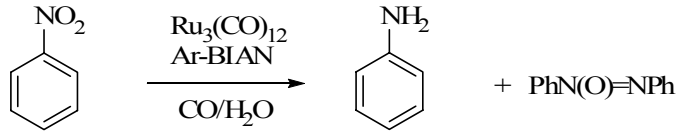

Scheme I.16 The Suzuki–Miyaura cross coupling.

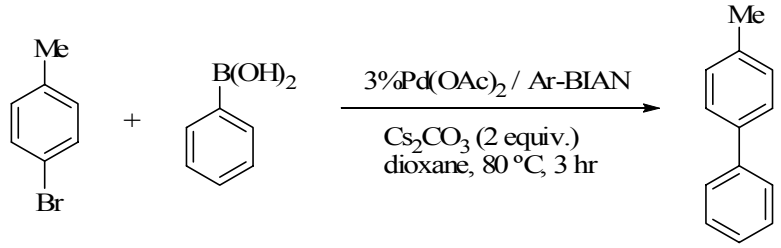

Scheme I.17 The synthesis of 4-quinolones and 2,3-dihydroquinolones from 2′-nitrochalcones and CO.

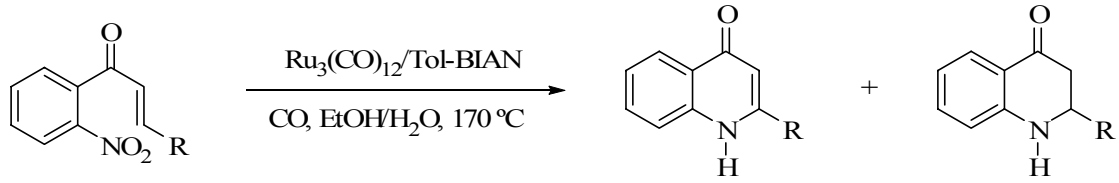

Scheme I.18 Heck arylation of olefins.

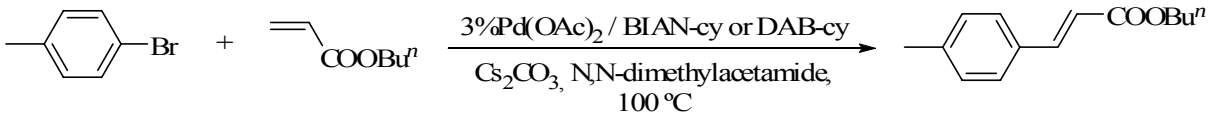

Scheme I.19 The synthesis of indoles from o-nitrostyrenes and CO.

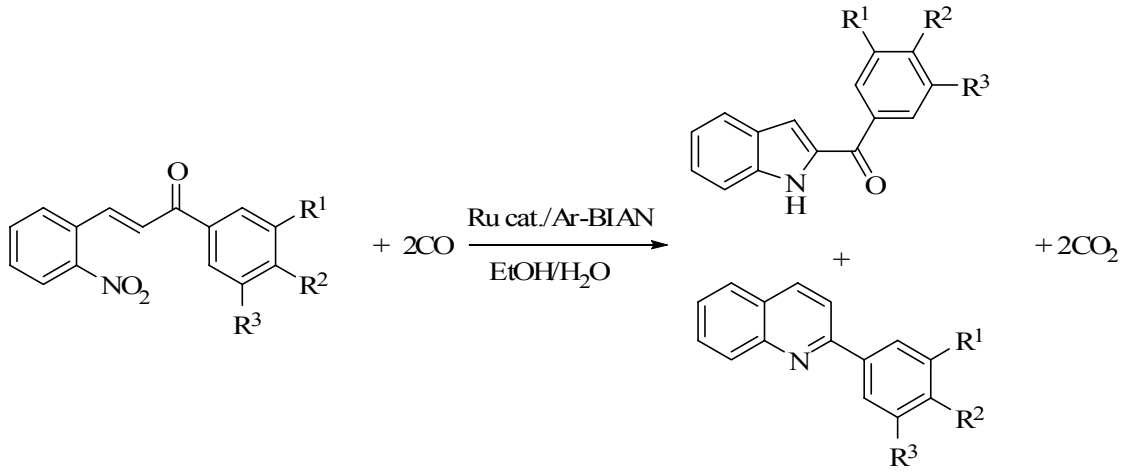

I.4 Catalysts bearing P,O type ligands

The use of late transition-metal complexes as single-site ethylene-oligomerisation and -polymerisation catalysts, by Keim in the early 70's, in a process known as SHOP (Shell Higher Olefins Process), was one of the most important achievements in homogeneous catalysis.[15-18] The catalyst was obtained through oxidative-addition of ketophosphorus ylides of type 1 to Ni(0) complexes such as [Ni(COD)$_2$], in the presence of a two-electron donor phosphine ligand, which leads to the migration of a phenyl group from phosphorus to nickel (Scheme I.20).[112, 113]

Scheme I.20 Synthetic route to SHOP type catalysts.

Since this discovery, the search for active complexes of functional phosphines became a subject of increasing interest as shown by the reviews recently published which illustrates

the importance of P, O chelating ligands in obtaining efficient catalyst for the oligomerisation and polymerization of ethylene.[114, 115]

There are different synthetic roots to the P,O phosphanylenolato chelating ligands, some of them rely in the synthesis of functional phosphines, by this we mean phosphine ligands which contain an additional functional group, capable of coordinating to a metal centre (Scheme I.21).

Scheme I.21 Example of one synthetic way to functional phosphines.

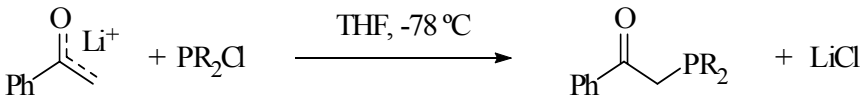

A great effort has been made throughout the years, in the synthesis of P, O ligands and their complexation to different transition metals, in order to understand the structural properties and the mechanisms for the catalytic reactions. In the case of the ligand (diphenylphosphino)acetophenone, Ph_2PCH_2COPh, Pd(II) complexes were obtained in which the ligand can behave as monodentate through the P atom or chelate through P atom and the keto group.[116] Some complexes with these P,O type of ligands and Co(II) and Co(III) were synthesized,[117, 118] as well as with Ni(II) and Pd(II).[119]

P, O chelating ligands can be modified by substituting the chelate backbone, which can be done by introducing electron withdrawing substituents in the phosphanylenolates[120] or by changing the phosphorous substituents, examples of good catalyst for the polymerization and oligomerization of ethylene are Ni(II) and Pd(II) complexes containing the bidentate phenacyldiarylphosphine ligands.[121]

In the chelate backbone of the P,O ligand we can substitute a C atom in the 5 member cycle by a N atom, in this case we obtain amide derived ligands $Ph_2PN(R)C(O)Me$ (R = H, CH_3)[122] and $Ph_2PN(H)C(O)R$ (R = Ph, NH_2, and 3-pyridyl)[123, 124] (Scheme I.22).

Scheme I.22 Amide derived ligands $Ph_2PN(R)C(O)Me$ (R = H, CH_3) and $Ph_2PN(H)C(O)R$ (R = Ph, NH_2, and 3-pyridyl).

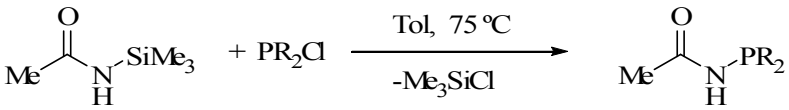

Acetamido derived ligands $Ph_2PNHC(O)Me$ acting as dissymmetric P,O chelate when complexated to palladium(II) gave stepwise ethene and/or methylacrilate/CO insertion into the Pd-C bond of Pd(II) cationic complexes.[125] Several structural studies of the $Ph_2PNHC(O)Me$ ligand and some of its complexes with Pd(II) have been performed.[126]

The synthesis of molybdenum arene complexes containing amide-derived heterodifuntional P,O ligands was investigated and the first example of a structurally characterized phosphinoiminolate complex was reported $Mo(\eta^3\text{-}C_3H_5)(\eta^6\text{-}C_6H_6)\{Ph_2PNHC(O)CH_3\text{-}\kappa^2\ P,O\}][PF_6]$.[127] Complexes of rhodium(I) containing the P,O ligand $PPh_2NHC(O)Me$ or its anion $[PPh_2N\text{-}C(\text{-}O)Me]^-$ were synthesized and structurally characterized in which mono or bidentate modes of the P,O ligand were found.[128] Monocyclopentadienyl complexes of Nb, Ta and W containing the P,O ligands $Ph_2PCH_2C(O)Ph$ and $Ph_2PCH_2C(O)NPh_2$ have been obtained and structurally characterized.[129] The bis-chelated palladium phosphino-iminolate complex $[Pd(dmba)\text{-}\{\kappa^2\ P,O\text{-}PPh_2N\text{-}C\text{-}(\text{-}O)CH_3\}]$ (dmba = ortometalateddemethylbenzylamine) has shown to behave as a metalloligand with electrophilic complexes of Cu, Ag and Au to form heterodi- or polynuclear complexes through metal coordination at the sp^2-hybridized nitrogen atom of the P,O-chelate.[130]

I.5 References

1. K. Ziegler, E. Holzkamp, H. Martin and H. Breil, *angew. Chem.*, 1955, **67**, 541.
2. K. Ziegler, E. Holzkamp, H. Breil and H. Martin, *Angew. Chem.*, 1955, **67**, 426.
3. G. Natta, *Angew. Chem.*, 1956, **68**, 393.
4. G. Natta, P. Pino, G. Mazzanti and U. Giannini, *J. Am. Chem. Soc.*, 1957, **79**, 2975.
5. D. S. Breslow and N. R. Newburg, *J. Am. Chem. Soc.*, 1957, **79**, 507.
6. W. Kaminsky, M. Miri, H. Sinn and R. Woldt, *Macromol. Rapid. Commun.*, 1983, **4**, 417.
7. in *Metalorganic Catalysts for Synthesis and Polymerization*, ed. W. Kaminsky, Springer Verlag, Heidelberg, Editon edn., 1999.
8. W. Kaminsky, *Macromol. Chem. Phys.*, 1996, **197**, 3907.
9. H. H. Brintzinger, D. Fischer, R. Mulhaupt, B. Rieger and R. Waymouth, *Angew. Chem.*, 1995, **34**, 1143.
10. A. L. McKnight and R. M. Waymouth, *Chem. Rev.*, 1998, **98**, 2587-2598.
11. J. A. Ewen, *Journal of the American Chemical Society*, 1984, **106**, 6355-6364.
12. W. Kaminsky, K. Kulper, H. H. Brintzinger and F. R. W. P. Wild, *Angewandte Chemie-International Edition in English*, 1985, **24**, 507-508.
13. J. A. Ewen, M. J. Elder, R. L. Jones, L. Haspeslagh, J. L. Atwood, S. G. Bott and K. Robinson, *Makromolekulare Chemie-Macromolecular Symposia*, 1991, **48-9**, 253-295.
14. G. W. Coates and R. M. Waymouth, *Science*, 1995, **267**, 217-219.
15. R. Bauer, H. Chung, K. W. Barnett, P. W. Glockner and W. Keim, *Shell Oil Company*, 1972, US 3 686 159.
16. R. Bauer, H. Chung, P. W. Glockner and W. Keim, 1972, (Shell Oil Co.) US-3635937.
17. D. M. Singleton, P. W. Glockner and W. Keim, 1974, (Shell Int. Res.) GB-1364870.
18. W. Keim, F. H. Kowaldt, R. Goddard and C. Krüger, *Angew. Chem. Int. Ed.*, 1978, **17**, 466-467.
19. *Late Transition Metal Polymerization Catalysis*, Wiley-VCH, Weinheim, 2003.
20. S. D. Ittel, L. K. Johnson and M. Brookhart, *Chem. Rev.*, 2000, **100**, 1169-1203.
21. G. J. P. Britovsek, V. C. Gibson and D. F. Wass, *Angew. Chem., Int. Ed.*, 1999, **38**, 428-447.
22. V. C. Gibson and S. K. Spitzmesser, *Chem. Rev.*, 2003, **103**, 283-315.

23. L. K. Johnson, C. M. Killian and M. Brookhart, *J. Am. Chem. Soc.*, 1995, **117**, 6414-6415.
24. L. K. Johnson, S. Mecking and M. Brookhart, *J. Am. Chem. Soc.*, 1996, **118**, 267-268.
25. C. M. Killian, D. J. Tempel, L. K. Johnson and M. Brookhart, *J. Am. Chem. Soc.*, 1996, **118**, 11664-11665.
26. C. M. Killian, L. K. Johnson and M. Brookhart, *Organometallics*, 1997, **16**, 2005-2007.
27. S. Mecking, L. K. Johnson, L. Wang and M. Brookhart, *J. Am. Chem. Soc.*, 1998, **120**, 888-899.
28. S. A. Svejda, L. K. Johnson and M. Brookhart, *J. Am. Chem. Soc.*, 1999, **121**, 10634-10635.
29. L. H. Shultz and M. Brookhart, *Organometallics*, 2001, **20**, 3975-3982.
30. D. Leatherman Mark, A. Svejda Steven, K. Johnson Lynda and M. Brookhart, *J. Am. Chem. Soc.*, 2003, **125**, 3068-3081.
31. A. C. Gottfried and M. Brookhart, *Macromolecules*, 2003, **36**, 3085-3100.
32. D. P. Gates, S. K. Svejda, E. Onate, C. M. Killian, L. K. Johnson, P. S. White and M. Brookhart, *Macromolecules*, 2000, **33**, 2320-2334.
33. D. J. Tempel, L. K. Johnson, R. L. Huff, P. S. White and M. Brookhart, *Journal of the American Chemical Society*, 2000, **122**, 6686-6700.
34. L. H. Shultz, D. J. Tempel and M. Brookhart, *Journal of the American Chemical Society*, 2001, **123**, 11539-11555.
35. A. C. Gottfried and M. Brookhart, *Macromolecules*, 2001, **34**, 1140-1142.
36. L. K. Johnson, C. M. Killian, S. D. Arthur, J. Feldman, E. McCord, S. J. McLain, K. A. Kreutzer, A. M. A. Bennett, E. B. Coughlin, S. D. Ittel, A. Parthasarathy, D. J. Tempel and M. Brookhart, 1996, DuPont WO patent 96/23010.
37. L. K. Johnson, A. M. A. Bennett, S. D. Ittel, L. Wang, A. Parthasarathy, E. Hauptman, R. D. Simpson, J. Feldman and E. B. Coughlin, 1998, World patent to DuPont WO 9830609.
38. C. Wang, S. Friedrich, T. R. Younkin, R. T. Li, R. H. Grubbs, D. A. Bansleben and M. W. Day, *Organometallics*, 1998, **17**, 3149-3151.
39. T. R. Younkin, E. F. Connor, J. I. Henderson, S. K. Friedrich, R. H. Grubbs and D. A. Bansleben, *Science*, 2000, **287**, 460-462.
40. D. Meinhard, M. Wegner, G. Kipiani, A. Hearley, P. Reuter, S. Fischer, O. Marti and B. Rieger, *J. Am. Chem. Soc.*, 2007, **129**, 9182-9191.
41. I. Gottker-Schnetmann, P. Wehrmann, C. Rohr and S. Mecking, *Organometallics*, 2007, **26**, 2348-2362.

42. B. Y. Lee, G. C. Bazan, J. Vela, Z. J. A. Komon and X. Bu, *J. Am. Chem. Soc.*, 2001, **123**, 5352-5353.

43. S. J. Diamanti, P. Ghosh, F. Shimizu and G. C. Bazan, *Macromolecules*, 2003, **36**, 9731-9735.

44. G. V. Z. Schulz, *Phys. Chem., Abt. B*, 1935, **30**, 379-398.

45. G. V. Z. Schulz, *Phys. Chem., Abt. B*, 1939, **43**, 25-46.

46. P. J. Flory, *J. Am. Chem. Soc.*, 1940, **62**, 1561-1565.

47. B. L. Small, M. Brookhart and A. M. A. Bennett, *J. Am. Chem. Soc.*, 1998, **120**, 4049-4050.

48. B. L. Small and M. Brookhart, *J. Am. Chem. Soc.*, 1998, **120**, 7143-7144.

49. G. J. P. Britovsek, V. C. Gibson, B. S. Kimberley, P. J. Maddox, S. J. McTavish, G. A. Solan, A. J. P. White and D. J. Williams, *Chem. Commun.*, 1998, 849-850.

50. G. J. P. Britovsek, M. Bruce, V. C. Gibson, B. S. Kimberley, P. J. Maddox, S. Mastroianni, S. J. McTavish, C. Redshaw, G. A. Solan, S. Strömberg, A. J. P. White and D. J. Williams, *J. Am. Chem. Soc.*, 1999, **121**, 8728-8740.

51. G. J. P. Britovsek, S. Mastroianni, G. A. Solan, S. P. D. Baugh, C. Redshaw, V. C. Gibson, A. J. P. White, D. J. Williams and M. R. J. Elsegood, *Chem. Eur. J.*, 2000, **6**, 2221-2231.

52. A. M. A. Bennett, 1998, (DuPont) WO Patent 98/27124.

53. J. Skupinska, *Chem. Rev.*, 1991, **91**, 613-648.

54. D. Vogt, *Applied Homogeneous Catalysis with Organometallic Compounds*, VHC, New York, 1996.

55. G. V. Parshall and S. D. Ittel, *Homogeneous Catalysis: The Applications and Chemistry of Catalysis by Soluble Transition Metal Complexes*, John Wiley and Sons, New York, 1992.

56. P. Braunstein, Y. Chauvin, S. Mercier, L. Saussine, A. DeCian and J. Fischer, *Chem. Commun.*, 1994, 2203-2204.

57. W. Keim, *Angew. Chem., Int. Ed.*, 1990, **29**, 235-244.

58. C. Bianchini, G. Mantovani, A. Meli, F. Migliacci and F. Laschi, *Organometallics*, 2003, **22**, 2545-2547.

59. C. Bianchini, G. Giambastiani, G. Mantovani, A. Meli and D. Mimeau, *J. Organomet. Chem.*, 2004, **689**, 1356-1361.

60. C. Bianchini, G. Giambastiani, I. G. Rios, G. Mantovani, A. Meli and A. M. Segarra, *Coordination Chemistry Reviews*, 2006, **250**, 1391-1418.

61. C. Bianchini, M. Frediani, G. Giambastiani, W. Kaminsky, A. Meli and E. Passaglia, *Macromolecular Rapid Communications*, 2005, **26**, 1218-1223.
62. S. Park, Y. Han, S. K. Kim, J. Lee, H. K. Kim and Y. Do, *Journal of Organometallic Chemistry*, 2004, **689**, 4263-4276.
63. G. Vankoten and K. Vrieze, *Advances in Organometallic Chemistry*, 1982, **21**, 151-239.
64. U. El-Ayaan and A. A. M. Abdel-Aziz, *European Journal of Medicinal Chemistry*, 2005, **40**, 1214-1221.
65. M. Sieger, K. Hubler, T. Scheiring, T. Sixt, S. Zalis and W. Kaim, *Zeitschrift Fur Anorganische Und Allgemeine Chemie*, 2002, **628**, 2360-2364.
66. M. Sieger, M. Wanner, W. G. Kaim, D. J. Stufkens, T. L. Snoeck and S. Zalis, *Inorganic Chemistry*, 2003, **42**, 3340-3346.
67. T. V. Laine, M. Klinga, A. Maaninen, E. Aitola and M. Leskela, *Acta Chemica Scandinavica*, 1999, **53**, 968-973.
68. M. J. Camazon, A. Alvarezvaldes, J. R. Masaguer and M. C. Navarroranninger, *Transition Metal Chemistry*, 1986, **11**, 334-336.
69. M. C. Barral, E. Delgado, E. Gutierrezpuebla, R. Jimenezaparicio, A. Monge, C. Delpino and A. Santos, *Inorganica Chimica Acta-Articles*, 1983, **74**, 101-107.
70. H. T. Dieck and M. Haarich, *Journal of Organometallic Chemistry*, 1985, **291**, 71-87.
71. B. Rieger, L. S. Baugh, S. Kacker and S. Striegler, *Late Transition Metal Polymerization Catalysis*, Weinheim, Wiley-VCH, 2003.
72. Y. Doi and T. Fujita, 1997, JP Patent 10298225 (Mitsui Chemicals Inc., Japan).
73. T. V. Laine, K. Lappalainen, J. Liimatta, E. Aitola, B. Löfgren and M. Leskelä, *Macromol. Rapid. Commun.*, 1999, **20**, 487-491.
74. M. X. Qian, M. Wang, B. Zhou and R. He, *Applied Catalysis a-General*, 2001, **209**, 11-15.
75. A. Togni and L. M. Venanzi, *Angewandte Chemie-International Edition in English*, 1994, **33**, 497-526.
76. F. Fache, E. Schulz, M. L. Tommasino and M. Lemaire, *Chemical Reviews*, 2000, **100**, 2159-2231.
77. A. K. Ghosh, M. Packiarajan and J. Cappiello, *Tetrahedron-Asymmetry*, 1998, **9**, 1-45.
78. F. Fache, B. Dunjic, P. Gamez and M. Lemaire, *Topics in Catalysis*, 1997, **4**, 201-209.
79. M. Gasperini and F. Ragaini, *Organometallics*, 2004, **23**, 995-1001.
80. M. Gasperini, F. Ragaini and S. Cenini, *Organometallics*, 2002, **21**, 2950-2957.
81. M. Gasperini, F. Ragaini, E. Gazzola, A. Caselli and P. Macchi, *Dalton Transactions*, 2004, 3376-3382.

82. I. L. Fedushkin, N. M. Khvoinova, A. Y. Baurin, G. K. Fukin, V. K. Cherkasov and M. P. Bubnov, *Inorganic Chemistry*, 2004, **43**, 7807-7815.
83. I. L. Fedushkin, V. A. Chudakova, A. A. Skatova, N. M. Khvoinova, Y. A. Kurskii, T. A. Glukhova, G. K. Fukin, S. Dechert, M. Hummert and H. Schumann, *Zeitschrift Fur Anorganische Und Allgemeine Chemie*, 2004, **630**, 501-507.
84. H. Vanderpoel, G. Vankoten and K. Vrieze, *Inorganica Chimica Acta-Articles*, 1981, **51**, 241-252.
85. H. Vanderpoel, G. Vankoten and K. Vrieze, *Inorganica Chimica Acta-Articles*, 1981, **51**, 253-262.
86. H. Vanderpoel, G. Vankoten, M. Kokkes and C. H. Stam, *Inorganic Chemistry*, 1981, **20**, 2941-2950.
87. Dvolaitz.M, *Comptes Rendus Hebdomadaires Des Seances De L Academie Des Sciences Serie C*, 1969, **268**, 1811-&.
88. I. Matei and T. Lixandru, *Bul. Ist. Politeh. Iasi*, 1967, **13**, 245.
89. R. Vanasselt, C. J. Elsevier, W. J. J. Smeets, A. L. Spek and R. Benedix, *Recueil Des Travaux Chimiques Des Pays-Bas-Journal of the Royal Netherlands Chemical Society*, 1994, **113**, 88-98.
90. R. Vanasselt and C. J. Elsevier, *Journal of Molecular Catalysis*, 1991, **65**, L13-L19.
91. S. A. Svejda and M. Brookhart, *Organometallics*, 1999, **18**, 65-74.
92. D. B. Llewellyn, D. Adamson and B. A. Arndtsen, *Organic Letters*, 2000, **2**, 4165-4168.
93. J. H. Groen, J. G. P. Delis, P. W. N. M. van Leeuwen and K. Vrieze, *Organometallics*, 1997, **16**, 68-77.
94. R. vanBelzen, H. Hoffmann and C. J. Elsevier, *Angewandte Chemie-International Edition in English*, 1997, **36**, 1743-1745.
95. R. van Belzen, R. A. Klein, H. Kooijman, N. Veldman, A. L. Spek and C. J. Elsevier, *Organometallics*, 1998, **17**, 1812-1825.
96. E. Shirakawa, H. Yoshida, Y. Nakao and T. Hiyama, *Journal of the American Chemical Society*, 1999, **121**, 4290-4291.
97. M. W. van Laren and C. J. Elsevier, *Angewandte Chemie-International Edition*, 1999, **38**, 3715-3717.
98. S. Cenini, F. Ragaini, S. Tollari and D. Paone, *Journal of the American Chemical Society*, 1996, **118**, 11964-11965.
99. F. Ragaini, S. Cenini, S. Tollari, G. Tummolillo and R. Beltrami, *Organometallics*, 1999, **18**, 928-942.

100. F. Ragaini, S. Cenini, E. Borsani, M. Dompe, E. Gallo and M. Moret, *Organometallics*, 2001, **20**, 3390-3398.

101. F. Ragaini, S. Cenini and M. Gasperini, *Journal of Molecular Catalysis a-Chemical*, 2001, **174**, 51-57.

102. F. Ragaini, S. Cenini and S. Tollari, *Journal of Molecular Catalysis*, 1993, **85**, L1-L5.

103. R. Vanasselt and C. J. Elsevier, *Organometallics*, 1992, **11**, 1999-2001.

104. R. Vanasselt and C. J. Elsevier, *Tetrahedron*, 1994, **50**, 323-334.

105. R. Vanasselt and C. J. Elsevier, *Organometallics*, 1994, **13**, 1972-1980.

106. G. A. Grasa, A. C. Hillier and S. P. Nolan, *Organic Letters*, 2001, **3**, 1077-1080.

107. S. Tollari, S. Cenini, F. Ragaini and L. Cassar, *Journal of the Chemical Society-Chemical Communications*, 1994, 1741-1742.

108. F. Ragaini, P. Sportiello and S. Cenini, *Journal of Organometallic Chemistry*, 1999, **577**, 283-291.

109. R. Annunziata, S. Cenini, G. Palmisano and S. Tollan, *Synthetic Communications*, 1996, **26**, 495-501.

110. S. Cenini, E. Bettettini, M. Fedele and S. Tollari, *Journal of Molecular Catalysis a-Chemical*, 1996, **111**, 37-41.

111. G. A. Grasa, R. Singh, E. D. Stevens and S. P. Nolan, *Journal of Organometallic Chemistry*, 2003, **687**, 269-279.

112. W. Keim, A. Behr, B. Gruber, B. Hoffmann, F. H. Kowaldt, U. Kürschner, B. Limbäcker and F. P. Sistig, *Organometallics*, 1986, **5**, 2356-2359.

113. Q. Huang, M. Xu, Y. Qian, W. Xu, M. Shao and Y. Tang, *J. Organomet. Chem.*, 1985, **287**, 419-426.

114. P. Kuhn, D. Semeril, D. Matt, M. J. Chetcuti and P. Lutz, *Dalton Transactions*, 2007, 515-528.

115. P. Braunstein, *Chemical Reviews*, 2006, **106**, 134-159.

116. S. E. Bouaoud, P. Braunstein, D. Grandjean, D. Matt and D. Nobel, *Inorg. Chem.*, 1986, **25**, 3765-3770.

117. P. Braunstein, D. G. Kelly, A. Tiripicchio and F. Ugozzoli, *Inorganic Chemistry*, 1993, **32**, 4845-4852.

118. P. Braunstein, D. G. Kelly, Y. Dusausoy, D. Bayeul, M. Lanfranchi and A. Tiripicchio, *Inorganic Chemistry*, 1994, **33**, 233-242.

119. J. Andrieu, P. Braunstein, M. Drillon, Y. Dusausoy, F. Ingold, P. Rabu, A. Tiripicchio and F. Ugozzoli, *Inorganic Chemistry*, 1996, **35**, 5986-5994.

120.P. Kuhn, D. Semeril, C. Jeunesse, D. Matt, M. Neuburger and A. Mota, *Chem.-Eur. J.*, 2006, **12**, 5210-5219.

121.J. M. Malinoski and M. Brookhart, *Organometallics*, 2003, **22**, 5324-5335.

122.P. Braunstein, C. Frison, X. Morise and R. D. Adams, *J. Chem. Soc., Dalton Trans.*, 2000, 2205-2214.

123.P. Bhattacharyya, T. Q. Ly, A. M. Z. Slawin and J. Derek Woollins, *Polyhedron*, 2001, **20**, 1803-1808.

124.T. Q. Ly, A. M. Z. Slawin and J. D. Woollins, *Polyhedron*, 1999, **18**, 1761-1766.

125.P. Braunstein, C. Frison and X. Morise, *Angew. Chem., Int. Ed.*, 2000, **39**, 2867-2870.

126.P. Braunstein, C. Frison and X. Morise, *C. R. Chimie*, 2002, **5**, 131-135.

127.N. G. Jones, M. L. H. Green, I. Vei, A. Cowley, X. Morise and P. Braunstein, *Journal of the Chemical Society-Dalton Transactions*, 2002, 1487-1493.

128.P. Braunstein, B. T. Heaton, C. Jacob, L. Manzi and X. Morise, *Dalton Transactions*, 2003, 1396-1401.

129.X. Morise, M. L. H. Green, P. Braunstein, L. H. Rees and I. C. Vei, *New Journal of Chemistry*, 2003, **27**, 32-38.

130.N. Oberbeckmann-Winter, P. Braunstein and R. Welter, *Organometallics*, 2005, **24**, 3149-3157.

Chapter II

Synthesis, solid state structures and EPR studies in polycrystalline and single crystal samples of α-diimine cobalt(II) complexes.

Published in:

V. Rosa; P. J. Gonzalez; T. Avilés; P. T. Gomes; R. Welter; A. C. Rizzi; M. C. G. Passeggi; C. D. Brondino.
Eur. J. Inorg. Chem., **2006**, 4761-4769.

Index

Synopsis

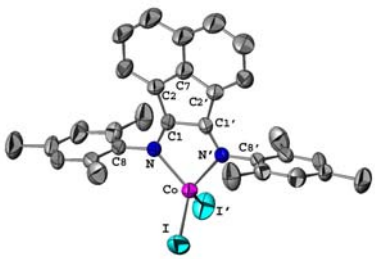

Compounds of Co(II) of general formulation CoX_2(α-diimine) where synthesized. α-Diimines are bis(aryl)acenaphthenequinonediimine) (Ar-BIAN) and 1,4-diaryl-2,3-dimethyl-1,4-diaza-1,3-butadiene (Ar-DAB). The single crystal X- ray structure of compounds[$CoCl_2$(Ph-DAB)] **1a**, [$CoCl_2$(*o,o',p*-$Me_3C_6H_2$-DAB)] **1b**, [$CoCl_2$(*o,o'-i*$Pr_2C_6H_3$-DAB)] **1c**, and [CoI_2(*o,o',p*-$Me_3C_6H_2$-BIAN)] **2'b** was determined, in all cases the cobalt atom is in a distorted tetrahedron. X-band EPR measurements in polycrystalline and single crystal samples performed on compounds **1b**, **1c** and **2'b** indicate high-spin Co(II) (S = 3/2) in an axially distorted environment.

II.1 Resumo

Compostos de cobalto de fórmula geral [CoX_2(α-diimina)], nos quais X = Cl ou I e as α-diiminas são as bis(arilo)acenaftenoquinonadiimina) (Ar-BIAN) e a 1,4-diaril-2,3-dimetil-1,4-diaza-1,3-butadieno (Ar-DAB), foram sintetizados por reacção directa a partir dos sais de cobalto $CoCl_2$ e CoI_2 com o correspondente ligando α-diimina em CH_2Cl_2 seco. Os compostos sintetizados foram [$CoCl_2$(Ph-DAB)] **1a**, [$CoCl_2$(*o*,*o'*,*p*-$Me_3C_6H_2$-DAB)] **1b**, [$CoCl_2$(*o*,*o'*-$^{i}Pr_2C_6H_3$-DAB)] **1c**, com os ligandos Ar-DAB, e [CoI_2(*o*,*o'*,*p*-$Me_3C_6H_2$-BIAN)] **2'b** com o ligando Ar-BIAN. As estruturas cristalinas dos compostos **1a**, **1b**, **1c** e **2´b** foram resolvidas por difracção de raio X de mono cristal. Em todos os casos os átomos de cobalto apresentavam uma geometria tetraédrica distorcida formada por dois haletos e pelos dois azotos do ligando α-diimina. Medidas de RPE na banda X de amostras policristalinas foram feitas com os compostos **1b**, **1c** e **2´b** mostrando um spin-alto do ião Co(II) (S = 3/2) num ambiente axial distorcido. Experiências de RPE de mono cristal dos compostos **1b** e **1c** permitiram-nos determinar a orientação do tensor ***g*** relativamente à estrutura molecular.

A minha contribuição para este trabalho consistiu na síntese de todos os compostos descritos neste trabalho assim como a sua caracterização.

II.2 Abstract

Cobalt compounds of general formula [CoX_2(α-diimine)], where X = Cl or I and the α-diimines are bis(aryl)acenaphthenequinonediimine (Ar-BIAN) and 1,4-diaryl-2,3-dimethyl-1,4-diaza-1,3-butadiene (Ar-DAB), were synthesized by direct reaction of the anhydrous cobalt salts $CoCl_2$ or CoI_2 and the corresponding α-diimine ligand in dried CH_2Cl_2. The synthesized compounds are [$CoCl_2$(Ph-DAB)] **1a**, [$CoCl_2$(*o*,*o'*,*p*-$Me_3C_6H_2$-DAB)] **1b**, [$CoCl_2$(*o*,*o'*-$^{i}Pr_2C_6H_3$-DAB)] **1c**, with the ligands Ar-DAB, and [CoI_2(*o*,*o'*,*p*-$Me_3C_6H_2$-BIAN)] **2'b** with the ligand Ar-BIAN. The crystal structures of compounds **1a**, **1b**, **1c** and **2´b** were solved by single crystal X-ray diffraction. In all cases the cobalt atom is in a distorted tetrahedron which is built by two halide atoms and two nitrogen atoms of the α-diimine ligand. X-band EPR measurements in polycrystalline samples performed on **1b**, **1c** and **2´b** compounds indicate high-spin Co(II) ion (S = 3/2) in an axially distorted environment. Single crystal EPR experiments on compounds **1b** and **1c** allowed us to evaluate the orientation of the ***g*** tensor in the molecular frame.

My contribution to this work was the synthesis of all the compounds described and their characterization.

II.3 Introduction

Cobalt is a 3d transition metal element which has been extensively studied in the last decades. Interest on cobalt compounds arises from their participation in many different processes, from industrial and technological applications as catalysts to the essential role in several biological systems of central importance in nature.[1-5]

A large number of late transition metal complexes bearing α-diimine[6] ligands have been extensively studied in the commercial production of polyolefin from ethene and propene.[7-10] However, reports on cobalt complexes containing this type of ligands are still scarce.[11-18] Recently some results in the insertion polymerization of ethylene have been reported using tetrahedral Co(II) complexes with related ligands.[19-21] α-Diimine ligands have also been the subject of different studies regarding the relative binding strengths,[22-24] as well as their reactivity with main group metals.[25, 26]

Less information exists about the magnetic properties of these types of compounds. The Co(II) ions can be present in two different spin configurations (high, $S = 3/2$ or low, $S = 1/2$), but in general they adopt the high spin configuration when they are in distorted coordination environments. A large amount of work has been directed to study the magnetic properties of Co(II) compounds in different coordination environments, some of them analyzing Co(II) in metalloproteins and compounds of biological interest.[27-34] Most of them have been focused on EPR studies in powder or frozen solutions and the evaluation of thermodynamic properties such as magnetic susceptibility and magnetization. In contrast, only few works have been devoted to study the correlation between the principal values and directions of the ***g*** tensor with the geometry of coordination in high-spin Co(II) compounds having low symmetry.[35-38] This type of information, which can be only obtained from oriented single crystal EPR experiments, is essential to understand the electronic and magnetic properties of those systems containing Co(II) ion complexes.

We report herein the synthesis and characterization of a series of Co(II) complexes of general formula $[CoX_2(\alpha\text{-diimine})]$, where X = Cl or I and the α-diimines are 1,4-diaryl-2,3-dimethyl-1,4-diaza-1,3-butadiene (Ar-DAB) or bis(aryl)acenaphthenequinonediimine) (Ar-BIAN), namely, $[CoCl_2(Ph\text{-}DAB)]$**, 1a**; $[CoCl_2(o,o',p\text{-}Me_3C_6H_2\text{-}DAB)]$**, 1b**; $[CoCl_2(o,o'\text{-}{}^{i}Pr_2C_6H_3\text{-}DAB)]$**, 1c**; $[CoI_2(o,o',p\text{-}Me_3C_6H_2\text{-}BIAN)]$**, 2'b**. The crystal structures of compounds **1a**, **1b**, **1c** and **2´b** were solved by single crystal X-ray diffraction. All compounds

with reported crystal structure (except **1a**) were studied by EPR on powdered samples. Compounds **1b** and **1c** were also studied by single crystal EPR spectroscopy. The EPR results obtained from both powder and single crystal samples were correlated with the structures of the compounds.

II.4 Results and Discussion

II.4.1 General characterization of the compounds

The reaction of equimolar quantities of CoX_2, where X = Cl or I, and α-diimine ligands in dried CH_2Cl_2 at room temperature yields crystalline solids of compounds of general formula [CoX_2(α-diimine)], in c.a. 75% to 85% yield (Scheme II.1).

Scheme II.1 Synthesised complexes

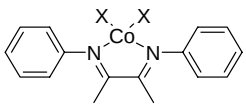

X=Cl, **1a**

[$CoCl_2$(Ph-DAB)]

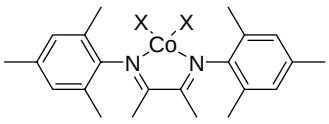

X=Cl, **1b**

[$CoCl_2$(*o,o',p*-$Me_3C_6H_2$DAB)]

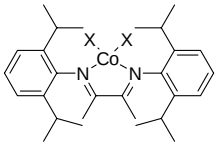

X=Cl, **1c**

[$CoCl_2$(*o,o'*-$^{i}Pr_2C_6H_3$-DAB)]

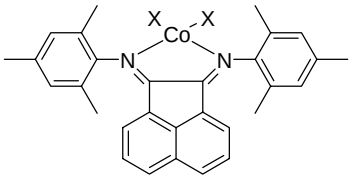

X=I, **2'b**

[CoI_2(*o,o',p*-$Me_3C_6H_2$-BIAN)]

All synthesized compounds, were characterized by elemental analyses, mass spectrometry, IR, and in some cases by EPR. The analytical data of the synthesized compounds are shown in Table II.1.

Table II.1 Analytical Data.

	Molecular mass [g mol^{-1}]; Molecular formula	MS(FAB) *m/z*[a]	Microanalysis (calc) [%] C	H	N	Colour
1a	366.15; $C_{16}H_{16}CoCl_2N_2$	$[L_1 + H^+]$ 237 (77%); $[L_1CoL_1]^{2+}$ 265.5 (100%); $[CoL_1Cl]^+$ 330 (36%); $[L_1CoL_1Cl]^+$ 566 (71%)	52.09 (52.48)	4.34 (4.40)	7.63 (7.65)	Green
1b	450.31; $C_{22}H_{28}CoCl_2N_2$	$[L_2CoCl]^+$ 414.2 (97%)	58.46 (58.68)	6.42 (6.27)	6.34 (6.22)	Green
1c	576.94; $C_{28}H_{40}CoCl_2N_2.1/2CH_2Cl_2$	$[CoL_3Cl]^+$ 498.3 (96%)	60.63 (59.33)	7.30 (7.16)	5.16 (4.86)	Green
2'b	729.30; $C_{30}H_{28}CoI_2N_2$	$[L_4 + H^+]$ 417.3 (16%); $[L_4CoI]^+$ 602.1 (30%)	49.26 (49.41)	4.16 (3.87)	3.65 (3.84)	Brown

[a] Ligand 1,4-diaryl-2,3-dimethyl-1,4-diaza-1,3-butadiene (Ar-DAB); L_1: Ar = Ph; L_2: Ar = *o,o',p*-$Me_3C_6H_2$; L_3: Ar = *o,o'* -$^iPr_2C_6H_3$; Ligand bis(aryl)acenaphthenequinonediimine (Ar-BIAN); L_4: Ar = *o,o',p*-$Me_3C_6H_2N$.

The IR spectra of the cobalt complexes recorded as Nujol mulls, display medium absorption bands in the region ν = 1652-1615 cm^{-1}, this is the absorption region for ν(C=N). Bands assigned to C=N stretching vibrations of the free ligand were observed in the region, ν = 1674-1633 cm^{-1}. The bands in the complexes are shifted to lower wave numbers, which is a criterion of the coordination of both diimine nitrogen atoms of the α-diimine ligands to the cobalt(II) ion. Selected IR absorption bands are displayed in Table II.2.

Table II.2 Selected IR data in Nujol mulls (values of ν given in cm^{-1})

	Ar-DAB*	**1**	*Ar*-BIAN*	**2'**
a	1633	1643		
b	1637	1635	1674, 1650	1621
c	1639	1641		

*free ligands

II.4.2 Crystal structures description.

*II.4.2.1 Complex **1a**.*

The complex **1a** crystallizes in an orthorhombic space group $P2_12_12_1$. An ATOMS[39] view of the asymmetric unit of the crystal structure is shown in Figure II.1. The cobalt atom is in a deformed tetrahedron which is built by two chloride atoms and two nitrogen atoms of the ligand (Co-Cl1: 2.214(1) Å; Co-Cl2 : 2.210(1) Å; Co-N1: 2.043(4) Å; Co-N2: 2.034(4) Å; Cl1-Co-Cl2: 119(1)°; N1-Co-N2: 80(1)°). The *[Co-N1-C1-C3-N2]* plane is strictly planar (maximum deviation from least-squares plane is 0.007(5) Å) and makes an angle of 56(1)° with both phenyl groups (*[C5-C10]* and *[C11-C16]*). No hydrogen bonds have been found in this crystal structure.

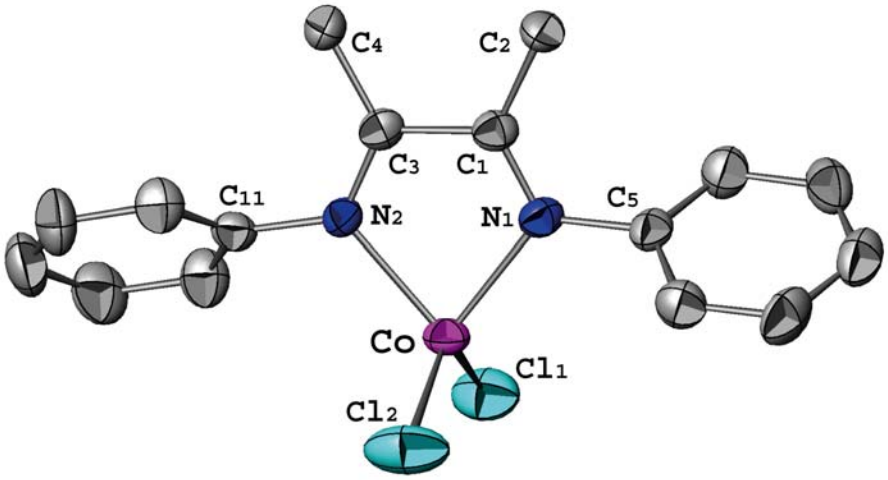

Figure II.1 Molecular structure of complex **1a** (ATOMS view) with partial labelling scheme. The hydrogen atoms are omitted for clarity. The thermal ellipsoids enclose 50% of the electronic density.

*II.4.2.2 Complex **1b**.*

The complex **1b** crystallizes in a monoclinic space group $P2_1/c$. An ATOMS view of the asymmetric unit of the crystal structure is shown in Figure II.2. In this case again, the cobalt atom is in a deformed tetrahedron (Co-Cl1: 2.224(1) Å; Co-Cl2: 2.212(1) Å; Co-N1:

2.050(3) Å; Co-N2: 2.051(3) Å; Cl1-Co-Cl2: 113(1)°; N1-Co-N2: 80(1)°). Two non classical intermolecular hydrogen bonds has been detected (PLATON software[40]) between C3 and Cl2 (H3B-CL2: 2.75(1) Å; C3-Cl2: 3.68(1) Å; C3-H3B-Cl2: 160(1)°) and C3 and Cl1 (H3C-CL1: 2.81(1) Å; C3-Cl1: 3.78(1) Å; C3-H3C-Cl1: 169(1)°). The angle between both phenyl groups is 14(1)° and these groups are quite perpendicular to the central plane *[Co-N1-C1-C2-N2]* (maximum deviation from least-squares plane is 0.035(2) Å) with angles of 88(1)° and 90(1)°, respectively.

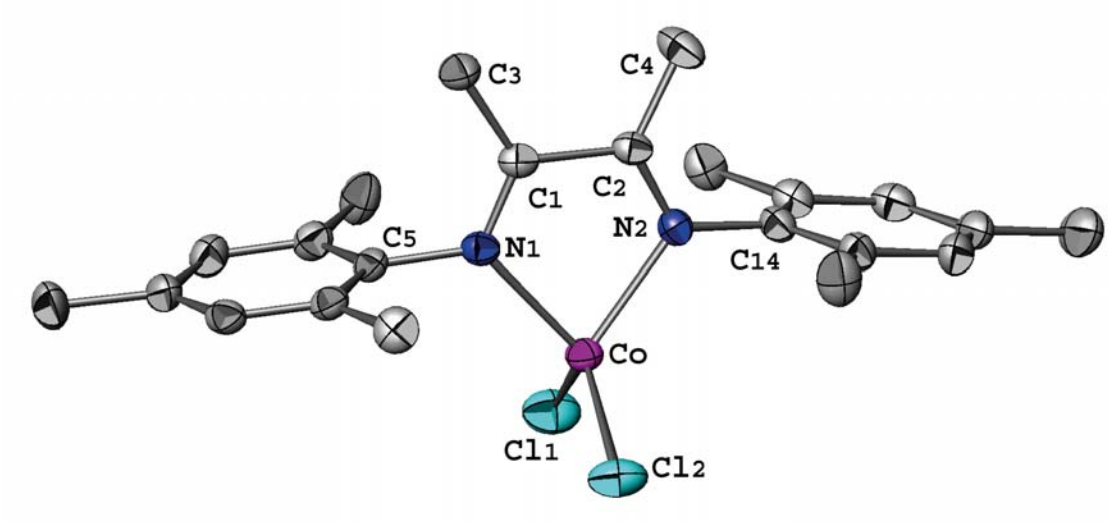

Figure II.2 Molecular structure of complex **1b** (ATOMS view) with partial labelling scheme. The hydrogen atoms and the solvent molecules (CH_2Cl_2) are omitted for clarity. The thermal ellipsoids enclose 50% of the electronic density.

*II.4.2.3 Complex **1c**.*

The complex **1c** crystallizes in an orthorhombic space group *Pnma*. An ATOMS view of the asymmetric unit of the crystal structure is shown in Figure II.3. The deformed tetrahedral site around the Co atom is characterized by the following distances and angles: Co-Cl1: 2.197(2) Å; Co-Cl2: 2.201(1) Å; Co-N: 2.050(3) Å Cl1-Co-Cl2: 113(1)°; N1-Co-N2: 80(1)°. Compare to what has been observed in both previous structures, the plane containing the Co atom is not well fitted by the least-squares planes calculation (SHELXL-97)[41] with a maximum deviation from the plane of 0.112(3) Å for both nitrogen atoms. This pseudo plane makes an angle of 87(1)° with both phenyl groups (identical by symmetry), these latter been tilted with an angle of 15(1)°, one compared to the other. At least, two non classical

intramolecular hydrogen bonds has been detected (PLATON software) between C9 and N (H9-N: 2.43(1) Å; C9-N: 2.94(1) Å; C9-H9-N: 111(1)°) and C12 and N (H12-N: 2.38(1) Å; C12-N: 2.88(1) Å; C12-H12-N: 110(1)°).

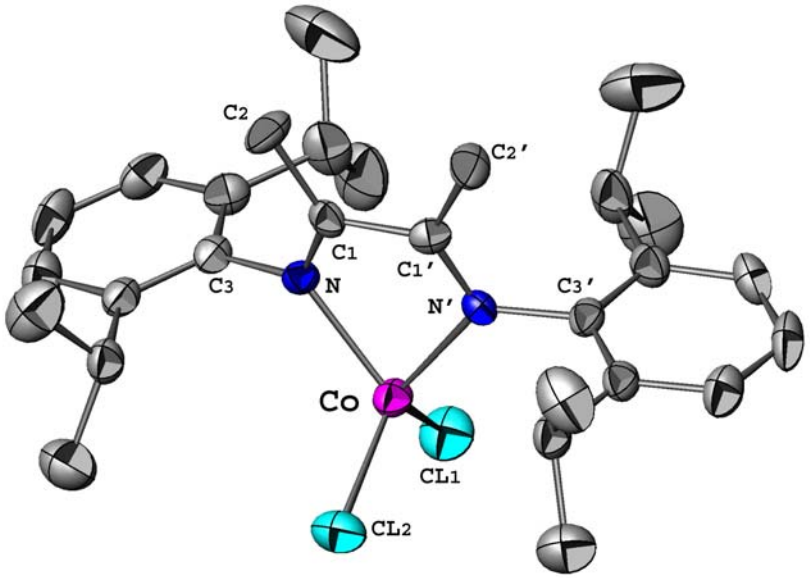

Figure II.3 Molecular structure of complex **1c** (ATOMS view) with partial labelling scheme. The hydrogen atoms are omitted for clarity. The thermal ellipsoids enclose 50% of the electronic density. Operators for generating equivalent atoms: x, y, -z+3/2.

*II.4.2.4 Complex **2'b**.*

The complex **2'b** crystallizes in an orthorhombic space group *Pcca*. An ATOMS view of the asymmetric unit of the crystal structure is shown in Figure II.4. The deformed tetrahedral site around the Co atom is characterized by the following distances and angles: Co-I: 2.509(1) Å; Co-N: 2.05(1) Å; I-Co-I': 111(1)°; N-Co-N': 82(1)°. The angle between both phenyl groups is 14(1)° and these groups make an angle of 85(1)° with the central plane *[Co-N-C1-C1'-N']* (maximum deviation from least-squares plane is 0.001(4) Å). It is important to note that the molecule of complex **2'b** is placed on a crystallographic mirror i.e. the following atoms are on the mirror (see Figure II.4)): Co, N, C8, C1, C2, C4, C5, C6, C7 and the corresponding equivalent atoms by the following symmetry operator : -x, y, -z+1/2. No H-bond has been detected in the case of this crystal structure. No H-bond has been detected in the case of this molecular structure.

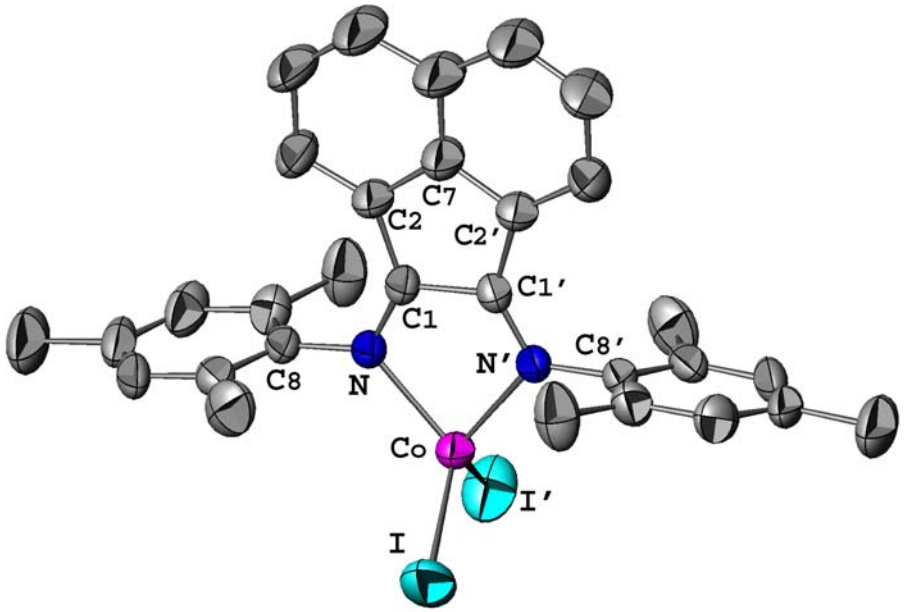

Figure II.4 Molecular structure of complex **2'b** (ATOMS view) with partial labelling scheme. The hydrogen atoms and the solvent molecules (kkk) are omitted for clarity. The thermal ellipsoids enclose 50% of the electronic density. Operators for generating equivalent atoms: -x, y, -z+1/2.

II.4.3 EPR measurements.

The X-band EPR spectra of polycrystalline samples of compounds **1b**, **1c** and **2´b** and their simulations are shown in Figure II.5. The peaks broaden at higher *T* and disappear at ~50 K. The hyperfine structure expected for the 100% abundant ^{59}Co isotope (^{59}I = 7/2) is not observed in any of the spectra of the powder samples. The values of the g-factors g_1, g_2 and g_3 are given in Table II.3 and are typical for Co(II) ions in a high spin S = 3/2 configuration.[31] The EPR spectrum obtained for compound **1a** (data not shown) is also compatible with a Co(II) ion in high spin configuration; however, a broad signal detected in the range 500-8000 Gauss and overlapped to the Co(II) ion transitions precluded the interpretation.

In a purely tetrahedral environment, Co(II) has the orbital singlet A_2 lowest,[27, 28] and since S = 3/2, there is a fourfold spin degeneracy. As for compounds **1b**, **1c**, and **2´b** the sites are distorted, the fourfold spin degeneracy is lifted into two Kramer's doublets. If the distortion is high enough (>>kT) as to separate neatly both doublets and at the low temperatures at which these experiments were performed, the observed spectra can be

assigned to transitions between the states of the lowest S' = 1/2 spin doublet, which is expected to be substantially populated.[42] The high anisotropy observed is also expected for Co(II) compounds in distorted tetrahedral coordination.[43, 44] Since the structural data do not show relevant chemical paths connecting the metal sites that could efficiently transmit exchange interactions, the principal g-values obtained from the powder spectra (Table II.3) can be considered as corresponding to isolated Co(II) ions, in which the resonance lines may be broaden by dipolar interactions. This could be the cause for the unobserved hyperfine structure in the EPR powder spectra.

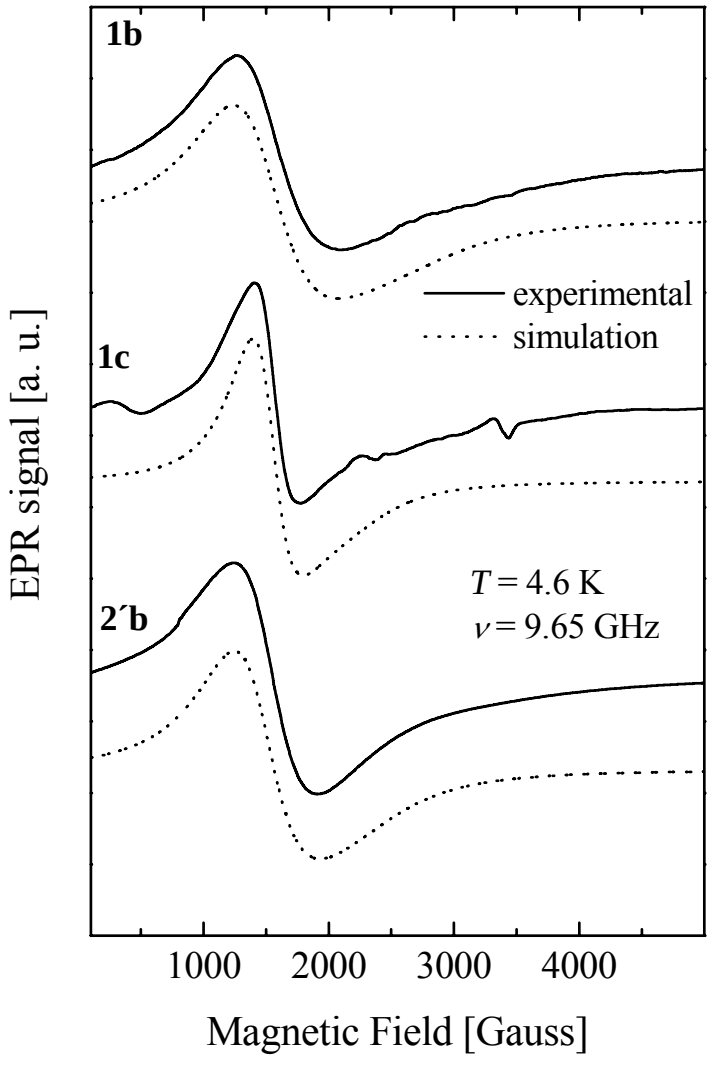

Figure II.5 EPR spectra of powdered samples of compounds **1b**, **1c**, and **2´b** together with simulations. The EPR parameters obtained from simulation are given in Table II.3. For compound **1c**, the peak at ~ 3300 Gauss correspond to Cu(II) impurities whereas the peak at ~ 500 Gauss to cavity background.

Table II.3 EPR parameters obtained from powder and single crystal samples for **1b**, **1c** and **2´b**. Linewidths (ΔB) are in Gauss. The components of the crystal ***g*** tensors are expressed in the *abc** (*c** = *a*×*b*) and *abc* coordinates system for compound **1b** and **1c**, respectively. They were obtained by least-squares analyses of the single crystal data.

Compound	**1b**	**1c**	**2´b**
powder sample			
g_1	4.83(5)	4.85(5)	4.87(5)
g_2	4.37(5)	4.35(5)	4.71(5)
g_3	2.58(9)	3.12(9)	3.08(9)
ΔB_1	580(20)	280(20)	580(20)
ΔB_2	680(20)	280(20)	480(20)
ΔB_3	900(20)	600(20)	800(20)
single crystal			
g_{aa}	2.66(2)	4.47(1)	-
g_{bb}	4.83(1)	3.12(2)	-
g_{cc}	4.32(1)	4.71(1)	-
g_{ac}	1.51(4)	0	-
g_{ab}	0	0	-
g_{cb}	0	0	-
$g_{//}$	2.58(2)	3.12(2)	3.08(9)
$g_{\perp}$	2.30(1)	2.30(1)	2.40(5)
$\frac{E}{D}$	0.03	0.04	0.01

Single crystal EPR measurements were performed on compounds **1b** and **1c**, as the size of the crystals of compounds **1a** and **2´b** were not appropriate for the EPR experiments. In order to understand the single crystal EPR experiment, it is important first to analyze the orientation of the Co sites as well as the symmetry operations relating them within the unit cell. The unit cell of compound **1b** contains four identical Co molecules, which are related by the symmetry operations of the space group $P2_1/c$ (Figure II.6a). Co1 at the general position (*x*,*y*,*z*) is related to Co2 by a C_{2b} rotation, as well as Co3 to Co4. Co1 and Co2 are related to Co3 and Co4, respectively, by an inversion. From the magnetic point of view, this compound

can be assumed as having two magnetically non-equivalent molecules per unit cell, because the Co sites related by an inversion are indistinguishable for EPR.

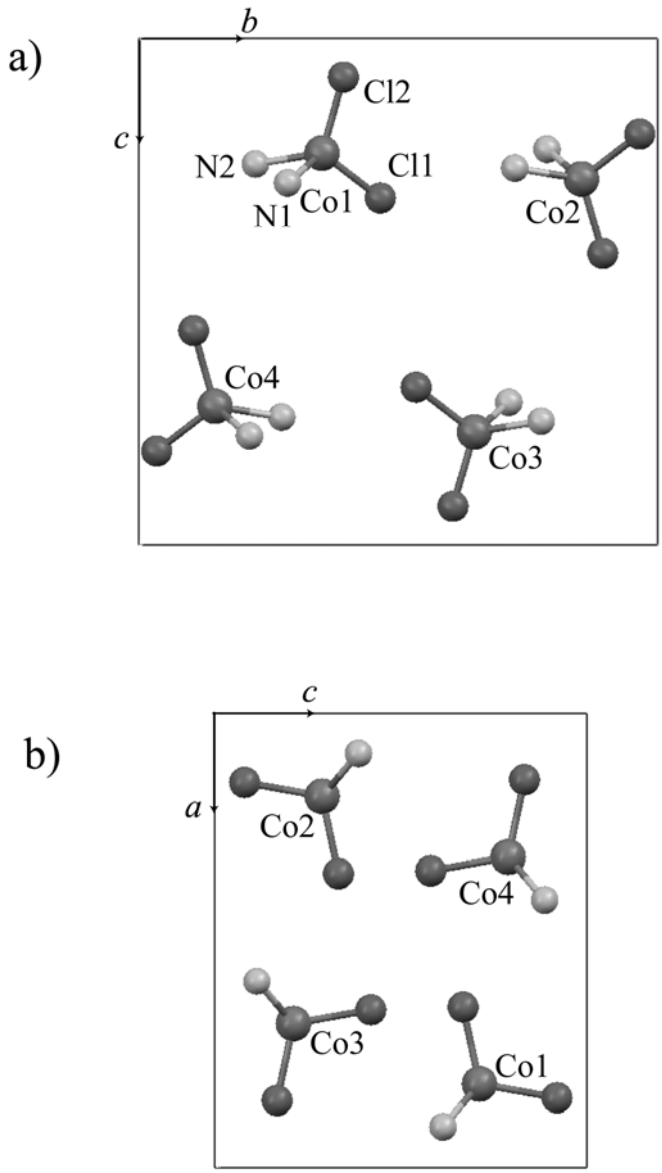

Figure II.6 (a) Projection along *a* of the four Co(II) ions and their ligands in the unit cell for compound **1b**. (b) Projection along *b* of the four Co(II) ions and their ligands in the unit cell for compound **1c**.

Compound **1c** has also four identical Co molecules in the unit cell, related by the symmetry operations of the space group P*nma* (Figure II.6b). Co1 at the special position (*x*,*1/4*,*z*) is related to Co2, Co3 and Co4 by C_{2b}, C_{2a} and C_{2c} rotations, respectively. These operations determine that there are two Co(II) ion pairs magnetically equivalent per crystal plane, and also that the four Co sites are magnetically equivalent along the crystal *a*,*b*,*c* axes. The Co molecule has a mirror plane defined by the Co(II) ion and the two Cl ligands, which is

parallel to the *ca* plane. This particular local symmetry together with the space orientation of the Co molecules in the unit cell determines that the non-equivalent pairs of Co(II) ions are equivalent in the planes *ab* and *cb.*

Single crystal EPR spectra were recorded with the magnetic field in three orthogonal crystal planes as explained in the experimental section. In all the planes and for the two compounds we observed one resonance line for all magnetic field orientations, except around the *b* axis in the orthorhombic compound **1c**. In the planes *ab* and *cb*, the signals become very broad around 90º, presumably due to non-resolved hyperfine structure and the position of the resonances in this zone could not be precisely evaluated. The position of the resonance line was obtained by least-squares fitting to a single Lorentzian line shape. Figure II.7 shows the angular variation of the g-factor as a function of the magnetic field orientation for both compounds. The data in Figure II.7 were least square fitted to a second rank tensor $g^2(\theta,\phi)$ = ***h.g.g.h***, in which ***h***=sinθcosϕ, sinθsinϕ, cosθ, is the magnetic field orientation, and ***g*** is the crystal ***g*** tensor defined as the average of the molecular ***g*** tensors of the non-equivalent Co(II) ions in the crystal lattice. The results are given in Table II.3 and were used to obtain the solid lines in Figure II.7. The overall symmetry of the evaluated ***g*** tensors follows the symmetry determined by the space group of each compound.

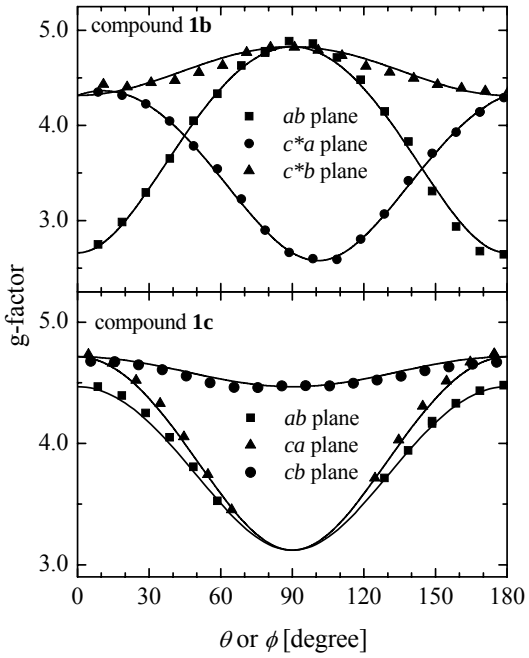

Figure II.7 Angular variation of the ***g*** factor obtained from oriented single crystal EPR measurements of compound **1b** and **1c** at 9.65 GHz and T = 4.6 K. The solid lines in both plots were calculated with the components of the $\boldsymbol{g}^2$ tensor given in Table II.3.

As discussed above, the angular variation of the g-factor in the orthorhombic compound **1c** can be associated with a single Co(II) ion in the planes *ab* and *cb*. By contrast, in the *ca* plane we would expect two resonance lines corresponding to the pairs Co1-Co2 and Co3-Co4. However, only one signal with a nearly isotropic angular variation was registered in this plane, which corresponds to the mirror Cl-Co-Cl plane. This fact can be due to either collapse by exchange interactions or resonance lines with similar g-factors. Taking into account that from the structural data we can discard the first possibility, the observed behaviour can only be explained assuming two resonance lines with similar g-factors which cannot be resolved by the EPR experiment at X-band.

The orientation of the molecular ***g*** tensor for compound **1c** in the molecular frame can be evaluated from both the analysis of the geometry of coordination of the metal site and the EPR results. One eigenvector must correspond to the *b* crystal axis (0, 1, 0) because, as explained above, the planes *ab* and *cb* are associated with a single Co(II) ion and the angular variation of the *g* factor is symmetric around the *b* crystal axis (g_3 = 3.12). Thus, the two remaining eigenvectors must be in the Cl-Co-Cl plane. The Co molecule can be considered as having a local pseudo-C_2 symmetry axis (-0.760, 0, 0.650) determined by the intersection of the Cl-Co-Cl plane (parallel to the *ca* crystal plane) and the N-Co-N plane. This C_2 symmetry axis must correspond to another eigenvector. The direction of the third eigenvector is straightforward (0.650, 0, 0.760). The orientation of the ***g*** tensor is shown in Figure II.8. This experiment allowed us to identify the eigenvalue along the *b* crystal axis, but not the remaining two eigenvalues because of the non-resolved EPR lines corresponding to the pairs Co1-Co2 or Co3-Co4. However, they should correspond to the highest g-values (4.35-4.85) of the ***g*** tensor obtained from the EPR powder spectra. This ***g*** tensor orientation is similar to that determined in the pseudo tetrahedral dichlorobis(triphenylphosphineoxide)cobalt(II).[36] This compound shows rhombic EPR spectra (g_1 = 5.67, g_2 = 3.69, g_3 = 2.16) with the two lowest g-values approximately included in the Cl-Co-Cl plane. Compound **1c** presents a nearly axial signal, with the lowest g value (g_3) lying along the normal to the Cl-Co-Cl plane. The main structural difference between both compounds is that **1c** contains the stronger N ligands instead of O ligands. Additional experimental work in a larger number of high spin Co(II) compounds with these structural characteristics is necessary to clarify whether the different EPR properties can be correlated with differences in the coordination environment of the metal ion.

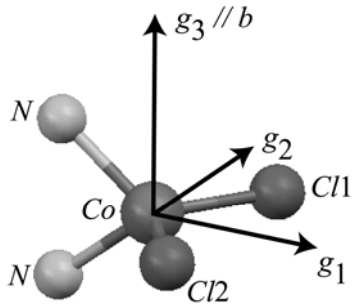

Figure II.8 Orientation of the principal axes of the ***g***-tensor for the Co(II) site in compound **1c**.

Structural data for compound **1b** show Co sites with coordination environments and space orientations similar to that of **1c**, but the local symmetry is lower (the local mirror plane cannot be defined in this case) and the Cl-Co-Cl plane is twisted near 10º from the *cb* crystal plane (Figure II.6 a) and b)). The structural similarities are reflected in Figure II.7: a nearly isotropic g-factor was obtained in the plane *c***b*, and the lowest g-value corresponds to a direction close to the normal of the Cl-Co-Cl plane. However, the fact of having non-resolved lines, in the *ab* and *cb* planes, precludes determining the ***g*** tensor associated with single Co(II) ions. Despite its lower symmetry, the coordination around Co(II) ions in both compounds shows no significant differences and we expect a ***g*** tensor orientation similar to that shown in Figure II.8 for **1b**. Although we were not able to perform single crystal EPR experiments on compounds **2´b**, the EPR data from powdered samples are similar for the three compounds. Consequently, we also expect similar ***g*** tensor orientation for the compounds in which I substitutes for Cl.

After this phenomenological assignment has been made, one is asked whether it might be possible to relate the highly anisotropic *g* factors corresponding to the effective *S'* = 1/2 of the lowest Kramer doublet with the distortions affecting the overall state of *S* = 3/2. The appropriate spin Hamiltonian within the *S* = 3/2 can be written as [Equation (1)]

$$H = \mu_B \mathbf{BgS} + \mathrm{D}\left(S_z - \frac{1}{3} S\left(S+1\right) \right) + \mathrm{E}\left(S_x^2 - S_y^2 \right) \qquad (1)$$

where D and E are the axial and rhombic ZFS parameters, respectively. The quantization axis *z* is assumed to be along the axial distortion. In principle, it is not required to assume that ***g*** will have its principal axes along any of these directions.

An effective Hamiltonian within the lowest *S*' = 1/2 (corresponding the either the originals |3/2, ±3/2> or the |3/2, ±1/2> states) Kramer doublet can be obtained under the form.[45-47]

$$H_{eff} = \mu_B \boldsymbol{B} \boldsymbol{g}' \boldsymbol{S}'$$

If the ground state is that derived from to the original |3/2, ±1/2> doublet and if one assumes now that the principal axes of ***g*** coincide with that of the axial distortion such that $g_z = g_{//}$ and $g_x = g_y = g_\perp$, one gets $g'_z = g_{//}$ while $g'_x = 2g_\perp(1-\frac{3}{2}\frac{E}{D})$ and $g'_y = 2g_\perp(1+\frac{3}{2}\frac{E}{D})$. Note that g'_x, g'_y, and g'_z correspond to g_2, g_1 and g_3, respectively, given in Table II.3. The experimental data are not consistent with assigning the ground state to that derived from original |3/2, ±3/2> doublet, in which $g'_z = 3g_{//}$ while $g'_x \sim 0$ and $g'_y \sim 0$.[48]

According with the previous discussion, adopting a coordinate system in which the *z*-axis lies along the g_3 direction (that in compound **1c** coincides with the crystal *b* axis), leads to $g'_z = g_{//}$. One can also estimate $g_\perp$ by using the other two eigenvalues obtained from the powder spectra, *e.g.* $g_\perp \cong (g'_x+g'_y)/4$. On the other hand, under the same assumptions, one gets

$$\left|\frac{E}{D}\right| = \frac{2\left|g'_x - g'_y\right|}{3\left(g'_x + g'_y\right)}$$

Table II.3 shows these parameters obtained for the three compounds using this model. The results indicate a weak rhombic distortion for all the compounds.

II.5 Conclusions

A series of cobalt(II) complexes of general formula [CoX_2(α-diimine)], **1a**, **1b**, **1c**, **2´b**, have been synthesized by direct reaction of equimolar quantities of the corresponding cobalt dihalide and the α-diimine ligand in dried CH_2Cl_2 in c.a. 75% to 85% yield. Single crystal X-ray structural data for compounds **1a**, **1b**, **1c**, and **2'b** show in all cases that the cobalt atom is in a distorted tetrahedral coordination which is built by two halide atoms and two nitrogen atoms of the α-diimine ligand. X-band EPR measurements in polycrystalline samples performed on **1b**, **1c**, and **2´b** indicate high-spin Co(II) (S = 3/2) in an axially distorted environment. The single crystal EPR experiment allowed us to determine the ***g*** tensor orientation for a low symmetry Co(II) compound. Structural and EPR results suggest similar ***g***-tensor orientations for all the compounds and the electronic properties of the Co(II) ions seem to be independent of the type of halide coordinated to the metal site.

II.6 Experimental Section

II.6.1 General Procedures and Materials

All reactions and manipulations of solutions were performed under an argon atmosphere using Schlenk techniques. Solvents were reagent grade and were dried according to literature methods. $CoCl_2$ and CoI_2 were purchased from Aldrich and the α-diimine ligands were synthesized as described elsewhere.[49-51]

II.6.2 Physical Methods

Infrared spectra were recorded as Nujol mulls on NaCl plates using a Mattson Satellite FTIR spectrometer. Elemental analyses were performed at the Analytical Services of the Laboratory of REQUIMTE. Mass spectra were recorded using a HP298S GC/MS system by the Mass Spectra Service of the Universitat Autònoma de Barcelona, Spain.

X-band CW EPR spectra of polycrystalline samples and single crystal samples were taken at 4.6 K with a Bruker EMX spectrometer using a rectangular cavity with 100 kHz field modulation, and equipped with an Oxford continuous flow cryostat. The EPR parameters of powdered samples were obtained from spectral simulations using the program Simfonia (v. 1.25, Bruker Instruments Inc.). Powder sample for EPR were obtained grinding single crystals.

The samples for the single crystal EPR measurements were oriented by gluing the *cb* and *ca* faces of **1b** and **1c**, respectively, to a cleaved KCl cubic holder, which defines a set of orthogonal laboratory axes. The habit of the crystals was determined by measuring the angles between crystal faces using a goniometric microscope. The sample holder was introduced into a 4 mm OD quartz tube, and positioned in the centre of the microwave cavity (see reference [52] for details). The tubes were attached to a goniometer and the sample was rotated in steps of 10° with the magnetic field in three crystal planes.

II.6.3 Synthesis of Complexes

*II.6.3.1 Synthesis of [$CoCl_2$(o,o',p-$Me_3C_6H_2$-DAB)], **1b***

A suspension of $CoCl_2$ (0.26 g, 2 mmol) in CH_2Cl_2 (20 mL) was treated with a yellow solution of *o,o',p*-$Me_3C_6H_2$-DAB, (0.64 g, 2 mmol) in CH_2Cl_2 (30 mL), a colour change was observed almost immediately, from a blue colour of the initial suspension to a green colour. The mixture was left stirring at room temperature for about 2 hours, until everything was dissolved. The solution was filtered, and concentrated by vacuum removal of the solvent. A green crystalline solid precipitated, which was separated by filtration, washed with diethyl ether (2×10mL) and petroleum ether (2×10mL), and then recrystallized from hot CH_2Cl_2**.** 0.76 g of **1b** were obtained (yield 85%).

Compounds **1a** and **1c** were obtained by this method. Yields obtained were between 75% and 85%. Compounds **1a**, **1b**, and **1c** are moisture sensitive.

*II.6.3.2 Synthesis of [CoI_2(o,o',p-$Me_3C_6H_2$-BIAN)], **2'b***

A green suspension of CoI_2 (0.16 g, 0.5 mmol) in CH_2Cl_2 (20 mL) was treated with a red solution of *o,o',p*-$Me_3C_6H_2$-BIAN (0.21 g, 0.5 mmol) in CH_2Cl_2 (30 mL). The mixture turned quickly to red wine colour; it was stirred over night, until everything was dissolved. After filtration of the solution the solvent was partially removed leaving a dark red solid, which was separated by filtration, washed with petroleum ether (2×10mL), and then recrystallised from CH_2Cl_2/petroleum ether. 0.29 g of **2'b** were obtained (yield 78%).

II.6.4 Crystallography

Single crystals of complexes **1a**, **1b**, **1c** and **2'b** were mounted on a Nonius Kappa-CCD area detector diffractometer (*MoKα* λ = 0.71073 Å). The complete conditions of data collection (DENZO software) and structure refinements are given below. The cell parameters were determined from reflections taken from one set of 10 frames (1.0° steps in phi angle), each at 20 s exposure. The structures were solved using direct methods (SHELXS97) and refined against F^2 using the SHELXL97 software.[41] The absorption was not corrected. All non-hydrogen atoms were refined anisotropically. Hydrogen atoms were generated according to stereo-chemistry and refined using a riding model in SHELXL97. Some disorders have been fixed for solvent molecules in the case of **1b** and **2'b** complexes (for details, see the corresponding cif files). The full labelled ORTEP views have been deposited as supplementary materials. Crystallographic data (excluding structure factors) have been deposited in the Cambridge Crystallographic Data Centre as Supplementary publication n° CCDC 297433 – 297436. Copies of the data can be obtained free of charge on application to CCDC, 12 Union Road, Cambridge CB2 1EZ, UK (fax: (+44)1223-336-033; e-mail: deposit@ccdc.cam.ac.uk).

1a Green single crystal; dimension : 0.10×0.10×0.10 mm^3; $C_{16}H_{16}Cl_2CoN_2$, *M*= 366.14 $g.mol^{-1}$; Orthorhombic; space group $P2_12_12_1$; *a* = 10.5880(4) Å ; *b* = 8.2160(3) Å ; *c* = 19.1880(9) Å; *Z* = 4; *Dc* = 1.457 $g.cm^{-3}$; μ (*MoKα*)= 1.342 mm^{-1}; a total of 14084 reflections; 2.20° < θ < 30.00°, 4806 independent reflections with 3211 having $I > 2\sigma(I)$; 191

parameters; Final results : R_1 = 0.1149; wR_2 = 0.1256, *Goof* = 1.179, Flack x ; 0.00(7), maximum residual electronic density = 0.614 $e^-.Å^{-3}$.

1b Green single crystal; dimension : 0.10×0.08×0.03 mm^3; $C_{22}H_{28}Cl_2CoN_2$, CH_2Cl_2, M = 535.22 $g.mol^{-1}$; Monoclinic; space group $P2_1/c$; a = 12.686(5) Å ; b = 14.514(5) Å ; c = 14.180(5) Å; Z = 4; Dc = 1.362 $g.cm^{-3}$; μ ($MoK\alpha$)= 1.079 mm^{-1}; a total of 9800 reflections; 2.13° < θ < 29.98°, 7555 independent reflections with 4498 having $I > 2\sigma(I)$; 268 parameters; Final results : R_1 = 0.0733; wR_2 = 0.2063, *Goof* = 1.037; maximum residual electronic density = 1.177 $e^-.Å^{-3}$.

1c Green single crystal; dimension : 0.13×0.10×0.08 mm^3; $C_{28}H_{40}Cl_2$ CoN_2, M= 534.45 $g.mol^{-1}$; Orthorhombic; space group *Pnma*; a = 10.4110(10) Å ; b = 12.707(2) Å ; c = 21.311(4) Å; Z = 4; Dc = 1.259 $g.cm^{-3}$; μ (*Mo* $K\alpha$)= 0.816 mm^{-1}; a total of 33608 reflections; 1.91° < θ < 29.83°, 3965 independent reflections with 2385 having $I > 2\sigma(I)$; 154 parameters; Final results : R_1 = 0.0614; wR_2 = 0.2027, *Goof* = 0.825, maximum residual electronic density = 0.324 $e^-.Å^{-3}$.

2'b Brown single crystal; dimension : 0.08×0.07×0.06 mm^3; $C_{30}H_{28}CoI_2N_2$, 0.2($C_4H_{10}O$), M = 744.10 $g.mol^{-1}$; Orthorhombic; space group *Pcca* ; a = 16.769(3) Å ; b = 11.676(2) Å ; c = 18.313(3) Å; Z = 4; Dc = 1.378 $g.cm^{-3}$; μ (*Mo* $K\alpha$)= 2.219 mm^{-1}; a total of 9862 reflections; 1.74° < θ < 30.04°, 5230 independent reflections with 3769 having $I > 2\sigma(I)$; 168 parameters; Final results : R_1 = 0.0710; wR_2 = 0.2249, *Goof* = 1.049, maximum residual electronic density = 1.424 $e^-.Å^{-3}$.

II.7 Acknowledgements

We thank Fundação para a Ciência e Tecnologia, Portugal, for funding (Project POCI/QUI/55519/2004) and for a Ph.D. grant (SFRH/BD/13777/2003) to V. R. and SEPCYT:PICT 2003-06-13872, CONICET PIP 02559/2000 and CAI+D-UNL in Argentina. We also thank CPU (France) and CRUP (Portugal) for the Portuguese-French Integrated Action-2006, Nº F-27/07. CDB and MCGP are members of CONICET-Argentina.

II.8 References

1. M. Kobayashi and S. Shimizu, *European Journal of Biochemistry*, 1999, **261**, 1-9.
2. R. Crabtree and M. Mingos, *Comprehensive Organometallic Chemistry III: From fundamentals to applications*, Elsevier, 2006.
3. J. J. R. F. d. Silva and R. J. P. Williams, *The Biological Chemistry of the Elements. The inorganic chemistry of life*, Clarendon Press, Oxford, 1991.
4. R. J. P. Williams and J. J. R. F. d. Silva, *The Natural Selection of the Chemical Elements*, Clarendon Press, Oxford, 1996.
5. S. J. Lippard and J. M. Berg, *Principles of Bioinorganic Chemistry*, University Science Books, Mill Valley, California, 1994.
6. G. Vankoten and K. Vrieze, *Advances in Organometallic Chemistry*, 1982, **21**, 151-239.
7. B. Rieger, L. S. Baugh, S. Kacker and S. Striegler, *Late Transition Metal Polymerization Catalysis*, Weinheim, Wiley-VCH, 2003.
8. S. D. Ittel, L. K. Johnson and M. Brookhart, *Chem. Rev.*, 2000, **100**, 1169-1203.
9. G. J. P. Britovsek, V. C. Gibson and D. F. Wass, *Angew. Chem., Int. Ed.*, 1999, **38**, 428-447.
10. V. C. Gibson and S. K. Spitzmesser, *Chem. Rev.*, 2003, **103**, 283-315.
11. M. C. Barral, E. Delgado, E. Gutierrezpuebla, R. Jimenezaparicio, A. Monge, C. Delpino and A. Santos, *Inorganica Chimica Acta-Articles*, 1983, **74**, 101-107.
12. H. T. Dieck and M. Haarich, *Journal of Organometallic Chemistry*, 1985, **291**, 71-87.
13. M. J. Camazon, A. Alvarezvaldes, J. R. Masaguer and M. C. Navarroranninger, *Transition Metal Chemistry*, 1986, **11**, 334-336.
14. Y. Doi and T. Fujita, 1997, JP Patent 10298225 (Mitsui Chemicals Inc., Japan).
15. T. V. Laine, M. Klinga, A. Maaninen, E. Aitola and M. Leskela, *Acta Chemica Scandinavica*, 1999, **53**, 968-973.
16. M. Sieger, K. Hubler, T. Scheiring, T. Sixt, S. Zalis and W. Kaim, *Zeitschrift Fur Anorganische Und Allgemeine Chemie*, 2002, **628**, 2360-2364.
17. M. Sieger, M. Wanner, W. G. Kaim, D. J. Stufkens, T. L. Snoeck and S. Zalis, *Inorganic Chemistry*, 2003, **42**, 3340-3346.
18. U. El-Ayaan and A. A. M. Abdel-Aziz, *European Journal of Medicinal Chemistry*, 2005, **40**, 1214-1221.

19. T. V. Laine, K. Lappalainen, J. Liimatta, E. Aitola, B. Löfgren and M. Leskelä, *Macromol. Rapid. Commun.*, 1999, **20**, 487-491.
20. M. X. Qian, M. Wang, B. Zhou and R. He, *Applied Catalysis a-General*, 2001, **209**, 11-15.
21. C. Bianchini, G. Mantovani, A. Meli, F. Migliacci and F. Laschi, *Organometallics*, 2003, **22**, 2545-2547.
22. M. Gasperini and F. Ragaini, *Organometallics*, 2004, **23**, 995-1001.
23. M. Gasperini, F. Ragaini and S. Cenini, *Organometallics*, 2002, **21**, 2950-2957.
24. M. Gasperini, F. Ragaini, E. Gazzola, A. Caselli and P. Macchi, *Dalton Transactions*, 2004, 3376-3382.
25. I. L. Fedushkin, V. A. Chudakova, A. A. Skatova, N. M. Khvoinova, Y. A. Kurskii, T. A. Glukhova, G. K. Fukin, S. Dechert, M. Hummert and H. Schumann, *Zeitschrift Fur Anorganische Und Allgemeine Chemie*, 2004, **630**, 501-507.
26. I. L. Fedushkin, N. M. Khvoinova, A. Y. Baurin, G. K. Fukin, V. K. Cherkasov and M. P. Bubnov, *Inorganic Chemistry*, 2004, **43**, 7807-7815.
27. A. Abragam and B. Bleaney, *Electron Paramagnetic Resonance of Transition Ions*, Clarendon Press, Oxford, 1970.
28. J. A. Weil, J. R. Bolton and J. E. Wertz, *Electron Paramagnetic Resonance. Elementary Theory and Practical Applications*, John Wiley & Sons, Inc., New York, 1994.
29. J. Zarembowitch and O. Kahn, *Inorganic Chemistry*, 1984, **23**, 589-593.
30. R. Carlin, *Magnetochemistry*, Springer, Berlin, 1986.
31. J. H. Pilbrow, *Transition Ion Electron Paramagnetic Resonance*, Clarendon Press, Oxford, 1990.
32. A. C. Rizzi, C. D. Brondino, R. Calvo, R. Baggio, M. T. Garland and R. E. Rapp, *Inorganic Chemistry*, 2003, **42**, 4409-4416.
33. A. Goni, L. M. Lezama, T. Rojo, M. E. Foglio, J. A. Valdivia and G. E. Barberis, *Physical Review B*, 1998, **57**, 246-251.
34. J. Krzystek, S. A. Zvyagin, A. Ozarowski, A. T. Fiedler, T. C. Brunold and J. Telser, *Journal of the American Chemical Society*, 2004, **126**, 2148-2155.
35. A. Bencini and D. Gatteschi, *Inorganic Chemistry*, 1977, **16**, 2141-2142.
36. A. Bencini, C. Benelli, D. Gatteschi and C. Zanchini, *Inorganic Chemistry*, 1979, **18**, 2137-2140.
37. A. Bencini, C. Benelli, D. Gatteschi and C. Zanchini, *Inorganic Chemistry*, 1979, **18**, 2526-2528.

38. L. C. Dickinson and J. C. W. Chien, *Journal of the American Chemical Society*, 1983, **105**, 6481-6487.

39. E. Dowty, 1994, ATOMS. Version 6.0. Shape Software, 521 Hidden Valley Road, Kingsport, TN 37663, USA.

40. A. L. Spek, *J. Appl. Crystallogr.*, 2003, **36**, 7-13.

41. G. M. Sheldrick, *SHELXL97, Program for the refinement of crystal structures*, University of Göttingen, Germany, 1997.

42. D. L. Pountney and M. Vasak, *European Journal of Biochemistry*, 1992, **209**, 335-341.

43. O. Y. Gavel, S. A. Bursakov, J. J. Calvete, G. N. George, J. J. G. Moura and I. Moura, *Biochemistry*, 1998, **37**, 16225-16232.

44. N. Bonander, T. Väangard, L. C. Tsai, V. Langer, H. Nar and L. Sjölin, Proteins: Structure, Function and Genetics 1997, **27**, 385-394.

45. C. A. Bates, J. M. Dixon, J. R. Fletcher and K. W. H. Stevens, *Journal of Physics Part C Solid State Physics*, 1968, **1**, 859-&.

46. K. W. H. Stevens, *Journal of Physics Part C Solid State Physics*, 1970, **3**, 2387-&.

47. M. C. G. Passeggi, *Phys. Stat. Solidi (b)*, 1972, **54**, 681-689.

48. M. T. Werth, S. F. Tang, G. Formicka, M. Zeppezauer and M. K. Johnson, *Inorganic Chemistry*, 1995, **34**, 218-228.

49. R. Vanasselt, C. J. Elsevier, W. J. J. Smeets, A. L. Spek and R. Benedix, *Recueil Des Travaux Chimiques Des Pays-Bas-Journal of the Royal Netherlands Chemical Society*, 1994, **113**, 88-98.

50. M. Svoboda and H. tom Dieck, *J. Organomet. Chem.*, 1980, **191**, 321-328.

51. H. tom Dieck, M. Svoboda and T. Greiser, *Z. Naturforsch.*, 1981, **36b**, 823-832.

52. J. M. Schveigkardt, A. C. Rizzi, O. E. Piro, E. E. Castellano, R. C. de Santana, R. Calvo and C. D. Brondino, *Eur. J. Inorg. Chem.*, 2002, 2913-2919.

Chapter III

Synthesis, characterization and solid state structures of α-diimine cobalt(II) complexes. Ethylene polymerization tests

Published in:

V. Rosa; S. A. Carabineiro; T. Avilés; P. T. Gomes; R. Welter; J.M. Campos; M.R. Ribeiro: Journal of Organometallic Chemistry, **2008**, *693*, 769-775.

Index

Synopsis

Compounds of Co(II) of general formulation [CoX_2(α-diimine)] (α-diimine = bis(aryl)acenaphthenequinonediimine or 1,4-diaryl-2,3-dimethyl-1,4-diaza-1,3-butadiene; X = Cl or I) were synthesised, characterised, and tested as ethylene polymerisation catalysts in the presence of methylaluminoxane (MAO).

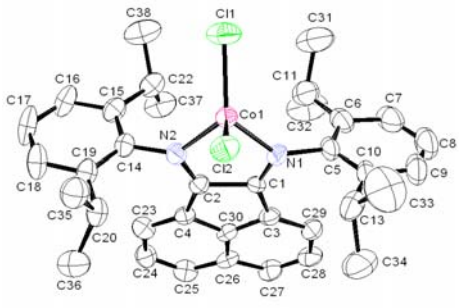

III.1 Resumo

Uma série de compostos de cobalto (II) do tipo [CoX_2(α-diimina)] foi sintetizada por reacção directa de sais anidros de $CoCl_2$ ou CoI_2 com o correspondente ligando α-diimina em CH_2Cl_2: [CoI_2(*o*,*o'*,*p*-$Me_3C_6H_2$-DAB)] (**1**), [CoI_2(*o*,*o'*-$^{i}Pr_2C_6H_3$-DAB)] (**2**), (no qual Ar-DAB = 1,4-bis(aril)-2,3-dimetil-1,4-diaza-1,3-butadieno), e [$CoCl_2$(*o*,*o'*,*p*-$Me_3C_6H_2$-BIAN)] (**3**), [$CoCl_2$(*o*,*o'*-$^{i}Pr_2C_6H_3$-BIAN)] (**4**), e [CoI_2(*o*,*o'*-$^{i}Pr_2C_6H_3$-BIAN)] (**5**) (no qual Ar-BIAN = bis(aril)acenaphthenoquinonadiimina). Todos os compostos obtidos foram caracterizados por análise elementar, IV, espectrometria de massa e difracção de raio X quando possível. As estruturas cristalinas dos compostos **2-4**, apresentaram em todos os casos, uma geometria tetraédrica distorcida do cobalto, composta pelos dois átomos haletos e pelos dois átomos de azoto do ligando α-diimina. Os compostos **3** e **4**, assim como os compostos ([$CoCl_2$(*o*,*o'*,*p*-$Me_3C_6H_2$-DAB)]) (**1a**), ([$CoCl_2$(*o*,*o'*-$^{i}Pr_2C_6H_3$-DAB)]) (**2a**), foram activados por metilaluminoxano (MAO) e testados como catalisadores para a polimerização de olefinas, mostrando uma fraca actividade catalítica. Determinadas amostras de polietileno (PE) foram caracterizadas por espectroscopias de ^{1}H RMN, ^{13}C RMN e IV, e por CDV, mostrando microestruturas ramificadas (2.5-5.5%).

A minha contribuição para este trabalho consistiu na síntese de todos os compostos descritos e sua caracterização.

III.2 Abstract

A series of cobalt(II) compounds of the type [CoX_2(α-diimine)] were synthesised by direct reaction of anhydrous $CoCl_2$ or CoI_2 and the corresponding α-diimine ligand, in CH_2Cl_2: [CoI_2(*o*,*o'*,*p*-$Me_3C_6H_2$-DAB)] (**1**), [CoI_2(*o*,*o'*-$^{i}Pr_2C_6H_3$-DAB)] (**2**), (where Ar-DAB = 1,4-bis(aryl)-2,3-dimethyl-1,4-diaza-1,3-butadiene), and [$CoCl_2$(*o*,*o'*,*p*-$Me_3C_6H_2$-BIAN)] (**3**), [$CoCl_2$(*o*,*o'*-$^{i}Pr_2C_6H_3$-BIAN)] (**4**), and [CoI_2(*o*,*o'*-$^{i}Pr_2C_6H_3$-BIAN)] (**5**) (where Ar-BIAN = bis(aryl)acenaphthenequinonediimine). All compounds were characterized by elemental analyses, IR, mass spectrometry, and X-ray diffraction whenever possible. The crystal structures of compounds **2-4** showed, in all cases, distorted tetrahedral geometries about the Co, built by two halogen atoms and two nitrogen atoms of the α-diimine ligand. Compounds **3** and **4**, as well as ([$CoCl_2$(*o*,*o'*,*p*-$Me_3C_6H_2$-DAB)]) (**1a**), and ([$CoCl_2$(*o*,*o'*-$^{i}Pr_2C_6H_3$-DAB)]) (**2a**), were activated by methylaluminoxane (MAO) and tested as catalysts for ethylene polymerization, showing low catalytic activities. Selected polyethylene (PE) samples were characterized by ^{1}H and ^{13}C NMR and FT-IR spectroscopies, and by differential scanning calorimetry (DSC), revealing branching microstructures (2.5-5.5%).

My contribution to this work was the synthesis of all the compounds described and their characterization.

III.3 Introduction

The commercial production of polyolefins from ethylene and propylene had an enormous development with the use of Ziegler-Natta type catalysts. This field has been remarkably renewed with the use of catalysts based on early-transition metallocenes.[1] In the mid-1990s, a new type of catalysts have been discovered, based on late transition metals and quite simple ligands, leading to novel polymer microstructures.[2-5] Among these ligands are the sterically demanding α-diimines.[6] These bidentate ligands are very rigid and it is possible to change easily their backbone and *N*-substituents, allowing the control of the steric and electronic effects at the metal centre. A great number of group 10 transition metal complexes bearing α-diimine ligands have been synthesized and characterized since then, and their employ as catalysts for the oligomerisation and polymerization of α-olefins have been extensively studied.[3] However, reports on cobalt complexes containing this type of ligands are scarce.[7-13] Recently, some results in the insertion polymerization of ethylene have been reported using tetrahedral Co(II) complexes with related ligands.[11, 14-16] The α-diimine ligands have also been object of different studies regarding the relative binding strengths[17-19] as well as their reactivity with main group metals.[20, 21]

We have been interested in the synthesis and characterization by X-ray diffraction and EPR spectroscopy of cobalt(II) complexes of the general formula [CoX_2(α-diimine)], where X = Cl, or I and α-diimines such as bis(aryl)acenaphthenequinonediimine (Ar-BIAN) and 1,4-bis(aryl)-2,3-dimethyl-1,4-diaza-1,3-butadiene (Ar-DAB).[22] The present paper reports on the synthesis and characterization of further α-diimine Co(II) halide complexes (Scheme III.1), namely, [CoI_2(*o,o',p*-$Me_3C_6H_2$-DAB)], (**1**); [CoI_2(*o,o'*-$^{i}Pr_2C_6H_3$-DAB)], (**2**); [$CoCl_2$(*o,o',p*-$Me_3C_6H_2$-BIAN)], (**3**); [$CoCl_2$(*o,o'*-$^{i}Pr_2C_6H_3$-BIAN)], (**4**); [CoI_2(*o,o'*-$^{i}Pr_2C_6H_3$-BIAN)], (**5**). Complexes **3** and **4**, and also the previously described BIAN analogues **1a** and **2a** (similar to **1** and **2**, respectively, but with X = Cl instead)[22] were activated by methylaluminoxane and tested as catalysts for ethylene polymerization.

Scheme III.1 α-diimine Co(II) halide complexes.

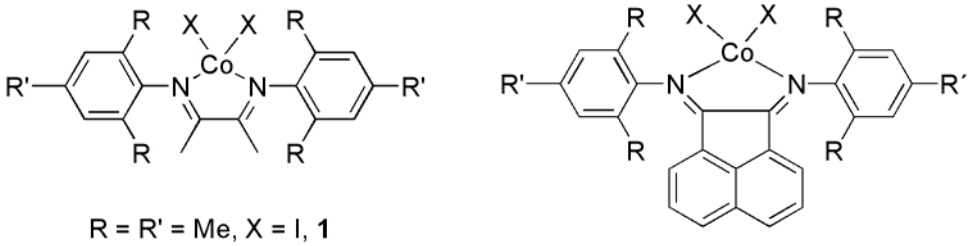

R = R' = Me, X = I, **1**
R = ^{i}Pr, R' =H, X = I, **2**
R = R' = Me, X = Cl, **1a**
R = ^{i}Pr, R' =H, X = Cl, **2a**

R = R' = Me, X = Cl, **3**
R = ^{i}Pr, R' = H, X = Cl, **4**
R = ^{i}Pr, R' = H, X = I, **5**

III.4 Results and Discussion

III.4.1 Synthesis and characterization of compounds

The reaction of equimolar quantities of anhydrous CoX_2 (X = Cl or I) and α-diimine ligands**,** in deoxygenated and dehydrated CH_2Cl_2, at room temperature, yielded red-brown crystalline solids **1**-**5**, with general formula [CoX_2(α-diimine)] (Scheme III.1), in *ca.* 75% to 94% yields. All synthesized compounds were characterized by elemental analyses, FT-IR and ^{1}H NMR spectroscopies and mass spectrometry (MALDI-TOF-MS) (see Experimental and Table SM III.1 supporting information).

The ^{1}H NMR spectra of compounds **1**-**5**, in CD_2Cl_2, at room temperature, exhibit paramagnetic contact shifts,[23] showing resonances spread from *ca.* δ 107 to -25. These contact shifts are due to the paramagnetic character of the Co(II) complexes that exhibit high spin S = 3/2 in the solid state,[22] although in solution they may be involved in equilibrium with their S = 1/2 square planar conformers.

A MALDI-TOF-MS study in dichloromethane was performed for all the synthesized complexes. The samples were dissolved in dichloromethane (1 μg/μL), and no matrix was added to obtain the mass spectra. All the complexes showed peaks attributed to the corresponding species $[CoXL]^{+}$, and to $[L + H^{+}]$, (where X = Cl or I, and L = α-diimine ligand). These species were formed by the dissociation of one halide or by protonation of the

dissociated neutral α-diimine ligand, to give cationic species in all cases. In compound **4**, the peak attributed to the parent ion [$CoCl_2L4\text{-}H^+$] was detected in the negative ionization mode (see Experimental and Table SM III.1 supporting information). These results agree very well with the proposed structures for the synthesized compounds.

The FT-IR spectra of the cobalt (II) complexes, recorded as Nujol mulls, display medium absorption bands in the range $\bar{\nu}$ = 1652-1615 cm^{-1}, which is the absorption region for $\bar{\nu}$(C=N). Bands assigned to the free ligand C=N stretching vibrations were observed in the range $\bar{\nu}$ = 1674-1637 cm^{-1}. In general, the bands in the complexes are shifted to lower wave numbers, which is a criterion of the coordination of both diimine nitrogen atoms of the α-diimine ligands to the cobalt (II) ion (see Table SM III.2 supporting information).

Crystals were obtained for complexes **2-4** enabling the determination of their crystal structures. Table III.1 lists selected bond distances (Å) and angles (º).

The molecular structure of compound **2** shows an asymmetric unit formed by a half molecule of [CoI_2(*o*,*o*'-$^i Pr_2C_6H_3$-DAB)] (where Ar-DAB = 1,4-bis(aryl)-2,3-dimethyl-1,4-diaza-1,3-butadiene) with the Co atom occupying a special position (0,0,0). The corresponding molecular structure is generated by symmetry, giving rise to a distorted tetrahedral geometry around the Co atom, which is built up of two iodine atoms and two nitrogen atoms of the ligand (Figure III.1). In fact, due to the symmetry exhibited, the dihedral angle formed by planes defined by I1-Co1-I2 and N1-Co1-N1_1 is exactly 90º. The I1-Co1-I2 angle is 111.68(3)º which is very close to ideal tetrahedral (109.47º), however the other two bonds to N atoms introduce some distortion since the bite angle N1-Co1-N1_1 is 80.15(16)º. The distances Co-I are 2.5200(7) and 2.5425(8) Å, while the Co-N is 2.045(3) Å. The planes formed by the aryl rings C5-C6-C7-C8-C9-C10 are nearly perpendicular to the plane defined by Co1-N1-C1-C1_1-N1_1 (89.63º). However, the aryl rings themselves are not exactly parallel to each other, making a dihedral angle of 16.79º. These features are similar to the ones found in previous α-diimine complexes synthesized by our group, namely **1a** and **2a**.[22]

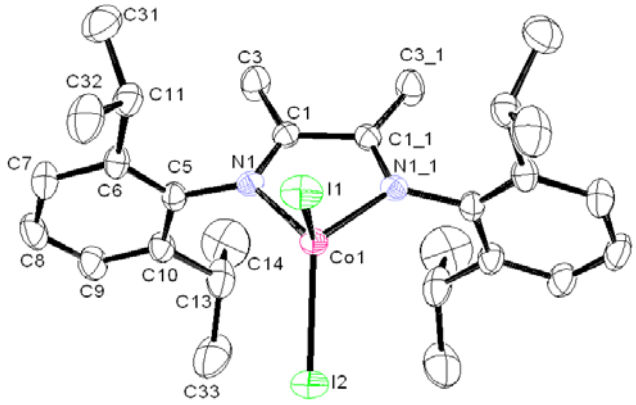

Figure III.1 ORTEP view of the complex **2**. The ellipsoids enclose 50% of the electronic density. Hydrogen atoms are omitted for clarity.

Table III.1 Selected bond distances (Å) and angles (º) for complexes **2-4**.

	2	**3**	**4**	
			molecule A	molecule B
Distances (Å)				
Co1-Cl1	-	2.2037(5)	2.192(2)	2.208(2)
Co1-Cl2	-	2.2105(5)	2.227(2)	2.195(2)
Co1-I1	2.5425(8)	-	-	-
Co1-I2	2.5200(7)	-	-	-
Co1-N1	2.045(3)	2.0753(12)	2.084(6)	2.092(5)
Co1-N2	-	2.0678(12)	2.067(6)	2.085(6)
C1-N1	1.279(4)	1.2795(19)	1.232(8)	1.278(8)
C2-N2	-	1.2773(19)	1.283(8)	1.257(8)
C2-C4	-	1.460(2)	1.473(9)	1.489(8)
C1-C3	1.490(5)	1.459(2)	1.464(9)	1.480(9)
C1-C2	-	1.520(2)	1.563(9)	1.504(9)
N1-C5	1.448(5)	1.4345(17)	1.450(9)	1.454(8)
N2-C14	-	1.4436(17)	1.428(9)	1.442(9)
C4-C30	-	1.416(2)	1.419(9)	1.416(9)
C3-C30	-	1.425(2)	1.430(10)	1.407(9)
Angles (º)				
Cl2-Co1-Cl1	-	112.51(2)	115.15(9)	117.27(8)
I2-Co1-I1	111.68(3)	-	-	-
N1-Co1-N2	80.15(16)	82.17(5)	81.5(2)	82.2(2)
N2-C2-C1	-	118.07(12)	117.1(6)	121.1(6)
N1-C1-C2	115.7(2)	118.03(12)	117.0(6)	117.6(6)
C5-N1-C1	121.9(3)	119.38(12)	115.8(6)	117.9(5)
C14-N2-C2	-	119.76(12	119.1(6)	121.3(6)

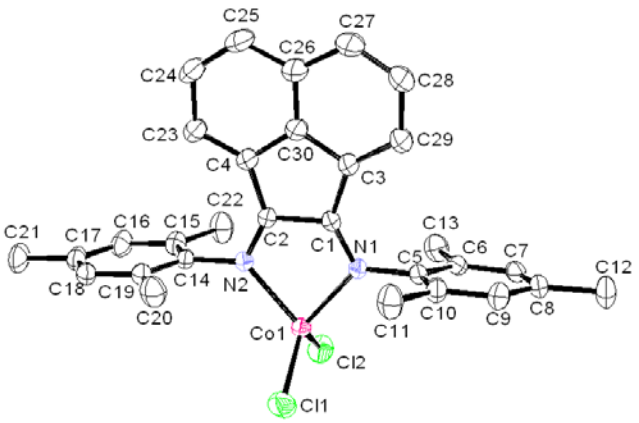

Figure III.2 ORTEP view of the complex **3**. The ellipsoids enclose 50% of the electronic density. Hydrogen atoms are omitted for clarity.

The molecular structure of compound **3** also shows a distorted tetrahedral geometry, just like in the case above, formed by two chloride atoms and two nitrogen atoms of the chelating ligand (Figure. III.2). The dihedral angle formed by planes defined by Cl1-Co1-Cl2 and N1-Co1-N2 is 89.25º. The Cl1-Co1-Cl2 angle is 112.51(2)º while the N1-Co1-N2 bite angle is 82.17(5). The distances Co-Cl are 2.2037(5) and 2.2105(5) Å, and the Co-N bond distances are similar to the ones found in complex **2**. The aryl rings C5-C6-C7-C8-C9-C10 and C14-C15-C16-C17-C18-C19 are almost parallel, forming an angle of 7.25º. They are nearly perpendicular to the plane defined by Co1-N1-C1-C2-N2 (83.39 and 87.87º).

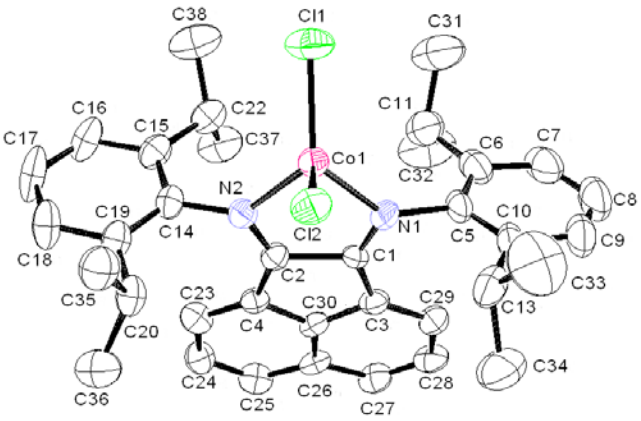

Figure III.3 ORTEP view of the complex **4** (molecule A). The ellipsoids enclose 50% of the electronic density. Hydrogen atoms are omitted for clarity.

The molecular structure of compound **4** consists of an asymmetric unit containing two independent molecules, also having distorted tetrahedral geometries (Figure. III.3). The

planes defined by Cl1-Co1-Cl2 and N1-Co1-N2 form angles of 89.11 and 87.83º, for molecules A and B, respectively. The Cl1-Co1-Cl2 angles are 115.15(9) and 117.27(8)º, while the N1-Co1-N2 bite angles are 81.5(2) and 82.2(2)º, for molecules A and B, respectively. The distances Co-Cl and Co-N are similar to the ones found in complexes **2** and **3**. As for the latter structures, the aryl rings are almost parallel to each other, being nearly perpendicular to the plane defined by Co1-N1-C1-C2-N2.

The coordinated imine C=N bond distances (1.232(8)-1.283(8) Å), as most of the other structural features of complexes **2-4**, are similar to those found for the other [CoX_2(α-diimine)] described in the literature,[11, 22, 24] and are slightly shorter than the C=N bond distances found in the free ligands (*e.g.* ligand L4: 1.250(6)-1.295(6) Å.[25]

III.4.2 Ethylene polymerisation tests

Complexes **3** and **4** (BIAN derivatives), were tested as catalysts for ethylene polymerisation in the presence of cocatalyst methylaluminoxane (MAO). In order to compare the influence of the ligand framework (DAB vs. BIAN), studies were also carried out for compounds **1a** and **2a**, described in a previous paper,[22] which only differ from **1** and **2** in the halide atom (having Cl instead of I). An experimental matrix encompassing temperature and cocatalyst/catalyst ratio was applied to determine critical factors and characteristics of polymerisation reactions. According to the rating of effectiveness of catalysts, based on its activities, provided by Gibson *et al.*,[4] the results obtained (Table III.2) are characteristic of very low to low activities.

The higher activities were observed at 20 ºC, for all catalysts studied. Except for **1a**/MAO system, an increase in the [Al]/[Co] ratio from 500 to 1000 led to improvements in the catalytic activities. Increasing the [Al]/[Co] ratio to 2000 caused a decrease in the activity. Catalyst system **3**/MAO, containing the mesityl-BIAN ligand showed the lowest activity, much lower than its *o,o'*-$^{i}Pr_2$Ph-BIAN analogue **4**/MAO. On the contrary, the *o,o'*-*i*Pr_2Ph-DAB based catalyst system **2a**/MAO, containing the bulkier ^{i}Pr substituents on the phenyl groups, showed lower activity in comparison with its mesityl analogue **1a**/MAO, the latter being the most active of all the catalysts studied. All these systems are less active than those reported by Laine et al.,[11] for the similar [$CoBr_2$(α-diimine)]/MAO system, where the α-

diimine used was 1,4-(bis-2,6-diisopropylphenyl)-1,4-diaza-1,3-butadiene, in which the chelating ligand has a less hindered framework than those used in the present work. However, the activities obtained by these authors were measured at higher ethylene pressures (3-5.5 bar), and the products obtained were mainly oily branched ethylene oligomers.

Table III.2 Ethylene polymerization catalyzed by **1a**, **2a**, **3** and **4**/MAO systems [a]

Entries	Complex	[Al]/[Co]	Temp. (ºC)	m PE (mg)	Activity (g/(mmol-cat.h.bar))
1	**1a**	500	0	33	0.83
2	**1a**	500	20	43	1.08
3	**1a**	500	40	[b]	
4	**1a**	500	60	0	
5	**1a**	1000	20	32	0.80
6	**1a**	2000	20	1	0.03
7	**2a**	500	0	4	0.10
8	**2a**	500	20	5	0.13
9	**2a**	500	40	[b]	
10	**2a**	500	60	[b]	
11	**2a**	1000	20	9	0.23
12	**2a**	2000	20	4	0.10
13	**3**	500	0	[b]	
14	**3**	500	20	[b]	
15	**3**	500	40	[b]	
16	**3**	500	60	0	
17	**3**	1000	20	4	0.10
18	**3**	2000	20	2	0.05
19	**4**	500	0	16	0.40
20	**4**	500	20	16	0.41
21	**4**	500	40	[b]	
22	**4**	500	60	[b]	
23	**4**	1000	20	26	0.65
26	**4**	2000	20	9	0.23

[a] Conditions: $P_{ethylene}$ = 2 bar (relative); $V_{toluene}$=50 ml; n_{cat} = 10 μmol; t = 2h. [b] traces

Selected polyethylene (PE) samples (runs no. 2, 5, 11, 17 and 23) were characterized (Table III.3) as white solids with branching degrees typical of low density polyethylene (LDPE), varying from 25-55 branches per 1000 carbon atoms, as determined by ^{1}H NMR spectroscopy. The corresponding FT-IR spectra (see Figure SM III.1 supporting information) showed in all samples the presence of a band at *ca.* $\bar{\nu}$ = 1378 cm^{-1}, in agreement with the presence of methyl groups associated with branching.[26, 27] Their melting temperatures were determined by DSC (see Figure SM III.2 supporting information), and lie in the range 77-110 ºC. The catalyst systems based on **1a** and **3** (entries 2, 5 and 17), which contain diimine

ligands with mesityl substituents, give rise to branching degrees of 25/1000 C, whereas **2a** and **4** (entries 11 and 23), containing the bulkier *o,o'*-$^{i}Pr_2Ph$ substituents, produce PE twice as branched as the others. This effect is also observed in the analogous nickel catalyst systems.[28] The fact that system **2a**/MAO (entry 11) produces PE with thermal features similar to those of **1a**/MAO (entries 2 and 5), but with a higher branching, may be explained by a variation of the PE molecular weight induced by the *o,o'*-$^{i}Pr_2Ph$ diimine substituents of **2a**. On the other hand, comparison of the thermal parameters of the PEs produced by **3** and **4**/MAO shows that the latter catalyst system presents a lower melting temperature and a lower crystallinity in agreement with the higher number of branches shown by this sample.

Table III.3 Number of branches per 1000 C and thermal analyses of selected polyethylene samples.

Entry	Reaction conditions [a]	No. branches/ 1000 C [b]	ΔH_m/J·g^{-1} [c]	T_{onset} [c]/ºC	T_{max} [c,d]/ºC
2	**1a**/500	25	90.8	84.5	103.7
5	**1a**/1000	25	89.4	85.7	103.6
11	**2a**/1000	55	90.0	85.2	103.5
17	**3**/1000	25	73.0	98.7	109.8
23	**4**/1000	46	47.4	51.0	76.6

[a] Complex/(Al/Co ratio); T = 20 ºC. [b] Estimated by ^{1}H NMR [29]. [c] Determined by DSC. [d] The peak value of the melting endotherm (ideally taken as the temperature at which the largest and most perfect crystals are melting) is frequently assigned as the melting temperature, i.e. $T_m \equiv T_{max}$.

III.5 Conclusions

A series of paramagnetic cobalt(II) complexes of general formula [CoX_2(α-diimine)]: [CoI_2(*o,o',p*-$Me_3C_6H_2$-DAB)] **1**, [CoI_2(*o,o'*-*i*$Pr_2C_6H_3$-DAB)] **2**, [$CoCl_2$(*o,o',p*-$Me_3C_6H_2$-BIAN)] **3**, [$CoCl_2$(*o,o'*-*i*$Pr_2C_6H_3$-BIAN)] **4** and [CoI_2(*o,o'*-*i*$Pr_2C_6H_3$-BIAN)] **5**, were synthesized by direct reaction of equimolar amounts of the corresponding cobalt dihalide and α-diimine ligand, in CH_2Cl_2, in *c.a.* 75% to 94% yields. Single crystal X-ray structural data for compounds **2-4** show, in all cases, the cobalt atom in a distorted tetrahedral coordination

generated by two halide atoms and two nitrogen atoms of the α-diimine ligand. Compounds **3** and **4**, as well as ([$CoCl_2$(*o*,*o'*,*p*-$Me_3C_6H_2$-DAB)]) **1a**, and ([$CoCl_2$(*o*,*o'*-$^{i}Pr_2C_6H_3$-DAB)]) **2a**, revealed low activities in ethylene polymerisation when activated with MAO. The resulting branched (2.5-5.5%) low molecular weight polyethylenes are solid samples, with melting points in the range 77-110 ºC.

III.6 Experimental

III.6.1 General

All reactions and manipulations of solutions were performed under nitrogen or argon atmospheres using standard Schlenk techniques. Reagent grade solvents were deoxygenated and dehydrated before use according to literature methods. $CoCl_2$ and CoI_2 were purchased from Aldrich and the α-diimine ligands were synthesized as described in literature.[30-32]

Elemental analyses were obtained from REQUIMTE, Chemistry Department, New University of Lisbon Service using a Thermo Finnigan-CE Flash-EA 1112-CHNS Instrument. Infrared spectra of complexes were recorded as Nujol mulls on NaCl plates using a Mattson Satellite FTIR spectrometer.

MALDI-TOF-MS analysis were obtained from REQUIMTE, MALDI-TOF-MS Service Laboratory, and have been performed in a MALDI-TOF-MS model voyager DE-PRO Biospectrometry Workstation equipped with a nitrogen laser radiating at 337 nm from Applied Biosystems (Foster City, United States). MALDI mass spectra were acquired and treated with Data Explorer software version 4 series. The MALDI-TOF-MS study in dichloromethane was carried out for complexes **1-5**. Samples were dissolved in dichloromethane (1 μg/μL), and 1 to 2 μL of the corresponding solution was spotted on a well of a MALDI-TOF-MS sample plate and allowed to dry. No matrix was added. Measurements were performed in the reflector positive ion mode, with a 20 kV accelerating voltage, 80 % grid voltage, 0.005 % guide wire, and a delay time of 200 ns, for complexes **1-5** and in the negative ion mode for complex **4**. Mass spectral analysis for each sample was based on the average of 500 laser shots.

^{1}H NMR of complexes **1-5** were recorded in a Bruker Avance III 400 spectrometer (at 400.13 MHz), in CD_2Cl_2, at room temperature. ^{1}H and ^{13}C NMR spectra of polyethylene samples were recorded in Bruker Avance III 400 (at 400.13 MHz) and Bruker Avance III 300 (at 75.47 MHz) spectrometers, at 110ºC. Polymer samples were previously dissolved in a boiling mixture of 3:1 trichlorobenzene:C_6D_6. All spectra taken in both devices were referenced internally to residual protio solvent (^{1}H) or solvent (^{13}C) resonances and reported relative to tetramethylsilane (δ 0). Deuterated solvents were dried with molecular sieves and freeze-pump-thaw-degassed prior to use.

Polyethylene thermal analyses were performed with a TA Instruments DSC2920 with MDSC® option, connected to a liquid N_2 cooling system and calibrated with standards. The sample weights were *ca.* 4-10 mg in all the experiments. A temperature range from 0 to 150 ºC has been studied and the heating and cooling rates used were 10 ºC min^{-1}. The second heating cycle was recorded.

Infrared spectra were collected on polymer films using a Thermo-Nicolet NEXUS FT-IR spectrophotometer. The spectra were normalized in relation to the intensity of the absorption band centered at 720 cm^{-1} (main polyethylene backbone). Films were prepared in a SpecAc press equipped with heating plates and a SpecAc 20160 temperature controller.

III.6.2 Synthesis of Complexes

*III.6.2.1 Synthesis of [CoI_2(o,o',p-$Me_3C_6H_2$-DAB)] (**1**)*

A green suspension of CoI_2 (0.2 g, 0.62 mmol) in CH_2Cl_2 (20 mL) was treated with a yellow solution of *o,o',p*-$Me_3C_6H_2$-DAB, (0.2 g, 0.64 mmol) in CH_2Cl_2 (30 mL). An almost immediate color change was observed from green to red-brown. The mixture was stirred overnight, at room temperature, until complete dissolution. The solution was filtered, and concentrated by vacuum removal of the solvent. A brown crystalline solid precipitated which was separated by filtration, washed with diethyl ether (2×10 mL) and petroleum ether (2×10

mL). After recrystallisation from CH_2Cl_2/petroleum ether 0.36 g of **1** were obtained (yield: 94%).

^{1}H NMR (CD_2Cl_2, 400 MHz): δ 107.11, 18.44, 15.22, 0.50. IR (nujol mull/NaCl plates), cm^{-1}: 1631 ($\bar{\nu}_{C=N}$). MS (MALDI-TOF); *m/z*: 506.7 $[CoIL]^+$ (54.25%), 321.8 $[L+H^+]$ (100%) (L = diimine ligand). Anal. Calc. for $C_{22}H_{28}CoI_2N_2$ (MW = 633.21): C, 41.73; H, 4.46; N, 4.42. Found: C, 41.67; H, 4.44; N, 4.71.

*III.6.2.2 Synthesis of [CoI_2(o,o'-$^i Pr_2C_6H_3$-DAB)] (**2**)*

Compound **2** was obtained using the procedure described for **1**. Yield: 77%. Crystals suitable for X-ray diffraction were obtained.

^{1}H NMR (CD_2Cl_2, 400 MHz): δ 95.22, 17.11, 7.59, 0.35, -3.00, -24.59. IR (nujol mull/NaCl plates), cm^{-1}: 1639 ($\bar{\nu}_{C=N}$). MS (MALDI-TOF); *m/z*: 590.76 $[CoIL]^+$ (16.38%), 405.9 $[L+H^+]$ (67.65%) (L = diimine ligand). Anal. Calc. for $C_{28}H_{40}CoI_2N_2$ (MW = 717.37): C, 46.88; H, 5.62; N, 3.90. Found: C, 46.55; H, 5.47; N, 4.04.

*III.6.2.3 Synthesis of [$CoCl_2$(o,o',p-$Me_3C_6H_2$-BIAN)] (**3**)*

A blue suspension of $CoCl_2$ (0.16 g, 1.2 mmol) in CH_2Cl_2 (20 mL) was treated with a red solution of *o,o',p*-$Me_3C_6H_2$-BIAN (0.5 g, 1.2 mmol) in CH_2Cl_2 (30 mL). The mixture turned quickly to dark red, and was further stirred for 2 hours, until complete dissolution. After filtration, the solvent was partially removed leaving a red-brown solid, which was separated by filtration, washed with petroleum ether (2×10 mL). Recrystallisation from CH_2Cl_2/petroleum ether afforded 0.49 g of **3** (yield: 75%). Crystals suitable for X-ray diffraction were obtained.

^{1}H NMR (CD_2Cl_2, 400 MHz): δ 24.73, 16.13, 7.76, 2.16, 1.29, 0.87, -1.40. IR (nujol mull/NaCl plates), cm^{-1}: 1652, 1628 ($\bar{\nu}_{C=N}$). MS (MALDI-TOF); *m/z*: $[CoClL]^+$ 510.59 (100%), 417.7 $[L+H^+]$ (4.49%) (L = diimine ligand). Anal. Calc. for $C_{30}H_{28}CoCl_2N_2 \cdot 1/2\ CH_2Cl_2$ (MW= 588.86): C, 62.21; H, 4.96; N, 4.76. Found: C, 62.86; H, 5.80; N, 4.18.

*III.6.2.4 Synthesis of [$CoCl_2$(o,o'-$^i Pr_2C_6H_3$-BIAN)] (**4**)*

Compound **4** was obtained using the procedure described for **3**. Yield: 83%. Crystals suitable for X-ray diffraction were obtained.

^{1}H NMR (CD_2Cl_2, 400 MHz): δ 24.89, 7.83, 4.00, 3.49, 3.44, -0.09, -19.94. IR (nujol mull/NaCl plates), cm^{-1}: 1649, 1619 ($\bar{\nu}_{C=N}$). MS (MALDI-TOF); *m/z*: 594.78 $[CoClL]^+$ (23.73%), 501.9 $[L+H^+]$ (38.23%) (L = diimine ligand). MS (MALDI-TOF, negative ionization mode); *m/z*: 629.77 $[CoCl_2L\text{-}H^+]$ (68%) (L = diimine ligand). Anal. Calc. for $C_{36}H_{40}CoCl_2N_2$ (MW = 630.56): C, 68.57; H, 6.39; N, 4.44. Found: C, 68.14; H, 6.29; N, 4.40.

*III.6.2.5 Synthesis of [CoI_2(o,o'-$^i Pr_2C_6H_3$-BIAN)] (**5**)*

A green suspension of CoI_2 (0.16 g, 0.5 mmol) in CH_2Cl_2 (20 mL) was treated with a red solution of *o,o'*-$^i Pr_2C_6H_3$-BIAN (0.25 g, 0.5 mmol) in CH_2Cl_2 (20 mL). The mixture turned quickly to dark red and was stirred overnight, until complete dissolution. After filtration, the solvent was removed to 1/4 of the volume, and petroleum ether (40-60 ºC) (5 mL) was added. A dark red solid, was formed by storage at -20 ºC. After filtration and washing with petroleum ether (2×10 mL), it was recrystallised from CH_2Cl_2/petroleum ether, yielding 0.37 g of complex **5** (yield: 91%).

^{1}H NMR (CD_2Cl_2, 400 MHz): δ 15.17, 11.35, 5.53, 4.99, 3.29, 2.63, -2.44, -22.14. IR (nujol mull/NaCl plates), cm^{-1}: 1640, 1615 ($\bar{\nu}_{C=N}$). MS (MALDI-TOF); *m/z*: 686.73 $[CoIL]^+$ (100%), 501.9 $[L+H^+]$ (71.99%) (L = diimine ligand). Anal. Calc. for $C_{36}H_{40}CoI_2N_2$ (MW = 813.46): C, 53.15; H, 4.96; N, 3.40. Found: C, 53.28; H, 4.96; N, 3.44.

III.6.3 Crystallographic details

Crystallographic and experimental details of crystal structure determinations are given in Table III.4. Single crystals of complexes **2**, **3**, and **4** were mounted on a Nonius Kappa-CCD area detector diffractometer (Mo-Kα λ = 0.71073 Å). The complete conditions of data

collection (DENZO software) and structure refinements are given below. The cell parameters were determined from reflections taken from one set of 10 frames (1.0° steps in phi angle), each at 20 s exposure. The structures were solved by direct methods (SHELXS97) and refined against F2 using the SHELXL97 software.[33] The absorption was not corrected. All non-hydrogen atoms were refined anisotropically. Hydrogen atoms were generated according to stereochemistry and refined using a riding model in SHELXL97. Figures were generated using ORTEP3.[34] Data was deposited in CCDC under the deposit numbers 665822 (**3**), 665823 (**2**) and 665824 (**4**).

Table III.4 Crystal data and structure refinement for compounds **2-4**.

Compound	**2**	**3**	**4**
Formula	$C_{28}H_{40}CoI_2N_2$	$C_{30}H_{28}CoCl_2N_2$	$C_{36}H_{40}CoCl_2N_2$
M	717.3	546.37	630.53
λ/ Å	0.71073	0.71073	0.71073
T/ K	173(2)	173(2)	173(2)
crystal system	orthorhombic	Orthorhombic	monoclinic
space group	Pnma	Pnab	$P2_1/a$
a/ Å	13.6130(2)	16.6540(3)	22.4880(5)
b/ Å	21.1000(2)	17.1900(2)	11.8010(4)
c/ Å	10.4930(5)	22.6670(4)	27.1090(6)
α / °	90.00	90.00	90.00
β / °	90.00	90.00	111.450(2)
γ / °	90.00	90.00	90.00
V/ $Å^3$	3013.95(15)	6489.16(18)	6695.9(3)
Z	4	8	8
ρ_{calc}/ g cm^{-3}	1.581	1.119	1.251
μ/ mm^{-1}	2.635	0.711	0.698
θ_{max}/ °	30.034	34.972	30.034
total data	4826	103035	161895
unique data	4519	14242	19531
R_{int}	0.0520	0.0000	0.0000
Reflections (*R* [*I*>3σ(*I*)])	4519	14242	19531
wR	0.1075	0.1768	0.3434
Goodness of fit	1.004	1.015	1.049
ρ min, ρ max	-1.273	-0.551	-0.839
	1.160	0.079	1.387

III.6.4 Polymerisation details

Ethylene polymerization tests were carried out in 200 mL crown capped pressure bottles sealed with neoprene septum and pump filled with nitrogen atmosphere (the bottles were previously dried in the oven at 150 ºC for several days and degassed with 3 cycles of vacuum/nitrogen). Freshly distilled toluene, dried over Na/K alloy, was added (50 mL) to each polymerization bottle and the resulting solvent was then saturated at an ethylene relative pressure of 2 bar, which was maintained throughout the polymerization reactions. Then the cocatalyst (MAO) was added in the proper Al/Co ratio via a glass syringe. Solutions were then brought to the desired temperatures and allowed to equilibrate for 15 min. After this, the corresponding amount of a toluene solution (1 mL) of the desired complex was added to the polymerization reactors with a glass syringe. The polymerizations were terminated after 2 h by quenching the mixture with 150 ml of an acidic methanol (1% HCl) solution. The absence of ethylene oligomers C_4-C_{24} was confirmed by GC chromatography, injecting aliquots of the gas and liquid phases of the polymerization reaction samples in a Perkin-Elmer Clarus 500 gas chromatograph, equipped with a capillary column Tracer/Teknorma TRB-5MS, 30m×0.25mm ID×0.25µm (film), using a temperature program from 60 to 240 ºC, and from 240 to 280 ºC, at ramp rates of 5 and 10 ºC/min, respectively. The obtained polymers were then filtered, washed several times with methanol and dried in a vacuum oven at 60 °C for 3 days. The filtrates were evaporated until all the methanol was removed, and the residual toluene fractions were extracted with distilled water (3×50 ml). After separation, the organic phases were evaporated to dryness and no organic materials were observed.

III.7 Acknowledgements

We thank Fundação para a Ciência e Tecnologia, Portugal, for funding (Projects PTDC/QUI/66440/2006 and POCI/QUI/59025/2004, co-financed by FEDER) and for doctoral and post-doctoral fellowships to V.R. (SFRH/BD/13777/2003) and S.A.C. (SFRH/BPD/34974/2007), respectively. We also thank CPU (France) and CRUP (Portugal) for the Portuguese-French Integrated Action-2006, No. F-27/07.

III.8 References

1. *Metalorganic Catalysts for Synthesis and Polymerization*, Springer Verlag, Heidelberg, 1999.
2. B. Rieger, L. S. Baugh, S. Kacker and S. Striegler, *Late Transition Metal Polymerization Catalysis*, Weinheim, Wiley-VCH, 2003.
3. S. D. Ittel, L. K. Johnson and M. Brookhart, *Chem. Rev.*, 2000, **100**, 1169-1203.
4. G. J. P. Britovsek, V. C. Gibson and D. F. Wass, *Angew. Chem., Int. Ed.*, 1999, **38**, 428-447.
5. V. C. Gibson and S. K. Spitzmesser, *Chem. Rev.*, 2003, **103**, 283-315.
6. G. Vankoten and K. Vrieze, *Advances in Organometallic Chemistry*, 1982, **21**, 151-239.
7. M. C. Barral, E. Delgado, E. Gutierrezpuebla, R. Jimenezaparicio, A. Monge, C. Delpino and A. Santos, *Inorganica Chimica Acta-Articles*, 1983, **74**, 101-107.
8. H. T. Dieck and M. Haarich, *Journal of Organometallic Chemistry*, 1985, **291**, 71-87.
9. M. J. Camazon, A. Alvarezvaldes, J. R. Masaguer and M. C. Navarroranninger, *Transition Metal Chemistry*, 1986, **11**, 334-336.
10. Y. Doi and T. Fujita, 1997, JP Patent 10298225 (Mitsui Chemicals Inc., Japan).
11. T. V. Laine, M. Klinga, A. Maaninen, E. Aitola and M. Leskela, *Acta Chemica Scandinavica*, 1999, **53**, 968-973.
12. M. Sieger, K. Hubler, T. Scheiring, T. Sixt, S. Zalis and W. Kaim, *Zeitschrift Fur Anorganische Und Allgemeine Chemie*, 2002, **628**, 2360-2364.
13. M. Sieger, M. Wanner, W. G. Kaim, D. J. Stufkens, T. L. Snoeck and S. Zalis, *Inorganic Chemistry*, 2003, **42**, 3340-3346.
14. T. V. Laine, K. Lappalainen, J. Liimatta, E. Aitola, B. Löfgren and M. Leskelä, *Macromol. Rapid. Commun.*, 1999, **20**, 487-491.
15. M. X. Qian, M. Wang, B. Zhou and R. He, *Applied Catalysis a-General*, 2001, **209**, 11-15.
16. C. Bianchini, G. Mantovani, A. Meli, F. Migliacci and F. Laschi, *Organometallics*, 2003, **22**, 2545-2547.
17. M. Gasperini and F. Ragaini, *Organometallics*, 2004, **23**, 995-1001.
18. M. Gasperini, F. Ragaini, E. Gazzola, A. Caselli and P. Macchi, *Dalton Transactions*, 2004, 3376-3382.

19. M. Gasperini, F. Ragaini and S. Cenini, *Organometallics*, 2002, **21**, 2950-2957.
20. I. L. Fedushkin, V. A. Chudakova, A. A. Skatova, N. M. Khvoinova, Y. A. Kurskii, T. A. Glukhova, G. K. Fukin, S. Dechert, M. Hummert and H. Schumann, *Zeitschrift Fur Anorganische Und Allgemeine Chemie*, 2004, **630**, 501-507.
21. I. L. Fedushkin, N. M. Khvoinova, A. Y. Baurin, G. K. Fukin, V. K. Cherkasov and M. P. Bubnov, *Inorganic Chemistry*, 2004, **43**, 7807-7815.
22. V. Rosa, P. J. Gonzalez, T. Aviles, P. T. Gomes, R. Welter, A. C. Rizzi, M. C. G. Passeggi and C. D. Brondino, *Eur. J. Inorg. Chem.*, 2006, 4761-4769.
23. C. Cremer and P. Burger, *Journal of the American Chemical Society*, 2003, **125**, 7664-7677.
24. M. Tanabiki, K. Tsuchiya, Y. Motoyama and H. Nagashima, *Chemical Communications*, 2005, 3409-3411.
25. U. El-Ayaan, A. Paulovicova and Y. Fukuda, *Journal of Molecular Structure*, 2003, **645**, 205-212.
26. F. J. B. Calleja and A. Hidalgo, *Kolloid-Zeitschrift and Zeitschrift Fur Polymere*, 1969, **229**, 21-&.
27. *Polymer Data Handbook*, Oxford University Press, New York, 1999.
28. L. K. Johnson, C. M. Killian and M. Brookhart, *J. Am. Chem. Soc.*, 1995, **117**, 6414-6415.
29. A. C. Gottfried and M. Brookhart, *Macromolecules*, 2003, **36**, 3085-3100.
30. R. Vanasselt, C. J. Elsevier, W. J. J. Smeets, A. L. Spek and R. Benedix, *Recueil Des Travaux Chimiques Des Pays-Bas-Journal of the Royal Netherlands Chemical Society*, 1994, **113**, 88-98.
31. M. Svoboda and H. tom Dieck, *J. Organomet. Chem.*, 1980, **191**, 321-328.
32. H. tom Dieck, M. Svoboda and T. Greiser, *Z. Naturforsch.*, 1981, **36b**, 823-832.
33. G. M. Sheldrick, *SHELXL97, Program for the refinement of crystal structures*, University of Göttingen, Germany, 1997.
34. L. J. Farrugia, *J. Appl. Crystallogr.*, 1997, **30**, 565.

III.9 Supplementary material

CCDC 665822-665824 contain the supplementary crystallographic data for compounds **3**, **2**, and **4**, respectively. These data can be obtained free of charge via http://www.ccdc.cam.ac.uk/conts/retrieving.html, or from the Cambridge Crystallographic Data Centre, 12 Union Road, Cambridge CB2 1EZ, UK; fax: (+44) 1223-336-033; or e-mail: deposit@ccdc.cam.ac.uk. Supplementary data associated with this article (analytical data of complexes **1**-**5**, selected FT-IR data of ligands and complexes, FT-IR spectra and DSC thermograms of selected polyethylene samples) can be found, in the online version, at doi: 10.1016/j.jorganchem.2007.12.007.

Table SM III.1 Analytical data for compounds **1-5**.

Complex[a]	^{1}H NMR (CD_2Cl_2)[b]	Molecular mass; Molecular formula	Mass spectrum,[c] MALDI-TOF-MS (*m/z*)	Microanalysis (calc) (%)		
				C	H	N
1	107.11, 18.44, 15.22, 0.50	633.21; $C_{22}H_{28}CoI_2N_2$	$[CoIL1]^+$ 506.7 (54.25%), $[L1+H^+]$ 321.8 (100%)	41.67 (41.73)	4.44 (4.46)	4.71 (4.42)
2	95.22, 17.11, 7.59, 0.35, -3.00, -24.59	717.37; $C_{28}H_{40}CoI_2N_2$	$[CoIL2]^+$ 590.76 (16.38%), $[L2+H^+]$ 405.9 (67.65%)	46.55 (46.88)	5.47 (5.62)	4.04 (3.90)
3	24.73, 16.13, 7.76, 2.16, 1.29, 0.87, -1.40	588.86; $C_{30}H_{28}CoCl_2N_2\cdot$ $\cdot 1/2\ CH_2Cl_2$	$[CoClL3]^+$ 510.59 (100%), $[L3+H^+]$ 417.7 (4.49%)	62.86 (62.21)	5.80 (4.96)	4.18 (4.76)
4	24.89, 7.83, 4.00, 3.49, 3.44, -0.09, -19.94	630.56; $C_{36}H_{40}CoCl_2N_2$	$[CoClL4]^+$ 594.78(23.73%), $[L4+H^+]$ 501.9 (38.23%) $[CoCl_2L4\text{-}H^+]$ 629.77(68%) [d]	68.14 (68.57)	6.29 (6.39)	4.40 (4.44)
5	15.17, 11.35, 5.53, 4.99, 3.29, 2.63, -2.44, -22.14	813.46; $C_{36}H_{40}CoI_2N_2$	$[CoIL4]^+$ 686.73(100%), $[L4+H^+]$ 501.9 (71.99%)	53.28 (53.15)	4.96 (4.96)	3.44 (3.40)

[a] Colour of complexes **1-5**: red-brown. [b] Referenced to $CDHCl_2$ peak at δ 5.32. [c] Legend: for ligand 1,4-bis(aryl)-2,3-dimethyl-1,4-diaza-1,3-butadiene (Ar-DAB), L1: Ar = *o,o',p*-$Me_3C_6H_2$ and L2: Ar = *o,o'-i*$Pr_2C_6H_3$; for ligand bis(aryl)acenaphthenequinonediimine (Ar-BIAN), L3: Ar = *o,o',p*-$Me_3C_6H_2N$ and L4: Ar = *o,o'-i*$Pr_2C_6H_3$; [d] Negative ionization mode.

Table SM III.2 Selected FT-IR data in Nujol mulls.

Free ligands [a]	$\bar{\nu}$ (cm^{-1})	Complexes	$\bar{\nu}$ (cm^{-1})
L1	1637	**1**	1631
L2	1639	**2**	1639
L3	1674, 1650	**3**	1652, 1628
L4	1672, 1651	**4**	1649, 1619
L4	1672, 1651	**5**	1640, 1615

[a] Legend for **L1-L4**: see Table SM III.1, footnote c.

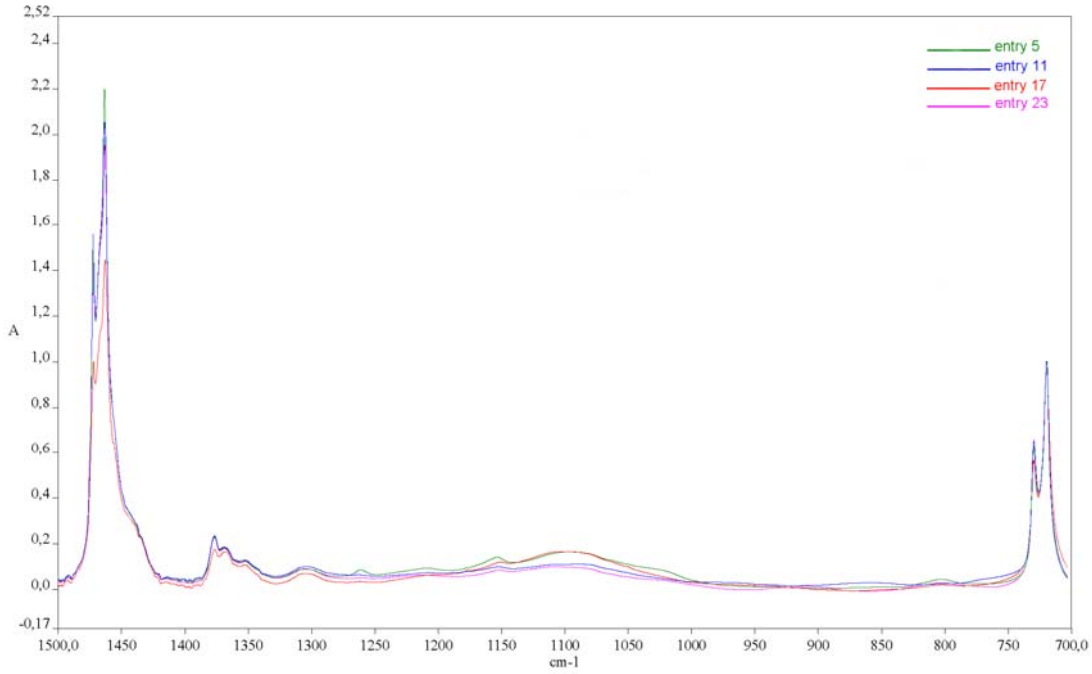

Figure SM III.1 FT-IR spectra of selected polyethylene samples.

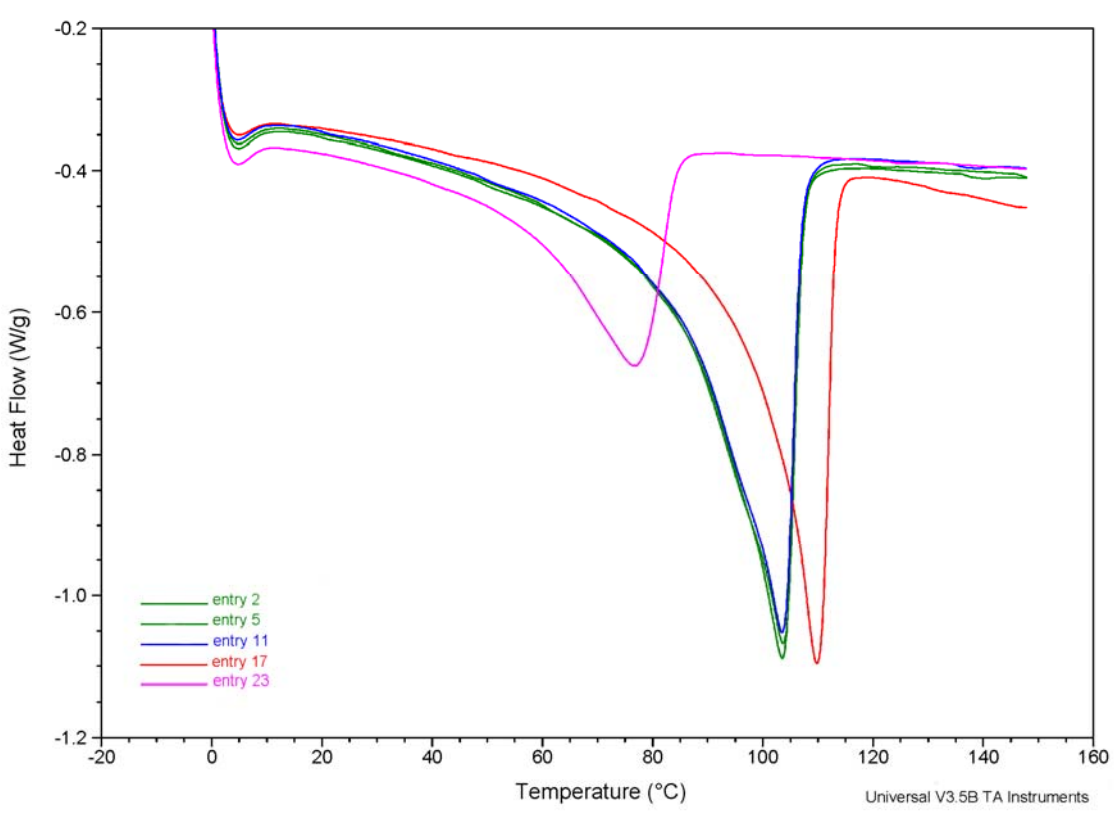

Figure SM III.2 DSC thermograms of selected polyethylene samples.

Chapter IV

A new bis(1-naphthylimino)acenaphthene compound and its Pd(II) and Zn(II) complexes: Synthesis, characterization, solid state structures and Density Functional Theory studies on the *syn* and *anti* isomers.

V. Rosa, T. Avilés, Gabriel Aullón, B. Covelo, C. Lodeiro.
Accepted for publication in Inorganic Chemistry, June **2008**.

Index

Synopsis

A new rigid bidentate ligand bis(1-naphthylimino)acenaphthene, **L1** and its Zn(II) and Pd(II) complexes, $ZnCl_2$(**L1**), **1** and $PdCl_2$(**L1**), **2**, have been synthesized. In all cases a mixture of the two possible *syn* and *anti*, isomers can be obtained. It has been shown by DFT calculations that isomerization is possible in the free ligand **L1** but is not in the square-planar palladium complex **2**. The solid state structures of **L1** and the *anti* isomer of compound **2** have been determined by single crystal X-ray diffraction.

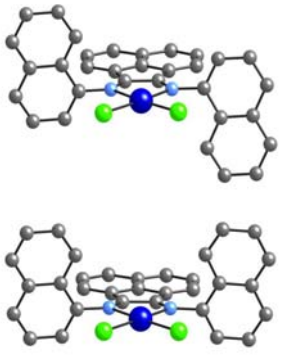

IV.1 Resumo

Um novo ligando rígido e bidentado, o bis(1-naftilolimino)acenafteno, **L1**, e os respectivos complexos de Zn(II) e Pd(II), [$ZnCl_2$(**L1**)], **1**, e [$PdCl_2$(**L1**)], **2**, foram sintetizados. **L1** foi preparado através do método *template*, fazendo reagir 1-naftiloamina e acenaftenoquinona na presença de $ZnCl_2$, dando **1**, que foi mais tarde desmetalado. Da reacção de 1-naftiloamina com acenaftenoquinona e $PdCl_2$ obteve-se dicloreto bis(1-naftilo)acenaftenoquinonadiimina) paládio, **2**. **L1**, **1** e **2** foram obtidos como uma mistura de isómeros *syn* e *anti*. **2**, também foi obtido por reacção de $PdCl_2$, activado por acetonitrilo em refluxo, seguido da adição de **L1**, dando também uma mistura de isómeros *syn* e *anti*, mas em proporções diferentes. As estruturas de estado sólido de **L1** e do isómero *anti* do composto **2** foram determinadas por difracção de raio-X de mono cristal. Todos os compostos foram caracterizados por análise elementar, MALDI-TOF-MS espectrometria, e por espectroscopias de IV, UV-vis, ^{1}H, ^{13}C, ^{1}H-^{1}H COSY, ^{1}H-^{13}C HSQC, ^{1}H-^{13}C HSQC-TOCSY e ^{1}H-^{1}H NOESY RMN quando necessário.

Estudos DFT mostraram que os confórmeros de [$PdCl_2$(BIAN)] são isoenergéticos e podem ser ambos obtidos experimentalmente. No entanto, pode-se prever que o processo de isomerização não é possível num complexo quadrangular planar, mas é possível para o ligando livre. A geometria molecular é muito semelhante para ambos os isómeros, sendo unicamente esperado observar diferentes orientações dos grupos naftilo.

A minha contribuição para este trabalho consistiu na síntese de todos os compostos e a sua caracterização.

IV.2 Abstract

A new rigid bidentate ligand bis(1-naphthylimino)acenaphthene, **L1**, and their Zn(II) and Pd(II) complexes [$ZnCl_2$(**L1**)], **1**, and [$PdCl_2$(**L1**)], **2**, were synthesized. **L1** was prepared by the "template method", reacting 1-naphthyl amine and acenaphthenequinone in the presence of $ZnCl_2$, giving **1**, that was further demetallated. Reaction of 1-naphthyl amine with acenaphthenequinone and $PdCl_2$ afforded dichloride bis(1-naphthyl)acenaphthenequinonediimine) palladium, **2**. **L1**, **1** and **2** were obtained as a mixture of *syn* and *anti* isomers. **2**, was also obtained by reaction of $PdCl_2$ activated by refluxing it in acetonitrile followed by addition of **L1**, by this route also a mixture of *syn* and *anti* isomers was obtained, but in a different rate. The solid state structures of **L1** and the *anti* isomer of compound **2** were determined by single crystal X-ray diffraction. All compounds were characterized by elemental analyses, MALDI-TOF-MS spectrometry, and by IR, UV-vis, ^{1}H, ^{13}C , ^{1}H-^{1}H COSY, ^{1}H-^{13}C HSQC, ^{1}H-^{13}C HSQC-TOCSY and ^{1}H-^{1}H NOESY NMR spectroscopies when applied.

DFT studies showed that both conformers for [$PdCl_2$(BIAN)] are isoenergetic, and they can be both obtained experimentally. However, we can predict that isomerization process is not available in square-planar complex, but is possible for the free ligand. The molecular geometry is very similar in both isomers, and only different orientations for naphthyl groups can be expected.

My contribution to this work was the synthesis of all the compounds and their characterization.

IV.3 Introduction

α-Diimine ligands have been known for a long time[1-4] and are well known to stabilize organometallic complexes.[5-7] They are derived from the condensation reaction of a diketone with two equivalents of an alkyl or arylamine often catalyzed by a Lewis or Brönsted acid. Using these synthetic routes, we can easily vary the backbone and the aryl substituent, enabling thus to modify the steric and electronic effects at the metal center. More recently Elsevier[8] described the synthesis and full characterization of the rigidly chelating bidentate nitrogen ligands (Ar-BIAN = bis(aryl)acenaphthenequinonediimine) by condensation of the rigid acenaphthenquinone with a proper amine. Palladium complexes with Ar-BIAN ligands, were shown to be efficient catalysts for homogeneous hydrogenation of electron-poor alkenes and carbon-carbon cross coupling reactions[9, 10] and for the selective hydrogenation of alkynes to alkenes.[11] A large number of late transition metal complexes bearing α-diimine ligands have been extensively employed in several other catalytic reactions.[12] We will recall among others the commercial production of polyolefins from ethene and propene,[13-15] and the alkene-CO copolymerization.[16, 17] It has been recently reported the synthesis of atactic polyketones catalyzed by Pd complexes with meta-substituted Ar-BIAN ligands.[18] Oligomerization of ethylene using modified α-diimine ligands, have been reported.[19] Ar-BIAN ligands with strong electron-withdrawing substituents on the aryl rings or mixed Ar,Ar'-BIAN having different substituents on the two aryl rings, have been synthesized and their relative binding strengths studied.[20-22] The reactivity of these ligands with main group metals calcium and magnesium and metalloid germanium has also been studied.[23-25]

We report herein the synthesis and characterization of a new ligand: bis(1-naphthylimino)acenaphthene, **L1** and its Zn(II) and Pd(II) complexes [$ZnCl_2$(**L1**)], **1**, and [$PdCl_2$(**L1**)], **2**. In **L1, 1**, and **2** *syn* and *anti* isomers are possible. The solid state structures of **L1**, and the *anti* isomer of compound **2** have been determined by single crystal X-ray diffraction. All complexes have been characterized by elemental analyses, MALDI-TOF-MS spectrometry, by IR, UV-Vis, ^{1}H, ^{13}C, ^{1}H-^{1}H COSY, ^{1}H-^{13}C HSQC, ^{1}H-^{13}C HSQC-TOCSY and ^{1}H-^{1}H NOESY NMR spectroscopy when applied. DFT studies showed that both conformers for [$PdCl_2$(BIAN)] are isoenergetic, and they can be both obtained experimentally. However, we can predict that isomerization process is not available in square-planar complex, but is possible for the free ligand. The molecular geometry is very similar in both isomers, and only different orientations for naphthyl groups can be expected.

IV.4 Experimental Section

IV.4.1 General Procedures and Materials

All reactions were performed in air, except the cases performed in an argon atmosphere using Shlenk techniques, as referred in the experimental section. Solvents were reagent grade and were dried according to literature methods. Elemental analyses were performed at the Analytical Services of the Laboratory of REQUIMTE-Departamento de Química, Universidade Nova de Lisboa, on a Thermo Finnigan-CE Flash-EA 1112-CHNS Instrument. Infrared spectra were recorded as Nujol mulls on NaCl plates using a Mattson Satellite FTIR spectrometer. NMR spectra were recorded using a Bruker AVANCE II 400 and 600 MHz, and program TOPSPIN 2.0 (Bruker).

IV.4.2 X-ray crystal structure determinations

Crystallographic data were collected on a Bruker Smart 1000 charged-coupled device diffractometer at CACTI (Universidade de Vigo) at 293 K using graphite monochromated Mo Kα radiation (λ = 0.71073 Å), and were corrected for Lorentz and polarization effects. The software SMART[26] was used for collecting frames of data, indexing reflections, and the determination of lattice parameters, SAINT[26] for integration of intensity of reflections and scaling. The data of **2** were corrected for absorption using the program SADABS.[27] The structures were solved by direct methods using the program SHELXS97.[28] All non-hydrogen atoms were refined with anisotropic thermal parameters by full-matrix least-squares calculations on F^2 using the program SHELXL97.[28] Hydrogen atoms were inserted at calculated positions and constrained with isotropic thermal parameters. Drawings were produced with PLATON[29] and MERCURY.[30] Special computations for the crystal structure discussions were carried out with PLATON.[29] Crystal data and structure refinement parameters are summarized in Table IV.1. The structural data have been deposited with the Cambridge Crystallographic Data Centre (CCDC) with reference numbers 671032 and

671033 for **L1** and **2**, respectively. The data can be obtained free of charge via www.ccdc.cam.uk/data_request/cif, by emailing data_request@ccdc.cam.ac.uk or by contacting The Cambridge Crystallographic Data Centre, 12 Union Road, Cambridge CB2 1EZ, UK.

IV.4.3 Spectrophotometric measurements

Absorption spectra were recorded on a Perkin Elmer lambda 35 spectrophotometer. The linearity of the absorption *vs.* concentration was checked in the concentration range used ($1.0.E^{-4}$-$1.0.E^{-6}$ M). All spectrophotorimetric titrations were performed as follows: the stock solutions of the ligand (*ca.* $1.0.E^{-3}$ M) were prepared by dissolving an appropriate amount of the ligand in a 50 mL volumetric flask and diluting to the mark with freshly dry CH_2Cl_2 UVA-sol. All measurements were performed at 298 K. The titration solutions ([**L1**] = $1.0.E^{-5}$M) were prepared by appropriate dilution of the stock solutions. Titrations of the ligand were carried out by addition of microliter amounts of standard solutions of the ions in dichloromethane.

IV.4.4 Mass spectrometry

MALDI-TOF-MS (Matrix Assisted Laser Desorption-Ionization Time-Of-Fly-Mass Spectrometry) analysis were obtained in the REQUIMTE-MALDI-TOF-MS Service Laboratory, and have been performed in a MALDI-TOF-MS voyager DE-PRO Biospectrometry Workstation equipped with a nitrogen laser radiating at 337 nm from Applied Biosystems (Foster City, United States). MALDI mass spectra were acquired and treated with Data Explorer software version 4 series. The MALDI-TOF-MS study in dichloromethane was carried out for **L** and **L1**, and for the Zn(II) and Pd(II) complexes **1** and **2**. Samples were dissolved in dichloromethane (1 μg/μL), and 1 to 2 μL of the corresponding solution was spotted on a well of a MALDI-TOF-MS sample plate and allowed to dry. No matrix was added. Measurements were performed in the reflector positive or negative ion mode, with a 20 kV accelerating voltage, 80 % grid voltage, 0.005 % guide wire, and a delay time of 200 ns. Mass spectral analysis for each sample was based on the average of 500 laser

shots. TOF-MS-EI (Time-of-Fly Mass Spectrometry Electron Impact) and TOF-MS-FD (Time-of-Fly Mass Spectrometry Field Desorption) spectra were obtained in the REQUIMTE-MS Service Laboratory using a Micromass GCT model.

IV.4.5 Computational details

Unrestricted calculations were carried out using the GAUSSIAN03 package.[31] The hybrid density function method known as B3LYP was applied.[32, 33] Effective core potentials (ECP) were used to represent the innermost electrons of the transition atoms and the basis set of valence double-ζ quality for associated with the pseudopotentials known as LANL2DZ.[34] Similar description was used for heavy elements as chlorine and germanium, supplemented with an extra *d*-polarization function.[35, 36] The basis set for the light elements as C, N and H was 6-31G*.[37, 38]The structural data were obtained through a systematic search in the *Cambridge Structural Database* (version 5.28).[39]

*IV.4.5.1 Mono(1-naphthylimino)acenaphthene (**L**)*

1-aminonaphtalene (0.8 g, 5.4 mmol) in methanol (10 mL) is slowly added to a solution of acenaphthenequinone (1 g, 5.4 mmol) in methanol (100 mL) in the presence of formic acid (1 mL). After 15 min a red precipitate was formed. The mixture was left stirring overnight at room temperature. After that, water was added (25 mL) to the reaction mixture and the desired product was extracted with dichloromethane (3 x 15 mL). The organic layer (CH_2Cl_2) was separated and dried with $MgSO_4$, filtered, and the solvent was removed with the rotary evaporator till dryness. The solid residue was washed with diethyl ether (2 x 5 mL) and petroleum ether (3 x 10 mL) giving 1.54 g of pure product. Yield: 92%. Red crystals were obtained by recrystalization from a saturated dichloromethane hot solution.

Anal calcd (%) for $C_{22}H_{13}NO$ (M=307.34): C, 85.97; H, 4.26; N, 4.56. Found: C, 85.63; H, 4.29; N, 4.54.

^{1}H NMR (400 MHz, CD_2Cl_2, 293 K): 8.21-8.18t (2H, Ar); 7.99-7.95t (2H, Ar); 7.91-7.81m (3H, Ar); 7.58-7.52m (2H, Ar); 7.42-7.39t (1H, Ar); 7.32-7.28t (1H, Ar); 7.12-7.10d (1H, Ar, J=7.11 Hz); 6.77-6.75d (1H, Ar, J=7.11 Hz).

^{13}C NMR (400 MHz, CD_2Cl_2, 293 K): 189.9 (C=O); 161 (C=N); 147.9 (C-N); 144.2; 134.9; 133.3; 131.8; 130; 128.8; 127.5; 125.8; 124.1; 122.6; 120.2; 112.6.

IR Nujol (cm^{-1}): ν(C=O) 1724, ν(C=N) 1652.

ESI: *m/z*: 308.1 [**L** + H]$^+$; 330.1 [**L** + Na]$^+$.

*IV.4.5.2 Bis(1-naphthylimino)acenaphthene zinc dichloride (**1**)*

The bis(1-naphthylimino)acenaphthene zinc dichloride complex was prepared in a manner similar to that reported in the literature.[8] A suspension of acenaphthenequinone (2 g, 11 mmol) and $ZnCl_2$ (1.71 g, 12.5 mmol) was prepared on glacial acetic acid (15 mL). The 1-aminonaphtalene (3.6 g, 25 mmol) was added and the reaction mixture was refluxed under stirring for 30 min. Then it was let to cool down to room temperature, and a purple solid precipitated. The solid was separated by filtration and washed with cold acetic acid (2 x 10 mL). Then it was washed with diethyl ether (5 x 10 mL), to remove all the remaining acetic acid, and dried under vacuum, giving 5.2 g of analytically pure purple product. Yield: 83%.

Anal calcd (%) for $C_{32}H_{20}Cl_2N_2Zn$ (M=568.81): C, 67.57; H, 3.54; N, 4.92. Found: C, 66.94; H, 3.59; N, 4.74.

^{1}H NMR (400 MHz, CD_2Cl_2, 293 K): 8.16-8.14d (2H, Ar); 8.11-8.07m (6H, Ar); 7.76-7.54m (8H, Ar); 7.43-7.39tt (2H, Ar); 6.80-6.78d (1H, Ar, J=7.35 Hz); 6.71-6.69d (1H, Ar, J=7.35 Hz).

^{13}C NMR (400 MHz, CD_2Cl_2, 293 K): 165.5 (C=N); 146 (C-N); 141.5; 135; 133.2; 131.5; 129.4; 129.2; 129; 127.9; 127.8; 127.4; 127.3; 126.6; 126.5; 125.9; 125.7; 125.6; 123.7; 123.6; 118.4; 118.2.

IR Nujol (cm^{-1}): ν(C=N) 1660, 1630.

MALDI-TOF-MS: 432.52 [**L1**]$^+$ 100 %, 533.4 [ZnCl(**L1**)]$^+$ 28%, 928.3 [Zn(**L1**)$_2$]$^+$ 9%.

ESI: *m/z*: 433.2 [**L1** + H]$^+$; 455.2 [**L1** + Na]$^+$; 928.3 [Zn(**L1**)$_2$]$^+$.

*IV.4.5.3 Bis(1-naphthylimino)acenaphthene (**L1**)*

The procedure for the synthesis of **L1** was the same as describe in the literature[22]: The Bis(1-naphthylimino)acenaphthene zinc dichloride (2 g, 3.3 mmol) was suspended in dichloromethane (200 mL), and a solution of potassium oxalate (0.181 g, 10 mmole) in water (10 mL) was added. The reaction mixture was left under strong agitation during 5 min. A white precipitate of $Zn(C_2O_4)$ was present, suspended in the aqueous phase. The two phases were separated and the organic layer was washed with water (3 x 20 mL), dried with $MgSO_4$, filtered and the solvent removed under vacuum, affording a red solid, 1.45 g. Yield of the crude product: 95%. The red solid was then dissolved in toluene and filtered. The toluene solution was concentrated and petroleum ether (b.p.: 110-130ºC) added, red crystals suitable for single crystal X-ray diffraction were formed while standing at room temperature.

Anal calcd (%) for $C_{32}H_{20}N_2$ (M = 432.51): C, 88.86; H, 4.66; N, 6.48. Found: C, 88.19; H, 4.97 N, 6.40.

^{1}H NMR (400 MHz, CD_2Cl_2, 293 K): 8.06-8.04d (2H, Ar); 8.0-7.98d (2H, Ar); 7.86-7.82t (4H, Ar); 7.63-7.55m (4H, Ar); 7.48-7.44t (2H, Ar); 7.26-7.22t + d overlapped (4H, Ar); 6.68-6.66d (2H, Ar, J = 7.29 Hz).

^{13}C NMR (400 MHz, CD_2Cl_2, 293 K): 162.4 (C=N); 148.9 (C-N); 142.3; 135; 131.7; 129.6; 128.6; 128.2; 127.2; 126.7; 126.3; 125.5; 125; 124.2; 124.0; 120.5; 112.7.

IR Nujol (cm^{-1}): ν(C=N) 1661, ν(C=N) 1628.

MALDI-TOF-MS: 432.6 $[\mathbf{L1}]^+$ 100 %, 864.5 $[2\mathbf{L1}]^+$ 9%.

ESI: *m/z*: 455.2 $[\mathbf{L1} + Na]^+$.

*IV.4.5.4 Bis (1-naphthylimino)acenaphthene palladium dichloride (**2**): Method A*

A suspension of acenaphthenequinone (0.21 g, 1.12 mmol) and $PdCl_2$ (0.2 g, 1.12 mmol) was prepared on glacial acetic acid (15 mL). 1-aminonaphtalene (0.32 g, 2.26 mmol) was added and the reaction mixture was refluxed under stirring for 30 min. Then it was left to cool down to room temperature, a red-orange solid precipitated. The solid was separated by filtration and washed with cold acetic acid (2 x 10 mL). Then it was washed with diethyl ether (5 x 10 mL), to remove all the remaining acetic acid. The dark red solid was dissolved in the minimum amount of CH_2Cl_2, filtered and a black powder ("black palladium") was left undissolved. The CH_2Cl_2 solution was concentrated by removal of the solvent under vacuum. Hexane was added and the solution left in the refrigerator. After one day, red crystals suitable for single crystal X-ray diffraction were formed. Yield 50%

Anal calcd (%) for $C_{32}H_{20}Cl_2N_2Pd$, (M = 609.84): C, 63.02; H, 3.31; N, 4.59. Found: C, 62.69; H, 3.84; N, 4.34.

^{1}H NMR (400 MHz, CD_2Cl_2, 293 K): 8.42-8.37m (2H, Ar); 8.14-8.12d (2H, Ar); 8.09-8.06t (4H, Ar); 7.76-7.62m (8H, Ar); 7.37-7.32tt (2H, Ar); 6.46-6.44d (1H, Ar); 6.41-6.39d (1H, Ar).

^{13}C NMR (400 MHz, CD_2Cl_2, 293 K): 177.3 (C=N); 148.2 (C-N); 142.5; 134.6; 133.2; 131.9; 129.9; 129.8; 129.6; 129.1; 127.9; 126.8; 125.9; 125; 123.5; 119.8.

IR Nujol (cm^{-1}): ν(C=N) 1618.

MALDI-TOF-MS: 432.6 [**L1**]$^+$ 100 %, 465.6 $[C_{24}H_{16}N_4Pd]^+$ 25%; 499.6 $[C_{24}H_{16}ClN_4Pd]^+$ 7.4 %, 537.5 [Pd(**L1**)]$^+$ 4%.

ESI: *m/z:* 432.2 [**L1**]$^+$; 610.03 [$PdCl_2$(**L1**)+H]$^+$

IV.4.5.5 Bis (1-naphthylimino)acenaphthene palladium dichloride (2): Method B

A suspension of $PdCl_2$, 0.3 g (1.69 mmol) in 50 mL of dry acetonitrile was warmed to 70 °C in argon atmosphere, to give a red solution. Then a solution of 0.73 g of **L1** (1.69 mmol) in acetonitrile (20mL) was added via cannula and the mixture refluxed for 1h. A red solid precipitated. After that, the mixture was cooled to 20 °C, and the solvent was partially removed and diethyl ether (20mL) was added to complete precipitation. The solid product was separated by filtration and washed with diethyl ether (2 x 20 mL). It was recrystallized from dichloromethane/hexane.0.92 g. Yield 89%.

Anal calcd (%) for $C_{32}H_{20}Cl_2N_2Pd$, (M = 609.84): C, 63.02; H, 3.31; N, 4.59. Found: C, 62.87; H, 3.36; N, 4.58.

^{1}H NMR (600 MHz, CH_2Cl_2 293 K): 8.42-8.37m (2H, Ar); 8.14-8.12d (2H, Ar); 8.09-8.06t (4H, Ar); 7.76-7.62m (8H, Ar); 7.37-7.32tt (2H, Ar); 6.46-6.44d (1H, Ar); 6.41-6.39d (1H, Ar).

^{13}C NMR (600 MHz, CH_2Cl_2 293 K): 177.4 (C=N); 148.3 (C-N); 142.5; 134.6; 133.2; 131.9; 129.8; 129.6; 129.2; 127.9; 126.8; 125.9; 124.9; 123.5; 119.8.

IR Nujol (cm^{-1}): ν(C=N) 1619.

MALDI-TOF-MS: 432.6 [**L1**]$^+$ 100 %, 465.6 $[C_{24}H_{16}N_4Pd]^+$ 16%; 499.6 $[C_{24}H_{16}ClN_4Pd]^+$ 3.52%, 537.5 [Pd(**L1**)]$^+$ 1%.

IV.5 Results and Discussion

IV.5.1 Synthesis and characterization

Attempts to obtain **L1** by direct reaction of 1-aminonaphtalene with acenaphthenequinone in methanol in the presence of formic acid, gives mono(1-naphthylimino)acenaphthene (**L**), independently of the stoichiometry (1:1) or (2:1) as red crystals in an almost quantitative yield, (Scheme IV.1).The single crystal X-ray structure of this compound was recently reported[40] but the full characterization has not been reported, therefore we include it, in order to compare with the bis(1-naphthylimino)acenaphthene, **L1**.

To be able to obtain bis(1-naphthylimino)acenaphthene, **L1**, the following method was adopted: firstly the bis(1-naphthylimino)acenaphthene zinc dichloride complex **1** was prepared in a manner similar to that reported in the literature[8] in 83% yield, by the reaction of 1-aminonaphtalene and acenaphthenequinone in a 2:1 stoichiometry, using the "template method", in the presence of $ZnCl_2$.

Secondly, subsequent demetallation of the ligand was obtained by treating a CH_2Cl_2 solution of [$ZnCl_2$**(L1)**] with an aqueous solution of potassium oxalate, to lead free **L1** in almost quantitative yield. It was then recrystallized from toluene/petroleum ether to yield red crystals, suitable for X-ray diffraction structure determination. The molecular structure of **L1** will be discussed below.

Scheme IV.1 Synthesis of ligand **L** and **L1**. i) Ethanol/Formic acid, ii) 1-$ZnCl_2$/Acetic acid, 2-Potassium oxalate.

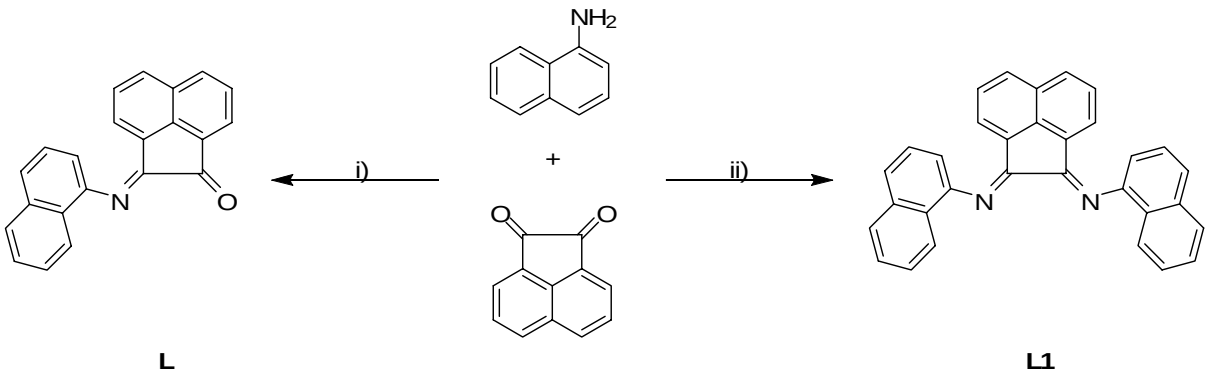

L **L1**

The complex bis(1-naphthylimino)acenaphthene palladium dichloride, **2**, was obtained by two different synthetic methods (A and B). In method A compound **2** was obtained in a manner similar to that of the zinc complex, using the "template effect", in a 50% yield. Presence of "black palladium" in the reaction due to metallic reduction, can explain this low yield. To try to improve this yield a second route was performed. Activation of $PdCl_2$, by refluxing it in acetonitrile, to give complex $[PdCl_2(NCCH_3)_2]$, as a non isolated intermediate, followed by addition of **L1** gave **2** in 89% yield. We could grow red-orange single crystals of the *anti* isomer of **2** from CH_2Cl_2/hexane from the crude of the reaction of method A, and the solid state structure was determined by X-ray diffraction. The molecular structure of **2** is discussed in the crystallographic section.

The FT-IR spectrum of **L1**, recorded in Nujol, shows bands assigned to C=N stretching vibrations in the region, ν = 1661-1628 cm^{-1}, while the IR spectrum of **L** shows frequencies at 1725 and 1652 cm^{-1} corresponding to C=O and C=N stretching vibrations, respectively. In the case of the metal complexes the FT-IR spectra display medium absorption bands in the region ν = 1660-1619 cm^{-1}, assigned to ν(C=N). The bands in the complexes are shifted to lower wave numbers, with respect to the free ligand, which is a criterion of the coordination of both diimine nitrogen atoms of the α-diimine ligands to the metallic ion. Selected IR absorption bands are listed in the experimental part. In the free ligand **L1** and in its metallic complexes *syn* and *anti* isomers are possible. The *syn* and *anti* isomers are formed due to the different orientation of the naphthyl-N=C units: the chiral *anti* conformation having the two 1-naphthyl groups on different sides of the acenaphthenequinone plane, and the achiral *syn* conformation on the same side.

The free ligands **L** and **L1** and the metallic complexes of **L1** (**1** and **2**) were studied by ^1H, ^{13}C, ^1H-^1H COSY, ^1H-^{13}C HSQC, ^1H-^{13}C HSQC-TOCSY and ^1H-^1H NOESY NMR spectroscopies. All the recorded spectra are included in the supplementary materials Figures SM IV.1 to SM IV.12. Comparison of the ^{13}C-NMR spectra of **L** and **L1** shows differences, since **L** shows a peak at δ 189.9 ppm (C=O); which is not present in the ^{13}C NMR spectrum of **L1**. Inspection in detail of the ^1H- and ^{13}C-NMR spectrum at 293 K of **L1** in CD_2Cl_2 solution see Figure SM IV.3, (supplementary material) shows that only a set of signals are present indicating that the *syn* and *anti* conformers are in fast exchange at that temperature on the NMR time scale. The variable-temperature ^1H NMR spectrum of **L1** was done at

temperatures from 223 K to 298 K, at 400 MHz in CD_2Cl_2, and it is shown in the supplementary materials Figure SM IV.13. The most important changes observed are in the region from 8.1 to 7.9 ppm, where two doublets are transformed into a triplet and in the region from 6.8 to 6.6 ppm, where a doublet shifts to higher field. The transformation of the two doublets into a triplet can be explained by their overlapping. These signals shifting is a fact normally encountered by lowering the temperature of the NMR sample solution. No further splitting was found therefore interconversion between the *syn* and *anti* isomers takes place at this temperature range.

By comparison of the ^{1}H NMR spectra of the metallic complexes **1** and **2** synthesized by the "template method", with that of **L1**, (Figure SM IV.14) we can see a duplication of the signals indicating the presence of two isomers *syn* and *anti* in a 1:1 ratio. In the case of the palladium complex **2**, the ^{1}H NMR spectra of the crude products obtained by methods A and B are different. The differences can be attributed to the existence of both isomers *syn* and *anti* in solution in a different proportion. In fact the spectra are identical in the chemical shifts, but different in the relative integration of the peaks. This is more apparent in the region 7.4-7.3 ppm and 6.5-6.3 ppm where we can see two superposed triplets and two doublets respectively. In Figure SM IV.15 is shown the amplified 7.5 to 6 ppm region of compounds **1** and **2** (obtained by method A and B).

Only the selected peaks in Figure SM IV.15 are assigned unequivocally. The doublets in the region of 6.5-6.3 ppm can be assign to the H(1,6) and the triplets in the region 7.4-7.3 ppm can be assign to the H(2,5) of the acenaphthene ring, by ^{1}H, ^{13}C, ^{1}H, ^{1}H COSY, ^{1}H, ^{13}C HSQC, ^{1}H, ^{13}C HSQC-TOCSY and ^{1}H, ^{1}H NOESY NMR experiments.

Scheme IV.2 NMR numbering of the compounds, R = O or N-Naphthyl.

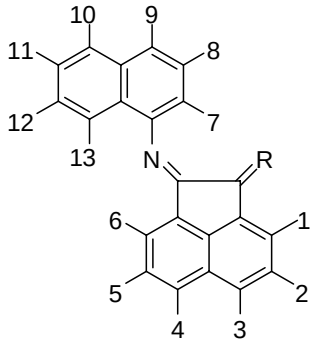

We can see therefore that in the crude of **2** obtained by the "template method", (method A) the doublets showed equal intensity, while when the product was obtained by the activation of the palladium chloride and further reaction with **L1**, (method B) the ratio in the intensities was different and equal to 1:3. That can be interpreted considering that in both reactions we get a mixture of both possible isomers *syn* and *anti* in a different rate, in the "template method" the probability of forming the isomer *syn* or *anti* is the same, as in the case of the complex **1** (ratio 1:1), when the reaction is done by the method B one orientation seems to be favored over the other, giving one of the isomers in a higher proportion (1:3). Once the isomers are formed there is no interconversion in solution as it is discussed in the performed theoretical calculations.

IV.5.2 Crystal structures description

The molecular structures of **L1** and **2** and the associated atom-numbering schemes are depicted in Figure IV.1 and IV.2 respectively. The free bis(1-naphthylimino)acenaphthene ligand (**L1**) exhibits the (*E,Z)* isomeric preference instead of the common *(E,E)* pattern in the crystalline state, like others α-diimine compounds.[23, 41, 42] The different configuration of the imino units do not lead to important differences in the bond lengths [C1-N1 1.270(3), N1-C101 1.419(3), C11-N2 1.264(3), N2-C201 1.440(3) Å] being similar to those in related α-diimines.[23, 41-44] The naphthalene moieties are almost perpendicular to each other, being the value of the dihedral angle 88.31(6)º. Concerning the arrangement of the naphthalene moieties in relation to the bis(imino)acenaphthene skeleton, the ligand shows *anti* orientation and the dihedral angles between the naphthalene planes and the bis(imino)acenaphthene are 57.82(5)º (*Z* imine naphthalene) and 71.45(5)º (*E* imine naphthalene).

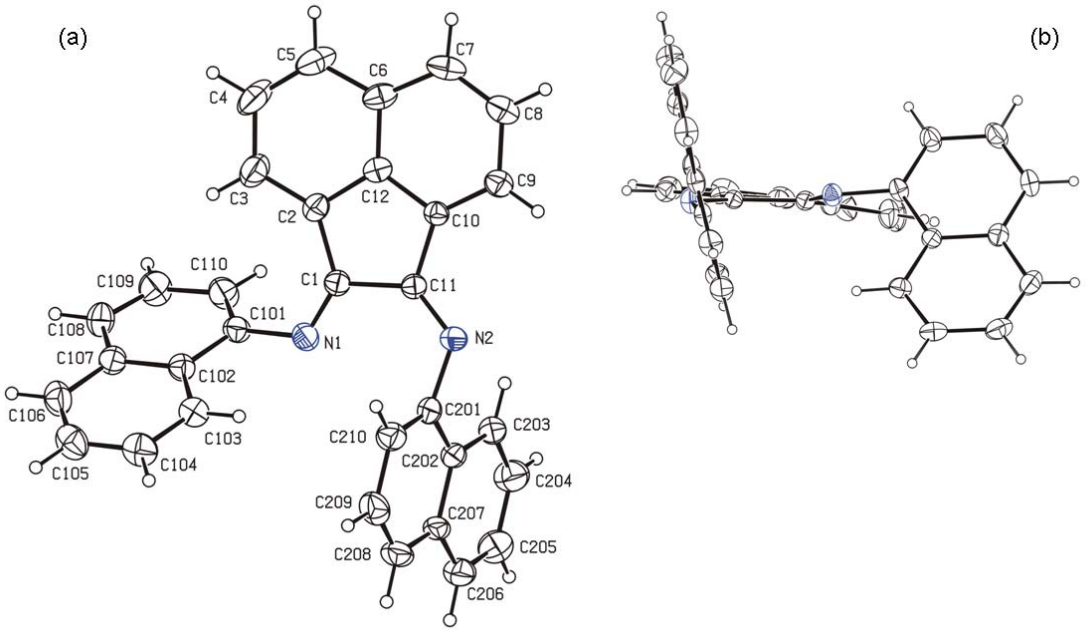

Figure IV.1 Displacement ellipsoid representations at the 30% probability level of **L1** (a) perpendicular and (b) parallel to the bis(imino)acenaphthene unit.

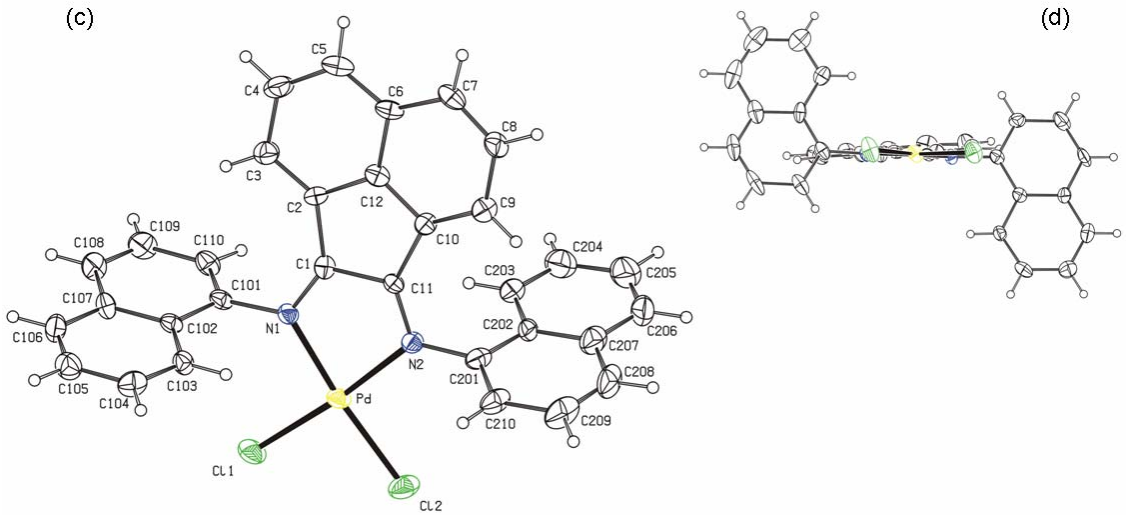

Figure IV.2 Displacement ellipsoid representation at the 30% probability level of **2** (c) perpendicular and (d) parallel to the bis(imino)acenaphthene unit. Selected bond lengths (Å) and angles (º) for **2**: Pd-N1 2.040(6); Pd-N2 2.050(6); Pd-Cl2 2.273(2); Pd-Cl1 2.278(2); N1-Pd-N2 81.4(2); N1-Pd-Cl2 174.59(18); N2-Pd-Cl2 93.30(19); N1-Pd-Cl1 93.51(18); N2-Pd-Cl1 174.60(19); Cl2-Pd-Cl1 91.75(9).

The coordination at the palladium in **2** is quite distorted from a regular square plane, where the relatively small N1-Pd-N2 bond angle of 81.4(2)º is a result of chelating ligand

steric constraints. The bond angles and distances in the Pd(II) coordination plane (Figure IV.2) are very similar to the found values in other α-diimine-$PdCl_2$ complexes.[43-46] Comparison with the structural data of the free bis(1-naphthylimino)acenaphthene (**L1**) (Figure IV.1) reveals some slight changes in the ligand which must be ascribed to the combined effects of changing the aromatic group on the imine N atoms and coordination to the palladium center. The imine C=N bonds C1-N1 and C11-N2 of 1.283(8) and 1.295(9) Å, respectively, are slightly longer than in the free ligand. Furthermore, upon coordination, the distance between the imine C atoms C1-C11 has decreased [1.531(3) Å in **L1** to 1.492(10) Å in **2**] and the diimine plane is more flat, the torsion angle N1-C1-C11-N2 is 10.4º in **L1** and 4.3º in **2**.[47] *E,Z* to *E,E* isomeric conversion of the α-diimine accompanies the coordination to the palladium atom. In this case both naphthalene units, practically parallel to each other [dihedral angle of 6.72(21)º], are almost perpendicular to the bis(imino)acenaphthene plane [dihedral angles of 70.97(14) and 65.91(14)º] and show also *anti* orientation.

The nature of the ligand allows the formation of supramolecular architectures based on C-H···π[48] in **L1** and on π···π[49] interactions in **2**. Each **L1** molecule is joined to seven neighbouring molecules through C-H···π interations (Cg(centroid)···H distance range 2.72-2.83 Å) generating a complicated 3D organization (Figure IV.3a). Supramolecular dimers of **2** are formed by π···π interactions involving the acenaphthene moieties ([C···C] = 3.547 Å, dihedral angle α: 2.56º). π···π interactions among the naphthalene units (d[C···C] = 3.400 Å, dihedral angle α: 6.75º), join the dimers, resulting in an infinite 1D ladder-like chain (Figure IV.3b).

(a)

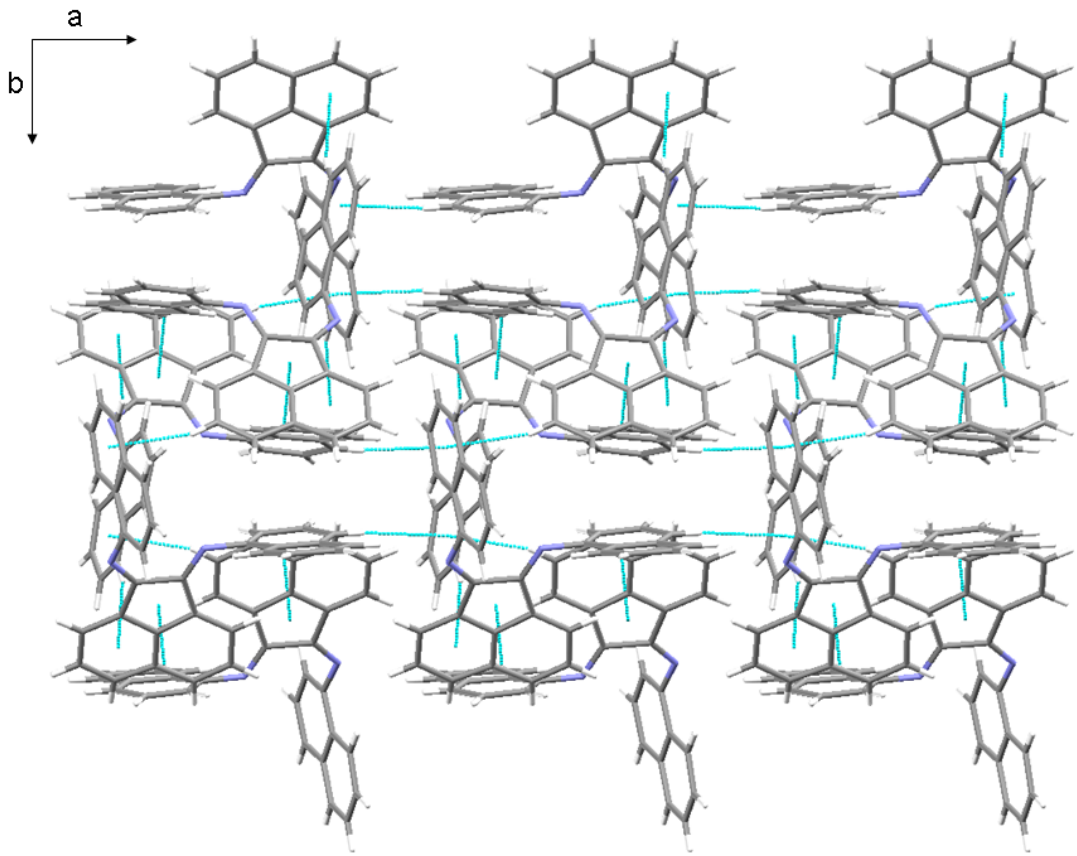

(b)

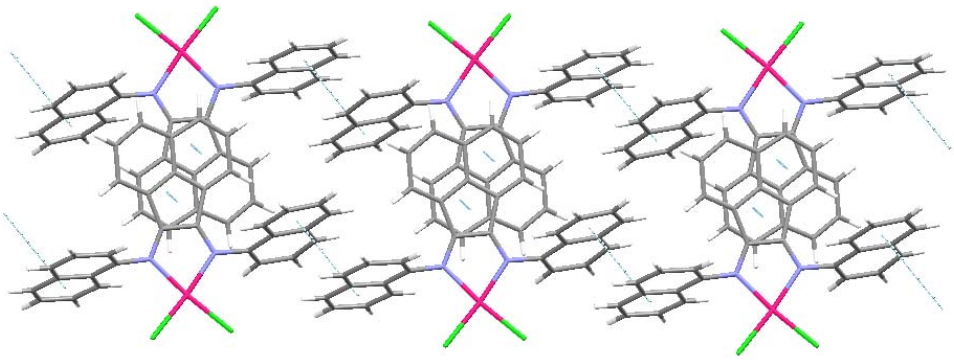

Figure IV.3 (a) Fragment of the infinite 3D network formed through C-H···π interactions among **L1** molecules, showing the packing in the *ab* plane. (b) Fragment of the infinite 1D ladder-like chain formed along of *a* axis through π···π interactions among molecules of **2**.

Table IV.1 Crystal and structure refinement data for **L1** and **2**.

	L1	**2**
Empirical formula	$C_{32}H_{20}N_2$	$C_{32}H_{20}Cl_2N_2Pd$
Formula weight	432.50	609.80
Crystal system; Space Group	Monoclinic; $P2_1/c$	Monoclinic; $P2_1/c$
Unit cell dimensions (Å, º)	a = 11.349(2)	a = 11.810(4)
	b = 15.356(3)	b = 11.816(4)
	c = 13.820(3)	c = 18.125(6)
	β = 109.032(4)	β = 95.041(6)
Volume ($Å^3$)	2276.8(8)	2519.6(15)
Z; ρ_{calc} ($g.cm^{-3}$)	4; 1.262	4; 1.608
F(000)	904	1224
Crystal size (mm^3)	0.49 x 0.40 x 0.18	0.24 x 0.19 x 0.07
Absorption coefficient (mm^{-1})	0.074	0.974
θ range (º)	1.90-28.01	1.73-27.98
Max./min.transmission	-	1.000/0.759
Reflections collected	10513	13536
Independent reflections (R_{int})	4531 (0.0477)	5651 (0.0990)
Final *R* indices [I > 2σ(I)]	R1 = 0.0623	R1 = 0.0943
	wR2 = 0.1476	wR2 = 0.1372

IV.5.3 Spectrophotometric studies

Compound **L1** is provided by two conjugated imine functions, but remarkably different from others diimine compounds such as 2,2-bipyridine or 1,10-phenanthroline. In our case, the exocyclic nature of both imine bonds, out of the heteroaromatic ring systems, impose better σ-donating and π-accepting properties as compared with bipyridine or phenanthroline.[50, 51] This phenomenon modulated the photophysical properties of this type of compounds.

The absorption spectra of **L1** in CH_2Cl_2 solution at 298 K at concentrations between $1.0E^{-6}$ to $1.0E^{-4}$ M are reported in Figure SM IV.16 (A). Two well defined bands are observed

in the spectrum. The first transition of compound **L1** appearing in the range $400 < \lambda < 550$ nm can be readily assigned to intraligand transitions of the free diimine compound as previously reported for similar BIAN diimine ligands,[52] whilst the second one at $250 < \lambda < 350$ nm can be assigned to the naphthalene moiety.[53-55] The naphthalene absorption contribution is also observed in Figure SM IV.17 (Supplementary material) where is represented the absorption spectra of both organic precursor of ligand **L1**: 1-naphthylamine and acenaphthenquinone. In both spectra, obtained in dichloromethane solution at $1.0E^{-5}$M at room temperature, the absorption band appear in the region $250 < \lambda < 350$ nm. The second band observed for ligand **L1** in the range $400 < \lambda < 550$ nm, is also present but with less intensity for the monoimine ligand **L** (Figure SM IV.17). The absence of bands in the infrared region of the absorption spectra of **L1**, confirms that no anionic states due to reduction are presents in this BIAN-derivate ligand.[56]

In Table IV.2 are summarized all optical data for ligands **L** and **L1** and the Zn(II) and Pd(II) complexes of **L1**. Figure SM IV.16 (B) shows the absorption spectra at different concentrations of complex **2** in freshly dichloromethane solution. Bands at 266, 327, 400*sh,* and 542*sh* nm are observed. The shoulder observed at 542 nm could be assigned to the MLCT transitions from the metal centre to the π* orbital of **L1**. The three previous bands at 266, 327 and 400 nm, presents also in the free ligand, are red shifted when compared with **L1**, and could be assigned to the π-π* transitions in the naphthalene moieties (intraligand transitions) observed in the free diimine compound.

Table IV.2 Optical Data for **L**, **L1** and its Zn(II) and Pd(II) complexes in freshly prepared dichloromethane solution at room temperature.

Absorption [a]	
Compounds	λ_{max}/ nm (10^{-3} ε, M^{-1} cm^{-1})
L	254 (37.5); 303 (19.3); 372*sh* (2.2); 457 (1.8)
L1	305 (42.3); 432 (5.2)
[$ZnCl_2$(L1)]	266 (426.4); 325*sh* (145.0); 468 (5.1)
[$PdCl_2$(L1)]	266 (478.6); 327 (373.7); 400*sh* (10.1); 542*sh* (1.7)

[a] in non degassed solutions.

sh = shoulder

The stoichiometry of the complex **2** has been obtained from a metal titration experiment using a freshly dichloromethane solution. This experiment is shown in Figure SM IV.18. The band centered at 300 nm is 16 nm red shifted after metal complexation. This effect confirms that metal complexation takes place. Detailed inspection of the inset in Figure SM IV.18, shows a plateau reached after the addition of an equivalent amount of Pd(II), which suggests that each **L1** unit is coordinated to one Pd(II) ion. This stoichiometry was confirmed in the solid state by the X-Ray structure.

Both ligands **L** and **L1** are not luminescent in dichloromethane. The expected fluorescence emission of **L1** as a naphthalene derivative is totally quenched even when the ligand is complexed to Zn(II).[57, 58] This behavior is probably due to the absence of any spacer between the emissive unit (naphthalene chromophore) and the chelation unit (imine nitrogen) that permits a fast electron transfer process from the lone pair of electrons presents in the imine nitrogen atoms to the emissive naphthalene chromophores.[59]

IV.5.4 Mass Spectrometry studies

Both organic ligands, **L** and **L1** and the Zn(II) and Pd(II) complexes of **L1**, has been study by mass spectrometric techniques: MALDI-TOF-MS, TOF-MS-EI and TOF-MS-FD. Samples were dissolved in freshly dichloromethane (1 μg/μL), and 1 to 2 μL of the corresponding solution was spotted on a well of a MALDI-TOF-MS sample plate and allowed to dry. For TOF-MS-EI$^+$ and TOF-MS-FD$^+$ the sample was introduced directly.

In all MALDI-TOF-MS studies no matrix was added, using the organic ligand as new *in situ* MALDI-TOF-MS matrix.[60] In this case, the measurements were performed in the reflector positive or negative ion mode, with a 20 kV accelerating voltage, 80 % grid voltage, 0.005 % guide wire, and a delay time of 200 ns.

Figure SM IV.19 shows the TOF-MS-FD$^+$ spectra of the complex **2**. The spectra shows peaks at 610.0 *m/z* assigned to the complex $[PdCl_2(\mathbf{L1})]^+$, and the fragmentations at 575.6, 538.0 and 433.1 *m/z*, assigned to the fragments $[PdCl(\mathbf{L1})]^+$, $[Pd(\mathbf{L1})]^+$, and $[\mathbf{L1}]^+$. At high mass region a peak corresponding to the dimeric species $[Pd(\mathbf{L1})_2]^+$ at 971.7 *m/z* also

appear. Similar peaks and fragmentations have been observed by MALDI-TOF-MS spectrometry (See Figure SM IV.20).

The peak at 610.0 m/z assigned to the complex $[PdCl_2(\mathbf{L1})]^+$, is shown in Figure SM IV.21 together with the isotopic theoretical model calculated with the software MASS LYNX by micromass, confirming our attribution.

In Figures SM IV.22 and SM IV.23 are shown the TOF-MS-EI and MALDI-TOF-MS spectra for ligands **L** and **L1** respectively. In both cases the molecular ion peaks at 307.09 *m/z* and 431.58 *m/z* assigned to $[\mathbf{L}+H]^+$ and $[\mathbf{L1}+H]^+$ respectively, are observed. Fragmentation peaks and peaks due to the formation of dimeric species for **L1** are also observed. Both spectra are very clear, suggesting the potential use of both organic compounds as MS matrices.

The MALDI-TOF-MS spectra of complex **1**, is also shown in supplementary material (Figure SM IV.24). Peaks at 532.4 and 433.5 *m/z*, assigned to the fragments $[ZnCl(\mathbf{L1})]^+$ and $[\mathbf{L1}]^+$ are observed. A peak at 930.3 *m/z*, assigned to the dimeric complex $[Zn(\mathbf{L1})_2]^+$ is also observed.

IV.5.5 Theoretical study

Density functional calculations have been performed in order to determine the relative stability of each isomer of compound **2**. The optimized molecular geometry is very similar in both isomers, and only a few differences can be found. In general, distances are identical in both isomers (*i.e.*, Pd-N and Pd-Cl are 2.12 and 2.31 Å, respectively), and angles around the palladium atom change only 0.1º. More significant is the variation in the angle between acenaphthylene and naphthyl groups, defined by τ in Scheme IV.3 (104.4 and 99.8º for *anti* and *syn*, respectively).

Scheme IV.3 Definition of parameter τ to describe the relative orientation between acenaphthylene and naphthyl groups.

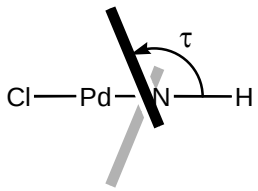

The full optimization of molecular structure shows that the *anti* isomer is more stable than *syn*-[$PdCl_2$(BIAN)]. However, the difference of energy is only 0.07 kJ·mol^{-1}, and we considerer both conformers as isoenergetic. Behind their similar stability, one can anticipate the possible formation of both complexes in solution. This result can be confirmed by a search of complexes having BIAN ligand, [ML_n(BIAN)], in *Cambridge Structural Database*, in which both isomers crystallize when the substituents are asymmetric: *anti*[23, 25, 61, 62] or *syn*.[23, 25, 63]

Similarly to complex [$PdCl_2$(BIAN)], free ligand BIAN can present *anti* and *syn* conformers, having same relative stability (*anti* is the most stable by 0.06 kJ·mol^{-1}) and similar structural parameters (*i.e.*, τ ≈ 125º). The interconversion between both isomers can be possible by rotating an N-$C_{naphthyl}$ bond. Consequently, a transition state is located having one coplanar naphthyl group to acenaphthylene rings (τ is 177 and 125º for each naphthyl group), and its energy, +18.7 kJ·mol^{-1}, is accessible a room temperature (Figure IV.4). However, when $PdCl_2$ fragment is introduced into the ligand, a corresponding transition state for the conversion between *anti* and *syn*-[$PdCl_2$(BIAN)] is computably unavailable, probably due to the proximity of the naphthyl moiety to the chloride ligand in a square-planar geometry. However, one cannot reject to obtain both isomers in different rates, by changing the experimental conditions as it is indicated above. In agreement, fluxionality has been detected by ^{1}H NMR spectroscopy in compounds having metallic fragments with less steric requirements such as Ge (R = 2,6-diisopropylphenyl).[25] Moreover, dynamic behavior in Mg or Ca complexes (R = 2,5-di-tert-butylphenyl) having terminal ligand perpendicularly to BIAN ligand has also been found.[23]

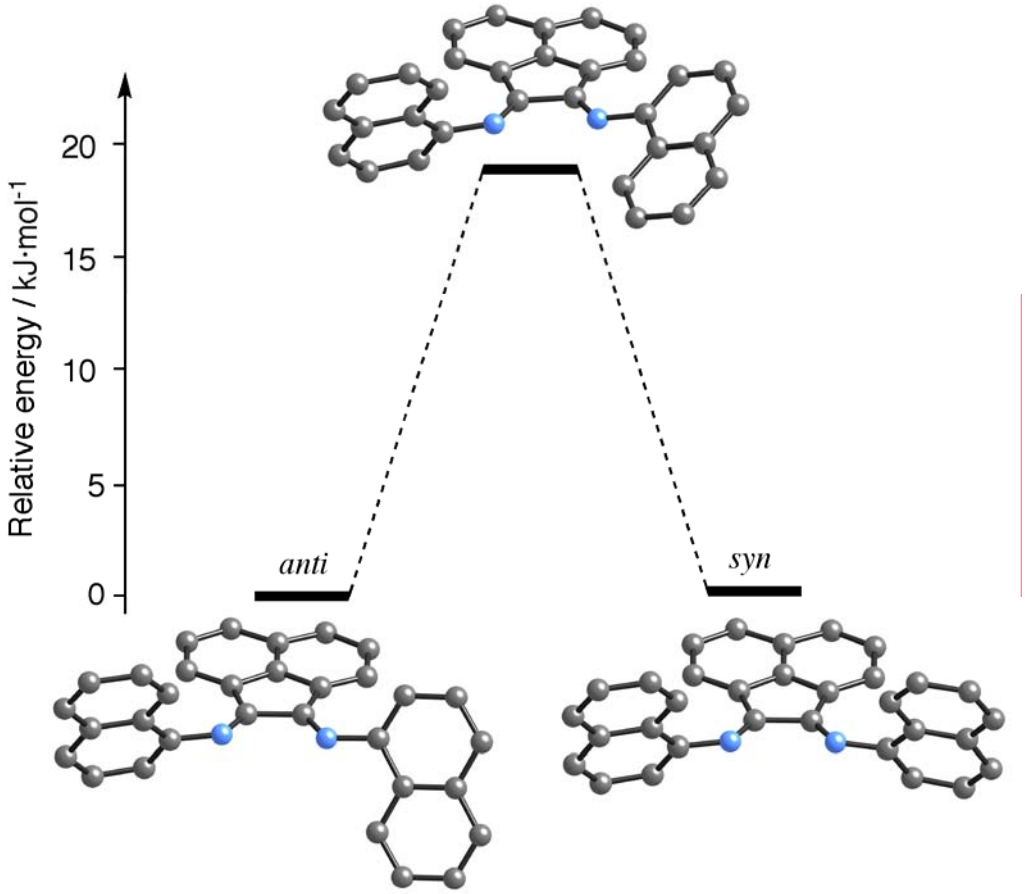

Figure IV.4 Energetic profile for free BIAN ligand. Atomic coordinates are available from Table SM IV.2.

To evaluate the possible conversion between *anti* and *syn* isomers, we have calculated the energy profile as a function of the torsion angle for N-$C_{naphthyl}$ bond, τ_1. In these partial optimizations, only this torsion angle is kept constant for one bond, and all other geometric parameters have been relaxed including the second N-$C_{naphthyl}$ bond, τ_2. As it is found in full optimization, one minimum is found for each conformer (*ca.* ~ 100º). When τ_1 angles are closed to transition state in the complex, such as 160º, the molecular energy increases ~ 40 kJ·mol^{-1} from the minimum in both conformations, and an estimation for coplanar rings (τ_1 = 180º) could reach values near to +80 kJ·mol^{-1}. In this case, the process is unfavoured and we will anticipate that this reaction does not occur. Finally, we notice that the inverse rotation by approaching a naphthyl moiety to acenaphthylene (τ = 0º) is always higher in energy.

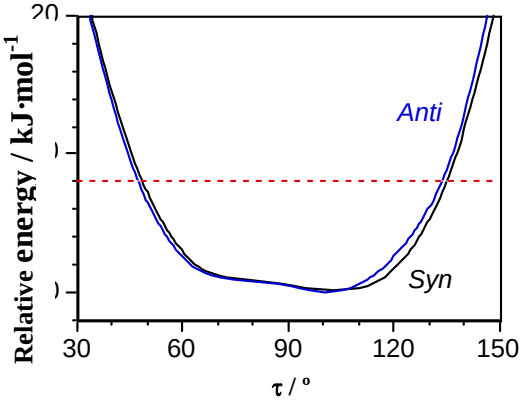

Figure IV.5 Energy as a function of τ angle in both isomers of compound [$PdCl_2$(BIAN)]. Zero values for each conformer are taken arbitrary to the minimum.

The second information can be obtained from Figure IV.5 it is due to the smooth profile for both conformers. If a limit of 8 kJ·mol^{-1} is assumed for intermolecular packing forces, available values for τ would be between 50 and 130º. Consequently, wide experimental range can be expected for τ by 80º, in agreement with experimental data having values of 68 and 109º for **2**. However, in an attempt to compare our results with structural data, we found impossible to define the relative orientation for symmetric substituent in *N*,*N*'-acenaphthylene ligand and differentiate τ and its complementary 180-τ (there are not significant data for asymmetric substituents) reduces the range to 50 – 90º. In accordance, experimental data in *Cambridge Structural Database* for related complexes show that most expected values are maxima between 70º and 90º, and range decreases when square-planar complexes are only considered (75 – 85º, see Figure SM IV.25). Moreover, the variation of τ for one naphthyl group has small influence in the other group. The second naphthyl prefers angles about 100 or 110º, except when τ is changed too. Experimental values show that differences between both substituents are normally less than 15º (Figure SM IV.26).

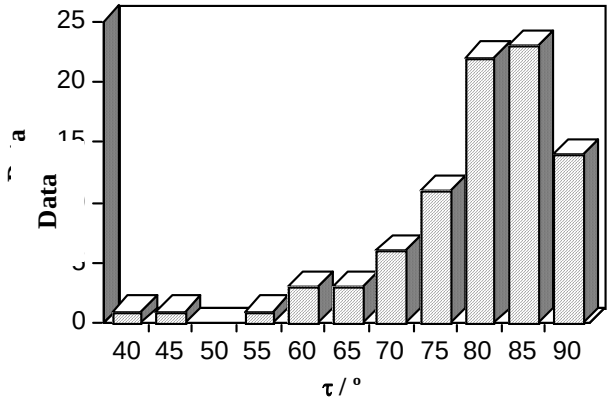

Figure IV.6 Experimental τ values in complexes [ML_n(BIAN)] in crystal structures having analogous ligand as BIAN. Data are retrieved for crystal structures from *Cambridge Structural Database*.

We continue searching other fragments ML_n attached to BIAN ligand in order to compare the geometry and relative stability of both conformers for complexes [ML_n(BIAN)]. These fragments are neutral and have different geometry in order to estimate the importance of external ligands in the coordination sphere of metal. The studied cases are: (*a*) Ge; (*b*) AuCl and CuCl; and (*c*) $NiCl_2$, $CoCl_2$, and $ZnCl_2$; for n = 0, 1 and 2, respectively. These results are shown in Table IV.3.

Table IV.3 Selected structural parameters for optimized complexes having BIAN ligand in both conformations. Distance are in Å, angles in degrees and energies kJ·mol^{-1}.

M	Geometry	Confor-mation	τ	M-N	M-Cl	N-M-N	N-M-Cl	Cl-M-Cl	ω[d]	Energy[e]
-	Free Ligand	*Anti* *Syn*	125.2 124.7	- -	- -	- -	- -	- -	- -	+0.06
Ge	Bent	*Anti* *Syn*	72.4 71.1	1.932 1.932	- -	- -	- -	- -	- -	-0.31
AuCl	Linear[a]	*Anti* *Syn*	97.8 95.8	2.112 2.110	2.318 2.318	66.9 66.9	175.0 174.9	- -	- -	+0.24
CuCl	Trigonar[b]	*Anti* *Syn*	115.7, 130.3 122.9	2.004, 2.398 2.151	2.151 2.165	76.7 78.5	160.9 122.3 140.8	- -	- -	+2.15
$PdCl_2$	Square-planar	*Anti* *Syn*	99.8 104.4	2.115 2.117	2.311 2.312	79.5 79.4	94.4 94.5	91.8 91.6	0.1 3.8	+0.07
$ZnCl_2$	Tetrahedral	*Anti* *Syn*	121.5 114.3	2.231 2.235	2.352 2.351	77.0 77.0	103.4, 112.5 105.8, 110.0	133.9 133.8	79.1 90.0	+2.86
$NiCl_2$[c]	Tetrahedral	*Anti* *Syn*	116.0 66.2, 112.1	2.088 2.077	2.249 2.248	81.7 81.8	98.9, 109.1 102.6, 104.9	142.9 143.3	79.1 85.8	+1.14
$CoCl_2$	Tetrahedral	*Anti* *Syn*	123.0 116.1	2.142 2.147	2.242 2.241	80.5 80.5	104.9, 114.9 108.2, 111.8	127.1 126.8	78.9 89.5	+3.29

[a] Second N-donor is not coordinated (N•••Au not-bonded distance are 2.932 and 2.936 Å, respectively). [b] Coordination of BIAN for *anti* isomer is asymmetric. [c] *Syn* isomer has two "different" orientations for naphthyl groups. [d] Angle ω is defined between BIAN and MCl_2 planes. [e] Positive values means that anti isomer must be the most stable.

In general, differences in geometric parameters between isomers are less than 0.01 Å for distances and 0.3º for bond angles, and we can suppose that energetic differences are introduced by only the coordination of metallic fragment ML_n. Germanium compound has an

important behavior with respect to transition metal complexes: the torsion angles τ is always less than 90º in both isomers. Only in this case, *syn* conformer is more stable than *anti* one, by only 0.3 kJ·mol^{-1}. We can confirm that the presence of Ge binding to *N*-donors does not change the small differences between isomers.

Similar result has been obtained by [AuCl(BIAN)]. Gold atom presents a lineal coordination (N-Au-Cl ≈ 175º) being coplanar to acenaphthylene ligand. The small influence due to the presence of chloride ligand is reflected in the small energetic difference between both structures, although *anti* form is in this case the most stable. This difference increases to 2 kJ·mol^{-1} for [CuCl(BIAN)], probably for the different coordination number in *syn* and *anti* isomers, having perfectly trigonal and intermediate geometries around copper atom (Scheme IV.4a).

Scheme IV.4 Molecular diagram for some complexes [ML$_n$(BIAN)] discussed in the text: (a) *anti*-[CuCl(BIAN)]; (b) *anti*-[MCl$_2$(BIAN)] (M = Zn, Co, Ni); and, (c) *syn*-[NiCl$_2$(BIAN)].

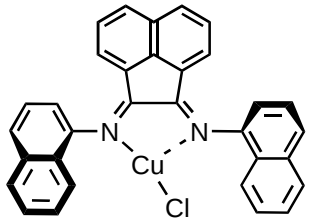

(a)

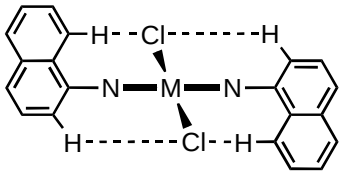

(b)

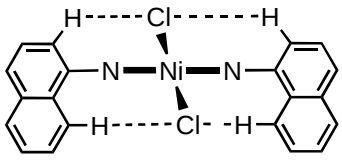

(c)

Calculations have also been performed for complexes of Zn(II), Co(II), and Ni(II) with tetrahedral environment. Structures for $ZnCl_2$ and $CoCl_2$ can be considered analogues to $PdCl_2$ square-planar complex, by changing the environment of transition metal. The energetic

difference is ~ 3 kJ·mol^{-1}, where *anti* conformer is stabilized by the best directionality of the hydrogen bonds such as (C)H···Cl(M) [64] (see Scheme 4b: H$^{(8)}$···Cl are ~ 2.87 and 2.80 Å for Zn and Co). As a result MCl_2 fragments are perpendicular to BIAN for *syn* conformer, but those are turned about 11º for *anti* one (Scheme IV.4b).

A special mention is done for Ni(II), which it can present two spinomers.[65] Six structures have been published having BIAN ligand, and its coordination is essentially tetrahedral, and only one compound with π-acid ligand such as allyl has square-planar environment. Consequently, we have considered tetrahedral geometry for [$NiCl_2$(BIAN)], in which relative energy decreases until 1.1 kJ·mol^{-1}. Since *anti* form is analogous to that of Co and Zn complexes (H$^{(8)}$···Cl ≈ 2.73 Å), *syn* one presents an asymmetric orientation for naphthyl groups (τ = 112 and 66º), being the only structure together with both of Ge compounds having τ < 90º. The molecular geometry implies two different short contacts for each chlorine atoms (H$^{(8)}$···Cl ≈ 2.77 and H$^{(2)}$···Cl' ≈ 2.89 Å) and a deviation from perpendicularity of 4º. These distortions from idealized geometry, such as Cl-Ni-Cl angle about 143º, can be assigned to a no spherical distribution of electronic density for a d^8 ion in tetrahedral environment.[66]

Finally, any octahedral complexes were calculated, however simple models suggest that conclusions obtained for square-planar ones, can be applied to these compounds.

IV.6 Conclusions

A new rigid bidentate ligand bis(1-naphthylimino)acenaphthene, **L1**, and their Zn(II) and Pd(II) complexes [$ZnCl_2$(**L1**)], **1**, and [$PdCl_2$(**L1**)], **2**, were synthesized. **L1** was prepared by the "template method", reacting 1-naphthyl amine and acenaphthenequinone in the presence of $ZnCl_2$, giving **1**, that was further demetallated. Reaction of 1-naphthyl amine with acenaphthenequinone and $PdCl_2$ afforded dichloride bis(1-naphthyl)acenaphthenequinonediimine) palladium, **2**. **L1**, **1** and **2** were obtained as a mixture of *syn* and *anti* isomers. **2** ,was also obtained by reaction of $PdCl_2$ activated by refluxing it in acetonitrile followed by addition of **L1,** by this route also a mixture of *syn* and *anti* isomers was obtained, but in a different rate. All compounds have been characterized by elemental

analyses, MALDI-TOF-MS spectrometry, and by IR, UV-vis, ^{1}H, ^{13}C , ^{1}H-^{1}H COSY, ^{1}H-^{13}C HSQC, ^{1}H-^{13}C HSQC-TOCSY and ^{1}H-^{1}H NOESY NMR spectroscopies when applied.

The solid state structures of **L1** and the *anti* isomer of compound **2** have been determined by single crystal X-ray diffraction. The coordination at the palladium in the *anti* isomer of compound **2** is quite distorted from an ideal square plane environment, where the relatively small N1-Pd-N2 bond angle of 81.4(2)º is a result of chelating ligand steric constraints. Theoretical calculations show that molecular geometry is very similar in both isomers and only an important variation in the orientation angle for naphthyl groups can be expected, in agreement with experimental structure. DFT studies showed that the *syn* and *anti* isomers of [$PdCl_2$(BIAN)] are isoenergetics, therefore they can both be obtained experimentally. However, no isomerization process is available in square-planar complexes, but it can occur for the free ligand. Finally, by replacing the metallic fragment ML_n, the structural choice can be affected, and one or both conformers can be obtained. Their relative stability will depend on the nature of the metal, including electronic configuration and environment, and on the terminal ligands

IV.7 Acknowledgements

We thank *Fundação para a Ciência e Tecnologia*, Portugal, for funding (Projects PTDC/QUI/66440/2006, PTDC/QUI/66250/2006 and for a doctoral fellowship to V.R. (SFRH/BD/13777/2003). We also thank the Portuguese-Spanish Integrated Action-2008, Nº. E-77/08. Financial support for this work was also provided by the *Spanish Dirección General de Investigación* (DGI) through grant CTQ2005-08123-C02-02/BQU and by the *Departament d'Universitats, Recerca i Societat de la Informació* (DURSI) of *Generalitat de Catalunya* through grant 2005SGR-0036. The computing resources at the *Centre de Supercomputació de Catalunya* (CESCA) were made available in part through a grant of *Fundació Catalana per a la Recerca* (FCR) and *Universitat de Barcelona*.

IV.8 References

1. Dvolaitz.M, *Comptes Rendus Hebdomadaires Des Seances De L Academie Des Sciences Serie C*, 1969, **268**, 1811-&.
2. M. Dvolaitzky, *Chem. Abstr.*, 1969, **71**, 61566b.
3. I. Matei and T. Lixandru, *Bul. Ist. Politeh. Iasi*, 1967, **13**, 245.
4. I. Matei and T. Lixandru, *Chem. Abstr.*, 1969, **70**, 3623m.
5. H. tom Dieck, M. Svoboda and T. Greiser, *Z. Naturforsch.*, 1981, **36b**, 823-832.
6. G. Vankoten and K. Vrieze, *Advances in Organometallic Chemistry*, 1982, **21**, 151-239.
7. V. Rosa, S. A. Carabineiro, T. Aviles, P. T. Gomes, R. Welter, J. M. Campos and M. R. Ribeiro, *J. Organomet. Chem.*, 2008, **693**, 769-775.
8. R. Vanasselt, C. J. Elsevier, W. J. J. Smeets, A. L. Spek and R. Benedix, *Recueil Des Travaux Chimiques Des Pays-Bas-Journal of the Royal Netherlands Chemical Society*, 1994, **113**, 88-98.
9. R. Vanasselt and C. J. Elsevier, *Journal of Molecular Catalysis*, 1991, **65**, L13-L19.
10. R. Vanasselt and C. J. Elsevier, *Organometallics*, 1992, **11**, 1999-2001.
11. M. W. van Laren and C. J. Elsevier, *Angewandte Chemie-International Edition*, 1999, **38**, 3715-3717.
12. B. Rieger, L. S. Baugh, S. Kacker and S. Striegler, *Late Transition Metal Polymerization Catalysis*, Weinheim, Wiley-VCH, 2003.
13. S. D. Ittel, L. K. Johnson and M. Brookhart, *Chem. Rev.*, 2000, **100**, 1169-1203.
14. G. J. P. Britovsek, V. C. Gibson and D. F. Wass, *Angew. Chem., Int. Ed.*, 1999, **38**, 428-447.
15. V. C. Gibson and S. K. Spitzmesser, *Chem. Rev.*, 2003, **103**, 283-315.
16. J. H. Groen, J. G. P. Delis, P. W. N. M. van Leeuwen and K. Vrieze, *Organometallics*, 1997, **16**, 68-77.
17. J. Durand and B. Milani, *Coord. Chem. Rev.*, 2006, **250**, 542-560.
18. A. Scarel, M. R. Axet, F. Amoroso, F. Ragaini, C. J. Elsevier, A. Holuigue, C. Carfagna, L. Mosca and B. Milani, *Organometallics*, 2008, **27**, 1486-1494.
19. B. L. Small, R. Rios, E. R. Fernandez and M. J. Carney, *Organometallics*, 2007, **26**, 1744-1749.
20. M. Gasperini and F. Ragaini, *Organometallics*, 2004, **23**, 995-1001.

21. M. Gasperini, F. Ragaini, E. Gazzola, A. Caselli and P. Macchi, *Dalton Transactions*, 2004, 3376-3382.

22. M. Gasperini, F. Ragaini and S. Cenini, *Organometallics*, 2002, **21**, 2950-2957.

23. I. L. Fedushkin, V. A. Chudakova, A. A. Skatova, N. M. Khvoinova, Y. A. Kurskii, T. A. Glukhova, G. K. Fukin, S. Dechert, M. Hummert and H. Schumann, *Zeitschrift Fur Anorganische Und Allgemeine Chemie*, 2004, **630**, 501-507.

24. I. L. Fedushkin, N. M. Khvoinova, A. Y. Baurin, G. K. Fukin, V. K. Cherkasov and M. P. Bubnov, *Inorganic Chemistry*, 2004, **43**, 7807-7815.

25. I. L. Fedushkin, A. A. Skatova, V. A. Chudakova, N. M. Khvoinova, A. Y. Baurin, S. Deckert, M. Hummert and H. Schumann, *Organometallics*, 2004, **23**, 3714-3718.

26. *SMART (control) and SAINT (integration) software*, Bruker Analytical X-Ray Systems, Madison, WI, 1994.

27. G. M. Sheldrick, *SADABS, Program for Empirical Absorption Correction of Area Detector Data*, University of Göttingen, Germany, 1996.

28. G. M. Sheldrick, *SHELXL97, Program for the refinement of crystal structures*, University of Göttingen, Germany, 1997.

29. A. L. Spek, *PLATON, A Multipurpose Crystallographic Tool*, Utrecht University, The Netherlands, 2004.

30. *MERCURY 1.4.1. Software for Visualising Crystal Structures*, The Cambridge Crystallographic Data Centre, Cambridge, UK, 2005.

31. M. J. Frisch, G. W. Trucks, H. B. Schlegel, G. E. Scuseria, M. A. Robb, J. R. Cheeseman, J. A. J. Montgomery, T. Vreven, K. N. Kudin, J. C. Burant, J. M. Millam, S. S. Iyengar, J. Tomasi, V. Barone, B. Mennucci, M. Cossi, G. Scalmani, N. Rega, G. A. Petersson, H. Nakatsuji, M. Hada, M. Ehara, K. Toyota, R. Fukuda, J. Hasegawa, M. Ishida, T. Nakajima, Y. Honda, O. Kitao, H. Nakai, M. Klene, X. Li, J. E. Knox, H. P. Hratchian, J. B. Cross, C. Adamo, J. Jaramillo, R. Gomperts, R. E. Stratmann, O. Yazyev, A. J. Austin, R. Cammi, C. Pomelli, J. W. Ochterski, P. Y. Ayala, K. Morokuma, G. A. Voth, P. Salvador, J. J. Dannenberg, V. G. Zakrzewski, S. Dapprich, A. D. Daniels, M. C. Strain, O. Farkas, D. K. Malick, A. D. Rabuck, K. Raghavachari, J. B. Foresman, J. V. Ortiz, Q. Cui, A. G. Baboul, S. Clifford, J. Cioslowski, B. B. Stefanov, G. Liu, A. Liashenko, P. Piskorz, I. Komaromi, R. L. Martin, D. J. Fox, T. Keith, M. A. Al-Laham, C. Y. Peng, A. Nanayakkara, M. Challacombe, P. M. W. Gill, B. Johnson, W. Chen, M. W. Wong, C. Gonzalez and J. A. Pople, *Gaussian 03 (Revission C.2)*, Gaussian Inc., Wallingford CT, 2004.

32. A. D. Becke, *Journal of Chemical Physics*, 1993, **98**, 5648-5652.

33. C. T. Lee, W. T. Yang and R. G. Parr, *Physical Review B*, 1988, **37**, 785-789.

34. P. J. Hay and W. R. Wadt, *Journal of Chemical Physics*, 1985, **82**, 299-310.

35. P. J. Hay and W. R. Wadt, *Journal of Chemical Physics*, 1985, **82**, 270-283.

36. A. Hollwarth, M. Bohme, S. Dapprich, A. W. Ehlers, A. Gobbi, V. Jonas, K. F. Kohler, R. Stegmann, A. Veldkamp and G. Frenking, *Chemical Physics Letters*, 1993, **208**, 237-240.

37. Harihara.Pc and J. A. Pople, *Theoretica Chimica Acta*, 1973, **28**, 213-222.

38. M. M. Francl, W. J. Pietro, W. J. Hehre, J. S. Binkley, M. S. Gordon, D. J. Defrees and J. A. Pople, *Journal of Chemical Physics*, 1982, **77**, 3654-3665.

39. F. H. Allen and O. Kennard, *Chem. Des. Autom. News*, 1993, **8**, 31.

40. A. C. Silvino, L. C. Ferreira, M. L. Dias, C. A. L. Filgueiras, M. Horner, L. D. C. Visentin and J. Bordinhao, *Acta Crystallographica Section E-Structure Reports Online*, 2007, **63**, O999-O1000.

41. H. Amii, M. Kohda, T. Katagiri and K. Uneyama, *Journal of Fluorine Chemistry*, 2006, **127**, 505-509.

42. J. A. Moore, K. Vasudevan, N. J. Hill, G. Reeske and A. H. Cowley, *Chemical Communications*, 2006, 2913-2915.

43. D. N. Coventry, A. S. Batsanov, A. E. Goeta, J. A. K. Howard and T. B. Marder, *Polyhedron*, 2004, **23**, 2789-2795.

44. E. K. Cope-Eatough, F. S. Mair, R. G. Pritchard, J. E. Warren and R. J. Woods, *Polyhedron*, 2003, **22**, 1447-1454.

45. D. H. Camacho, E. V. Salo, Z. B. Guan and J. W. Ziller, *Organometallics*, 2005, **24**, 4933-4939.

46. M. Schmid, R. Eberhardt, M. Klinga, M. Leskela and B. Rieger, *Organometallics*, 2001, **20**, 2321-2330.

47. R. Vanasselt, C. J. Elsevier, W. J. J. Smeets and A. L. Spek, *Inorganic Chemistry*, 1994, **33**, 1521-1531.

48. M. Nishio, *Crystengcomm*, 2004, **6**, 130-158.

49. C. Janiak, *Journal of the Chemical Society-Dalton Transactions*, 2000, 3885-3896.

50. L. K. Johnson, C. M. Killian and M. Brookhart, *J. Am. Chem. Soc.*, 1995, **117**, 6414-6415.

51. J. Reinhold, R. Benedix, P. Birner and H. Hennig, *Inorganica Chimica Acta*, 1979, **33**, 209-213.

52. A. Paulovicova, U. El-Ayaan, K. Shibayama, T. Morita and Y. Fukuda, *European Journal of Inorganic Chemistry*, 2001, 2641-2646.

53. J. S. de Melo, M. T. Albelda, P. Diaz, E. Garcia-Espana, C. Lodeiro, S. Alves, J. C. Lima, F. Pina and C. Soriano, *Journal of the Chemical Society-Perkin Transactions 2*, 2002, 991-998.

54. J. Pina, J. S. de Melo, F. Pina, C. Lodeiro, J. C. Lima, A. J. Parola, C. Soriano, M. P. Clares, M. T. Albelda, R. Aucejo and E. Garcia-Espana, *Inorganic Chemistry*, 2005, **44**, 7449-7458.

55. R. Aucejo, J. Alarcon, E. Garcia-Espana, J. M. Llinares, K. L. Marchin, C. Soriano, C. Lodeiro, M. A. Bernardo, F. Pina, J. Pina and J. S. de Melo, *European Journal of Inorganic Chemistry*, 2005, 4301-4308.

56. I. L. Fedushkin, A. N. Lukoyanov, S. Y. Ketkov, M. Hummert and H. Schumann, *Chemistry-a European Journal*, 2007, **13**, 7050-7056.

57. M. R. Bermejo, M. Vazquez, J. Sanmartin, A. M. Garcia-Deibe, M. Fondo and C. Lodeiro, *New Journal of Chemistry*, 2002, **26**, 1365-1370.

58. M. Fondo, A. M. Garcia-Deibe, N. Ocampo, J. Sanmartin, M. R. Bermejo, E. Oliveira and C. Lodeiro, *New Journal of Chemistry*, 2008, **32**, 247-257.

59. F. Pina, J. C. Lima, C. Lodeiro, J. S. de Melo, P. Diaz, M. T. Albelda and E. Garcia-Espana, *Journal of Physical Chemistry A*, 2002, **106**, 8207-8212.

60. B. Pedras, H. M. Santos, L. Fernandes, B. Covelo, A. Tamayo, E. Bertolo, J. L. Capelo, T. Aviles and C. Lodeiro, *Inorganic Chemistry Communications*, 2007, **10**, 925-929.

61. D. P. Gates, S. K. Svejda, E. Onate, C. M. Killian, L. K. Johnson, P. S. White and M. Brookhart, *Macromolecules*, 2000, **33**, 2320-2334.

62. A. E. Cherian, J. M. Rose, E. B. Lobkovsky and G. W. Coates, *Journal of the American Chemical Society*, 2005, **127**, 13770-13771.

63. R. J. Maldanis, J. S. Wood, W. A. Chandrasekaran, M. D. Rausch and J. C. W. Chien, *J. Organomet. Chem.*, 2002, **645**, 158-167.

64. G. Aullon, D. Bellamy, L. Brammer, E. A. Bruton and A. G. Orpen, *Chemical Communications*, 1998, 653-654.

65. J. Cirera, E. Ruiz and S. Alvarez, *Inorganic Chemistry*, 2008, **47**, 2871-2889.

66. E. Ruiz, J. Cirera and S. Alvarez, *Coordination Chemistry Reviews*, 2005, **249**, 2649-2660.

IV.9 Supplementary Material

Figure SM IV.1a) ^{1}H NMR spectrum of **L** b) ^{13}C NMR spectrum of **L** measured at 400 MHz in CD_2Cl_2.

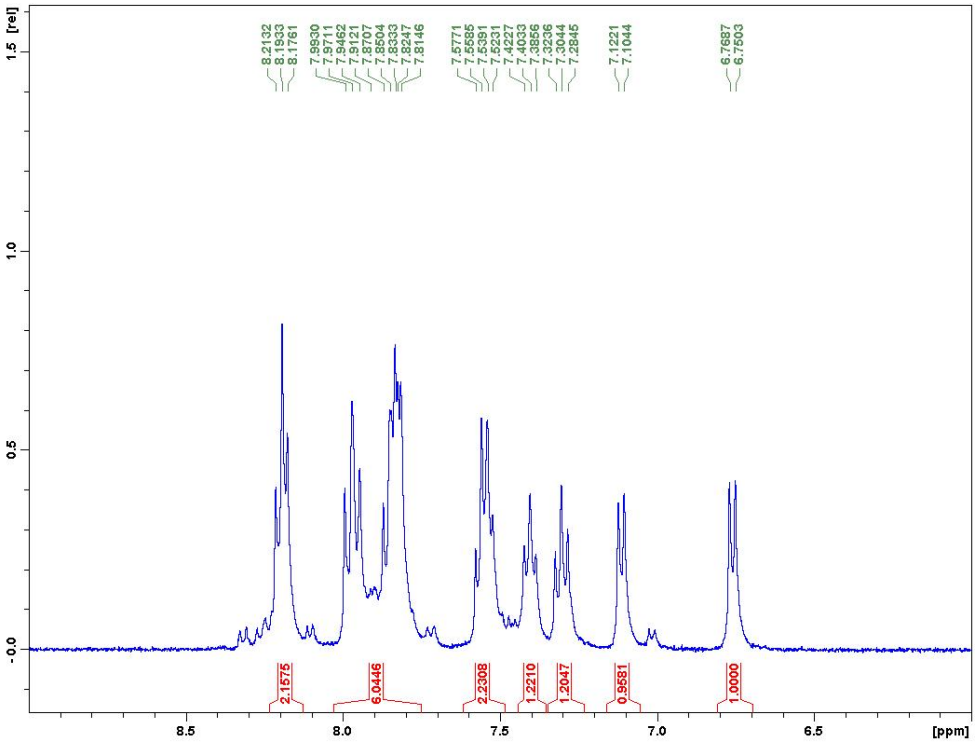

a)

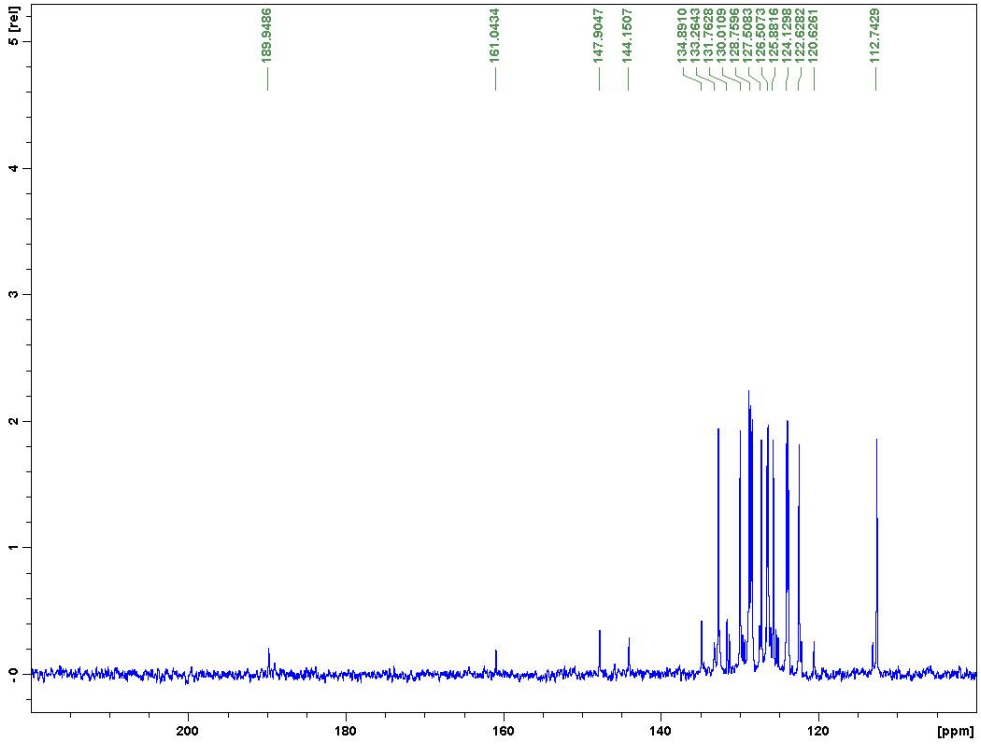

b)

Figure SM IV.2 $^{1}H,^{1}H$ COSY NMR spectrum of **L** measured at 400 MHz in CD_2Cl_2.

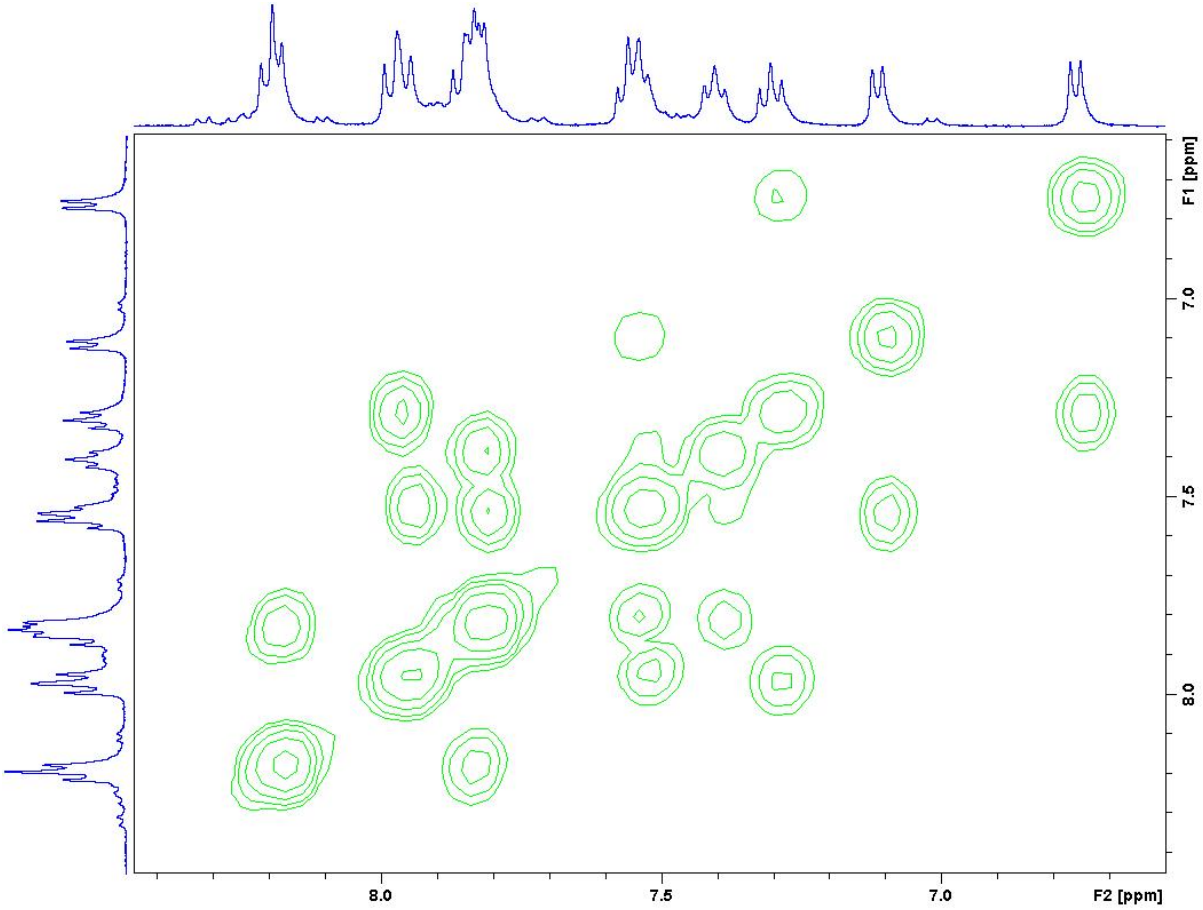

Figure SM IV.3 a) ^{1}H NMR spectrum of **L1** b) ^{13}C NMR spectrum of **L1** measured at 400 MHz in CD_2Cl_2.

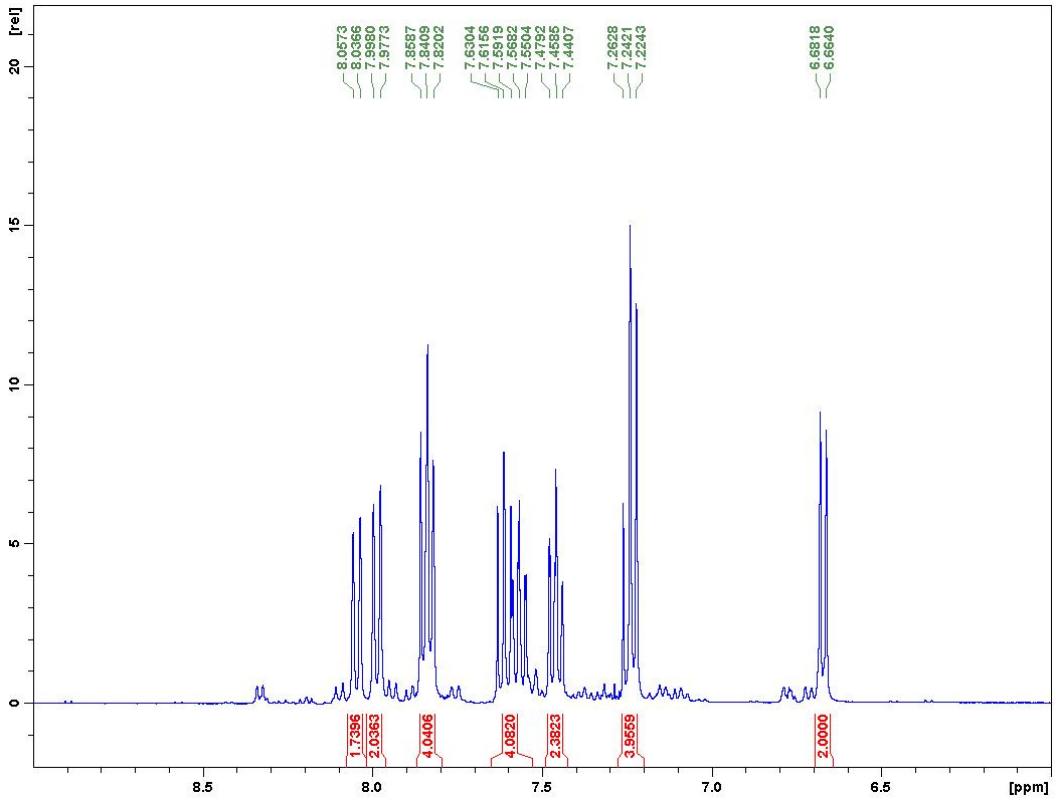

a)

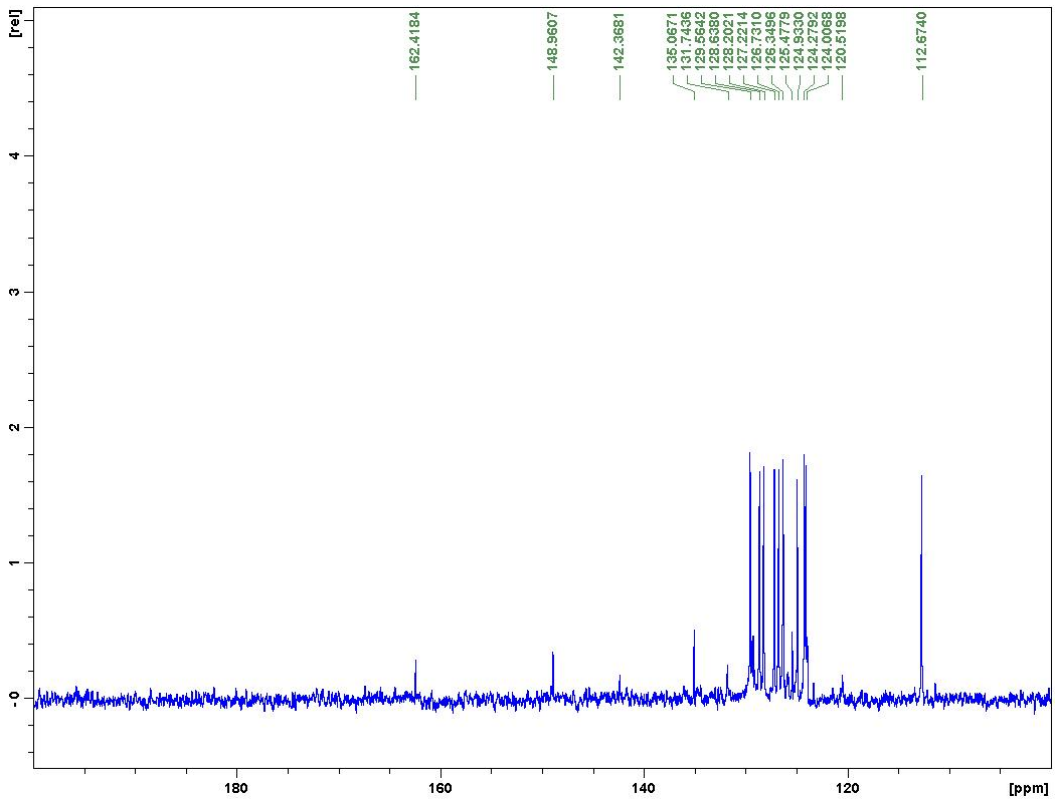

b)

Figure SM IV.4 $^{1}H,^{1}H$-COSY NMR spectrum of **L1** measured at 400 MHz in CD_2Cl_2.

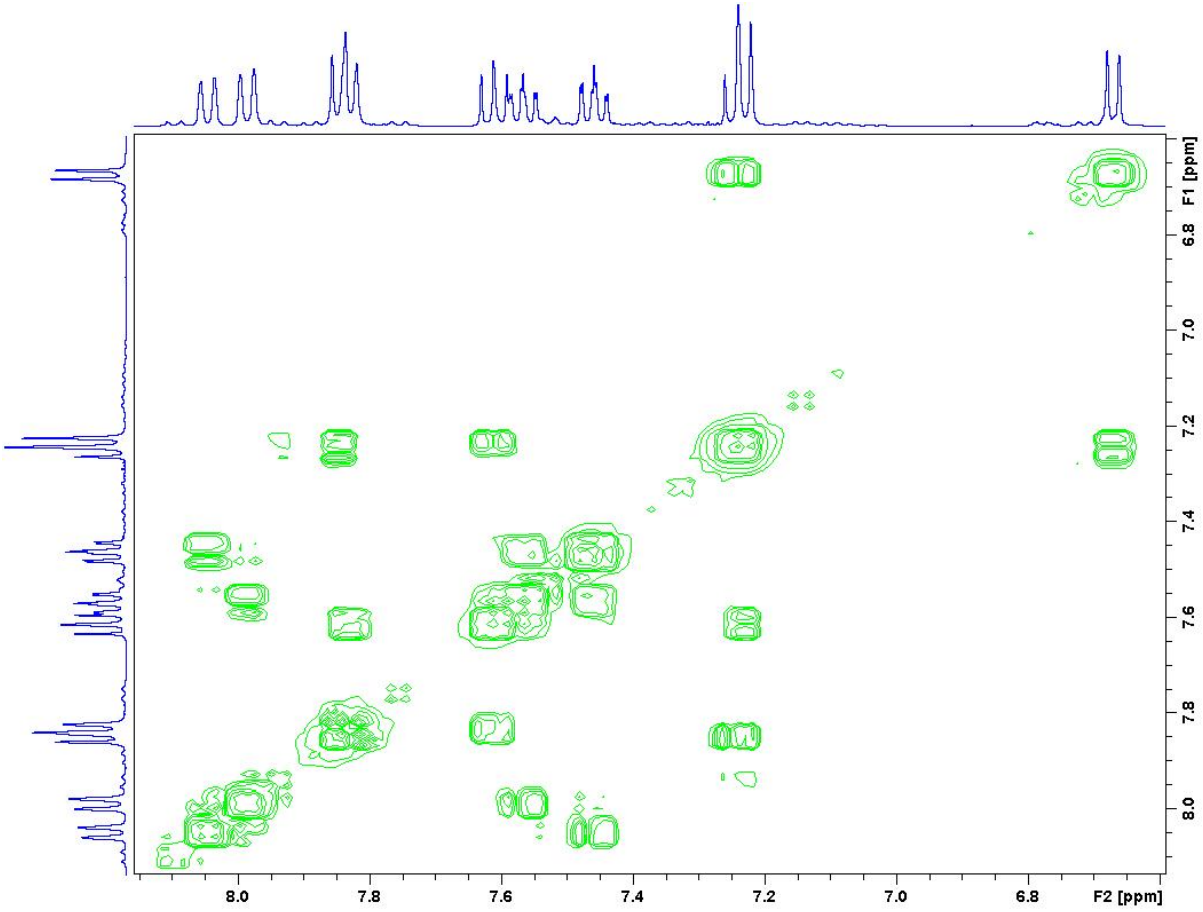

Figure SM IV.5a) ^{1}H NMR spectrum of **1** b) ^{13}C NMR spectrum of **1** measured at 400 MHz in CD_2Cl_2.

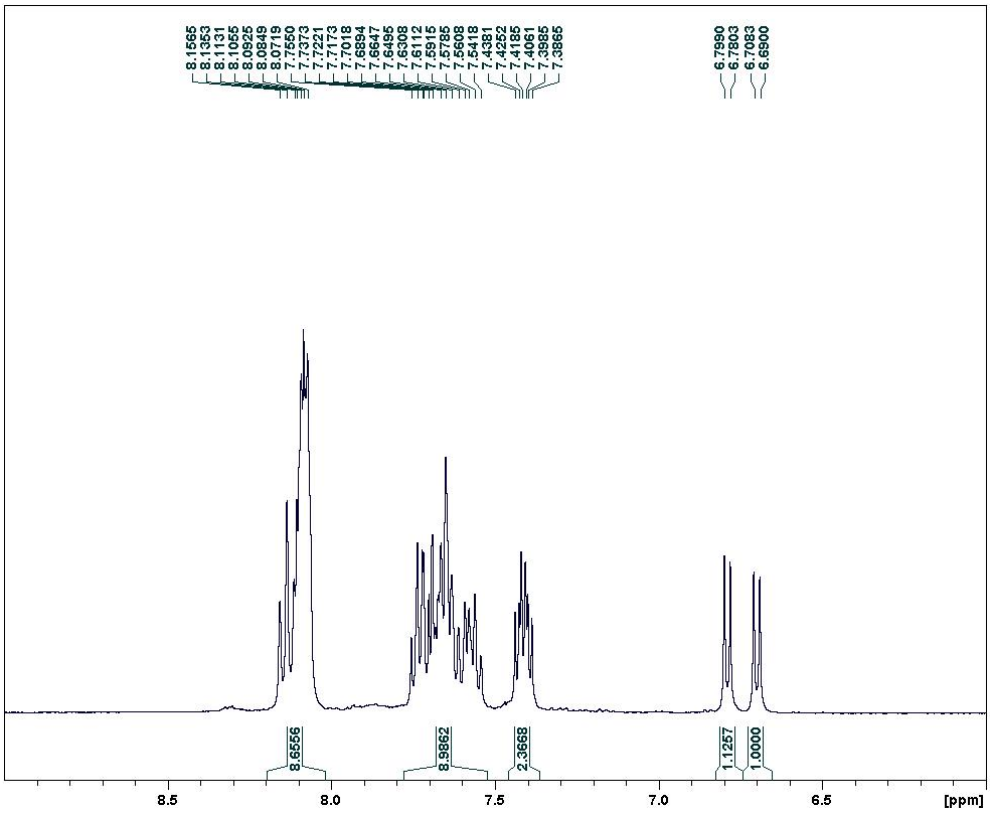

a)

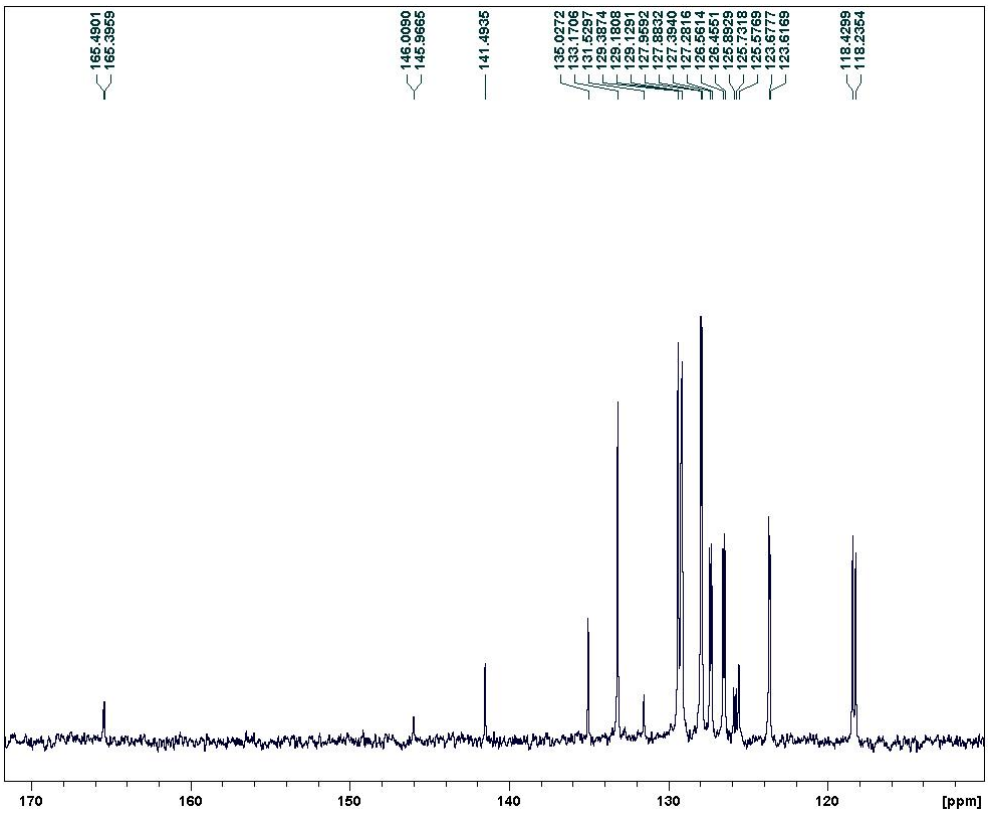

b)

Figure SM IV.6a) ^{1}H NMR spectrum of **2** (method A). b) ^{13}C NMR spectrum of **2** (method A) measured at 400 MHz in CD_2Cl_2.

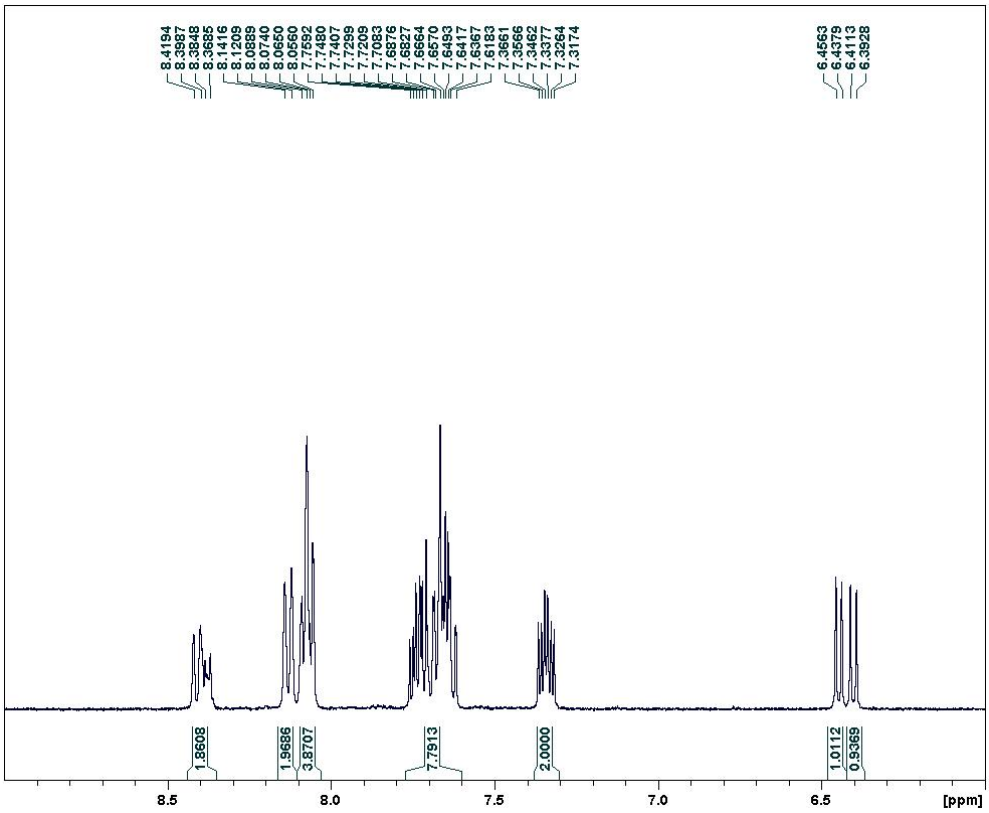

a)

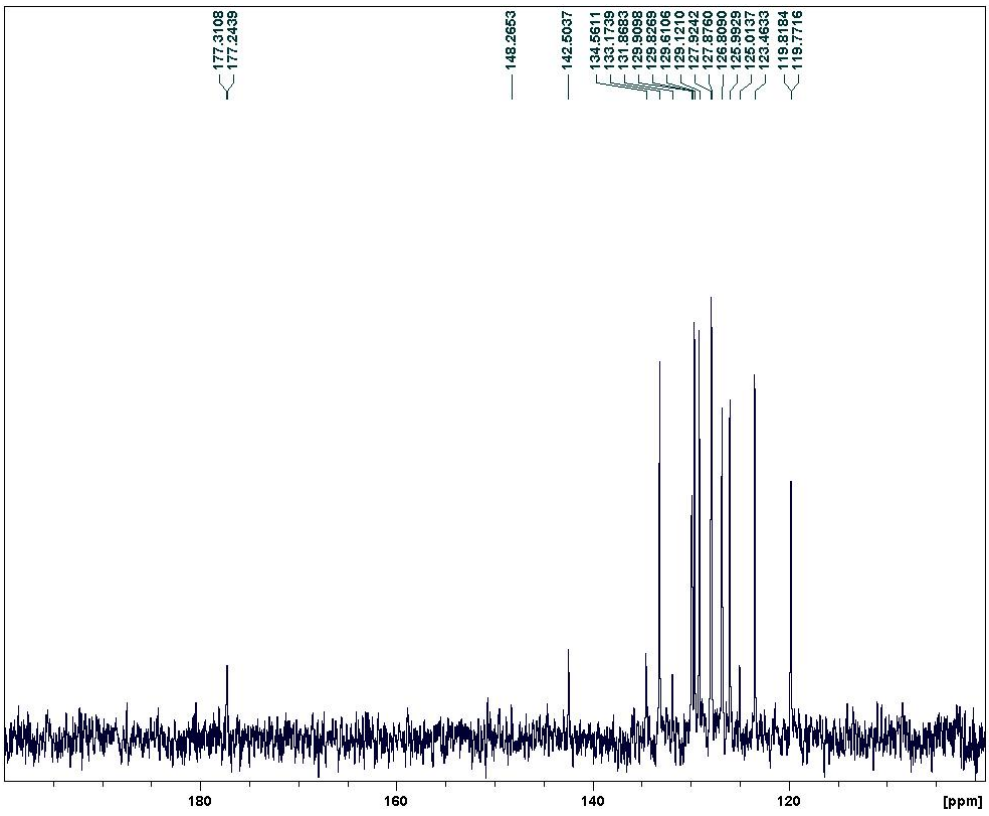

b)

Figure SM IV.7 $^{1}H,^{1}H$ COSY NMR spectrum of **2** (method A) measured at 400 MHz in CD_2Cl_2.

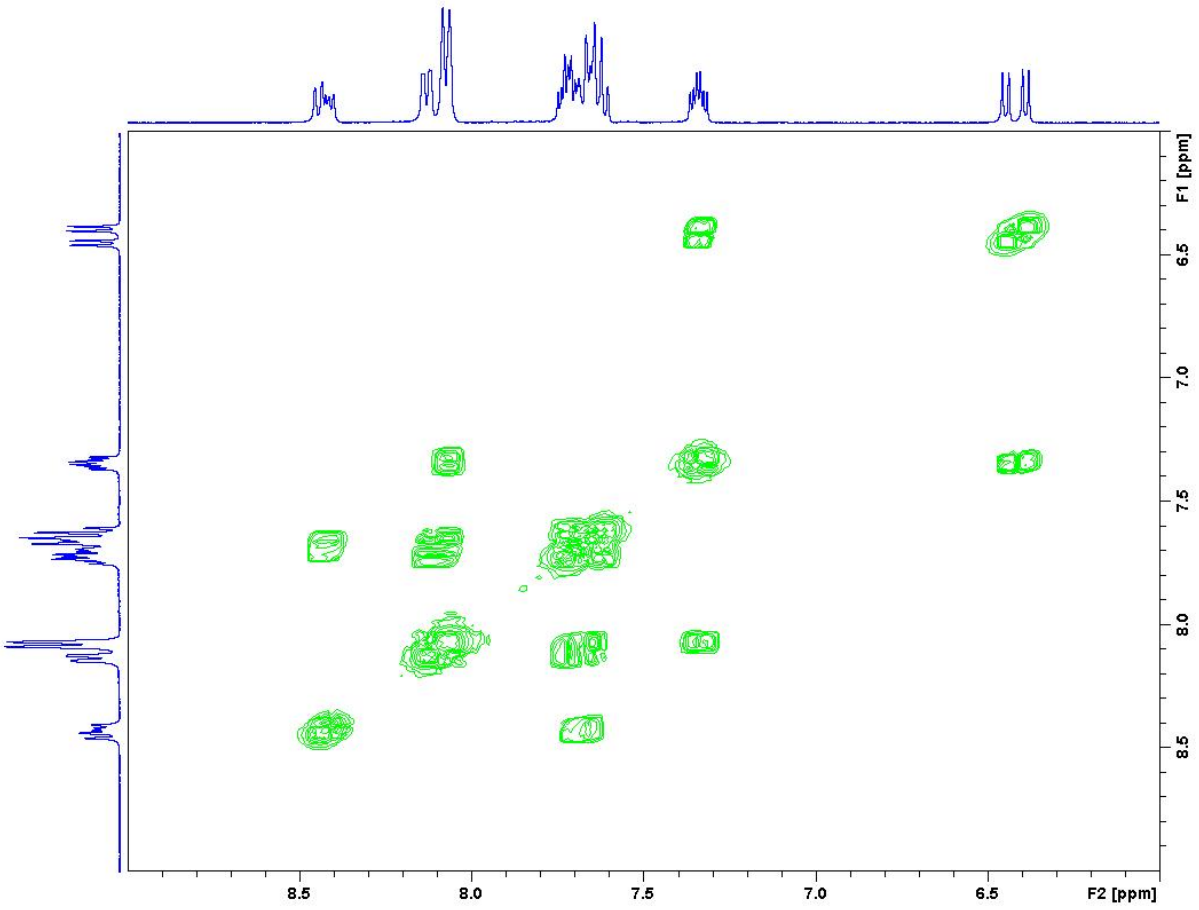

Figure SM IV.8 ^{1}H NMR spectrum of **2** (method B) measured at 400 MHz in CD_2Cl_2.

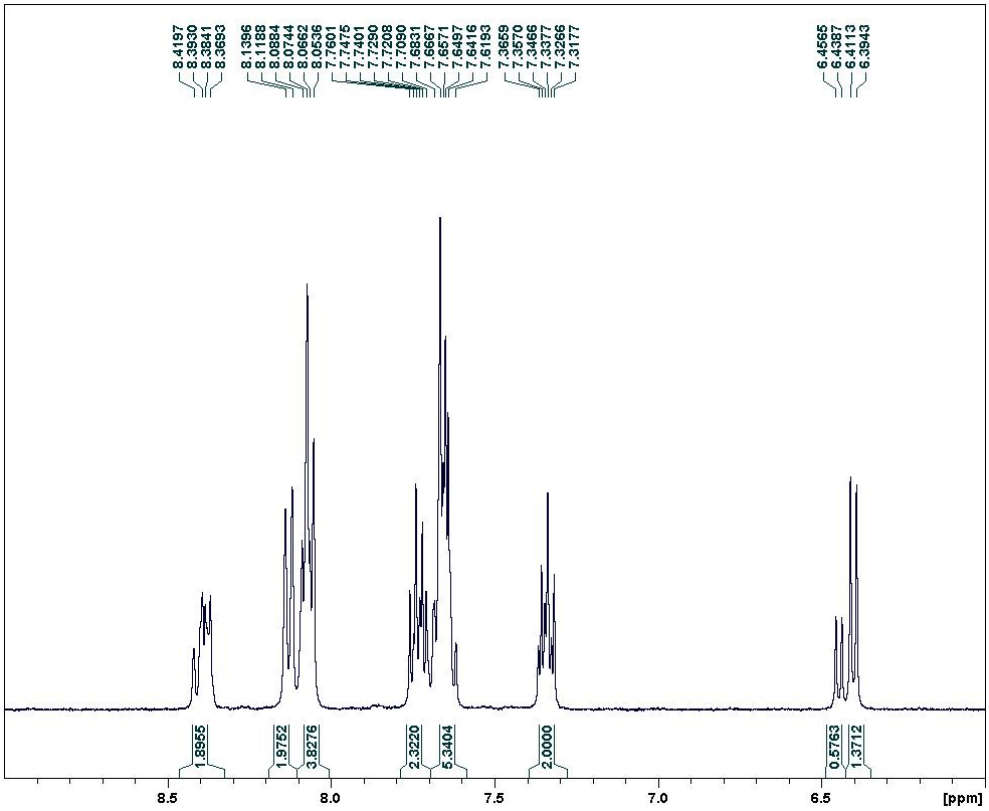

Figure SM IV.9 ^{1}H NMR spectrum of **2** (method B). b) ^{13}C NMR spectrum of **2** (method B) measured at 600 MHz in CD_2Cl_2.

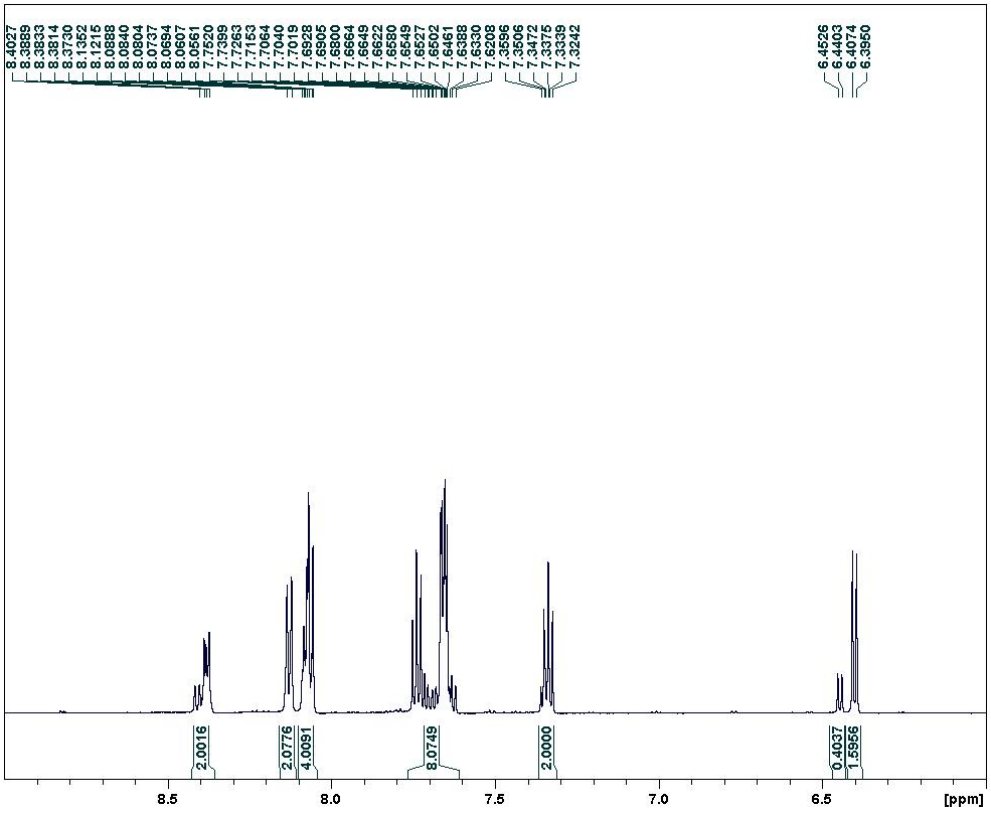

a)

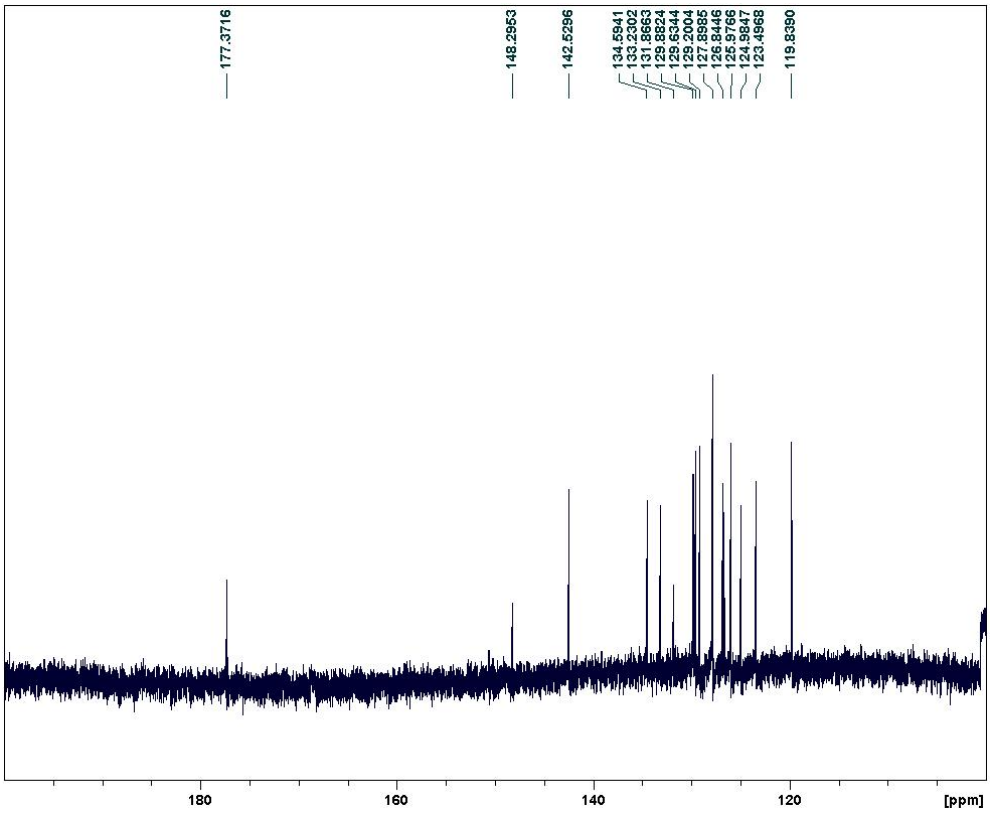

b)

Figure SM IV.10 $^{1}H,^{1}H$ COSY NMR spectrum of **2** (method B) measured at 600 MHz in CD_2Cl_2.

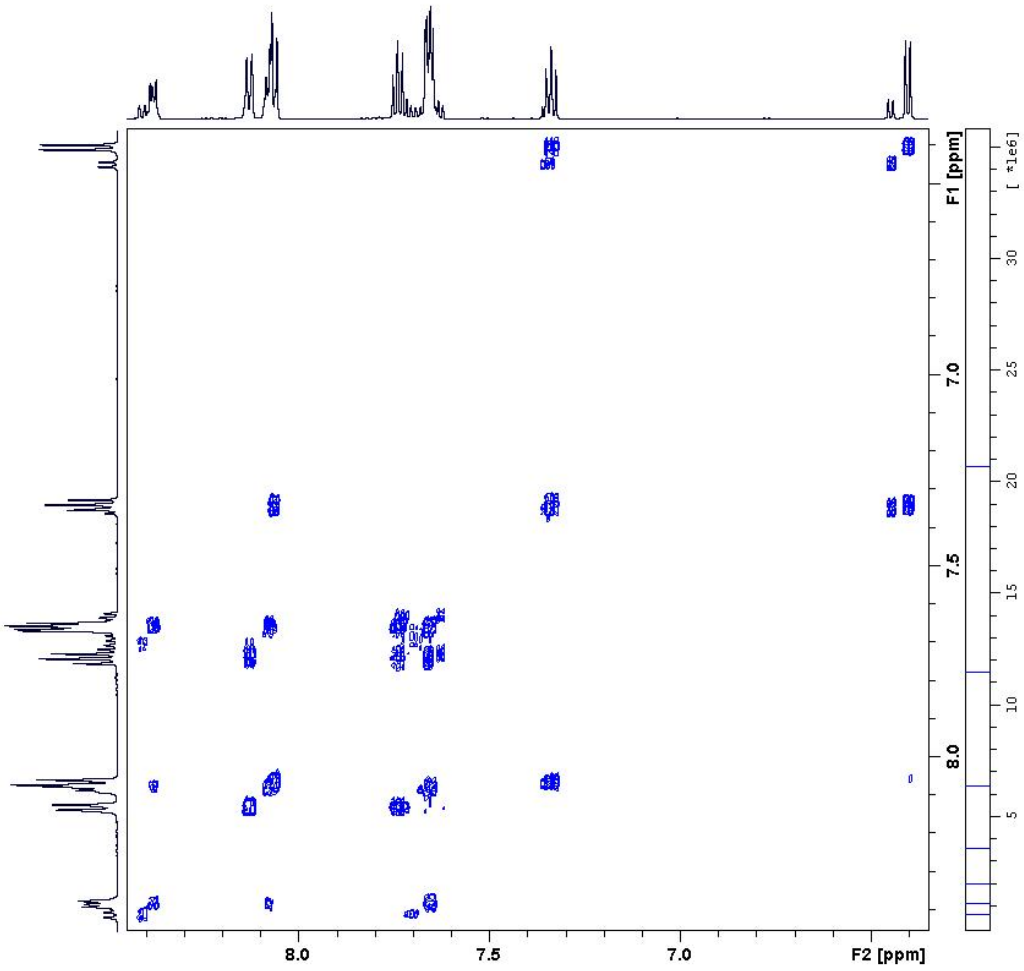

Figure SM IV.11 ^{1}H, ^{13}C HSQC-TOCSY NMR spectrum of **2** (method B) measured at 600 MHz in CD_2Cl_2.

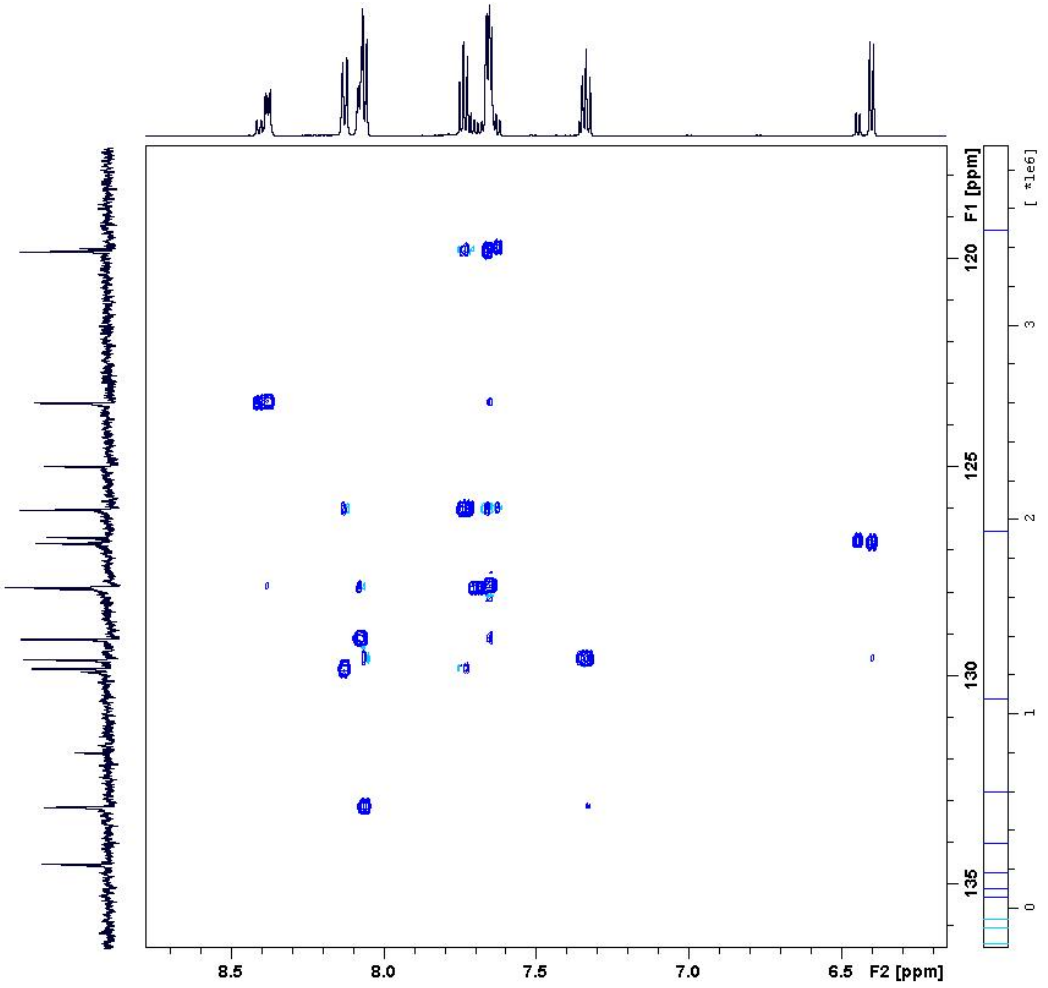

Figure SM IV.12 ^{1}H, ^{1}H NOESY NMR spectrum of **2** (method B) measured at 600 MHz in CD_2Cl_2.

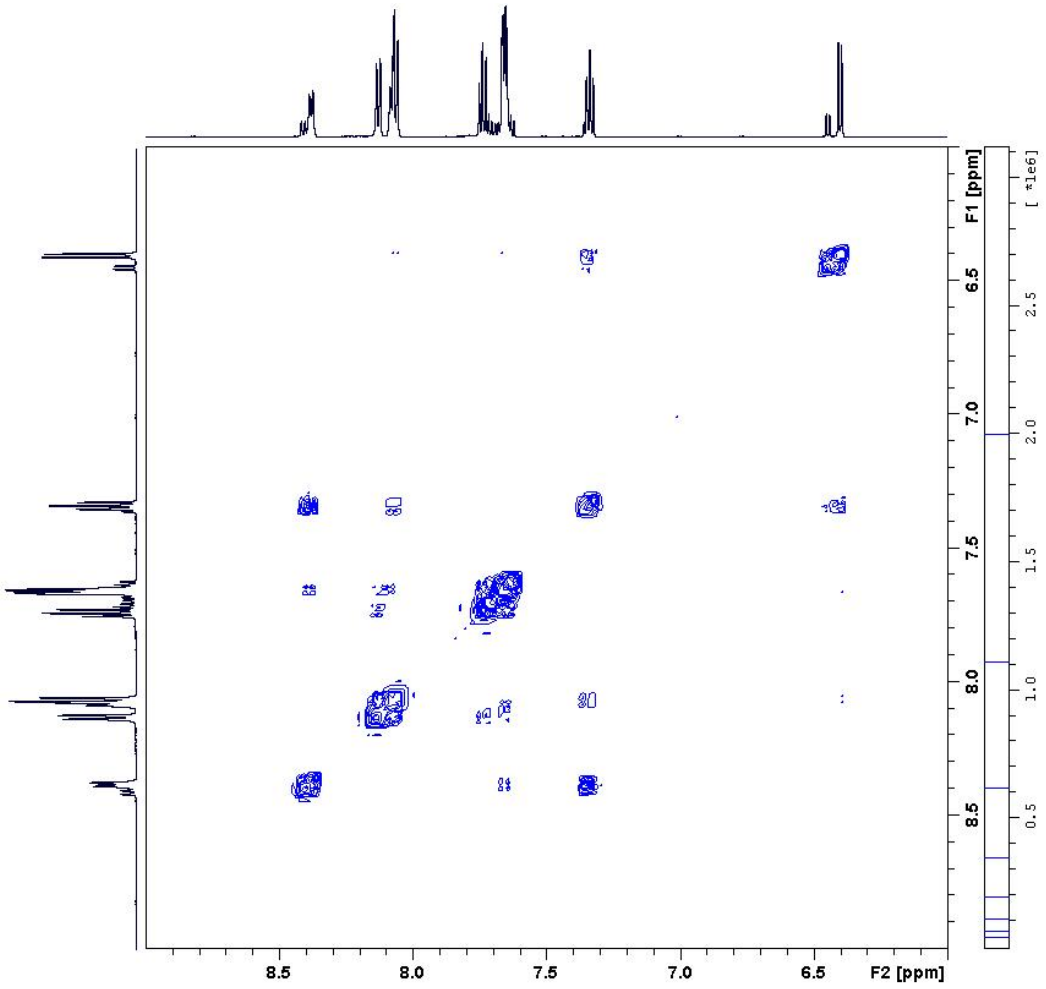

Figure SM IV.13 a) Variable temperature ^{1}H NMR spectrum of **L1** measured at 400 MHz in CD_2Cl_2 b) and c) amplified selected regions.

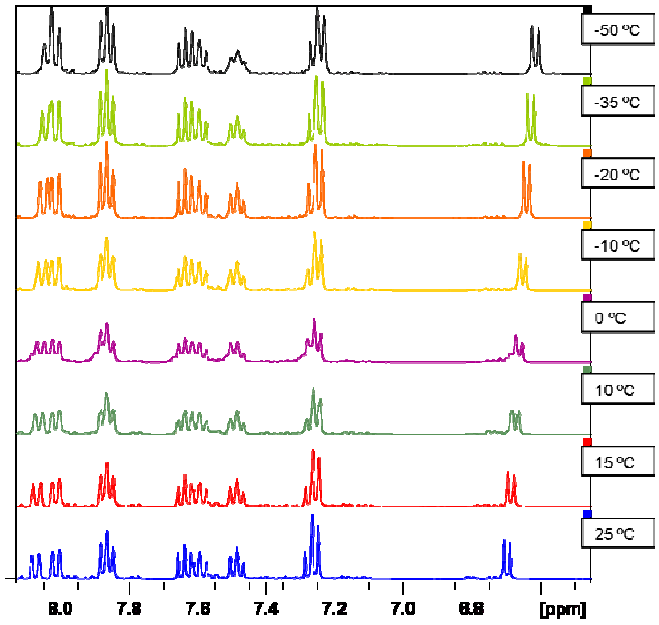

a)

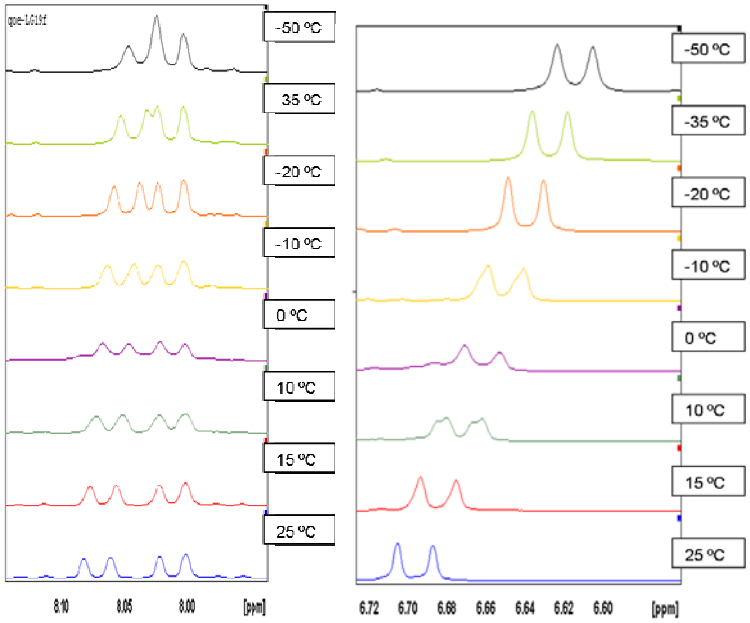

b) c)

Figure SM IV.14 ^{1}H-NMR spectra of **L1**, **1**, **2** (method A) and **2** (method B) measured at 400 MHz in CD_2Cl_2, for comparison purposes.

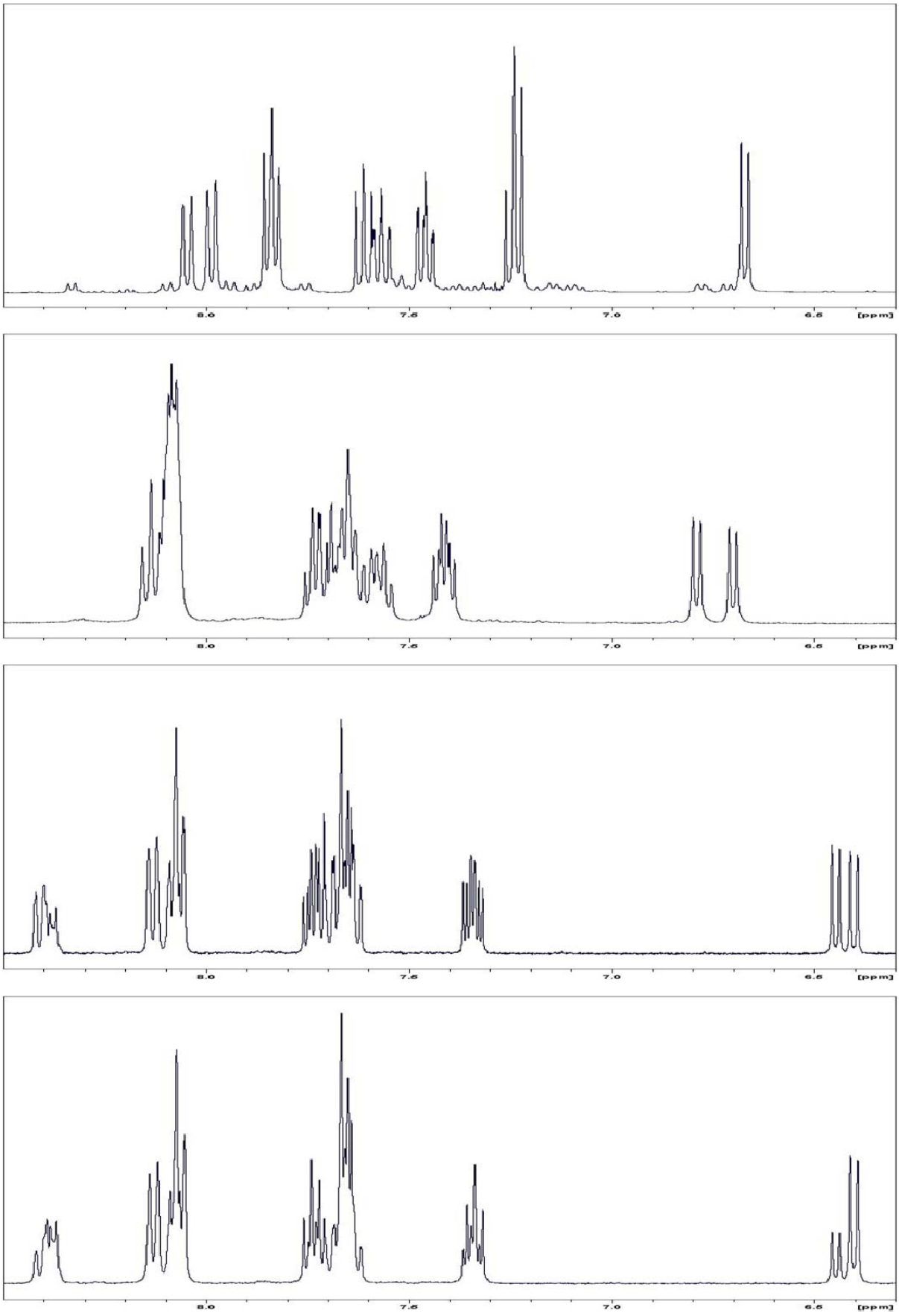

Figure SM IV.15 Amplified region (7.5-6ppm) of ^{1}H-NMR spectra of compound **1** (A) and **2** (B, C) obtained by the two methods.

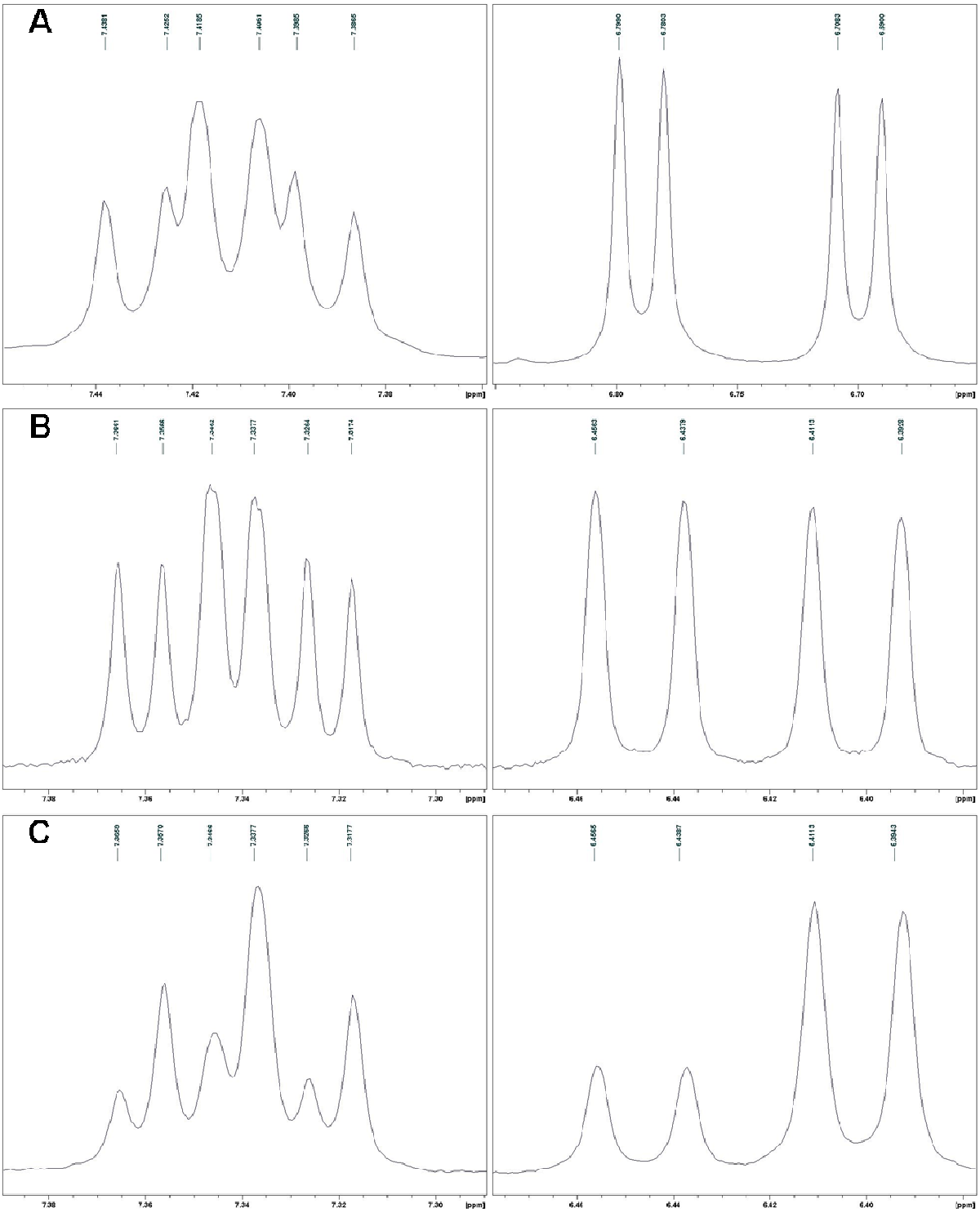

Figure SM IV.16 Absorption spectra of **L1** (A) and complex **2** (B) in freshly prepared dichloromethane solution ([**L1**] and [**2**] = $1.0E^{-6}$ to $1.0E^{-4}$ M).

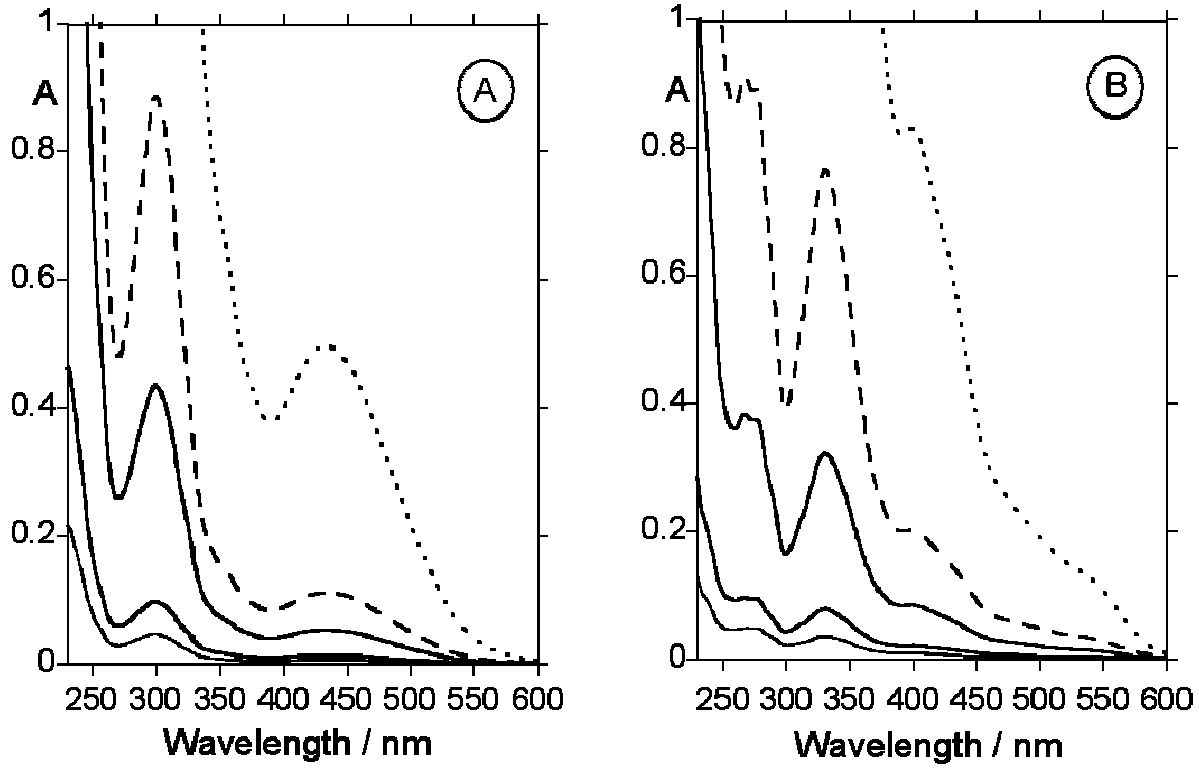

Figure SM IV.17 Absorption spectra of precursors 1-naphthylamine, acenaphthenquinone and **L**, and Absorption spectra of ligand **L1** for comparative purpose in freshly prepared dichloromethane solution ([**L**] = **L1**] = $1.0E^{-5}$ M).

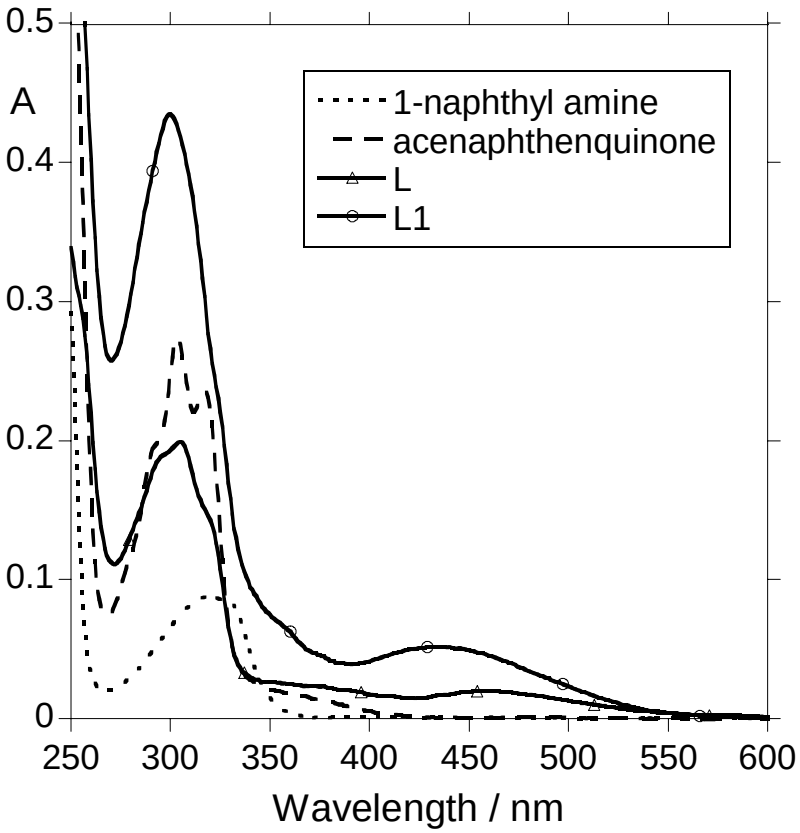

Figure SM IV.18 Absorption spectra of ligand **L1** in freshly prepared dichloromethane solution in the presence of increased amount of Pd(II) ([L1] = $1.0E^{-5}$ M). In the inset is represented the absorption at 300 nm.

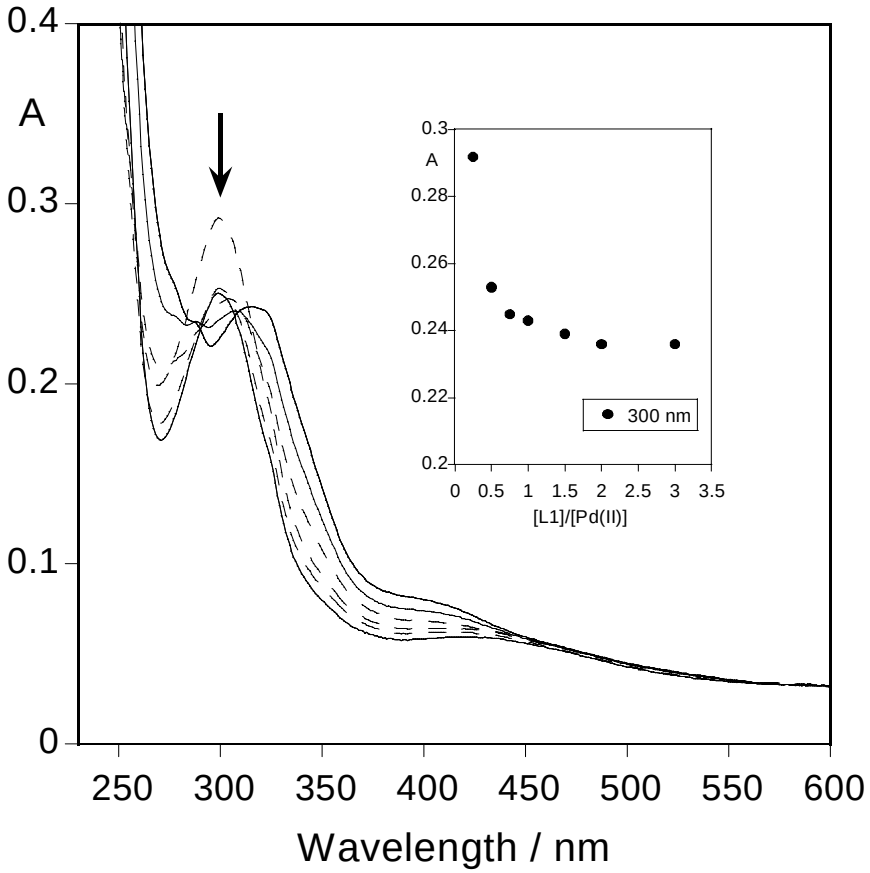

Figure SM IV.19 Fragmentation observed by TOF-MS-FD$^+$ spectroscopy for the metal complex **2**.

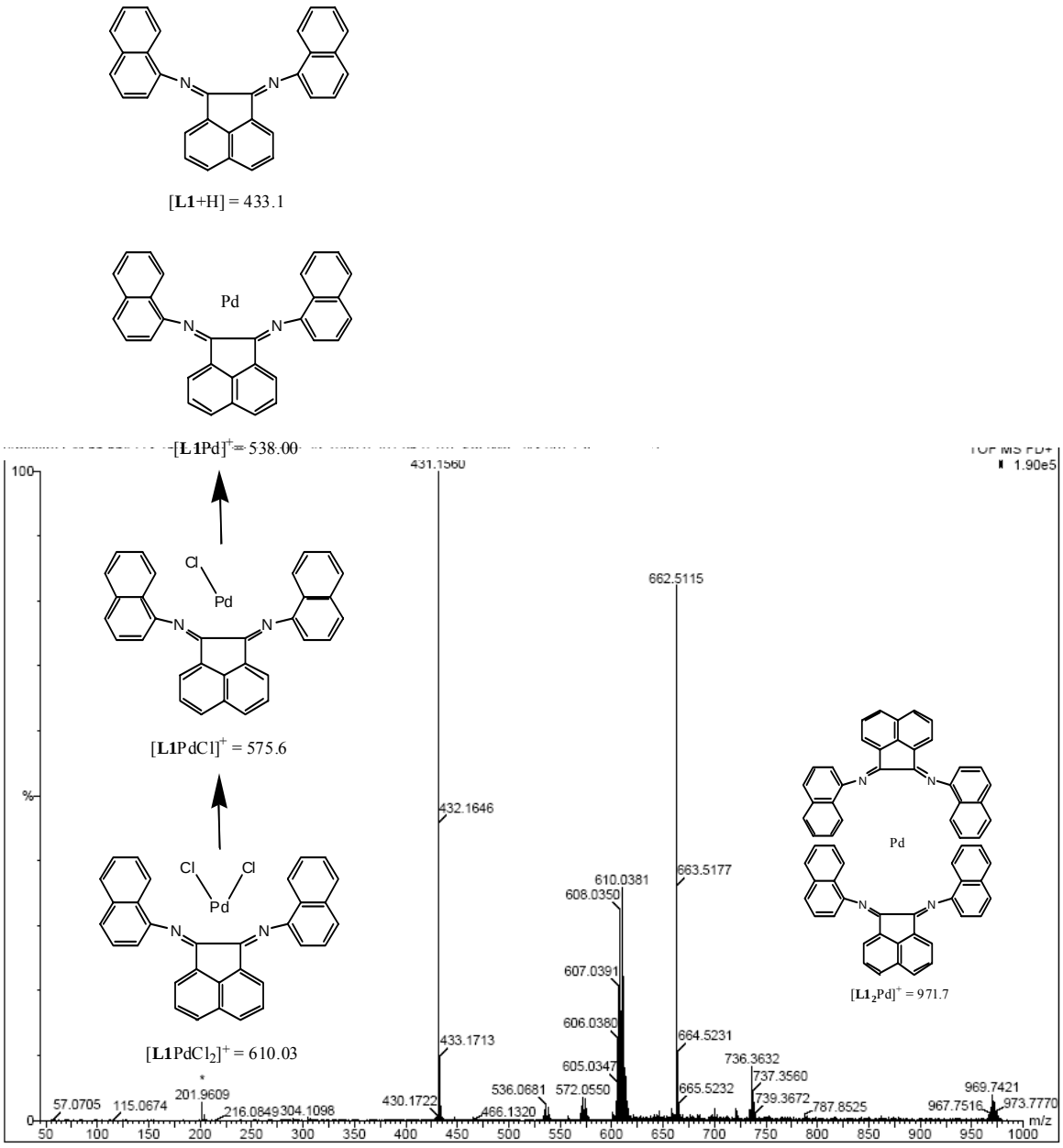

Figure SM IV.20 Fragmentation observed by MALDI-TOF-MS spectroscopy for the metal complex **2**.

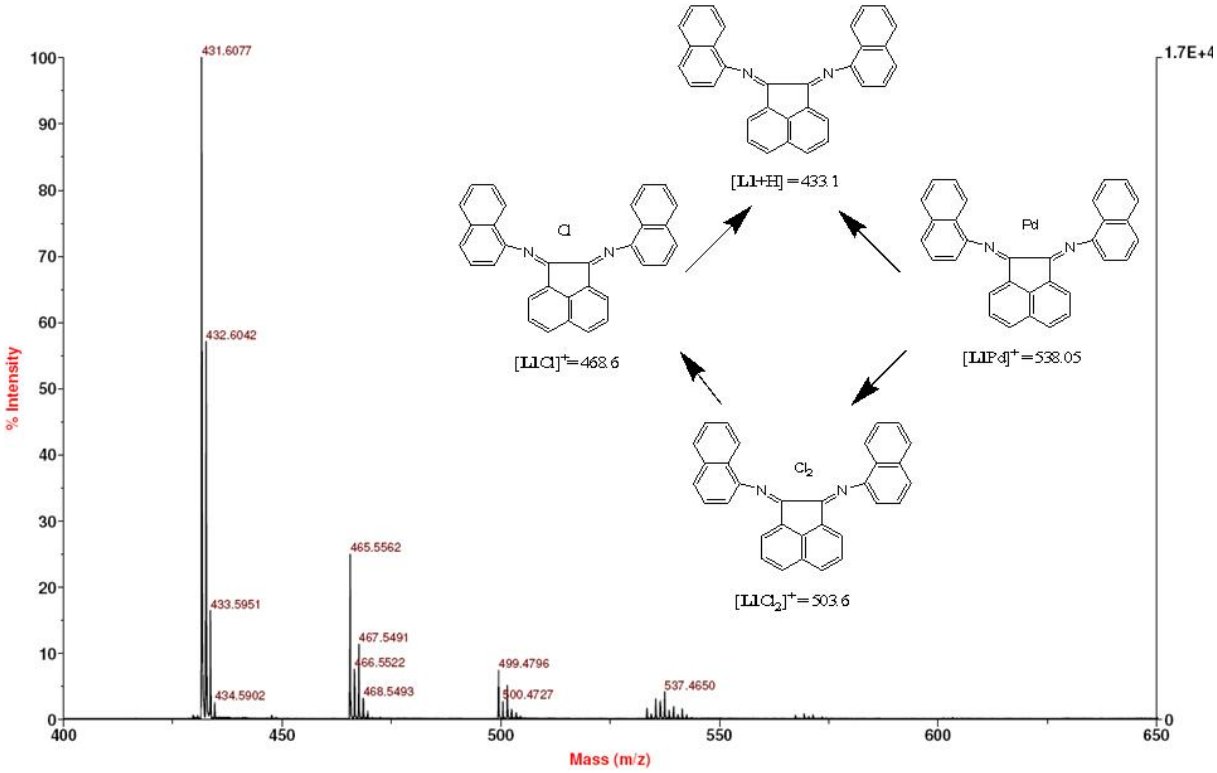

Figure SM IV.21 Isotopic fragmentation observed by TOF-MS-FD$^+$ spectroscopy for the peak at 610.00 *m/z* (down) assigned to the metal complex **2** with the isotopic theoretical model (top).

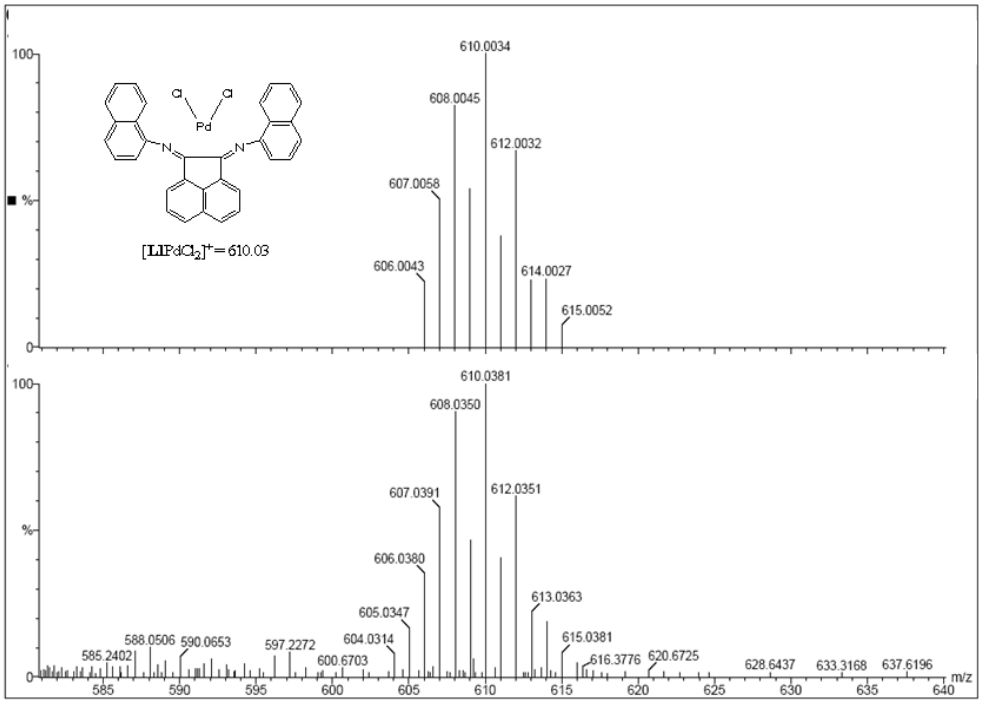

Figure SM IV.22 Fragmentation observed by TOF-MS-EI$^+$ spectroscopy for the precursor **L**.

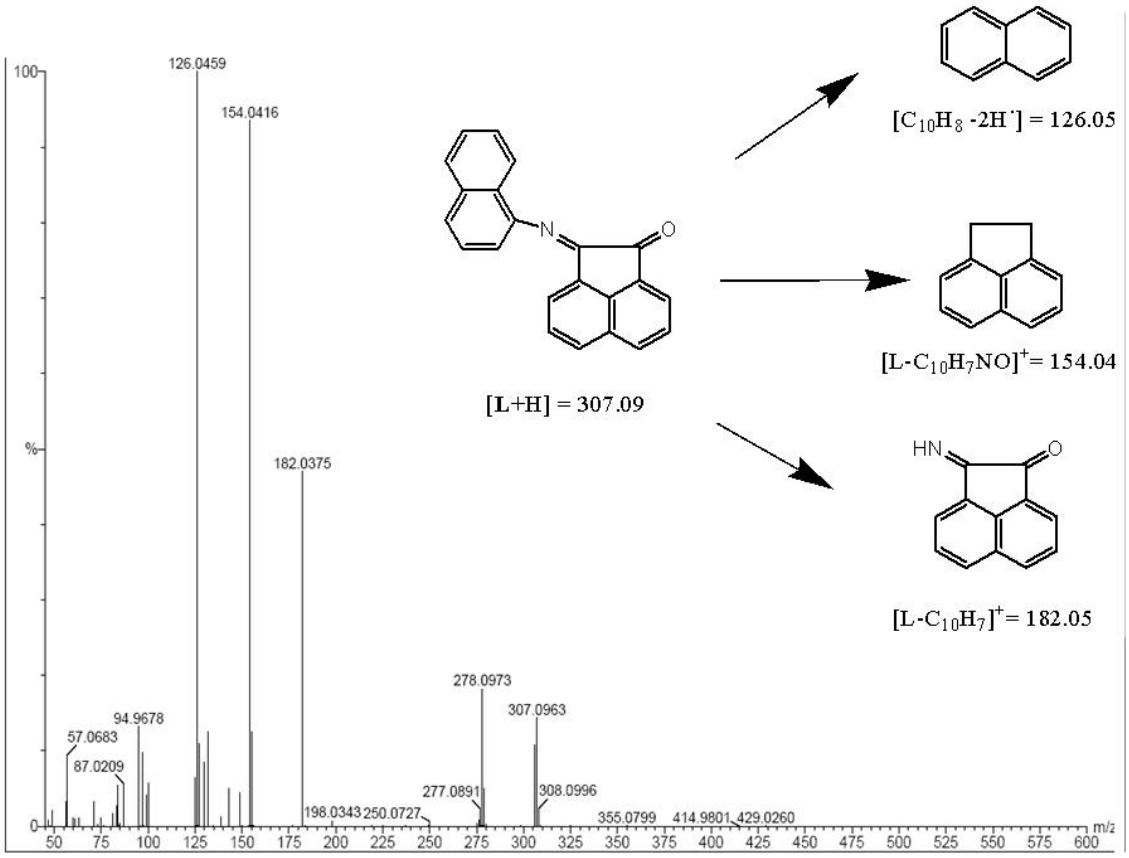

Figure SM IV.23 Fragmentation observed by MALDI-TOF-MS ligand **L1**.

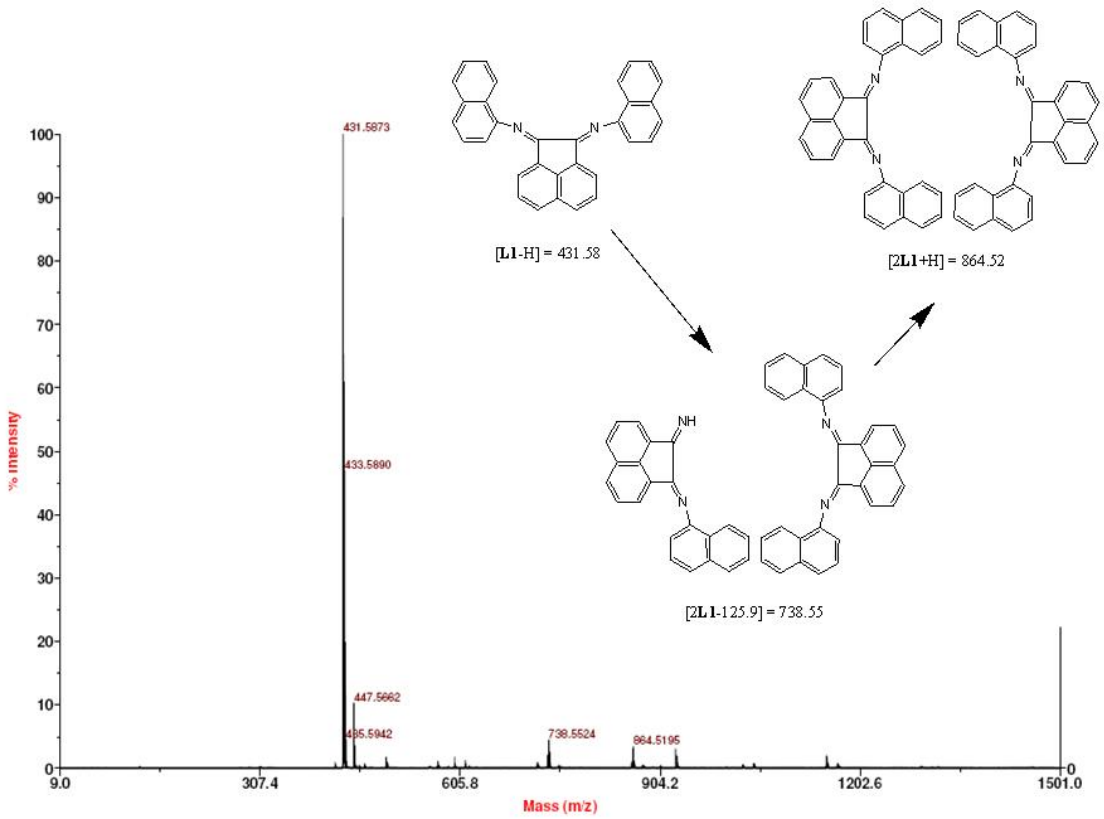

Figure SM IV.24 Fragmentation observed by MALDI-TOF-MS spectroscopy for the metal complex **1**. A dimer structure is observed in the spectra.

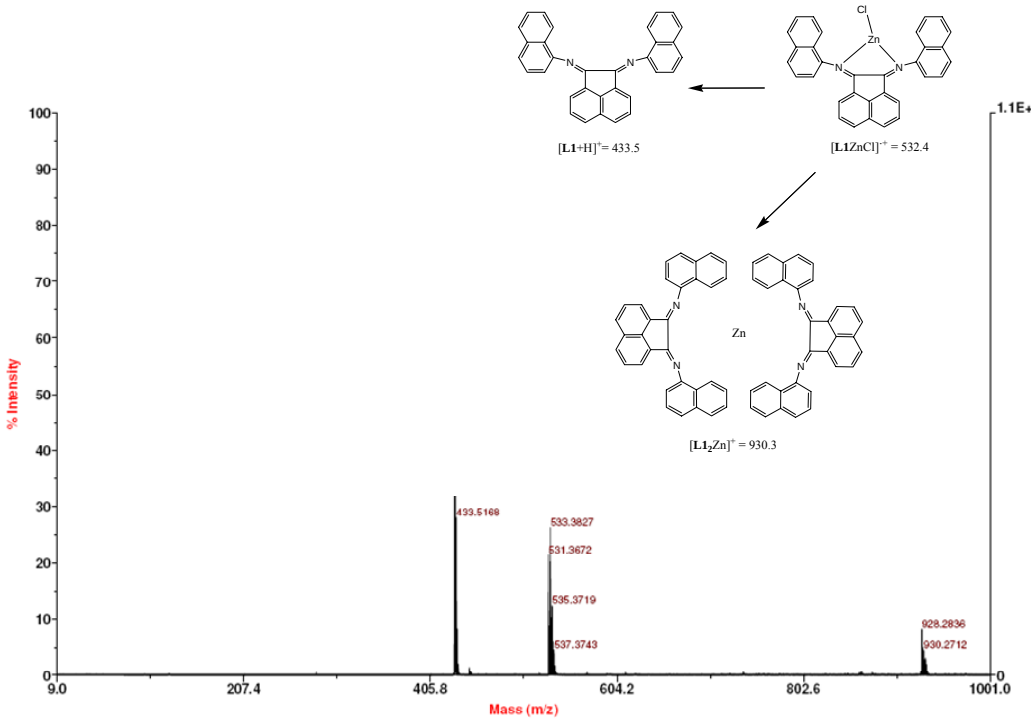

Figure SM IV.25 Experimental τ values in crystal structures retrieved from *Cambridge Structural Database*. Only complexes having square-planar coordination for transition metal are represented (19 data, which 15 have Pd).

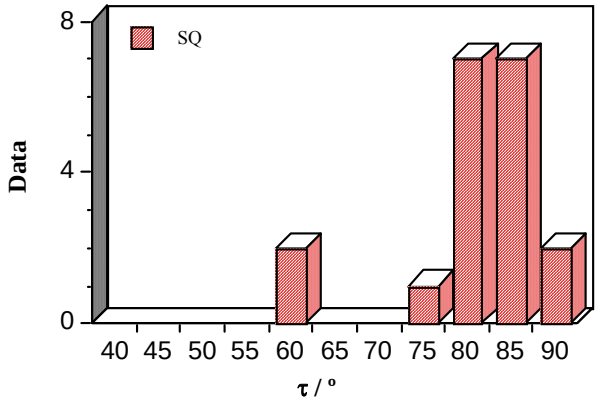

Figure SM IV.26 a) Relation between both τ angles in partial optimized structures of $[PdCl_2(BIAN)]$ when only one, τ_1, is fixed. b) Differences between both τ values in experimental structures retrieved from *Cambridge Structural Database*.

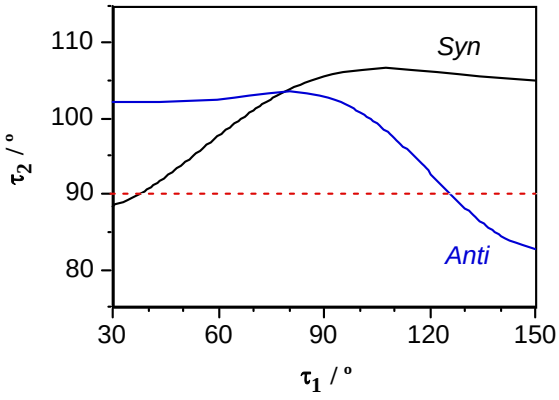

a)

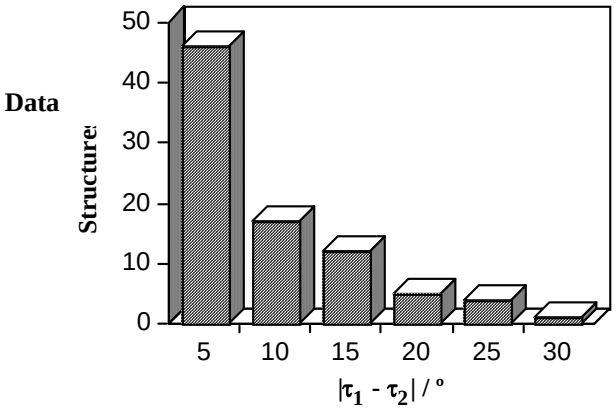

b)

Table SM IV.1 Atomic coordinates of optimized structures for [$PdCl_2$(BIAN)] complex.

(a) *anti*-[PdCl2(BIAN)]

Pd	0.334613	-1.761189	-0.031002
Cl	-0.995176	-3.650791	-0.065889
Cl	2.264669	-3.031882	-0.051139
N	1.359568	0.089117	-0.009645
N	-1.297405	-0.415979	0.003559
C	0.552935	1.101379	0.018727
C	-0.918320	0.821879	0.014834
C	-1.615034	2.115530	0.040301
C	-0.589480	3.102280	0.054258
C	0.726550	2.560480	0.041492
C	-2.938090	2.519739	0.060044
C	-3.220671	3.909826	0.092072
C	-2.222039	4.869681	0.098406
C	-0.852507	4.486343	0.078415
C	0.280872	5.345652	0.080095
C	1.561943	4.819253	0.060450
C	1.809035	3.422151	0.043822
H	-3.750851	1.803461	0.047315
H	-4.259496	4.225845	0.108682
H	-2.483068	5.924605	0.118439
H	0.136723	6.422837	0.097285
H	2.412379	5.494576	0.061127
H	2.827912	3.053850	0.037626
C	-2.687691	-0.750799	-0.037409
C	-3.343428	-0.736955	-1.251121
C	-4.714375	-1.072915	-1.320762
C	-5.404671	-1.412850	-0.179760
C	-4.752719	-1.445627	1.082168
C	-5.446239	-1.794671	2.272432
C	-4.797796	-1.826555	3.485854
C	-3.419668	-1.512262	3.563906
C	-2.715552	-1.164645	2.432704
C	-3.358938	-1.120268	1.167584
H	-2.793704	-0.484124	-2.152441
H	-5.214053	-1.064519	-2.284966
H	-6.459256	-1.671497	-0.230231

H	-6.502888	-2.041738	2.204220
H	-5.339557	-2.100278	4.386927
H	-2.911755	-1.555885	4.523156
H	-1.655569	-0.943920	2.497775
C	2.938480	-0.007210	-2.453027
C	3.714078	-0.035231	-3.590523
C	5.111976	0.174864	-3.514043
C	5.711040	0.402179	-2.296119
C	4.945134	0.433491	-1.099486
C	5.547424	0.661403	0.166957
C	4.787557	0.687133	1.314082
C	3.388465	0.499485	1.246772
C	2.776007	0.286107	0.029117
C	3.528585	0.228112	-1.183052
H	2.789851	0.503537	2.152391
H	5.255279	0.846376	2.281200
H	6.623725	0.805638	0.215620
H	6.785125	0.557364	-2.229325
H	5.710841	0.148480	-4.420149
H	3.251622	-0.230299	-4.553914
H	1.870952	-0.188133	-2.517566

(b) *syn*-[$PdCl_2$(BIAN)]

Pd	0.294692	-1.798529	-0.168582
Cl	2.187510	-3.107723	0.046090
Cl	-1.081842	-3.647402	0.009789
N	1.372230	0.003916	-0.422073
N	-1.296956	-0.428580	-0.442988
C	0.599695	1.010681	-0.680367
C	-0.878185	0.771746	-0.691606
C	-1.533025	2.060482	-0.960486
C	-0.477169	3.005702	-1.092729
C	0.820157	2.439360	-0.945791
C	-2.841920	2.496023	-1.069581
C	-3.079965	3.873676	-1.311309
C	-2.051607	4.792098	-1.442695
C	-0.695805	4.376946	-1.332502
C	0.463318	5.195152	-1.431158
C	1.726232	4.644661	-1.288486
C	1.928498	3.261844	-1.043699
H	-3.676810	1.811638	-0.978699
H	-4.107962	4.213218	-1.396551
H	-2.278383	5.838586	-1.629241
H	0.353043	6.260217	-1.617888
H	2.597071	5.288831	-1.365718
H	2.934341	2.872693	-0.940939
C	-2.690598	-0.740209	-0.484445
C	-3.309018	-0.879042	-1.710686
C	-4.680747	-1.210258	-1.781314
C	-5.410893	-1.390857	-0.628522
C	-4.799486	-1.262757	0.647359
C	-5.534955	-1.446690	1.849292
C	-4.925530	-1.325753	3.077234
C	-3.546715	-1.015505	3.158942
C	-2.803064	-0.824604	2.015712
C	-3.404817	-0.942481	0.735529
H	-2.726712	-0.755991	-2.618631
H	-5.149161	-1.326640	-2.754167
H	-6.466311	-1.645991	-0.678800
H	-6.592130	-1.690798	1.779271
H	-5.498745	-1.474710	3.988033
H	-3.070070	-0.937066	4.131950
H	-1.743410	-0.604033	2.084502

C	2.793734	0.153698	-0.430526
C	3.458620	0.170045	-1.639609
C	4.865643	0.296570	-1.674348
C	5.581793	0.408130	-0.504311
C	4.925036	0.385033	0.755261
C	5.645238	0.497555	1.975076
C	4.993742	0.467872	3.186928
C	3.586399	0.321981	3.233764
C	2.854397	0.215454	2.072173
C	3.499216	0.243745	0.807681
H	2.894403	0.061016	-2.560577
H	5.374392	0.298038	-2.633817
H	6.664199	0.504954	-0.527691
H	6.726462	0.603374	1.931818
H	5.557697	0.549669	4.111896
H	3.081593	0.284883	4.194964
H	1.778096	0.088391	2.115840

Table SM IV.2 Atomic coordinates of optimized structures for free ligand BIAN.

(a) *anti*-BIAN.

N	1.503993	-0.383936	-0.072197
N	-1.250685	-0.910803	0.075537
C	0.670679	0.582611	-0.000841
C	-0.830936	0.295990	0.038993
C	-1.512869	1.616934	0.076503
C	-0.492603	2.603742	0.048497
C	0.818999	2.062412	-0.000282
C	-2.831550	2.026901	0.164983
C	-3.117017	3.416338	0.206970
C	-2.122693	4.377441	0.150398
C	-0.757530	3.991620	0.066253
C	0.369332	4.854829	-0.002301
C	1.647231	4.328794	-0.078445
C	1.893684	2.931238	-0.072433
H	-3.645318	1.312432	0.192730
H	-4.155046	3.729929	0.275640
H	-2.381942	5.433132	0.170605
H	0.221790	5.931978	0.004748
H	2.496608	5.004048	-0.134784
H	2.913213	2.567628	-0.114779
C	-2.593985	-1.292836	0.007128
C	-3.378251	-1.013275	-1.103757
C	-4.693687	-1.518122	-1.205669
C	-5.232434	-2.287716	-0.198842
C	-4.459920	-2.609807	0.949950
C	-4.978976	-3.409611	2.004126
C	-4.206642	-3.729165	3.098549
C	-2.871667	-3.266613	3.187240
C	-2.338755	-2.480929	2.188233
C	-3.114570	-2.128692	1.053262
H	-2.960440	-0.417292	-1.909711
H	-5.280308	-1.288221	-2.091310
H	-6.247965	-2.668123	-0.274293
H	-6.002616	-3.769146	1.928202
H	-4.618109	-4.343810	3.894862
H	-2.264318	-3.537165	4.046784

H	-1.313106	-2.131099	2.243320
C	3.055321	-1.379932	-2.240525
C	3.821722	-1.881742	-3.270132
C	5.234525	-1.819004	-3.206841
C	5.854758	-1.269562	-2.106935
C	5.097025	-0.751542	-1.021600
C	5.717299	-0.202108	0.133209
C	4.951374	0.281492	1.170330
C	3.540687	0.267319	1.094442
C	2.894608	-0.247124	-0.021299
C	3.667474	-0.799845	-1.099106
H	2.947621	0.641529	1.923649
H	5.428059	0.684160	2.060238
H	6.802741	-0.182162	0.188991
H	6.940057	-1.226764	-2.050501
H	5.828812	-2.213005	-4.027089
H	3.341145	-2.331956	-4.134550
H	1.972180	-1.433139	-2.276443

(b) *syn*-BIAN

N	1.522115	-0.573007	-0.255321
N	-1.253252	-1.033078	-0.288689
C	0.724772	0.339266	-0.662555
C	-0.783868	0.090469	-0.677658
C	-1.415831	1.352754	-1.146064
C	-0.362245	2.276895	-1.372599
C	0.927734	1.737299	-1.127287
C	-2.721415	1.778263	-1.317934
C	-2.959147	3.116957	-1.724318
C	-1.930451	4.014537	-1.951499
C	-0.578513	3.615014	-1.771650
C	0.577790	4.425257	-1.933590
C	1.835752	3.902347	-1.689561
C	2.031690	2.557258	-1.281858
H	-3.559741	1.112502	-1.152189
H	-3.986980	3.442204	-1.859726
H	-2.152657	5.032563	-2.261887
H	0.468006	5.461478	-2.243877
H	2.707899	4.538725	-1.811782
H	3.035909	2.193557	-1.101046
C	-2.598483	-1.405708	-0.371426
C	-3.253098	-1.510896	-1.591154
C	-4.573886	-2.006655	-1.662713
C	-5.246855	-2.384471	-0.522303
C	-4.609686	-2.306880	0.745760
C	-5.269542	-2.696536	1.942910
C	-4.627656	-2.634130	3.159606
C	-3.288160	-2.182397	3.235418
C	-2.620923	-1.787564	2.096101
C	-3.260163	-1.833416	0.829986
H	-2.728682	-1.226516	-2.498556
H	-5.056805	-2.083843	-2.633338
H	-6.266343	-2.757596	-0.577417
H	-6.296073	-3.050161	1.879165
H	-5.145997	-2.938203	4.065180
H	-2.784470	-2.151132	4.197820
H	-1.591324	-1.448531	2.143538
C	2.917128	-0.491290	-0.307404
C	3.597040	-0.393765	-1.513831
C	5.008455	-0.435689	-1.553692

C	5.742331	-0.560661	-0.395242
C	5.086596	-0.677844	0.860312
C	5.810598	-0.816797	2.075599
C	5.156601	-0.950293	3.280055
C	3.741704	-0.957150	3.324613
C	3.007732	-0.814979	2.166920
C	3.654993	-0.666585	0.912730
H	3.029054	-0.306139	-2.435263
H	5.511687	-0.364140	-2.514393
H	6.828691	-0.583547	-0.426330
H	6.897453	-0.818700	2.035644
H	5.725415	-1.057727	4.199887
H	3.233928	-1.078993	4.277625
H	1.923016	-0.828812	2.191063

(c) *TS*-BIAN

N	1.571493	-0.266818	-0.335175
N	-1.190852	-0.514044	-0.171467
C	0.847192	0.763464	-0.575627
C	-0.673106	0.611305	-0.490871
C	-1.254953	1.949976	-0.772445
C	-0.169416	2.804443	-1.092241
C	1.097673	2.161136	-1.021521
C	-2.535738	2.474201	-0.763180
C	-2.719983	3.841481	-1.093488
C	-1.664986	4.662052	-1.452646
C	-0.337806	4.154801	-1.472951
C	0.834430	4.861569	-1.855114
C	2.060294	4.220880	-1.856851
C	2.210746	2.872814	-1.440742
H	-3.396022	1.860988	-0.523857
H	-3.728067	4.246709	-1.081305
H	-1.847374	5.698270	-1.726674
H	0.760039	5.902485	-2.159874
H	2.944717	4.765211	-2.176497
H	3.195335	2.422350	-1.472247
C	-2.561604	-0.786696	-0.152624
C	-3.339277	-0.715417	-1.300657
C	-4.694700	-1.112621	-1.282350
C	-5.279631	-1.568849	-0.122131
C	-4.516639	-1.673650	1.072390
C	-5.082521	-2.150667	2.286000
C	-4.320489	-2.265998	3.427226
C	-2.949598	-1.913454	3.406601
C	-2.370100	-1.437951	2.250088
C	-3.133475	-1.300645	1.061506
H	-2.886957	-0.366916	-2.224331
H	-5.275271	-1.050421	-2.199134
H	-6.325211	-1.865983	-0.107165
H	-6.134251	-2.427722	2.295582
H	-4.768422	-2.634854	4.346258
H	-2.352065	-2.022401	4.307711
H	-1.317833	-1.174512	2.222629
C	2.910891	-0.420313	-0.022137
C	3.778287	0.600337	0.368037
C	5.088375	0.322727	0.805389

C	5.552922	-0.973893	0.861111
C	4.699810	-2.058160	0.527120
C	5.138072	-3.407544	0.618569
C	4.284399	-4.447365	0.328014
C	2.949399	-4.180750	-0.060211
C	2.495631	-2.883545	-0.169705
C	3.355218	-1.790785	0.112668
H	3.427018	1.623679	0.389523
H	5.732941	1.146465	1.100701
H	6.569887	-1.183531	1.183786
H	6.162054	-3.602644	0.928755
H	4.629953	-5.474969	0.404394
H	2.276468	-5.007833	-0.270504
H	1.472569	-2.665629	-0.454606

Chapter V

Synthesis and characterization of Co and Ni complexes stabilized by keto and acetamide-derived phosphine P,O type ligands

M. Agostinho, V. Rosa, Teresa Avilés, R. Welter and P. Braunstein.

To be submitted.

Index

V.1 Resumo

Os ligandos β-keto fosfinas $R_2PCH_2C(O)Ph$ (**HL1**, R = ^{i}Pr; **HL2**, R = Ph) foram preparados por reacção de $PhC(O)CH_2Li$ com a correspondente clorofosfina. O novo fosfino-ligando derivado de acetamido $(^{i}Pr)_2PNHC(O)Me$ (**HL3**) foi preparado fazendo reagir $(^{i}Pr)_2PCl$ com N-trimetilosililoacetamida, de maneira semelhante à do ligando **HL4** [$Ph_2PNHC(O)Me$] descrito anteriormente na literatura.

Os ligandos **HL2** e **HL4** reagiram com o complexo de cobalto ciclopentadienilo [(η^5-C_5H_5)$CoI_2(CO)$] obtendo-se os mono-aductos [(η^5-C_5H_5)CoI_2{$Ph_2PCH_2C(O)Ph$}] (**3**) e [(η^5-C_5H_5)CoI_2{$Ph_2PNHC(O)Me$}] (**5**). Por tratamento de **3** e **5** com um excesso de Et_3N, sintetizou-se o complexo η^2-fosfinoenolato [(η^5-C_5H_5)CoI{Ph_2PCH⋯C(⋯O)Ph}] (**4**) e o complexo η^2-acetamidofosfina [(η^5-C_5H_5)CoI{Ph_2PN⋯C(⋯O)Me}] (**6**). **HL4** reagiu com $NiCl_2$ na presença de NaOMe obtendo-se *cis*-[Ni(Ph_2PN⋯C(⋯O)$Me)_2$] (**10**). A reacção de **HL3** com $NiCl_2.6H_2O$ em etanol seguida da adição de NaOEt resultou na obtenção do complexo *cis*-[Ni(($^{i}Pr)_2PN$⋯C(⋯O)$Me)_2$] (**11**).

A estrutura de estado sólido do ligando **HL3** foi determinada por difracção raio-X de cristal único e comparada com a do **HL4**. Os complexos **3**, **5**, **6**, **9**, **10** e **11** também foram caracterizados por cristalografia de raio-X de monocristal e a conformação dos ligandos em redor do centro metálico discutidas e comparadas com as dos outros complexos relacionados.

A minha contribuição para este trabalho consistiu na síntese do ligando **HL3** e dos complexos **3**, **5**, **4**, **6** e **11** e sua caracterização.

V.2 Abstract

The β-keto phosphine ligands $R_2PCH_2C(O)Ph$ (**HL1**, R = ^{i}Pr; **HL2**, R = Ph) were prepared by reacting $PhC(O)CH_2Li$ with the corresponding chlorophosphine. The new acetamide-derived phosphine ligand ($^{i}Pr)_2PNHC(O)Me$ (**HL3**) was prepared by reacting ($^{i}Pr)_2PCl$ with N-trimethylsilylacetamide, similar to the ligand **HL4** [$Ph_2PNHC(O)Me$] reported previously.

Ligands **HL2** and **HL4** reacted with the cobalt cyclopentadienyl complex [(η^5-C_5H_5)$CoI_2(CO)$] to afford the phosphine mono-adducts [(η^5-C_5H_5)CoI_2{$Ph_2PCH_2C(O)Ph$}] (**3**) and [(η^5-C_5H_5)CoI_2{$Ph_2PNHC(O)Me$}] (**5**). Treatment of **3** and **5** with excess Et_3N yielded the η^2-phosphinoenolate complex [(η^5-C_5H_5)CoI{Ph_2PCH⋯C(⋯O)Ph}] (**4**) and the η^2-acetamidophosphine complex [(η^5-C_5H_5)CoI{Ph_2PN⋯C(⋯O)Me}] (**6**), respectively. **HL4** reacted with $NiCl_2$ in the presence of NaOMe to give the *cis*-[Ni(Ph_2PN⋯C(⋯O)$Me)_2$] (**10**). The reaction of **HL3** with $NiCl_2.6H_2O$ in ethanol followed by the addition of NaOEt afforded complex *cis*-[Ni(($^{i}Pr)_2PN$⋯C(⋯O)$Me)_2$] (**11**).

The solid state structure of ligand **HL3** was determined by single crystal X-ray diffraction. Complexes **3**, **5**, **6**, **9**, **10** and **11** have also been characterized by X-ray crystallography and the conformation of the ligands around the metal centre discussed and compared with that of related complexes.

My contribution to this work was the synthesis of the ligand **HL3** and the complexes **3**, **4**, **5**, **6** and **11** and their characterization.

V.3 Introduction

Much research has been performed on the synthesis of functional phosphine ligands of the P, O-type and their complexation to different transition metals in order to understand their structural features and their relevance to catalytic reactions.[1-3] With softer metal ions, P-coordination is invariably observed, with or without interaction of the oxygen donor, in a chelating or, more rarely, a bridging mode. In even rarer cases involving early transition metals, the P,O ligand was found to interact with the metal solely via the oxygen function. With the ligand (diphenylphosphino)acetophenone, $Ph_2PCH_2C(O)Ph$ (**HL2**), Pd(II) complexes have been obtained in which the ligand can behave as monodentate through the P atom or chelate through P atom and the keto group.[4] Numerous transition metal complexes with these P,O-type ligands have been synthesized, including of Co(II) and Co(III).[5-9]

In the chelate backbone of the P,O ligand, a C-H atom in the five-membered cycle can be replaced with a N atom, as in the amide-derived ligands $Ph_2PN(R)C(O)Me$ (R = H, CH_3)[10] and $Ph_2PN(H)C(O)R$ (R = Ph, NH_2, and 3-pyridyl).[11, 12]

In addition to the possible occurrence of hemilabile behaviour, which can lead to enhanced reactivity in catalysis by making a coordination site more readily available, P,O chelates can lead to reactivity of their metal complexes not observed with symmetrical P,P chelates. Thus, cationic palladium(II) complexes with the acetamido-derived ligand $Ph_2PNHC(O)Me$ allowed a stepwise ethene and/or methylacrylate/CO insertion into their Pd-C bond.[13]

The synthesis of molybdenum arene complexes containing amide-derived heterodifuntional P,O ligands was investigated and the first example of a structurally characterized phosphinoiminolate complex was reported $Mo(\eta^3\text{-}C_3H_5)\{Ph_2PNHC(O)CH_3\text{-}\kappa^2 P,O\}(\eta^6\text{-}C_6H_6)][PF_6]$.[14] Complexes of rhodium(I) containing the P,O ligand $PPh_2NHC(O)Me$ or its anion $[PPh_2N\text{-}C(\text{-}O)Me]$ were synthesized and structurally characterized in which mono or bidentate modes of the P,O ligand were found.[15] Monocyclopentadienyl complexes of Nb, Ta and W containing the P,O ligands $Ph_2PCH_2C(O)Ph$ and $Ph_2PCH_2C(O)NPh_2$ have been obtained and structurally characterised.[16] The bis-chelated palladium phosphino-iminolate complex of formulation $[Pd(dmba)\text{-}\{\kappa^2P,O\text{-}PPh_2N\text{-}C\text{-}(\text{-}O)CH_3\}]$ (dmba=ortometalateddemethylbenzylamine) have shown to behave as a metalloligand with

electrophilic complexes of Cu, Ag and Au to form heterodi- or polynuclear complexes through metal coordination at the sp^2-hybridized nitrogen atom of the P,O-chelate.[17]

In this article we present the synthesis of the β-keto phosphine ligands $R_2PCH_2C(O)Ph$ (**HL1**, R = ^{i}Pr; **HL2**, R = Ph), prepared by reaction of $PhC(O)CH_2Li$ with the corresponding chlorophosphine,[4, 18] and the new acetamide-derived phosphine ligand $(^iPr)_2PNHC(O)Me$ (**HL3**), prepared similarly to the known ligand $Ph_2PNHC(O)Me$ (**HL4**).[10] The solid state structure of ligand **HL3** was determined by single crystal X-ray diffraction, and compared to that of **HL4**.[10] The coordination properties of the ligands **HL2** and **HL4** towards the cobalt cyclopentadienyl precursor $[(\eta^5\text{-}C_5H_5)CoI_2(CO)]$ have been investigated, a series of Co complexes in which the ligands display η^1-phosphine or η^2- phosphinoenolate (**HL2**) and η^2-phosphinoiminolate (**HL4**) coordination modes have been synthesised and characterised. The coordination behaviour of ligands **HL1**-**HL4** towards $NiCl_2$ was also investigated. **HL4** reacted with $NiCl_2$ in the presence of NaOMe to give the *cis*-$[Ni(Ph_2PN{\cdots}C({\cdots}O)Me)_2]$ (**10**). The reaction of **HL3** with $NiCl_2.6H_2O$ in ethanol followed by the addition of NaOEt afforded complex *cis*-$[Ni((^iPr)_2PN{\cdots}C({\cdots}O)Me)_2]$ (**11**). In addition, cobalt complexes $[(\eta^5\text{-}C_5H_5)CoI_2$(**HL2**)] (**3**), $[(\eta^5\text{-}C_5H_5)CoI_2$(**HL4**)] (**5**) and $[(\eta^5\text{-}C_5H_5)CoI($**L4**$^-)]$ (**6**) have also been structurally characterized, as well as nickel complexes **9** and **10** and **11**.

V.4 Results and Discussion

V.4.1 Synthesis and characterization of the ligands

The ligands $R_2PCH_2C(O)Ph$ (**HL1**, R = ^{i}Pr; **HL2**, R = Ph) were obtained in high yields by the previously reported procedure,[4, 18] which consists of the reaction of $PhCOCH_2Li$ with the corresponding chlorophosphine in THF at low temperature (Scheme V.1). Additional characterizing data to those previously reported for **HL1**[18] are given in the Experimental Section.

Scheme V.1 Synthesis of ligands **HL1** and **HL2**.

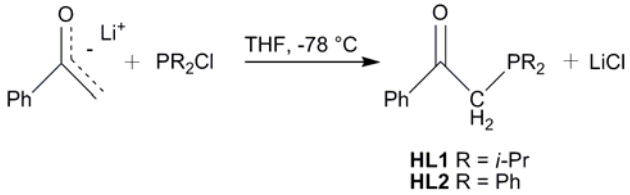

In the ^{1}H NMR spectrum of ligand **HL1**, the PCH_2 protons appear as a doublet (δ = 3.11, $^{2}J_{PH}$ = 1.3 Hz, Table V.1) and the CH protons of the ^{i}Pr substituents on the phosphorus appear as a septet of doublets (δ = 1.83, $^{2}J_{PH}$ = 1.0 Hz, $^{3}J_{HH}$ = 7.1 Hz), in agreement with values recently reported for related oxazoline ligand ($^{i}Pr)_2PCH_2$(oxazoline).[19] The ^{31}P NMR spectrum contains a singlet at δ 9.9 and the characteristic ν_{CO} band appears in the IR spectrum at 1673 cm^{-1} (Table V.1). In contrast to ligand **HL2**, which was obtained as a white solid,[4] **HL1** is an orange liquid that can be exposed to air for short periods of time, but is best kept under an inert atmosphere. Comparative spectroscopic data are presented in Table V.1.

Table V.1 Selected IR and NMR data for the ligands and complexes.

	IR	NMR[d]	
		^{1}H	^{31}P
HL1	1673[b] (s, ν_{CO})	3.11 (d, $^{2}J_{PH}$ = 1.3 Hz, 2H, PCH_2)	9.9
HL2	1670[a] (s, ν_{CO})	3.80 (s, $^{2}J_{PH}$ ~ 0 Hz 2H, PCH_2)	-17.1
HL3	1695[a] (s, ν_{CO})	2.00 (s, 3H, MeC(=O)), 5.54 (br, 1H, NH)	47.7
HL3'		2.18 (d, $^{4}J_{PH}$ = 2.7 Hz, MeC(OH)), 2.08 (br, 1H, OH)	57.5
HL4	1715[b] (s, ν_{CO})	2.13 (s, 3H, MeC(=O)), 6.15 (br, 1H, NH)	21.6
HL4'		2.30 (s, 3H, MeC(OH)), OH not observed	31.1
3	1671[a] (s, ν_{CO})	4.54 (d, $^{2}J_{PH}$ = 9.7 Hz, 2H, PCH_2)	34.6
4	1518[a] (s, ν_{CC+CO})	5.02 (s, 1H, PCH)	60.6
5	1699[a] (s, ν_{CO})	1.20 (s, 3H, Me), 6.30 (d, $^{2}J_{PH}$ = 16.7 Hz, 1H, NH)	70.7
6	1487[a] (s, ν_{CN+CO})	2.19 (s, 3H, Me)	111.1
7	1662[a] (s, ν_{CO})		
8	1515[a] (s, ν_{CC+CO})	4.55 (s, 2H, PCH)	28.2
9	1517[a] (s, ν_{CC+CO})		
10	1439[a] (s, ν_{CN+CO})	3.76 (d, $^{4}J_{PH}$ = 11.1 Hz, 6H, Me)	34.4
11	1519 (s, ν_{CN+CO})	1.40-1.23 (m, Me ^{i}Pr) , 2.16 (s, MeCO)	115.9

[a]In KBr, [b]in CH_2Cl_2, cm^{-1}. [d]In $CDCl_3$, ppm, *J* in Hz.

The new acetamido phosphine $(^{i}Pr)_2PNHC(O)Me$ **HL3** has now been synthesized by a similar procedure to that used for $Ph_2PNHC(O)Me$ (**HL4**),[10] which consists in the

condensation of N-trimethylsilylacetamide with the corresponding chlorophosphine in toluene (Scheme V.2).

Scheme V.2 Synthesis of ligands **HL3** and **HL4**.

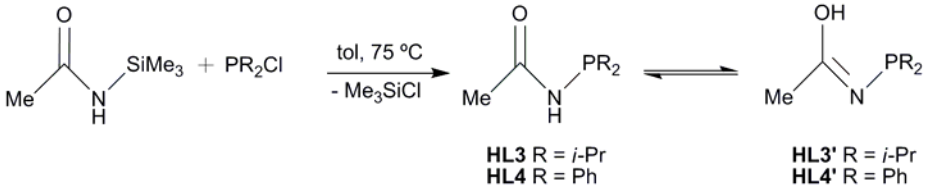

In contrast to **HL1** and **HL2**, the ^{31}P NMR ($CDCl_3$) spectrum of **HL3** consists of two signals at δ 47.7 and 57.5 (ratio 20/80). This is explained by a tautomeric equilibrium between the acetamido and the iminol forms **HL3** and **HL3'**, respectively (Scheme V.2). The N=C bond having a deshielding effect on the nearby atoms, the ^{31}P signal of **HL3'** is expected to occur at lower field than that of **HL3**. We therefore assign the signal at δ 57.5 (major tautomer) to the iminol form **HL3'**. An equilibrium of this type has already been observed for **HL4**,[10] however in that case the major tautomer in $CDCl_3$ solution was the acetamido form **HL4** (60%). The suggested tautomeric equilibrium is solvent dependent: in acetone-d_6 the acetamido forms **HL3** and **HL4** are favoured, in the case of **HL4** it is the only isomer observed, and as for **HL3** it represents 20% in $CDCl_3$. In the ^{1}H NMR spectrum the signals due to the CH_3 protons of **HL3** and **HL3'** occurred at δ 2.0 and δ 2.18, respectively (Table V.1). The ^{13}C signal of the HN-C=O moiety in **HL3** was observed at δ 172.8 and that of N=C-OH in **HL3'** at δ 177.3, the latter showing a $^2J_{PC}$ value of 18.8 Hz. Two different signals were observed for the carbon atom of the methyl group, a doublet at δ 21.8 ($^3J_{PC}$ = 14.8 Hz) and a singlet at 22.7 ppm, corresponding each to one of the tautomeric forms of the ligand (tentative assignment in the experimental section).

The solid state structure of **HL3** has been determined by single crystal X-ray diffraction. An ORTEP view as well as packing diagram build on the unique hydrogen bond detected in this compound (d_{H1-O}: 2.38 Å, N-H1-O : 161°) in show in Figures V.1 and V.2. The refined crystal structure clearly shows that only HL3 tautomer (and not the HL3') was present in the crystal. The H1 hydrogen is unambiguously observed by Fourier differences and no hydrogen atom can be stabilized (from spatial position and electronic density point of view) around the O atom (see Figure V.1).

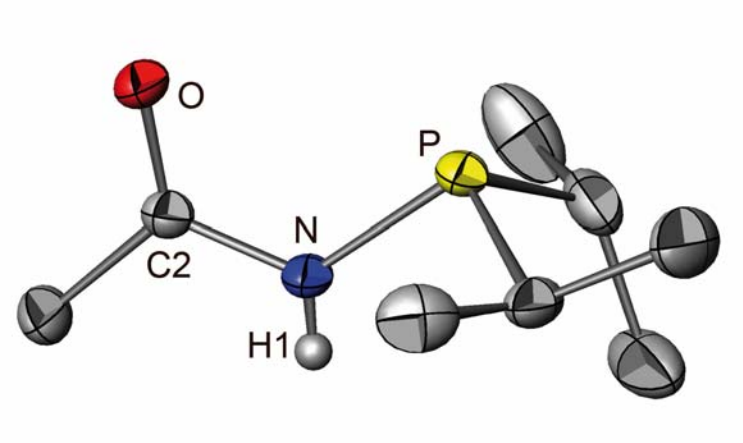

Figure V.1 ORTEP view of ligand **HL3** (hydrogen atoms have been omitted for clarity, except the H1 one on the nitrogen atom founded by Fourier differences). Displacement ellipsoids are drawn at 50% probability level.

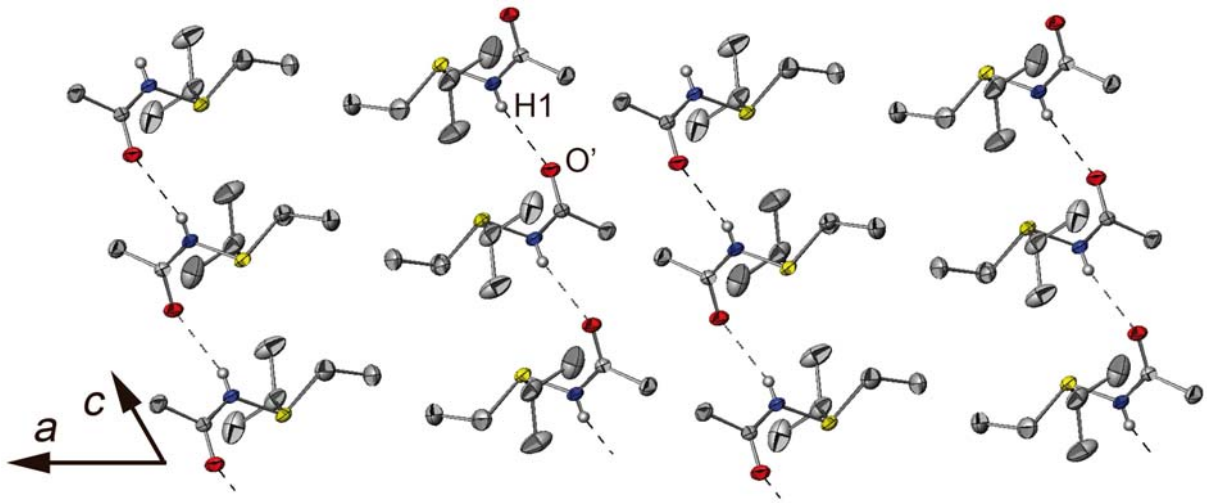

Figure V.2 Crystal packing diagram of ligand **HL3** showing the N-H···O hydrogen bonding. Symmetry code for equivalent positions: x, -y+1/2, z-1/2. Dashed lines indicate the hydrogen bonds.

V.4.2 Cobalt Complexes

The reaction between [(η^5-C_5H_5)CoI_2(CO)] and $Ph_2PCH_2C(O)Ph$ (**HL2**), in toluene resulted in the cleavage of the Co-CO bond to afford the phosphine mono-adduct [(η^5-C_5H_5)CoI_2(HL2)] (**3**), as a dark blue solid (Scheme V.3).

Scheme V.3 Synthesis of complexes **3** and **4**.

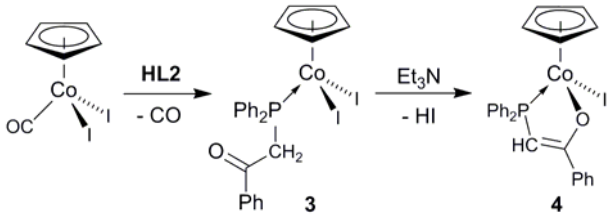

The ^{31}P NMR spectrum of **3** displayed a resonance at δ 34.6 ppm, shifted ca. 52 ppm downfield of the free phosphine (δ -17.1 ppm),[4] consistent with the coordination of the phosphorus to a cobalt center.[20] The methylene protons were observed to be magnetically equivalent, giving rise to a doublet in the ^{1}H NMR spectrum (δ = 4.54, $^2J_{PH}$ = 9.7, Table V.1). The IR spectrum confirmed that the carbonyl fragment of the ketophosphine was not coordinated to the metal center (ν_{CO} = 1671 cm^{-1} for **3** vs 1670 cm^{-1} for the free ligand, Table V.1).[4] The solid state structure of **3** was determined by X-ray diffraction and an ORTEP view is shown in Figure V.3 (selected distances and angles are given in the caption). The angle between the C15/C20 and C9/C14 phenyl rings is 67 (1)°, and a π-π interaction exists between the latter ring and the C3/C8 phenyl rings (21(1)° between both rings, see dashed line in Figure V.3). The other distances and angles are typically classical in such cobalt complex. No hydrogen bond has been detected in this crystal structure while intramolecular CH-π interactions occur between C7-H7 and C8-C8, and the C15/C20 and C9/C14 phenyl rings, respectively.

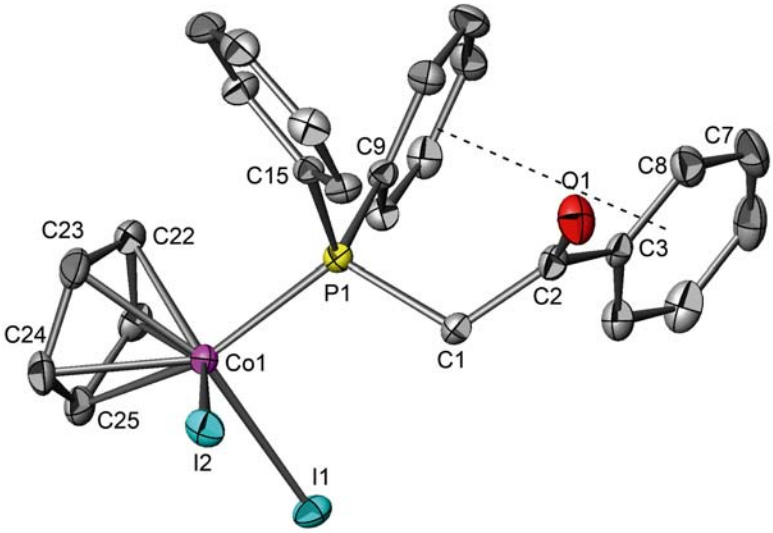

Figure V.3 ORTEP view of complex **3** (the hydrogen atoms have been omitted for clarity). Displacement ellipsoids are drawn at 50% probability level. Selected distances and angles: I1-Co1, 2.593(1) Å; I2-Co1, 2.569(1) Å, Co1-P1, 2.231(1) Å; P1-C1, 1.85(1) Å; C1-C2, 1.51(1) Å; O1-C2, 1.21(1) Å; P1-Co1-I2, 88.9(1)°; C1-P1-Co1, 114.4(1)°, C9-P1-C15, 105.6(1)°.

Treatment of **3** with excess triethylamine yielded the η^2-phosphinoenolate complex [(η^5-C_5H_5)CoI(L2)] (**4**) as a dark solid (Scheme V.3). The IR spectrum confirmed that the oxygen was now coordinated to the metal center (ν_{CC+CO} = 1518 cm^{-1}). The ^{31}P NMR resonance of **4** at 60.6 ppm is shifted 26 ppm downfield to that for the corresponding phosphine complex **3**.

The reaction between [(η^5-C_5H_5)CoI_2(CO)] and the (diphenylphosphino)acetamide ligand **HL4** in toluene resulted in the cleavage of the Co-CO bond to afford the *P* mono-aduct complex [(η^5-C_5H_5)CoI_2(**HL4**)] **5**, as a dark purple cristalline solid (Scheme V.4).

Scheme V.4 Synthesis of complexes **5** and **6**.

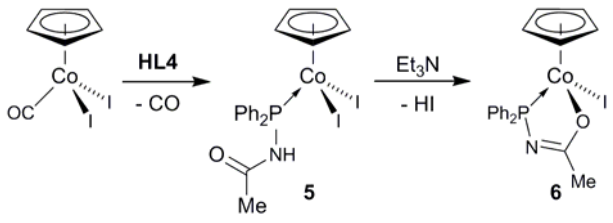

The IR spectrum confirmed that the carbonyl fragment was not coordinated to the metal centre (ν_{CO} = 1699 cm^{-1} for 5 vs 1715 cm^{-1} for the free ligand).[10] The ^{31}P NMR of **5** shows a peak at δ 69.7 which corresponds to a downfield of 48 ppm relative to the free ligand (δ -21.6ppm).[10] The acetamide N*H* proton was observed in the ^{1}H NMR spectrum at δ 6.34 and the Me protons at δ 1.20 (Table V.1). The solid state structure of **5** was determined by X-ray diffraction and an ORTEP view is shown in Figure V.4 (selected distances and angles are given in the caption).

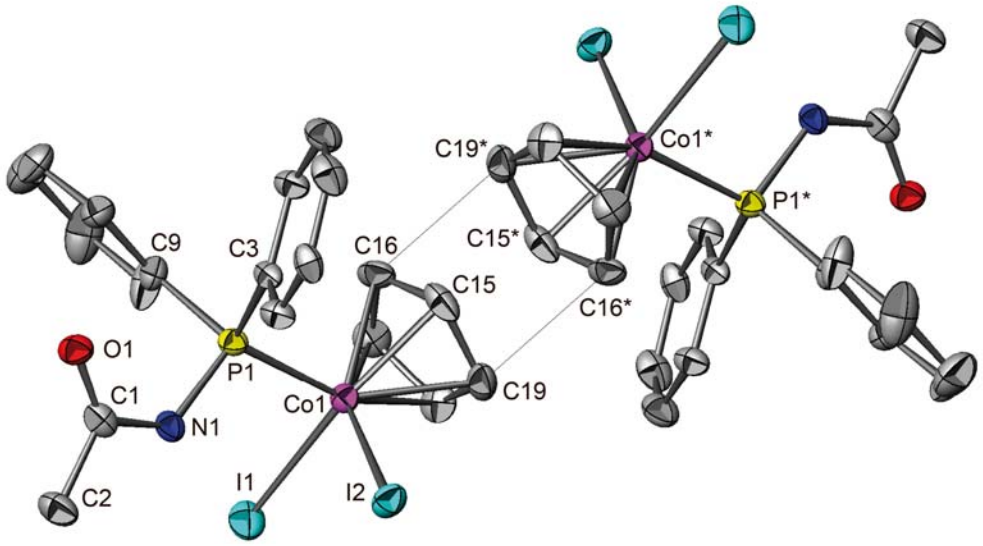

Figure V.4 ORTEP view of pseudo dimer of the complexes **5** (the hydrogen atoms have been omitted for clarity). Displacement ellipsoids are drawn at 50% probability level. Symmetry operator * for equivalent positions: 2-x, -1-y, 1-z. Selected distances and angles: I1-Co1, 2.596(1) Å; I2-Co1, 2.577(1) Å, Co1-P1, 2.198(2) Å; P1-N1, 1.71(1) Å; N1-C1, 1.35(1) Å; O1-C1, 1.23(1) Å; I1-Co1-I2, 93.4(1)°; N1-P1-Co1, 109.8(2)°, C9-P1-C3, 105.9(3)°.

Two quasi identical molecules of complex **5** crystallize in the asymmetric unit. Only one of them is described. The angle between the phenyl rings C3/C8 and C9/14 is 62(1)°, a value very close to that found in complex **3**. A short π–π intermolecular interaction is observed between the two cyclopentadienyl rings C15/C19 with a distance between the centroids of 3.31(1) Å. This situation allows us to describe this crystal structure as that of pseudo-dimers, as shown in Figure V.4. From the crystal packing point of view, these pseudo-

dimers are connected to each other by some CH-π interactions and numerous van der Waals contacts but no classical hydrogen bond has been found in this structure.

Table V.2 Crystal data and X-ray refinement details for **HL3**, complex **3** and complex **5**,$CHCl_3$,1/2(CH_2Cl_2).

Compound	Ligand **HL_3**	Complex **3**	Complex **5**, solvent
Formula	$C_8H_{18}NOP$	$C_{25}H_{22}CoIOP$	$2(C_{19}H_{18}CoI_2NOP)$, $CHCl_3$,0.5(CH_2Cl_2)
Formula weight	175.20	682.13	1384.19
Crystal system	monoclinic	monoclinic	triclinic
Space group	P 2_1/c	P2_1/c	P-1
a (Å)	15.5860(5)	10.2740(2)	8.0520(3)
b (Å)	7.8790(4)	8.19200(10)	15.4070(5)
c (Å)	9.1420(12)	28.0720(6)	19.8740(7)
alpha (°)	90.00	90.00	89.393(2)
beta (°)	105.741(2)	94.9260(8)	82.027(2)
gamma (°)	90.00	90.00	76.3740(14)
V (A^3)	1080.55(16)	2353.94(7)	2372.33(14)
Z	4	4	2
Density ($g.cm^{-3}$)	1.077	1.925	1.938
M (Mo Kα) (mm^{-1})	0.209	3.435	3.601
F(000)	384	1312	1321
Data collection			
Temperature (K)	173(2)	173(2)	173(2)
Theta min - max	1.36 - 29.15	1.46 - 30.02	1.36 - 30.07
Dataset[h, k, l]	-21/21, -8/10, -12/12	-14/14, -10/11, -39/39	-11/11, -21/20, -27/25
Tot., Uniq. Data, R(int)	5114, 2898, 0.0466	11181, 6859, 0.0288	19144, 13854, 0.0342
Observed data >2σ(I)	1559	4838	8377
Refinement			
Nreflections, Nparameters	2898, 104	6859, 271	13854, 494
R2, R1, wR2, wR1, Goof	0.1227, 0.0568, 0.1650, 0.1410, 1.040	0.0622, 0.0337, 0.0688, 0.0602, 1.014	0.1162, 0.0613, 0.1912, 0.1643, 1.043
Max. and Av. Shift/Error	0.020, 0.001	0.002, 0.000	0.002, 0.000
Min,Max.($e.A^{-3}$)	-0.259, 0.320	-0.925, 0.846	-1.530, 1.501

Treatment of **5** with excess triethylamine yielded the η^2-acetamidophosphine complex [(η^5-C_5H_5)CoI(**L4**)] (**6**) as a dark solid (Scheme V.4). The IR spectrum confirmed that the oxygen atom was now coordinated to the metal centre (ν_{CN+CO} = 1487 cm^{-1}, Table V.1). The solid state structure of **6** was also determined by X-ray diffraction and an ORTEP view of its molecular structure is shown in Figure V.5 (selected distances and angles are given in the caption).

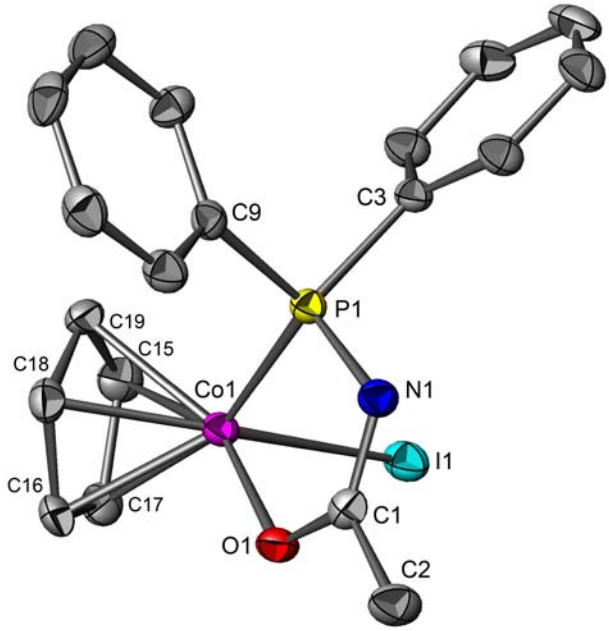

Figure V.5 ORTEP view of complex **6** (the hydrogen atoms have been omitted for clarity). Displacement ellipsoids are drawn at 50% probability level. Selected distances and angles: I1-Co1, 2.572(1) Å; O1-Co1, 1.924(2) Å, Co1-P1, 2.190(1) Å; P1-N1, 1.676(2) Å; N1-C1, 1.32(1) Å; O1-C1, 1.29(1) Å; O1-Co1-P1, 82.6(1)°; I1-Co1-P1, 94.45(2)°; N1-P1-Co1, 102.2(1)°, C9-P1-C3, 102.1(2)°.

The crystal structure confirms that a five-member heteroatomic ring was effectively formed which contains five different chemical elements. This ring is almost planar with a maximum deviation from the ring of 0.03 Å for both Co1 and P1 atoms. This ring makes an angle of 41(1)°, 59(1)° and 76°(1) with the cyclopentadienyl ring, the C3/C8 phenyl ring and the C9/C14 phenyl ring, respectively. The angle between the two phenyl rings is 89(1)°, against 67° and 62° in complexes **3** and **5**, respectively. No specific π–π interaction or classical H-bond was observed. From the crystal packing point of view, the main intermolecular interaction are three short CH-pi interactions (C5-H5 →cyclopentadienyl ring,

C7-H7 → C3/C8 phenyl ring and C13-H13 → C9/C14 phenyl ring, with distances from the hydrogen atoms to the centroids of 2.90(1) Å, 2.72(1) Å and 3.00(1) respectively).

V.4.3 Nickel Complexes

We previously reported the preparation of complex **7** [$NiCl_2$(**HL2**)$_2$] by addition of ligand **HL2** to a solution of $NiCl_2 \cdot 6H_2O$ in ethanol (Scheme V.5). Treating a stirred suspension of **7** in ethanol with NaOEt afforded complex *cis*-[Ni(**L2**)$_2$] (**8**) (Scheme V.5).[21] Complex **8** can also be obtained by reacting $Ni(COD)_2$ with 2 mol equiv. of **HL2.**[21]

Scheme V.5 Synthesis of complexes **7** and **8**.

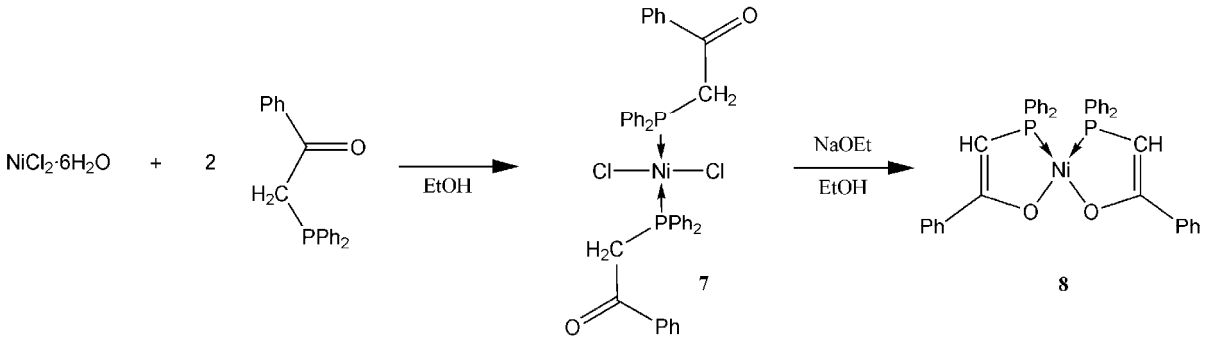

The *cis* arrangement of the ligand was inferred from the presence in the ^{1}H NMR spectrum of a singlet for the PCH proton,[21] and confirmed by the solid state structure of **8** obtained independently by reacting the ylide $Ph_3PCHC(O)Ph$ with $Ni(COD)_2$ in the presence of $AsPh_3$.[22] Note that complex **8** corresponds to the deactivated form of oligo- or polymerization SHOP catalysts of type **2,** but can be converted to an active ethylene homo-polymerization catalyst by alkylation with trimethylaluminum.[23, 24]

We have found that complex **9**, prepared by a similar reaction pathway but from **HL1** (Scheme V.6), is obtained as a mixture of *cis*-[Ni(**L1**)$_2$] and *trans*-[Ni(**L1**)$_2$] isomers which are in equilibrium in solution.[7]

Scheme V.6 Synthesis of complex and solution equilibrium of complex **9**.

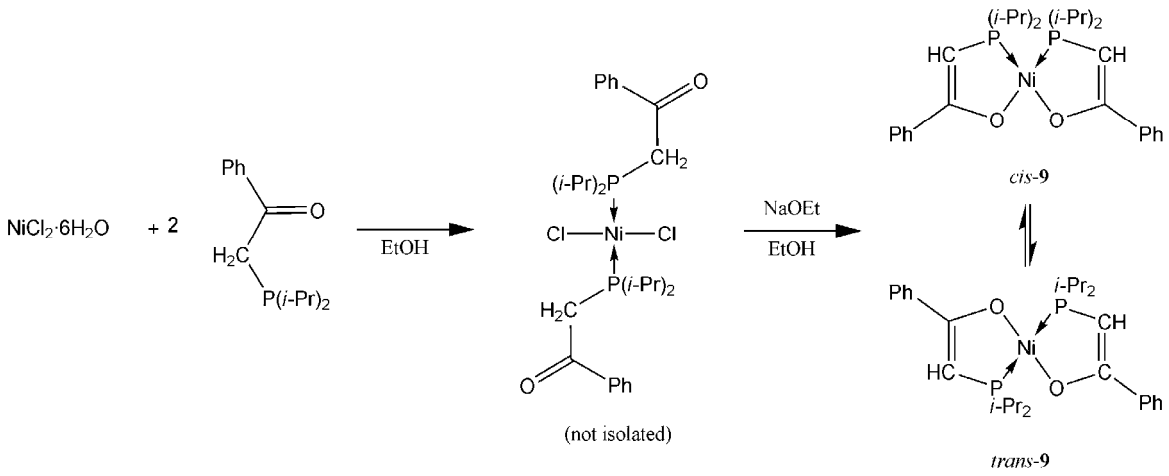

The formation of both *cis*- and *trans*-**9** can be explained by opposite steric and electronic effects, the former favoring the *trans*-arrangement while the latter favors the *cis*-arrangement due to the *trans* effect of the phosphorus donor atoms. Slow diffusion of hexane into a CH_2Cl_2 solution of the isomers afforded crystals suitable for X-ray diffraction, which revealed to be the *trans*-**9** isomer. An ORTEP view of this *trans*-**9** complex is shown in Figure V.6 and selected bond distances and angles are given in the caption.

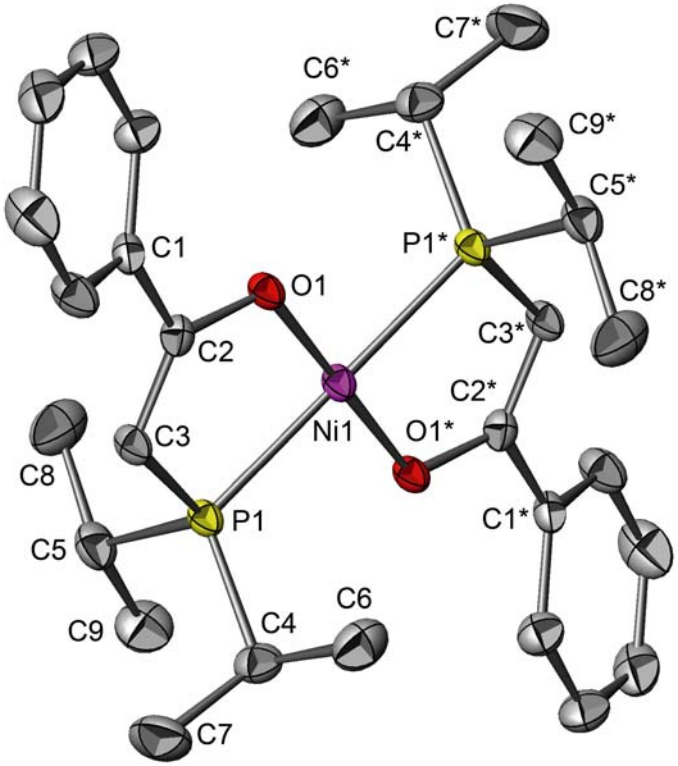

Figure V.6 ORTEP view of complex *trans*-**9** (the hydrogen atoms have been omitted for clarity). Displacement ellipsoids are drawn at 50% probability level. Symmetry code for equivalent positions *: -x, 2-y, -z. Selected distances and angles: Ni1-O1, 1.850(1) Å; Ni1-P1, 2.199(1) Å, P1-C3, 1.769(2) Å; C3-C2, 1.354(3) Å; C2-O1, 1.32(1) Å; C2-C1, 1.49(1) Å; P1-C5, 1.841(2) Å; P1-C4, 1.836(2) Å; O1-Ni1-P1, 87.0(1)°; O1-Ni1-O1*, 180.0(1)°; C3-P1-Ni1, 97.9(1)°; C2-O1-Ni1, 119.4(2)°; O1-C2-C3, 123.0(2)°.

The crystal structure clearly reveals the square planar coordination environment of the nickel centre (the nickel centre is on the crystallographic -1 inversion centre). The five-member heteroatomic ring Ni1-P1-C3-C2-O1 is almost planar, with a maximum deviation from the Least-squares plane of +0.31(1) Å and -0.30(1) Å for Ni1 atom and P1 atom, respectively. This ring makes an angle of 30(1)° with the phenyl ring. The crystal packing reveals many intermolecular CH-π interactions and especially a short one involving the phenyl ring and the C8-H8 group (2.73(1) Å between the hydrogen atom and the ring centroid with an angle of 146(1)°).

In contrast to the equilibrium found with **9**, the *t*-Bu substituted analogue of **8**, [Ni{(*t*-Bu)$_2$PCH^{---}C($^{---}$O)Ph}$_2$], was observed only as the *trans* isomer, however no crystal structure was reported.[25]

The reaction of **HL4** with $NiCl_2$ in methanol, in the presence of NaOMe, afforded *cis*-[Ni(**L4**)$_2$] (**10**) (Scheme V.7). Its ^{31}P NMR resonance is shifted ca. 13 ppm downfield of the free ligand (δ 21.6 ppm).[10] In the ^{1}H NMR spectrum the Me protons were observed at δ 1.20 ppm (Table V.1). The IR spectrum confirmed that the oxygen atom was coordinated to the metal center (ν_{CN+CO} = 1439 cm^{-1}, Table V.1).

Scheme V.7 Synthesis of complex **10**.

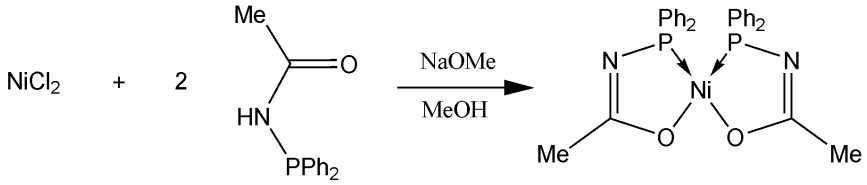

10

The solid-state structure of **10** was determined by single crystal X-ray diffraction, a ORTEP view of its molecular structure is shown in Figure V.7 and selected distances and angles are given in the caption.

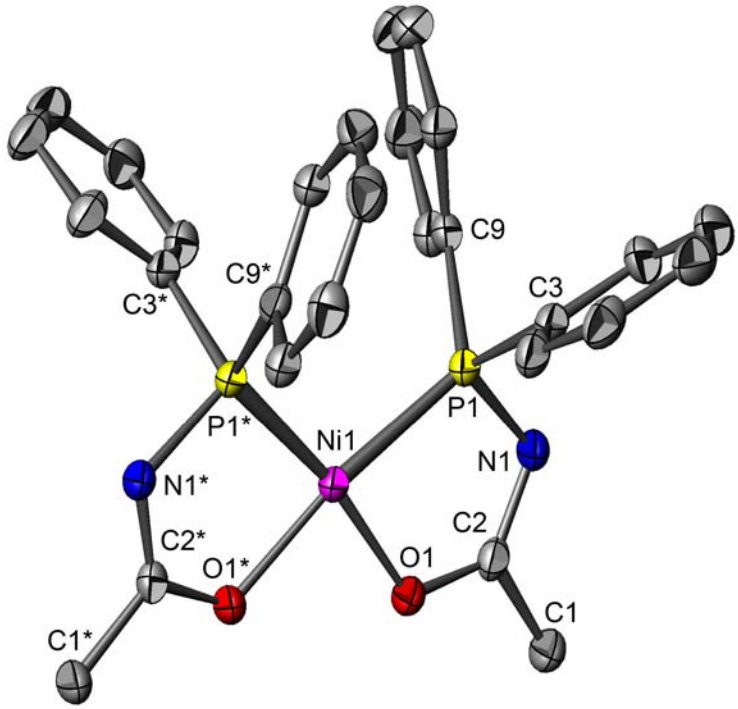

Figure V.7 ORTEP view of complex **10** (the hydrogen atoms have been omitted for clarity). Displacement ellipsoids are drawn at 50% probability level. Symmetry code for equivalent positions *: 1-x, y, 1/2-z. Selected distances and angles: Ni1-O1, 1.891(1) Å; Ni1-P1, 2.153(1) Å, P1-C3, 1.816(2) Å; P1-C9, 1.805(2) Å; P1-N1 1.686(2) Å; O1-C2, 1.299(2) Å; C2-C1, 1.497(3) Å; C2-N1, 1.313(3) Å; P1-Ni1-P1* 105.2(1)°; O1-Ni1-O1*, 87.8(1)°; P1-Ni1-O1, 171.3(1)°; C2-O1-Ni1, 118.0(1)°; O1-C2-C1, 125.0(2)°.

As clearly shown in Figure V.7, the nickel atom has a square-planar coordination and lies on the crystallographic twofold axis. The five-member heteroatomic ring Ni1-O1-C2-N1-P1 is almost planar with a maximum deviation from the least-squares plane of +0.065(1) and -0.071(1) for Ni1 and P1, respectively. The angle between both phenyl rings is 75(1)° and the angles between the heteroatomic ring and the phenyl rings are almost the same i.e. 70(1)° and 73(1)° for C3/C8 and C9/C14, respectively. No specific π–π stacking or classical hydrogen bond was detected is this crystal structure. Only four significant CH-π interactions can be described from a crystal packing point of view.

The reaction of **HL3** with $NiCl_2.6H_2O$ in ethanol followed by the addition of NaOEt afforded the complex *cis*-[Ni(**L3**)$_2$] **(11)** (Scheme V.8). Its ^{31}P NMR spectrum displayed a single peak at δ = 115.9 ppm, indicating the presence of only one isomer.

The CH_3 protons of the ^{i}Pr substituents of the phosphorus appear as two doublet of doublets (δ = 1.24-1.29, $^{3}J_{PH}$ = 14.5 Hz, $^{3}J_{HH}$ = 7 Hz and δ = 1.35-1.41, $^{3}J_{PH}$ = 17.1 Hz, $^{3}J_{HH}$ = 7.2 Hz). The multiplet assigned to the ^{i}PrC*H* was not sufficiently well defined to allow us to determine the J_{HH} and J_{PH} coupling constants.

A crystal structure determination showed that the only isomer formed is the *cis*-**11**, although steric effects favor a *trans*-arrangement. The *trans* effect of the phosphorous donor atoms favoring the *cis*-arrangement appears in this case to be the dominant effect. The IR spectrum confirmed that the oxygen atom was coordinated to the metal center (ν_{CN+CO} = 1519 cm^{-1}, Table V.1)

Scheme V.8 Synthesis of complex **11**.

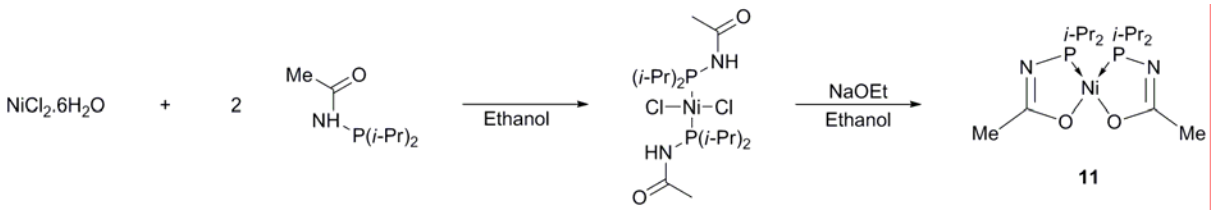

The solid state structure of **11** was determined by single crystal X-ray diffraction. An ORTEP view is shown in Figure V.8 and selected distances and angles are given in Figure V.8 caption.

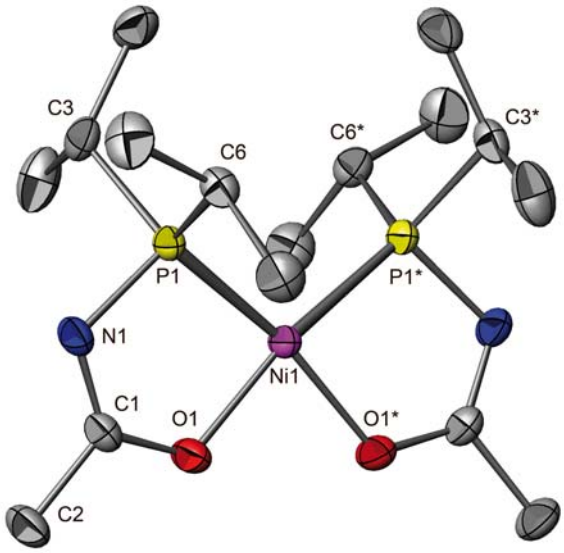

Figure V.8 ORTEP view of complex **11** (the hydrogen atoms have been omitted for clarity). Displacement ellipsoids are drawn at 50% probability level. Symmetry code for equivalent positions *: -x+2, y, -z+3/2. Selected distances and angles: Ni1-O1, 1.887(2) Å; Ni1-P1, 2.175(1) Å, P1-C3, 1.831(2) Å; P1-C6, 1.841(2) Å; P1-N1 1.690(2) Å; O1-C1, 1.291(2) Å; C2-C1, 1.502(3) Å; C1-N1, 1.302(3) Å; P1-Ni1-P1* 109.4(1)°; O1-Ni1-O1*, 85.2(1)°; P1-Ni1-O1, 166.2(1)°; C1-O1-Ni1, 118.5(1)°; O1-C1-N1, 125.7(2)°.

The nickel atom is in a square planar coordination environment and lies on the crystallographic twofold axis (space group C2/c). The five member heteroatomic ring Ni1-O1-C2-N1-P1 is almost planar with a maximum deviation from the least-squares plane of +0.027(1) and -0.026(2) for Ni1 and O1, respectively. No specific π–π stacking or classical hydrogen bond has been detected is this crystal structure but numerous CH-π interactions exist in the crystal packing.

Table V.3 Crystal data and X-ray refinement details for complexes **6**, **9**, **10** and **11**.

Compound	Complex **6**	Complex **9**	Complex **10**	Complex **11**
Formula	$C_{19}H_{18}CoINOP$	$C_{28}H_{40}NiO_2P_2$	$C_{28}H_{26}N_2NiO_2P_2$	$C_{16}H_{34}N_2NiO_2P_2$
Formula weight	493.14	529.25	543.16	407.10
Crystal system	Monoclinic	Triclinic	Monoclinic	monoclinic
Space group	$P2_1/c$	P-1	C2/c	C 2/c
a (Å)	12.6820(2)	8.3590(2)	15.5110(8)	12.4880(9)
b (Å)	8.3580(2)	10.0440(4)	8.9890(12)	9.9680(7)
c (Å)	17.9100(4)	10.1440(3)	19.733(3)	17.9220(12)
alpha (°)	90.00	63.3780(16)	90.000(7)	90.00
beta (°)	100.1030(13)	66.9910(16)	112.010(9)	108.706(3)
gamma (°)	90.00	80.8330(14)	90.000(5)	90.00
V (A^3)	1868.95(7)	700.67(4)	2550.8(5)	2113.1(3)
Z	4	1	4	4
Density ($g.cm^{-3}$)	1.753	1.254	1.414	1.280
M (Mo Kα) (mm^{-1})	2.661	0.828	0.915	1.079
F(000)	968	282	1128	872
Data collection				
Temperature (K)	173(2)	173(2)	173(2)	173(2)
Theta min - max	1.63 - 30.00	2.27 - 30.03	2.83 - 29.11	2.40 - 26.37
Dataset[h, k, l]	-17/17, -10/11, -25/25	-11/11, -13/14, -14/14	-21/21, -12/10, -26/26	-15/15, -12/11, -15/22
Tot., Uniq. Data, R(int)	9352, 5456, 0.0298	5962, 4082, 0.0303	5084, 3377, 0.0253	4974, 2097, 0.0556
Observed data >2σ(I)	4025	2681	2742	1899
Refinement				
Nreflections, Nparameters	5456, 217	4082, 151	3377, 159	2097, 105
R2, R1, wR2, wR1, Goof	0.0591, 0.0358, 0.0886, 0.0793, 1.046	0.0821, 0.0418, 0.1085, 0.0933, 1.019	0.0576, 0.0408, 0.1110, 0.1039, 1.139	0.0436, 0.0356, 0.1065, 0.1027, 1.198
Max. and Av. Shift/Error	0.003, 0.000	0.001, 0.000	0.001, 0.000	0.001, 0.000
Min,Max.($e.A^{-3}$)	-1.093, 0.892	-0.562, 0.501	-0.697, 0.453	-0.683, 0.472

V.5 Conclusion

β-keto phosphine ligands $R_2PCH_2C(O)Ph$ (**HL1**, R = ^{i}Pr; **HL2**, R = Ph) were prepared by reacting $PhC(O)CH_2Li$ with the corresponding chlorophosphine. The new acetamide-derived phosphine ligand $(^iPr)_2PNHC(O)Me$ (**HL3**) was prepared by reacting $(^iPr)_2PCl$ with N-trimethylsilylacetamide, similar to the ligand **HL4** [$Ph_2PNHC(O)Me$] reported previously. Ligands **HL2** and **HL4** reacted with the cobalt cyclopentadienyl complex [(η^5-C_5H_5)CoI_2(CO)] to afford the phosphine mono-adducts [(η^5-C_5H_5)CoI_2{$Ph_2PCH_2C(O)Ph$}] (**3**) and [(η^5-C_5H_5)CoI_2{$Ph_2PNHC(O)Me$}] (**5**). Treatment of **3** and **5** with excess Et_3N yielded the η^2-phosphinoenolate complex [(η^5-C_5H_5)CoI{Ph_2PCH---C(---O)Ph}] (**4**) and the η^2-acetamidophosphine complex [(η^5-C_5H_5)CoI{Ph_2PN---C(---O)Me}] (**6**), respectively. **HL4** reacted with $NiCl_2$ in the presence of NaOMe to give the *cis*-[Ni(Ph_2PN---C(---O)$Me)_2$] (**10**). The reaction of **HL3** with $NiCl_2.6H_2O$ in ethanol followed by the addition of NaOEt afforded complex *cis*-[Ni(($^iPr)_2PN$---C(---O)$Me)_2$] (**11**). The solid state structure of ligand **HL3** was determined by single crystal X-ray diffraction. Complexes **3**, **5**, **6**, **9**, **10** and **11** have also been characterized by X-ray crystallography

V.6 Experimental section

The ^1H, ^{13}C and ^{31}P NMR spectra were recorded at 300.13, 75.48 and 121.49 MHz, respectively, on FT Bruker AC300, Avance 300, unless otherwise stated. IR spectra in the range 4000–400 cm^{-1} were recorded on a Bruker IFS66FT and a Perkin Elmer 1600 Series FTIR. Elemental analyses were preformed by the "Service de Microanalyse, Université Louis Pasteur (Strasbourg, France)". All reactions were carried out under purified N_2, using Schlenk techniques, and the solvents were freshly distilled under nitrogen prior to use. Ligands **HL2**[4] and **HL4**[10] were prepared according to literature procedures, as were complexes [(η^5-C_5H_5)CoI_2(CO)][26], **7**, **8**[21, 27] and **9**.[7] Other chemicals were commercially available and used as received.

*V.6.1 Preparation and spectroscopic data for **HL1***

HL1 was prepared similarly to **HL2** [$Ph_2PCH_2C(O)Ph$],[4] but starting from acetophenone and $^{i}Pr_2PCl$, it was obtained as a clear yellow liquid. We first reported **HL1** in 1996,[18] now we report additional analytical data. IR (CH_2Cl_2): 1673 (s, ν_{CO}) cm^{-1}. ^1H NMR (300.13 MHz, $CDCl_3$, room temp.): δ 1.08 [dd, $^3J_{PH}$ = 5.7 Hz, $^3J_{HH}$ = 7.1 Hz, 6H, $(CH(CH_3)(CH_3))_2$], 1.12 [dd, $^3J_{PH}$ = 3.3 Hz, $^3J_{HH}$ = 7.1 Hz, 6H, $(CH(CH_3)(CH_3))_2$], 1.83 [septd, $^2J_{PH}$ = 1.0 Hz, $^3J_{HH}$ = 7.1 Hz, 2H, $(CH(CH_3)_2)_2$], 3.11 (d, $^2J_{PH}$ = 1.3 Hz, 2H, PCH_2), 7.40-7.55 (complex m, 3H, aromatic), 7.91-8.02 (m, 2H, aromatic). ^{13}C NMR (75.48 MHz, $CDCl_3$, room temp.): δ 18.8 [d, $^2J_{PC}$ = 10.5 Hz, $(CH(CH_3)(CH_3))_2$], 19.6 [d, $^2J_{PC}$ = 15.5 Hz, $(CH(CH_3)(CH_3))_2$], 24.1 [d, $^1J_{PC}$ = 15.3 Hz, $(CH(CH_3)_2)_2$], 34.6 (d, $^1J_{PC}$ = 29.8 Hz, PCH_2), 128.3-137.0 (aromatics), 199.5 [d, $^2J_{PC}$ = 8.2 Hz, C(O)]. ^{31}P NMR (121.49 MHz, $CDCl_3$, room temp.): δ 9.9 (s).

*V.6.2 Preparation and spectroscopic data for **HL3***

The compound $MeC(O)NHSiMe_3$ (0.759 g, 5.78 mmol) was dissolved in toluene (20 mL), $P(^{i}Pr)_2C1$ (0.882 g, 5.78 mmol) was added to the solution and the mixture was placed under vacuum for 30 s, before being heated to 60 ºC. The mixture was placed under vacuum for 10 s every 5 min in order to eliminate $ClSiMe_3$ which was formed. After 30 min, the solution was allowed to cool to ambient temperature. The solvent was then evaporated under reduced pressure and residue thus obtained dried in vacuum overnight. After this period a crystalline material with a melting point close to room temperature was obtained, keeping this material at 5 ºC overnight afforded suitable crystals for X-ray diffraction. Overall yield: 0.700 g (69%). **HL3** is soluble in most common solvents (including petroleum ether) and therefore it was difficult to purify, however, the crude product could be used for metal complexation and the resulting complexes were easier to purify. IR (KBr): 1695 (s, ν_{CO}) cm^{-1}. ^1H NMR (300.13 MHz, $CDCl_3$, room temp.): δ 1.02 [dd, $^3J_{PH}$ = 0.9 Hz, $^3J_{HH}$ = 7.0 Hz, 6H, $(CH(CH_3)(CH_3))_2$], 1.07 [dd, $^3J_{PH}$ = 4.2 Hz, $^3J_{HH}$ = 7.0 Hz, 6H, $(CH(CH_3)(CH_3))_2$], 1.72 [septd, $^2J_{PH}$ = 2.4 Hz, $^3J_{HH}$ = 7.0 Hz, 2H, $(CH(CH_3)_2)_2$], 2.00 [s, $CH_3C(=O)$], 2.08 (br, OH), 2.18 [d, $^4J_{PH}$ = 2.7 Hz, $CH_3C(OH)$], 5.54 (br, NH), see text. ^{13}C NMR (75.48 MHz, $CDCl_3$, room temp.): δ 16.9 [d, $^2J_{PC}$ = 7.8 Hz, $(CH(CH_3)(CH_3))_2$], 18.3 [d, $^2J_{PC}$ = 19.8 Hz,

($CH(CH_3)(CH_3)$)$_2$], 21.8 [d, $^3J_{PC}$ = 14.8 Hz, $CH_3C(OH)$], 22.7 [s, $CH_3C(=O)N$], 25.9 [d, $^1J_{PC}$ = 12.1 Hz, ($CH(CH_3)_2$)$_2$], 172.8 [s, C(O)], 177.3 [d, $^2J_{PC}$ = 18.8 Hz, NC(OH)]. ^{31}P NMR (121.49 MHz, $CDCl_3$, room temp.): δ 47.7 (s, minor isomer 20% **HL3**), 57.5 (s, major isomer 80% **HL3'**).

*V.6.3 Preparation and spectroscopic data for **3***

The complex [(η^5-C_5H_5)CoI_2(CO)] (0.750 g, 1.85 mmol) was suspendend in toluene (50 ml) and **HL2** (0.560 g, 1.84 mmol) was added. The reaction mixture was stirred at room temperature for 1 h. The solvent was then evaporated under reduced pressure affording a dark blue residue. The latter was washed with diethylether (5 mL) and pentane (2 × 10 mL) and dried under vacuum (dark blue powder, 1.16 g, 92%). IR (KBr): 1671 (s, ν_{CO}) cm^{-1}. ^{1}H NMR (300.13 MHz, $CDCl_3$, room temp.): δ 4.54 (d, $^2J_{PH}$ = 9.7 Hz, 2H, PCH_2), 5.06 (s, 5H, η^5-C_5H_5), 7.17 (t, *J* = 7.6 Hz, 2H, aromatic), 7.31-7.45 (complex m, 7H, aromatic), 7.57 (d, *J* = 7.6 Hz, 2H, aromatic), 8.07 (t, *J* = 8.9 Hz, 4H, aromatic). ^{31}P NMR (121.49 MHz, $CDCl_3$, room temp.): δ 34.6 (s). Anal. Calcd for $C_{25}H_{22}CoI_2OP$: C, 44.02; H, 3.25. Found: C, 44.30; H, 3.30.

*V.6.4 Preparation and spectroscopic data for **4***

To a solution of complex **3** (0.124 g, 0.18 mmol) in toluene (20 ml) was added excess Et_3N (1 ml, 7.12 mmol). The reaction mixture was stirred at room temperature for 1 h. The solution was then filtered through dry Celite and the solvent evaporated under reduced pressure. The residue was washed with diethylether (5 mL) and pentane (2 × 10 mL) and dried under vacuum overnight. Complex **4** was obtained as a black solid (74 mg, 73%). IR (KBr): 1518 (s, ν_{CC+CO}) cm^{-1}. ^{1}H NMR (300.13 MHz, $CDCl_3$, room temp.): δ 5.02 (s, 1H, PCH), 5.16 (s, 5H, η^5-C_5H_5), 7.26-7.29 (m, 2H, aromatic), 7.44-7.52 (complex m, 7H, aromatic), 7.63-7.73 (m, 4H, aromatic), 7.82-7.88 (m, 2H, aromatic). ^{31}P NMR (121.49 MHz, $CDCl_3$, room temp.): δ 60.6 (s). Anal. Calcd for $C_{25}H_{21}CoIOP$: C, 54.18; H, 3.82. Found: C, 53.89; H, 3.97.

*V.6.5 Preparation and spectroscopic data for **5***

Complex **5** was obtained using a similar procedure to that described above for **3,** from [(η^5-C_5H_5)CoI_2(CO)] (0.120 g, 0.30 mmol) and **HL4** (0.073 g, 0.30 mmol). It was obtained has a dark purple crystalline solid (0.151 g, 81%). IR (KBr): 1699 (s, ν_{CO}) cm^{-1}. ^{1}H NMR (300.13 MHz, $CDCl_3$, room temp.): δ 1.20 (s, 3H, CH_3), 5.08 (s, 5H, η^5-C_5H_5), 6.30 (d, $^2J_{PH}$ = 16.7 Hz, 1H, NH), 7.47-7.57 (complex m, 6H, aromatic), 8.07-8.16 (complex m, 4H, aromatic). ^{31}P NMR (121.49 MHz, $CDCl_3$, room temp.): δ 70.7 (s). Anal. Calcd for $C_{19}H_{19}CoI_2NOP$: C, 36.74; H, 3.08; N, 2.26. Found: C, 36.84; H, 3.10; N, 2.20.

*V.6.6 Preparation and spectroscopic data for **6***

Complex **6** was obtained using a similar procedure to that described above for **4,** from **5** (0.176 g, 0.28 mmol) and Et_3N (1 ml, 7.12 mmol). It was obtained has a dark purple solid (0.113 g, 81%). IR (KBr): 1487 (s, ν_{CN+CO}) cm^{-1}. ^{1}H NMR (300.13 MHz, $CDCl_3$, room temp.): δ 2.19 (s, 3H, CH_3), 5.09 (s, 5H, η^5-C_5H_5), 7.45-7.55 (complex m, 8H, aromatic), 7.93-8.01 (complex m, 2H, aromatic). ^{31}P NMR (121.49 MHz, $CDCl_3$, room temp.): δ 111.1 (s). Anal. Calcd for $C_{18}H_{19}CoINOP$: C, 46.27; H, 3.68; N, 2.84. Found: C, 46.00; H, 3.90; N, 2.60.

*V.6.7 Preparation and spectroscopic data for **10***

NaOMe (0.030 g, 0.564 mmol) was dissolved in the minimum amount of methanol and **HL4** (0.135 g, 0.555 mmol) dissolved in 15 mL of dichloromethane was added. Anhydrous $NiCl_2$ (0.036 g, 0.278 mmol) was then added and the yellow solution thus obtained was stirred at ambient temperature for 48 h. After removal of the solvent under vacuum, the yellow residue was treated with toluene, and the solution was filtered in order to remove NaCl. The toluene was then evaporated under reduced pressure and the complex washed with cold petroleum ether (0.132 g, 0.243 mmol, 87%). IR (KBr): 1439 (s, ν_{CN+CO})

cm^{-1}. ^{1}H NMR (300.13 MHz, $CDCl_3$, room temp.): δ 3.76 (d, $^{4}J_{PH}$ = 11.1 Hz, 6H, CH_3), 7.42-7.56 (complex m, 6H, aromatic), 7.77-7.85 (m, 4H, aromatic). ^{31}P NMR (121.49 MHz, $CDCl_3$, room temp.): δ 34.4 (s). Anal. Calcd for $C_{28}H_{26}N_2NiO_2P_2$: C, 61.92; H, 4.82; N, 5.16. Found: C, 62.11; H, 4.95; N, 4.99.

*V.6.8 Preparation and spectroscopic data for **11***

A mixture of $NiCl_2.6H_2O$ (0.2 g, 0.85 mmol) and **HL3** (0.3 g, 1.71 mmol) was dissolved in ethanol (20 mL) giving a dark green solution. After stirring for 1 hour, a solution of NaOEt (prepared from 0.04 g of Na and 10 mL of ethanol) was slowly added (20 min) the colour changed to light green-yellow. After being stirred for an hour, the colour of the solution changed to yellow-orange. The solvent was removed under reduced pressure. And the orange solid extracted with dry toluene to give an orange solution, that was filtered in order to remove NaCl, and pentane added. It was let in the fridge over night to give compound **11** as yellow crystals (0.210 g, 0.515 mmol, 60%). IR: 1519 (s, ν_{CN+CO}) cm^{-1}. ^{1}H NMR (300.13 MHz, $CDCl_3$, room temp.): δ 1.24-1.29 (dd, $^{3}J_{PH}$ = 14.5 Hz, $^{3}J_{HH}$ = 7 Hz, 12H, $(CH(CH_3)(CH_3))_2$), 1.35-1.41 (dd, $^{3}J_{PH}$ = 17.1 Hz, $^{3}J_{HH}$ = 7.2 Hz, 12H, $(CH(CH_3)(CH_3))_2$), 1.97-2.07 (m, 4H, ^{i}PrCH), 2.16 (s, 6H, MeC=N). ^{31}P NMR (121.49 MHz, $CDCl_3$, room temp.): δ 115.9 (s).

V.7 Crystal structure determinations

Crystals of **HL3** suitable for an X-ray diffraction study were obtained by placing a schlenk with the ligand at 5 ºC overnight. Crystals of **3**, **5**, **6**, **9** and **10** were obtained by slow diffusion of hexane into a CH_2Cl_2 solution of the respective complex at 5 ºC. Crystals of **11** were obtained from a mixture of toluene/pentane at -25ºC overnight. Diffraction data were collected on a Kappa CCD diffractometer using graphite-monochromated Mo Kα radiation (λ = 0.71073 Å) (Table V.2 and V.3). Data were collected using phi-scans and the structures were solved by direct methods using the SHELXL 97 software,[28-30] and the refinement was performed by full-matrix least squares on F^2. The absorption was not corrected. All non-

hydrogen atoms were refined anisotropically. Hydrogen atoms were generated according to stereo-chemistry and refined using a riding model in SHELXL97.

V.8 Acknowledgements

We thank Dr. A. DeCian (ULP Strasbourg) for his contribution to the crystal structure determinations and A. Degrémont (LCC) for assistance. We are also grateful to the European Commission (Palladium Network HPRN-CT-2002-00196), the "Centre National de la Recherche Scientifique" (France), the French "Ministère de la Recherche" for financial support. We also thank "Fundação para a Ciência e Tecnologia", Portugal, for funding (Project PTDC/QUI/66440/2006) and for a doctoral fellowship to V.Rosa (SFRH/BD/13777/2003) and CPU (France) and CRUP (Portugal) for the Portuguese-French Integrated Action-2006, Nº F-27/07

V.9 References

1. P. Braunstein, *Chem. Rev.*, 2006, **106**, 134-159.
2. M. P. Batten, A. J. Canty, K. J. Cavell, T. Ruther, B. W. Skelton and A. H. White, *Inorg. Chim. Acta*, 2006, **359**, 1710-1724.
3. I. Gottker-Schnetmann, B. Korthals and S. Mecking, *J. Am. Chem. Soc.*, 2006, **128**, 7708-7709.
4. S. E. Bouaoud, P. Braunstein, D. Grandjean, D. Matt and D. Nobel, *Inorg. Chem.*, 1986, **25**, 3765-3770.
5. A. Kermagoret and P. Braunstein, *Dalton Transactions*, 2008, 1564-1573.
6. Q. Z. Yang, A. Kermagoret, M. Agostinho, O. Siri and P. Braunstein, *Organometallics*, 2006, **25**, 5518-5527.
7. J. Andrieu, P. Braunstein, M. Drillon, Y. Dusausoy, F. Ingold, P. Rabu, A. Tiripicchio and F. Ugozzoli, *Inorg. Chem.*, 1996, **35**, 5986-5994.
8. P. Braunstein, D. G. Kelly, Y. Dusausoy, D. Bayeul, M. Lanfranchi and A. Tiripicchio, *Inorganic Chemistry*, 1994, **33**, 233-242.
9. P. Braunstein, D. G. Kelly, A. Tiripicchio and F. Ugozzoli, *Inorganic Chemistry*, 1993, **32**, 4845-4852.
10. P. Braunstein, C. Frison, X. Morise and R. D. Adams, *J. Chem. Soc., Dalton Trans.*, 2000, 2205-2214.
11. P. Bhattacharyya, T. Q. Ly, A. M. Z. Slawin and J. Derek Woollins, *Polyhedron*, 2001, **20**, 1803-1808.
12. T. Q. Ly, A. M. Z. Slawin and J. D. Woolins, *Polyhedron*, 1999, **18**, 1761.
13. P. Braunstein, C. Frison and X. Morise, *Angew. Chem., Int. Ed.*, 2000, **39**, 2867-2870.
14. N. G. Jones, M. L. H. Green, I. Vei, A. Cowley, X. Morise and P. Braunstein, *J. Chem. Soc. Dalton Trans.*, 2002, 1487-1493.
15. P. Braunstein, B. T. Heaton, C. Jacob, L. Manzi and X. Morise, *J. Chem. Soc., Dalton Trans.*, 2003, 1396-1401.
16. X. Morise, M. L. H. Green, P. Braunstein, L. H. Rees and I. Vei, *New J. Chem.*, 2003, **27**, 32-38.
17. N. Oberbeckmann-Winter, P. Braunstein and R. Welter, *Organometallics*, 2005, **24**, 3149-3157.

18. P. Braunstein, Y. Chauvin, J. Nähring, A. DeCien, J. Fischer, A. Tiripicchio and F. Ugozzoli, *Organometallics*, 1996, **15**, 5551-5567.
19. M. Agostinho and P. Braunstein, *C. R. Chimie*, 2007, In press.
20. S. J. Landon and T. B. Brill, *Inorg. Chem.*, 1984, **23**, 1266-1271.
21. P. Braunstein, D. Matt, D. Nobel, F. Balegroune, S. E. Bouaoud, D. Grandjean and J. Fischer, *J. Chem. Soc., Dalton Trans.*, 1988, 353-361.
22. H. Qichen, X. Minzhi, Q. Yanlong, X. Weihua, S. Meichen and T. Youqui, *J. Organomet. Chem.*, 1985, **287**, 419-426.
23. U. Klabunde and S. D. Ittel, *J. Mol. Catal. A: Chem.*, 1987, **41**, 123-134.
24. U. Klabunde, R. Mühlhaupt, T. Herskowitz, A. H. Janowicz, J. Calabrese and S. D. Ittel, *J. Polym. Sci., Part A: Polym. Chem.*, 1987, **25**, 1989-2003.
25. C. J. Moulton and B. L. Shaw, *J. Chem. Soc., Dalton Trans.*, 1980, 299-301.
26. R. F. Heck, *Inorg. Chem.*, 1965, **4**, 855-857.
27. P. Braunstein, D. Matt, D. Nobel and J. Fischer, *J. Chem. Soc., Chem. Commun.*, 1987, 1530-1532.
28. B. V. Nonius, *Kappa CCD Operation Manual*, Delft, The Nederlands, 1997.
29. R. Welter, *Acta Crystallographica Section A*, 2006, **62**, s252.
30. G. M. Sheldrick, SHELXL97, Program for the refinement of crystal structures, University of Göttingen, Germany, Editon edn., 1997.

Chapter VI

Conclusions

A series of cobalt(II) complexes of general formula [Co(α-diimine)X_2], where α-diimine was R-DAB or R-BIAN, R= Me or i-propyl and X= Cl or I were obtained , by direct reaction of equimolar quantities of the corresponding CoX_2 salt and the α-diimine ligand in dried CH_2Cl_2, in c.a. 75% to 94% yield. The synthesized compounds are [Co(Ph-DAB)Cl_2] **II-1a**, [Co(*o,o',p*-$Me_3C_6H_2$-DAB)Cl_2] **II-1b**, [Co(*o,o'*-$^{i}Pr_2C_6H_3$-DAB)Cl_2] **II-1c**, [Co(*o,o',p*-$Me_3C_6H_2$-DAB)I_2] **II-1´b**, [Co(*o,o',p*-$Me_3C_6H_2$-BIAN)I_2] **II-2´b**, [CoI_2(*o,o',p*-$Me_3C_6H_2$-DAB)] **III-1**, [CoI_2(*o,o'*-$^{i}Pr_2C_6H_3$-DAB)] **III-2**, [$CoCl_2$(*o,o',p*-$Me_3C_6H_2$-BIAN)] **III-3**, [$CoCl_2$(*o,o'*-$^{i}Pr_2C_6H_3$-BIAN)] **III-4** and [CoI_2(*o,o'*-$^{i}Pr_2C_6H_3$-BIAN)] **III-5**.

The crystal structures of compounds[Co(Ph-DAB)Cl_2] **II-1a**, [Co(*o,o',p*-$Me_3C_6H_2$-DAB)Cl_2] **II-1b**, [Co(*o,o'*-$^{i}Pr_2C_6H_3$-DAB)Cl_2] **II-1c**, [Co(*o,o',p*-$Me_3C_6H_2$-BIAN)I_2] **II-2´b**, [$CoCl_2$(*o,o',p*-$Me_3C_6H_2$-BIAN)] **III-3** and [$CoCl_2$(*o,o'*-$^{i}Pr_2C_6H_3$-BIAN)] **III-4** were solved by single crystal X-ray diffraction. Single crystal X-ray structural data for these compounds shows, in all cases, that the cobalt atom is in a distorted tetrahedral coordination which is built by two halide atoms and two nitrogen atoms of the α-diimine ligand.

X-band EPR measurements in polycrystalline samples performed on [Co(*o,o',p*-$Me_3C_6H_2$-DAB)Cl_2] **II-1b**, [Co(*o,o'*-$^{i}Pr_2C_6H_3$-DAB)Cl_2] **II-1c**, and [Co(*o,o',p*-$Me_3C_6H_2$-BIAN)I_2] **II-2´b** indicate high-spin Co(II) (S = 3/2) in an axially distorted environment.

Single crystal EPR measurements were performed on compounds [Co(*o,o',p*-$Me_3C_6H_2$-DAB)Cl_2] **II-1b** and [Co(*o,o'*-$^{i}Pr_2C_6H_3$-DAB)Cl_2] **II-1c**, which allowed us to determine the ***g*** tensor orientation for a low symmetry Co(II) compound. Structural and EPR results suggest similar ***g*** tensor orientations for all the compounds and the electronic properties of the Co(II) ions seem to be independent of the type of halide coordinated to the metal site.

The ^{1}H NMR spectra of compounds CoI_2(*o,o',p*-$Me_3C_6H_2$-DAB)] **III-1**, [CoI_2(*o,o'*-$^{i}Pr_2C_6H_3$-DAB)] **III-2**, [$CoCl_2$(*o,o',p*-$Me_3C_6H_2$-BIAN)] **III-3**, [$CoCl_2$(*o,o'*-$^{i}Pr_2C_6H_3$-BIAN)] **III-4** and [CoI_2(*o,o'*-$^{i}Pr_2C_6H_3$-BIAN)] **III-5**, in CD_2Cl_2, at room temperature, exhibit paramagnetic contact shifts. These contact shifts are due to the paramagnetic character of the Co(II) complexes that exhibit high spin S = 3/2 in the solid state, although in solution they may be involved in equilibria with their S = 1/2 square planar conformers.

The catalytic activity towards ethylene polymerization was tested for some of the [Co(α-diimine)X_2] compounds. **III-3** and **III-4**, as well as ([$CoCl_2$(*o,o',p*-$Me_3C_6H_2$-DAB)]) **III-1a**, and ([$CoCl_2$(*o,o'*-$^{i}Pr_2C_6H_3$-DAB)]) **III-2a**, revealed low activities in ethylene polymerization when activated with MAO. The resulting branched (2.5-5.5%) low molecular weight polyethylenes are solid samples, with melting points in the range of 77-110 ºC.

A new rigid bidentate ligand bis(1-naphthylimino)acenaphthene, **IV-L1**, and its Zn(II) and Pd(II) complexes [$ZnCl_2$(**L1**)], **IV-1**, and [$PdCl_2$(**L1**)], **IV-2**, were synthesized.

Bis(1-naphthylimino)acenaphthene **IV-L1** was prepared by the "template method", reacting 1-naphthyl amine and acenaphthenequinone in the presence of $ZnCl_2$, giving [$ZnCl_2$(**L1**)] **IV-1**, that was further demetallated.

Reaction of 1-naphthyl amine with acenaphthenequinone and $PdCl_2$ afforded dichloride bis(1-naphthyl)acenaphthenequinonediimine) palladium [$PdCl_2$(**L1**)] **IV-2**.

Bis(1-naphthylimino)acenaphthene **IV-L1**, [$ZnCl_2$(**L1**)] **IV-1** and [$PdCl_2$(**L1**)] **IV-2** were obtained as a mixture of *syn* and *anti* isomers.

[$PdCl_2$(**L1**)] **IV-2**, was also obtained by reaction of $PdCl_2$ activated by reflux in acetonitrile followed by addition of bis(1-naphthylimino)acenaphthene **IV-L1,** by this route a mixture of *syn* and *anti* isomers was also obtained, but in a different proportion.

Bis(1-naphthylimino)acenaphthene **IV-L1**, [$ZnCl_2$(**L1**)] **IV-1** and [$PdCl_2$(**L1**)] **IV-2** were characterized by elemental analyses, MALDI-TOF-MS spectrometry, and by IR, UV-vis, ^{1}H, ^{13}C, ^{1}H-^{1}H COSY, ^{1}H-^{13}C HSQC, ^{1}H-^{13}C HSQC-TOCSY and ^{1}H-^{1}H NOESY NMR spectroscopies when applied.

The solid state structures of bis(1-naphthylimino)acenaphthene **IV-L1** and the *anti* isomer of compound [$PdCl_2$(**L1**)] **IV-2** were determined by single crystal X-ray diffraction. The coordination at the palladium in the *anti* isomer of compound [$PdCl_2$(**L1**)] **IV-2** is quite distorted from an ideal square plane environment, where the relatively small N1-Pd-N2 bond angle of 81.4(2)º is a result of chelating ligand steric constraints.

Theoretical calculations showed that molecular geometry is very similar in both isomers and only an important variation in the orientation angle for the naphthyl groups can be expected, in agreement with experimental structure.

DFT studies showed that the *syn* and *anti* isomers of [$PdCl_2$(BIAN)] are isoenergetic, therefore they can both be obtained experimentally. However, no isomerization process is available in square-planar complexes, but it can occur for the free ligand. Finally, by replacing the metallic fragment ML_n, the structural choice can be affected, and one or both conformers can be obtained. Their relative stability will depend on the nature of the metal, including electronic configuration and environment, and on the terminal ligands

Three new ligands: the β-keto phosphine ligands $R_2PCH_2C(O)Ph$ (**V-HL1**, R = ^{i}Pr; **V-HL2**, R = Ph) and the new acetamide-derived phosphine ligand (^{i}Pr)$_2$PNHC(O)Me (**V-HL3**) were prepared. (^{i}Pr)$_2$PCH$_2$C(O)Ph **V-HL1** and Ph$_2$PCH$_2$C(O)Ph **V-HL2** were prepared by reacting PhC(O)CH$_2$Li with the corresponding chlorophosphine. (^{i}Pr)$_2$PNHC(O)Me **V-HL3** was prepared by reacting (^{i}Pr)$_2$PCl with N-trimethylsilylacetamide.

A series of cobalt (III) and nickel (II) complexes bearing these ligands were obtained. Ligands Ph$_2$PCH$_2$C(O)Ph **V-HL2** and [Ph$_2$PNHC(O)Me] **V-HL4** reacted with the cobalt cyclopentadienyl complex [(η^5-C$_5$H$_5$)CoI$_2$(CO)] to afford the phosphine mono-adducts [(η^5-C$_5$H$_5$)CoI$_2${Ph$_2$PCH$_2$C(O)Ph}] (**V-3**) and [(η^5-C$_5$H$_5$)CoI$_2${Ph$_2$PNHC(O)Me}] (**V-5**). Treatment of [(η^5-C$_5$H$_5$)CoI$_2${Ph$_2$PCH$_2$C(O)Ph}] **V-3** and [(η^5-C$_5$H$_5$)CoI$_2${Ph$_2$PNHC(O)Me}] **V-5** with excess Et$_3$N yielded the η^2-phosphinoenolate complex [(η^5-C$_5$H$_5$)CoI{Ph$_2$PCH⋯C(⋯O)Ph}] (**V-4**) and the η^2-acetamidophosphine complex [(η^5-C$_5$H$_5$)CoI{Ph$_2$PN⋯C(⋯O)Me}] (**V-6**), respectively.

Cis-[Ni(Ph$_2$PN⋯C(⋯O)Me)$_2$] (**V-10**) was obtained by reaction of [Ph$_2$PNHC(O)Me] **V-HL4** with NiCl$_2$ in the presence of NaOMe. The reaction of (^{i}Pr)$_2$PNHC(O)Me **V-HL3** with NiCl$_2$.6H$_2$O in ethanol followed by the addition of NaOEt afforded complex *cis*-[Ni((^{i}Pr)$_2$PN⋯C(⋯O)Me)$_2$] (**V-11**).

The solid state structure of ligand (^{i}Pr)$_2$PNHC(O)Me **V-HL3** was determined by single crystal X-ray diffraction. Complexes [(η^5-C$_5$H$_5$)CoI$_2${Ph$_2$PCH$_2$C(O)Ph}] **V-3**, [(η^5-C$_5$H$_5$)CoI$_2${Ph$_2$PNHC(O)Me}] **V-5**, [(η^5-C$_5$H$_5$)CoI{Ph$_2$PN⋯C(⋯O)Me}] **V-6**, **V-9**, *cis*-

[Ni($Ph_2PN^{\cdots}C(^{\cdots}O)Me)_2$] **V-10** and *cis*-[Ni(($^{i}Pr)_2PN^{\cdots}C(^{\cdots}O)Me)_2$] **V-11** were also characterized by X-ray crystallography.